UNIVERSIDAD AUTÓNOMA DE MADRID
Programa de Doctorado en Biociencias Moleculares

Mechanisms involved in quiescent blood vessel homeostasis

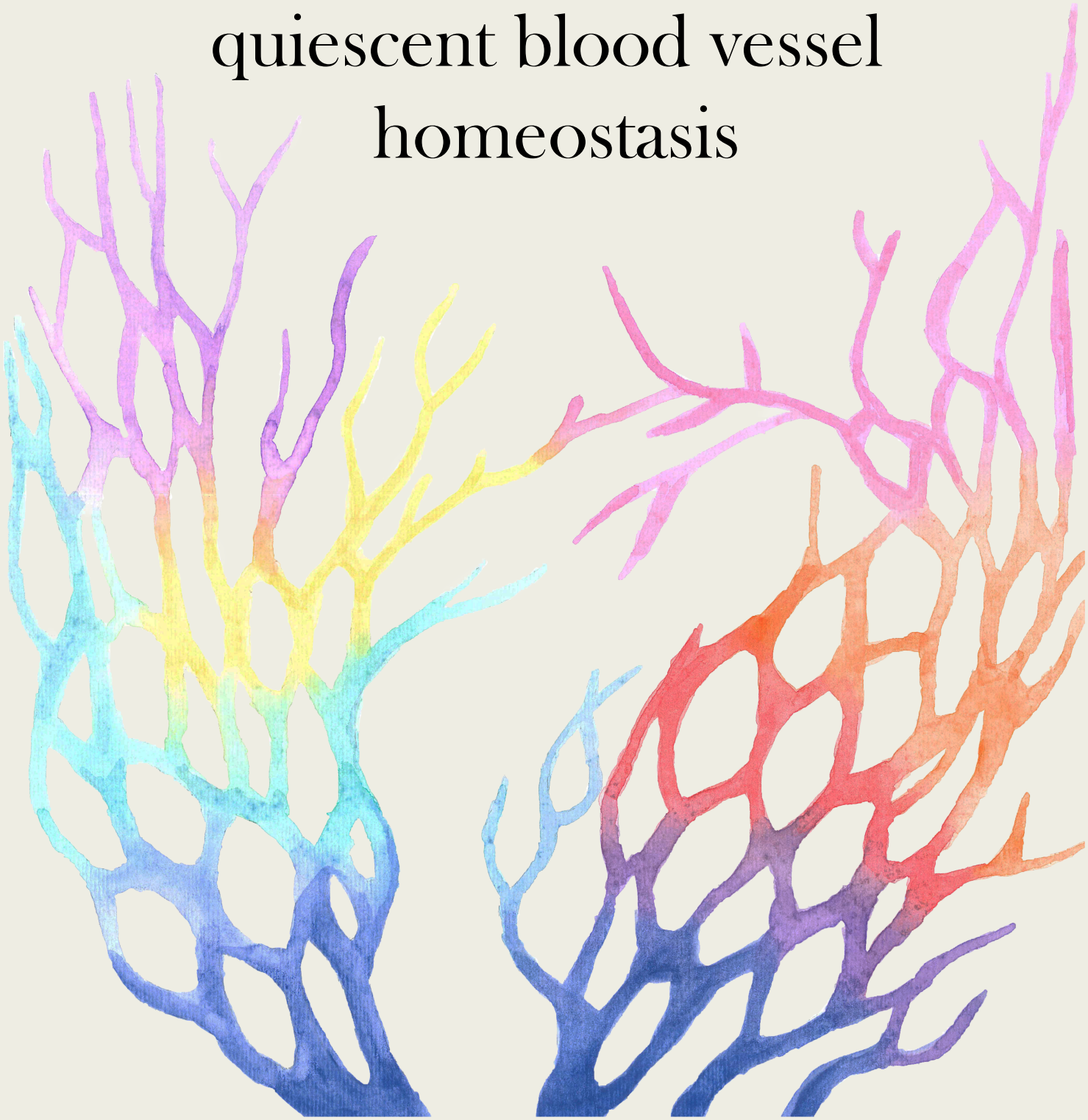

Macarena Fernández Chacón
Madrid, 2020

Imagen de portada:

Acuarela pintada por Blanca y Macarena Fernández Chacón

en Jerez de la Frontera el 1 de noviembre de 2020.

Representa la heterogeneidad de los vasos sanguíneos

Cover image:

Watercolor painted by Blanca and Macarena Fernández Chacón

en Jerez de la Frontera el 1 de noviembre de 2020,

It represents blood vessel heterogeneity.

POSTGRADUATE PROGRAMME IN MOLECULAR BIOSCIENCES

DEPARTMENT OF BIOCHEMISTRY

FACULTY OF MEDICINE

UNIVERSIDAD AUTÓNOMA DE MADRID

Mechanisms involved in quiescent blood vessel homeostasis

Macarena Fernández Chacón

BSc Biotechnology

MSc Molecular Biomedicine

Director: Rui Benedito

Spanish National Center for Cardiovascular Research (CNIC)

Director: Dr. Rui Benedito

Spanish National Center for Cardiovascular Research (CNIC)

This work was performed in Dr. Rui Benedito's laboratory in the Cellular and Developmental Biology Department at the Spanish National Center for Cardiovascular Research (CNIC) in Madrid.

This study was supported by the following grants from the Ministerio de Economía, Industria y Competitividad (MEIC: SAF2013-44329-P, SAF2013-42359-ERC and RYC2013-13209) and the European Research Council (ERC-2014-StG – 638028 AngioGenesHD).

Macarena Fernández Chacón was supported by a PhD fellowship from Fundación la Caixa (CX_E-2015-01).

The thesis director Dr. Rui Benedito certifies that this doctoral thesis has been performed under his supervision,

Rui Benedito

Thesis director

A lo mejor de mi vida,

a mi familia.

ACKNOWLEDGMENTS

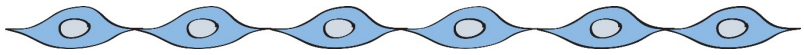

Showing gratitude is one of the simplest yet most powerful things humans can do for each other.

The Last Lecture, Randy Pausch

If you want to go fast, go alone. If you want to go far, go together.

African proverb

> Siempre he asistido como espectadora a mis propios conflictos y gracias a un peculiar desdoblamiento todas mis actividades me parecen ejecutadas por otra persona. Por lo cual, como un conflicto ajeno tiene importancia relativa para el que desde fuera le está mirando, nunca he tomado demasiado en serio -aunque de veras me hayan dolido o regocijado- ni mis penas ni mis alegrías; las unas no han logrado jamás hundirme en desesperación, ni las otras embriagarme; soy mi propio espejo y mi propio fantasma; sé, lo he sabido siempre, que todo pasa y que de todo he de salir por misericordiosas puertas de la muerte.
>
> *Gregorio y yo,* Maria Lejárraga

Espectadora de mi propia vida. Así me siento 6 años después de haber puesto por primera vez un pie en el CNIC. Un sueño que bajo mi punto de vista ha pasado demasiado rápido, pero que a la vez he disfrutado de él cómo nada en este mundo. Un sueño lleno de inmensas alegrías, pero no os voy a engañar, también con alguna que otra pena. Sin embargo, como dice Maria Lejárraga estas "no han logrado jamás hundirme en desesperación", ya que en mi caso tengo la enorme suerte de no haber pasado por este camino sola, sino rodeada de personas maravillosas. Durante estos años, no ha habido un solo día en el que no me haya levantado con ganas de ir al CNIC y hacer ciencia. Eso es una gran suerte y no hay nada que lo supere.

I would like to start thanking Rui for the opportunity to work in his laboratory. Not everyone has the chance to get sequenced 106 RNA-seq samples! I have learnt that in science one has to be precise, because details are important. I have grown up as a scientist in your group and I will always be grateful. Thanks a lot Susana for the effort in the paper and thesis correction. You made my work much better. Gracias a mi tutora de la Universidad, Teresa González, por la supervisión a lo largo de estos años.

A mis queridas compañeras de grupo, a mis clonators y beneditas, tanto a las antiguas con las que empecé, como a las nuevas que se han ido incorporando y continuarán: os debo todas las alegrías. Vosotras habéis hecho del grupo un lugar donde pasarlo bien, porque trabajar duro puede ir de la mano de reír y disfrutar. Todas sois unas grandes personas y me habéis demostrado una gran calidad humana. Hemos sido una gran familia y os estaré eternamente agradecida. A Sofía, por ser una compañera y amiga. Todos los comienzos son difíciles, y tú siempre me lo hiciste más fácil. ¡Echo de menos nuestro querido corner! Tania, no he visto a persona con más pasión y más entregada por la ciencia que tú. Me alegra ver que todo esfuerzo tiene su recompensa, y que la tuya ha llegado ahora. A Luis, por acompañarme en esos primeros años de Máster. No había día en el que yo me fuera a casa y tú no siguieras a altas horas de la noche mirando las digestiones. Gracias por tus consejos. Briane, it has been a pleasure to start this PhD trip with you, and I have always appreciated your willingness to party with me. You rock! Irene, la gran guerrera del grupo. Tu coraje y tu valentía siempre son necesarios en esta sociedad. Nunca cambies. Gracias a ti también Elena, porque aunque fuera poco tiempo aprendí mucho de ti. Si algo sé del mundo de los ratoncillos es por Gonzalo: gracias por invertir tiempo no sólo en enseñarme cómo manejarlos, sino también en escucharme, aconsejarme y darme apoyo. Néstor, todo un maestro clonator que nos ha deleitado con su alegría y su música de pachangueo. ¡La sanidad te necesita ahora más que nunca! Macarenita, por mucho que hayamos bromeado, espero que nunca pierdas ese entusiasmo de florecilla, y que pocos días te sientas Calamardo. Lourdes, nuestra instagramer del grupo. Gracias por darme una segunda oportunidad para ser tu hero. Fue toda una suerte poder trabajar contigo y compartir mi experiencia. Confío en ti, en tu ciencia y en tus imágenes tan preciosas de los mosaicos. Aroa, ¡tu rincón de la felicidad nos ha dado de los mejores momentos en el laboratorio! Tu empatía no entiende de límites. Severin, it was great that you joined our group. You gave us so many reasons to get together and celebrate. We needed that impulse. Thanks! Ivana, gracias por dejarme disfrutar contigo tantos momentos dentro, y últimamente fuera del laboratorio. No cualquier persona te hace una mudanza en una tarde o te acompaña al fisio para que no te de miedo. Eso lo sé. Eres increíblemente fuerte (y no me refiero físicamente, ¡ya que eso nadie lo pone en duda!). Te debo mucho y aquí me tendrás siempre. Wen, I cannot imagine my PhD without you. We are all so lucky to have you in the group all these years and I can tell you I have enjoyed every moment at your side. You always supported and helped me. You are a true friend, and I cannot wait to visit you wherever your next career step is. A Verónica, la cual ha recorrido este camino conmigo desde el principio hasta el final. Has sido un pilar fundamental durante todos estos años: mi guía, mi apoyo y mi comprensión. Gracias por tu ayuda científica y personal. Siempre has confiado en

mí y me has recordado quien soy en aquellos momentos en los que no vi clara la dirección. Sin ti, llegar aquí hubiera sido sino imposible, cuanto menos muy complicado. Amiga, este PhD también es tuyo. A todas las estudiantes que he tenido el placer de supervisar y acompañar: me habéis enseñado más a mí, que yo a vosotras. Especial mención a mis querida Carla, que en dos meses con su sonrisa nos robó el corazón a todos. Nunca olvidaré nuestra emoción al ver la caspasi brillar en el confocal. A todos los miembros del grupo que se están uniendo (Álvaro, Anahita…) y a todos los que se unirán en un futuro: disfrutad juntos.

A mi segunda familia en el CNIC, a los que hicieron que ver un punto rojo brillante dentro de la tinción de Isolectina fuera para mí algo digno de orgullo. No es casualidad que más de una vez en administración o en alguna Unidad se creyeran que yo era de vuestro grupo. Todos los pomperos siempre han sido para mí un punto de referencia y de consulta. A Juli, Gaetano, Tania, Dimitris: You were all so inspiring that encouraged me to work hard in my project. Marcos, ir por el pasillo y no escuchar algunos de tus comentarios sería extraño y triste. Aunque nunca lo reconocerás, siempre has estado ahí para ayudarme y han abundado los "más" que los "menos". Tengo suerte de haber compartido este doctorado contigo. Gracias. A Alejandro, un cachas con chulería que esconde un corazón enorme. He disfrutado mucho estos últimos años a tu lado, incluso de tus comentarios junto con el anterior mencionado. A Rebeca T, desde el Máster hasta la escritura de la tesis: ¡ya está hecho! Al Dr. Luna, por su sabiduría y sus irónicas respuestas. A mi Piñe, la cual ha sido indispensable durante esta última etapa: nunca me habría imaginado que pudiera encontrar tanto apoyo y tanto amor a mitad del viaje. Soy una afortunada por tener a una gran amiga como tú. Lao, al poco de conocernos me dijiste que yo era "soleada". Para mí el sol ha sido tenerte a mi lado durante cuatro años, dentro y fuera del laboratorio. Un trocito de mi corazón y de mi alegría se fueron contigo a EEUU, y sueñan con volverse a reencontrar. Nunca olvides la carta de la suerte.

Y es que la 3N quizás ha sido (y espero que siga siendo) de las alas más singulares del CNIC. Gracias al grupo de Miguel Torres, Nacho Flores y Nadia por hacer de nuestra planta un lugar de encuentro y conversación. Héctor, un apasionado de la ciencia con su propia perspectiva del mundo. Me alegra haber compartido contigo la pasión por Notch en estos últimos años. María, siempre velando por toda la planta. Nos haces falta y agradezco los momentos pasados a tu lado. Teresa Casaseca, una madre dentro del CNIC.

Sin embargo, cualquier ala o planta del CNIC esconde verdaderas joyas. Especial mención al grupo de Miguel Manzanares: esa visión y pasión por la ciencia compartida por Miguel, y que pasa por todos los PhD, postdocs, técnicos y estudiantes de su grupo hace de la investigación un mundo mejor. Julio, Melisa, María, Antonio, Isabel: gracias por compartir ese entusiasmo conmigo. Jesús, una vida tan paralela y a la vez tan diferentes ¡Ya van diez años! Sergio, sin darnos cuenta nos convertimos en grandes amigos, y siempre me has demostrado que sigues ahí, aun teniendo yo una agenda tan difícil como ha sido a veces: gracias por entenderme y quererme así. Y a un sinfín de personas, que incluso sin compartir ni grupo ni ala ni planta han hecho de estos años un recorrido inmejorable: Javito, Itziar, Ana, Jose…

Quisiera recalcar aquí el papel de los verdaderos héroes, que en mi opinión pasan desapercibidos demasiadas veces, pero que son los que realmente sacan las castañas del fuego, y hacen que nuestros proyectos pasen del papel a una realidad tangible. Estas son las Unidades Técnicas del CNIC. Sin vosotros, mi proyecto hubiera sido imposible. Microscopía: Valeria, Moreno, Verónica y Elvira, habéis sido esenciales para obtener nuestras fotos en el confocal. Verónica, ¡tus macros! Eternamente agradecida. Genómica: Ana, Alberto, Rebeca, gracias por iniciarnos en el maravilloso mundo de la NGS. Siempre habéis estado ahí para sacar un RNA-seq de dónde no había casi RNA. Sois verdaderos magos. Proteómica: gracias a Emilio y a Jesús. Las reuniones con vosotros siempre fueron increíblemente fructíferas, y me quedo con las ganas de haber hecho más experimentos junto a vosotros. Emilio, gracias por tu disponibilidad inmediata. Medicina comparativa: Pedro, gracias por aceptar mis cassettes llenos de órgano y hacer de ellos una nueva terminología en el CNIC. Merche, Sandra, Gonzalo, gracias por cuidar de todos nuestros animalitos y hacer nuestro trabajo mucho más sencillo. Bioinformática: en especial a Fátima y Manuel, gracias por analizar, reanalizar y volver a re-reanalizar todos mis experimentos. Por vuestra paciencia y compartir vuestro conocimiento conmigo. Informática: Juan Carlos, que haríamos todo el CNIC sin ti…Celómica: después de mi planta, es donde quizás más tiempo he pasado. Eternas horas de sorting para intentar sacar células de colores de poblaciones imposibles. Jose, Raquel, Mariano, Elena...He aprendido del mundo de la citometría

gracias a vosotros. Nunca he tenido problema en tener un día completo de FACS, aunque eso significara salir a las 21h, cansada, con el centro casi vacío y el campus a oscuras, ya que eso también significaba que iba a pasar unas horas con Elena. Jamás he visto a una persona tan involucrada en los proyectos, teniendo incluso más interés que yo en encontrar a mis queridas células endoteliales. Elena no sólo me ha salvado los experimentos, sino que me ha salvado de las tinieblas… He disfrutado las eternas horas de sorting, y si os digo la verdad, las echo de menos porque echo de menos estar allí con ella. No tendría espacio suficiente para darte las gracias por todos estos años.

Gracias inmensas al personal de limpieza, en especial a Tere, que no ha dejado que me perdiera entre mis papeles del escritorio. Al servicio de cafetería y a Ángel, a mantenimiento, a seguridad, almacén…todos ellos han hacen que nuestro trabajo sea posible.

Me gustaría agradecer a todas las jefas de grupo que he tenido la suerte de encontrarme en el terreno profesional y personal: Silvia Martín Puig, Fátima Sánchez, Guadalupe Sabio, Hannah Carter, Maria Luisa Toribio… Para mi sois un ejemplo a seguir, y me recordáis día a día que podemos conseguirlo. Gracias por luchar por ello.

Agradecer también a la Fundación la Caixa por la beca concedida para realizar la tesis doctoral en el CNIC y a la Boehringer Ingelheim Fonds por la beca de viaje para irme de estancia a San Diego durante la tesis. A la UFV y a la Escuela de Liderazgo por toda la formación académica y el acompañamiento durante estos años. Gracias a Pepelu y a Sabrina.

In the middle of my PhD, I had the opportunity to spend six wonderful months in San Diego. Thanks Hannah, for given me the chance of joining your group. In such a little time you showed me the enormous scientist and person you are. You gave to a wet lab student the time, space and tools to learn from you and all your group experience about the incredible bioinformatic world. Two years later still I cannot believe how lucky I was to be part of your group. Because of that I met my two American friends: Rachel and Clara. Rachel, I was so honored to share all those important moments of your life. You let me be part of your family and I will always be grateful. My stay in San Diego would have been completely different without you. Clara, I miss our talks in the beach, running, climbing, our parties and trips together. Thanks for visiting me so many times and open your heart. Rachel, Daniel, Clara and Judd, I miss you and I hope I can visit you soon in California. Here you will have always your home. A David y Laura, que me abrieron las puertas de su hogar desde el primer día. Gracias por las conversaciones nocturnas y el bueno vino, que me dejaron conoceros y pasar muy buenos momentos a vuestro lado. Echo de menos estar con vosotros en Hygeia.

Volver a casa después de una larga jornada nunca ha sido duro gracias a las personas con las que he tenido la suerte de compartir piso. Mis amigas, mis compañeras de Biotecnología y unas científicas de los pies a la cabeza. Hemos compartido tantos momentos juntas que nos conocemos a la perfección. Paula, ir al CNIC en el 147 ya no tiene sentido si no voy contigo. Compartir reflexiones a las 08:00 de la mañana o tras una jornada intensiva ha sido un verdadero placer. Carmen, gracias por tu responsabilidad, tu tranquilidad y paz a nuestra casa. Ana, nos diste una alegría enorme al venirte. Gracias por hacer de nosotras un grupo. Sois unas hermanas para mí, y espero poder seguir disfrutando de todos vuestros logros (que han sido, y seguirán siendo muchos). A ti Pablo, qué decirte que no sepas. Gracias por leer a través de mis ojos todos estos años. Eres único en el mundo. Andrés, gracias por tu apoyo en el CNIC y fuera de él. Sólo con saber que estás unos días por el centro ya me alegra el corazón. Nuestros caminos seguirán juntos. Juan y Jose: os sigo echando de menos.

A Claudia y Pepe, que han sido y son mi familia en Madrid. Ellos saben muy bien lo que supuso mudarme de Sevilla-Jerez a Madrid con unos maletones enormes y un doctorado por empezar. Me alegra haber crecido y ver crecer a vuestra familia a vuestro lado. Gracias por dejarme compartir todos esos momentos y por quererme tal y como soy.

A mis amigas de toda la vida, mis amigas de Jerez: Paula, Maru, Carmela e Inma. Gracias por toda una vida de amistad y buenos momentos a vuestro lado. Aunque muchos de ellos me los haya perdido, ellas siempre han estado ahí cuando yo he podido volver, y siguen esperándome con muchas ganas de pasarlo bien.

También tengo que agradecer a la Residencia de Estudiantes el haberme concedido una beca para estar allí durante este último año de doctorado. He conocido a personas de una calidad intelectual enorme y he tenido el privilegio de vivir entre sus paredes. Sin embargo, nadie imaginaba que una pandemia mundial iba a paralizar el mundo aquel 13 de marzo. No pudimos disfrutar del año que quisimos, pero yo me he llevado algo mucho mejor que todo aquello. Incluso me cuesta imaginar cómo hubiera podido escribir esta tesis sin tenerte delante escribiendo la tuya. Gracias Hedgar, por ver en mí a una Emilia Pardo Bazán, a una María Lejárraga o a una Concha Méndez. Gracias por creer en mí y por no dudar ni un segundo en estar a mi lado. Tú eres nuestro lugar y nuestro dónde. Me alegra saber que tendremos tiempo para todo lo que aún no hemos podido hacer juntos.

> I won the parent lottery. I was born with the winning ticket, a major reason I was able to live out my childhood dreams.
>
> *The last Lecture,* Randy Pausch

Siempre me he sentido así. Siento que he ganado la lotería de la familia. Mi familia es especial, y todos los que me conocéis bien lo sabéis. Lo que soy en esta vida os lo debo a vosotros. Si he conseguido algo ha sido por vuestro esfuerzo, vuestro sacrificio y vuestro amor. Habéis dado todo lo que estaba en vuestra mano para que yo hiciera de mí todo aquello que he querido y yo jamás tendré cómo agradecéroslo. Todas las veces que me derrumbé estabais ahí para sujetarme y volverme a levantar. Todas las veces que lo logré estabais junto a mí para alegraros y celebrarlo. Gracias por querer mi felicidad, aunque eso significara volar lejos y no estar a vuestro lado. Mi corazón está siempre pendiente de volver. Gracias mamá, por tu amor incondicional, por haberme esperado en las vías del tren de la estación de Jerez con la misma ilusión y ganas ya más de 100 veces durante estos 10 años. Por ser mi acompañante al otro lado del teléfono de vuelta a casa, por ser mi agenda personal y pensar más en mí que en ti. Por quererme demasiado como tú dices. Gracias papá, por ser mi entrenador personal y mi coach. Por enseñarme que la guerra no se gana en la primera batalla, y que hay que coger el toro por los cuernos. Eres un contador de historias nato y yo disfruto como nadie escuchándolas. Eres un mirlo blanco y todo el mundo debería tener un padre como tú. Gracias Blanca, por ser una hermana, una segunda madre y una amiga. Gracias Quique, por haberte unido a esta familia. Mi hermana es la persona con el corazón más grande que conozco, con una generosidad desbordante. Gracias por confiar en mí y dejarme ser de vez en cuando tu Pepito Grillo. Has sido siempre mi referente y me has hecho el camino mucho más fácil. Tampoco sabré nunca cómo agradecerte todo lo que has velado y lo que has cuidado de mí.

Gracias a todos por dejarme compartir estos maravillosos años con vosotros

> How lucky I am to have something that makes saying goodbye so hard.
>
> *The complete tales of Winnie-the-Pooh,* A.A. Milne

There is no science which does not spring from pre-existing knowledge, and no certain and definite idea which has not derived its origin from the senses.

On the Motion of the Heart and Blood in Animals, William Harvey

Finally, the story teaches us the importance of questioning dogmas when the evidence calls for it.

William C. Aird

ABSTRACT

Our vascular system is an organized and hierarchical blood vessel network lined by a monolayer of endothelial cells (ECs) that supplies oxygen and nutrients to all tissues and organs in our body. Importantly, they are not passive conduits for blood flow and they contribute to organ physiology and homeostasis throughout the entire life of the organisms. Therefore, it is not surprising that an imbalance of this vascular network is involved the pathogenesis of many diseases such as cancer, stroke or myocardial infarction.

The Notch signalling pathway is a critical regulator in the process of angiogenesis, participating in the tip-stalk specification, arterial-venous differentiation, vessel stabilization and maturation. Importantly, pharmacological compounds targeting distinct members of the Notch signalling pathway have been used in the clinics but their effect on the homeostasis of different types of blood vessels is unknown.

In this thesis, we have developed and used a wide range of novel genetic tools, loss-of-function mouse models, imaging, trancriptomic and proteomic approaches to uncover the role of several Notch signalling members in the regulation of organ-specific vascular homeostasis at high cellular and molecular resolution.

We found that Dll4/Notch signalling is active in most quiescent endothelium of several organs, such as the heart, lung, liver and brain. However, despite being active in all the mentioned vascular tissues, only in heart and liver vessels it plays an essential role in the maintenance of vascular quiescence by actively repressing EC proliferation. By using comparative transcriptomic and proteomic approaches, we found that Dll4/Notch1 actively supresses the Myc pathway to sustain vascular quiescence in the liver.

By analysing a series of Notch signalling mutants, we found that while loss of the ligand Dll4 leads to an intermediate increase in p-ERK levels and cell cycle entry, resulting in EC hyperproliferation; loss of the co-factor Rbpj or the receptor Notch1 induces even higher ERK signalling activity but not EC proliferation. At high p-ERK levels there is an increase in the expression of the cell cycle inhibitor p21, which arrests EC proliferation. These arrested cells have also several features of endothelial senescence.

In addition, we observed that the loss of Dll4/Notch signalling in liver ECs, promotes the transient increase in the proliferation of neighboring hepatocytes prior to their own expansion, suggesting the existence of angiocrine factors secreted by ECs after the loss of Notch signalling.

Moreover, the effect of Notch on liver endothelial cell proliferation was very heterogenous and zonated. ECs located close to the central veins had a higher proliferation potential compared to the endothelium located in oxygen-rich periportal zones. Using multispectral genetic mosaics, we also identified a rare population of liver ECs that is able to clonally expand more than most of their neighbours, suggesting the existence of liver-resident endothelial progenitor cells.

In addition to these studies on the role of Notch in vascular biology, we also used and validated an inducible dual reporter-Cre mouse allele (*iSuRe-Cre*), which by significantly increasing Cre activity in reporter-expressing cells, it provides certainty that these cells have completely recombined floxed alleles.

RESUMEN

Nuestro sistema vascular es una red de vasos sanguíneos organizada y jerárquica, cuyo interior está recubierto por células endoteliales (ECs), y que se encarga de proporcionar oxígeno y nutrientes a todos los tejidos y órganos de nuestro cuerpo. Sin embargo, no son meros conductos pasivos de flujo sanguíneo, sino que contribuyen a la fisiología y la homeostasis de todos los tejidos y órganos a lo largo de nuestra vida. Por lo tanto, no sorprende que un desequilibrio en estos vasos sanguíneos esté involucrado en la patogénesis de muchas enfermedades, tales como el cáncer, los accidentes cerebrovasculares o el infarto de miocardio.

La vía de señalización de Notch desempeña un papel fundamental en la regulación de la angiogénesis: participa en la especificación de las células *tip-stalk*, la especificación arterio-venosa y la estabilización y maduración de dichos vasos. Además, se están utilizando en la clínica compuestos farmacológicos dirigidos contra diferentes componentes de la vía de señalización de Notch. Sin embargo, aún se desconoce su efecto en la homeostasis de los diferentes tipos de vasos sanguíneos.

En esta tesis, hemos desarrollado y usado una amplia gama de novedosas herramientas genéticas, modelos murinos de pérdida de función, así como técnicas de transcriptómica y proteómica para analizar el papel de los distintos elementos de la vía de señalización de Notch en la regulación de la homeostasis vascular específica de órgano con alta resolución celular y temporal.

Hemos observado que la vía de señalización de Notch, a través del eje Dll4/Notch1, está activa en el endotelio quiescente adulto de distintos órganos analizados, tales como el corazón, el pulmón, el hígado y el cerebro. Sin embargo, a pesar de encontrarse la vía activa en los tejidos mencionados, sólo en el corazón y el hígado juega un papel esencial en el mantenimiento de la vasculatura, reprimiendo de manera activa la proliferación de dichas ECs. Usando enfoques transcriptómicos y proteómicos, hemos descubierto que Dll4/Notch1 suprime activamente la vía de Myc para mantener la quiescencia de manera específica en el hígado.

Analizando diferentes mutantes de la vía de señalización de Notch, hemos observado que, mientras que la pérdida del ligando Dll4 da a lugar a niveles intermedios de p-ERK y una reentrada en ciclo celular que resulta en una hiperproliferación endotelial, la pérdida del co-factor Rbpj o del receptor Notch1 da lugar a niveles más altos de la señalización ERK, pero no a la proliferación de las ECs. Altos niveles de ERK resultan en un incremento de la expresión del inhibidor de ciclo celular p21, que detiene la proliferación de las ECs. Estas células detenidas presentan características de senescencia endotelial.

Además, hemos observado que la pérdida de la señalización de Dll4/Notch en las ECs del hígado da lugar a un incremento transitorio de la proliferación de los hepatocitos circundantes antes de promover la propia expansión del compartimento endotelial, sugiriendo así la existencia de factores angiocrinos secretados por las ECs después de la pérdida de la señalización de Notch.

El efecto de Notch en la proliferación endotelial del hígado es muy heterogéneo y zonificado. Las ECs que se encuentran cerca de la vena central tienen un potencial mayor de proliferación comparadas con el endotelio localizado en el área portal rica en oxígeno. Usando mosaicos genéticos multiespectrales, hemos identificado en el hígado una población de ECs

poco frecuente, que es capaz de expandirse de manera clonal más que el resto de células ECs, lo cual implicaría la presencia de células progenitoras endoteliales en el hígado.

Además de estos estudios sobre el papel de Notch en la biología vascular, hemos usado y validado un alelo de ratón inducible de doble reportero-Cre (*iSuRe-Cre*), el cual, mediante una elevada actividad de la Cre en las células que expresan el reportero, es capaz de proporcionar certeza sobre la recombinación completa de los alelos floxeados.

Index

ACKNOWLEDGMENTS **7**

ABSTRACT **17**

RESUMEN **19**

ABBREVIATIONS AND ACRONYMS **25**

HISTORICAL BACKGROUND **31**

INTRODUCTION **35**

Notch at the center of vascular development 37
Role of Notch in arterial-venous specification 41
Regulation of sprouting angiogenesis by Notch signalling 43
Role of Notch in vascular maturation and quiescence 47
Notch maintains the quiescence of some organ vascular beds 50
Angiocrine functions of endothelial Notch signalling 52
Role of Notch on organ-specific endothelial cell heterogeneity 53
Zonal and single-cell Notch vascular heterogeneity 56

OBJECTIVES **59**

MATERIALS AND METHODS **63**

Mice 65
Genotyping 65
Recombinant DNA and ES cell culture 66
Immunofluorescence on cryosections 67
Vibratome immunofluorescence and 3D imaging 68
Immunofluorescence on paraffin sections 69
Immunofluorescence on mouse retinas 69
Image acquisition and analysis 71
Western blot analysis 72
Endothelial cell isolation and RNA/DNA extraction 72
qRT-PCR and competitive PCR 74
Next Generation Sequencing – RNA-seq 74
RNA-seq data analysis 75
Liver endothelial cell proteomics 76
Preparation of protein extracts and on-filter tryptic digestion 76
Multiplexed stable isotope labeling of tryptic peptides 77
Peptide fractionation 77
Liquid chromatography coupled to tandem mass spectrometry 77
Protein identification based on database searching 78
Statistical analysis of proteomics data 78
Statistical analysis 79

Data availability 79
RESULTS 81
Chapter I: The role of Notch signalling members in the regulation of organ-specific vascular homeostasis 83
Notch signalling is active in quiescent endothelial cells of several organs 85
Dll4 deletion leads to cell cycle entry and hyperproliferation of liver and heart ECs 90
Transcriptomic analysis after the loss of Dll4/Notch signalling in quiescent ECs of several organs 95
Differentially expressed proteins after the loss of Dll4/Notch signalling in liver ECs 97
Possible genetic compensation mechanisms in lung and brain ECs after loss of Dll4/Notch signalling 99
Myc is essential for the proliferation of liver ECs after the loss of Dll4/Notch signalling 102
Deletion of *Rbpj* and *Notch1* in quiescent blood vessels does not phenocopy Dll4 deletion 104
Transcriptional differences after the loss of *Notch1* and *Rbpj* 109
Loss of Notch signalling increases nuclei size and the number of binucleated cells 111
High-ERK activation after the loss of *Notch1* and *Rbpj* 114
Notch signalling prevents EC senescence 122
p21 induces EC senescence and prevents apoptosis after the loss of *Rbpj* 126
Temporal course of *Dll4*^{iDEC} liver phenotype 129
Heterogeneous and zonal response of liver vessels to *Dll4* deletion 132
The expression of Notch signalling members is spatially zonated in the liver endothelium 134
Multispectral clonal analysis reveals that only a very small fraction of liver ECs have the potential to proliferate and expand over time 138
Chapter II: *iSuRe-Cre*: a genetic tool to reliably induce and report Cre-dependent genetic modifications 141
Design and testing of *iSuRe-Cre* constructs 143
iSuRe-Cre reliably reports cells with full gene deletion 146
iSuRe-Cre enables deletion of multiple genes and epistasis analysis 150
DISCUSSION 153
Although Dll4/Notch1 signalling is active in different organ-specific ECs, only in some vascular beds its activity is essential to maintain EC quiescence 155
Myc is a Notch downstream target in liver quiescent ECs that controls proliferation 157
Why do not some organ proliferate after *Dll4* deletion? 158
Deletion of different Notch pathway components does matter: let's forget about an equal Notch loss-of-function response 160
Notch signalling regulates p-ERK signalling to balance EC quiescence, proliferation and cell cycle-arrest 161
High mitogenic stimuli after *Rbpj* and *Notch1* deletion in liver quiescent ECs leads to cell cycle exit by p21 expression 163
Liver EC senescence is prevented by Notch signalling pathway 163
Temporal proliferation analysis of *Dll4*^{iDEC} liver ECs 166
Liver EC zonation: Notch signalling and EC proliferation in *Dll4*^{iDEC} livers 167
There is a specific liver EC population with the potential to proliferate and expand over time 169
On the importance of reliable gene deletion experiments 170
Concluding remarks and outlook 171
CONCLUSIONS / CONCLUSIONES 173

BIBLIOGRAPHY **179**

PUBLICATIONS **199**

ABBREVIATIONS AND ACRONYMS

53BP1	p53-binding protein 1
Acvrl1	Activin A receptor like type 1
Adm	Adrenomedullin
ANG1	Angiopoietin 1
ANOVA	Analysis of variance
Apln	Apelin
BBB	Blood brain barrier
bHLH	Basic helix-loop-helix
BM	Basement membrane
BSA	Bovine serum albumin
Bub1	Budding uninhibited by benzimidazoles 1
CD31	Cluster of differentiation 31
CD34	Cluster of differentiation 34
CD36	Cluster of differentiation 36
CD45	Cluster of differentiation 45
Cdc42	Cell division cycle 42
Cdh5	Cadherin 5
CDK	Cyclin-dependent kinase
CDKI	Cyclin-dependent kinase inhibitor
Cdkn1a	Cyclin dependent kinase inhibitor 1A
Cdkn1b	Cyclin dependent kinase inhibitor 1B
Cdkn1b	Cyclin dependent kinase inhibitor 1B
Cdkn1c	Cyclin dependent kinase inhibitor 1C
Cdkn2a	Cyclin dependent kinase inhibitor 2A
cDNA	Complementary DNA
COUP-TFII	COUP transcription factor 2
CPM	Counts per million
CreERT2	Tamoxifen-inducible Cre-ERT2 fusion protein
CV	Central vein
CX40	Connexin 40

Cxcl1	C-X-C motif chemokine ligand 1
CXCR4	C-X-C motif chemokine receptor 4
DAPI	4′,6-Diamidino-2-phenylindole dihydrochloride
DEG	Differentially expressed gene
Dll1	Delta-like 1
Dll3	Delta-like 3
Dll4	Delta-like 4
DMEM	Dulbecco's modified eagle medium
DNA	Deoxyribonucleic acid
DNAseI	Deoxyribonuclease I
DTT	Dithiothreitol
E	Embryonic day
EC	Endothelial cell
EDTA	Ethylenediaminetetraacetic acid
Efnb2	Ephrin B2
EGF	Epidermal growth factor
EPC	EC progenitor cells
Ephb4	EPH Receptor B4
ERG	ETS-related gene
ERK	Extracellular signal-regulated kinase
ES	Embryonic stem
Esm1	Endothelial cell specific molecule 1
Fab	Antigen-binding fragment
Fabp	Fatty acid binding protein
FACS	Fluorescence-activated cell sorting
FBS	Fetal bovine serum
FGF	Fibroblast growth factor
Fgfr3	Fibroblast growth factor receptor 3
G2M	Gap 2 phase mitosis
GFP	Green fluorescence protein
GO	Gene ontology
GSEA	Gene set enrichment analysis
H&E	Hematoxylin and eosin

HB-EGF	Heparin-binding *EGF*-like growth factor
HGF	Hepatocyte growth factor
HPLC	High performance liquid chromatography
HRP	Horseradish peroxidase
HS4	Hypersensitive site-4
HSC	Hematopoietic stem cell
iChr2-Mosaic	2^{o}generation of the chromatin-localized FPs mosaic
ifgMosaic	Inducible fluorescent and genetic mosaic
Igfbp7	Insulin like growth factor binding protein 7
Igfbp6	Insulin like growth factor binding protein 6
Il33	Interleukin 33
iMb2-Mosaic	2^{o}generation of the membrane-localized FPs mosaic
Jag1	Jagged 1
Jag2	Jagged 2
Kdr	Kinase insert domain receptor
KO	Knock-out
LC-MS/MS	Liquid chromatography coupled to tandem mass spectrometry
Lfng	Lunatic fringe
Lgr6	Leucine rich repeat containing G protein-coupled receptor 6
LIF	Leukemia inhibitory factor
LoxP	Locus of X-over P1
LSL-EYFP	Lox-stop-Lox -enhanced yellow fluorescent protein
MAML	Mastermind-like
MAPK	Mitogen-activated protein kinase
MbTomato	Membrane tomato
Mcm	Mini chromosome maintenance complexes
MEF	Mouse embryonic fibroblasts
MEOX2	Mesenchyme homeobox 2
Mfng	Manic fringe
Mif	Inflammatory mediator macrophage migration inhibitory factor
MMTS	S-methyl methanethiosulfonate
mRNA	Messenger RNA
N1ICD	Notch1 intracellular domain

NEAA	Non-essential amino acids
NGS	Next generation sequencing
NICD	Notch intracellular domain
N-PhiM	Noncytotoxic modified PhiYFP
NRG1	Neuregulin 1
NSC	Neural stem cells
Nts	Neurotensin
OCT	Optimal cutting temperature
P1	Postnatal day 1
P3	Postnatal day 3
PAC	P1-derived artificial chromosomes
PBS	Phosphate-buffered saline
PC12	Rat phaeochromocytoma cells
PCR	Polymerase chain reaction
Pdgfβ	Platelet derived growth factor subunit B
PDGFR-β	Platelet-derived growth factor receptor beta
Pen/Strep	Penicillin-streptomycin
p-ERK	Phosphorylated extracellular signal-regulated kinase
PFA	Paraformaldehyde
PhiYFP	Yellow fluorescent protein
Plaur	Plasminogen activator urokinase receptor
Prom1	Prominin 1
psrc1	Proline and serine rich coiled-coil 1
PV	Portal vein
qRT-PCR	Real-Time quantitative reverse transcription PCR
RAC1	Rac family small GTPase 1
RBPJk	Recombination signal binding protein for immunoglobulin kappa J region
Rfng	Radical fringe
RNA	Ribonucleic acid
RNase	Ribonuclease
RNA-seq	RNA sequencing
Rpl	Ribosomal proteins
RT	Room temperature

Runx1	Runt-related transcription factor 1
SASP	Senescence-associated secretory phenotype
SBT	Systems biology triangle
scRNA-seq	Single-cell RNA sequencing
SD	Standard deviation
SDS–PAGE	Sodium dodecyl sulfate polyacrylamide gel electrophoresis
Ska1	Spindle and kinetochore associated complex subunit 1
SMC	Smooth muscle cells
TFC15	Secretion cluster MPF-G protein
Tg	Transgene
TGF-β	Transforming growth factor beta
Tgfbr2	Transforming growth factor beta receptor 2
TMM	Trimmed mean of m-values
TSA	Tyramide signal amplification
Ubc	Ubiquitous
Unc5b	Unc-5 netrin receptor B
USS	Urea sample solution
V1744	Valine 1744
VEGF	Vascular endothelial growth factor
VEGFR2	Vascular endothelial growth factor receptor 2
VSMC	Vascular smooth muscle cells
Wnt2	Wingless family member 2
Wnt9b	Wingless family member 9b
WPRE	Woodchuck hepatitis virus posttranscriptional regulatory element
WSPP	Weighted scan-peptide-protein
YFP	Yellow fluorescence protein

HISTORICAL BACKGROUND

"The tree of the veins".

"The plant never arises from the branchings, for the plant first exists before the branches, and the heart exists before the veins. The heart is the seed which engenders the tree of veins"(Da Vinci, 1983). That is how Leonardo da Vinci described the cardiovascular system on his drawings in the 16th century: hierarchical patterned trees of vessels with specific paths and positions, ramified through the whole body. As would happen in a tree, in our body we can also find main stems that continue their path subdividing themselves into smaller branches. In a tree, these branches will grow to give to the leaves the most light possible. In our body, the vascular branches, otherwise called blood vessels, will grow to give to every tissue or organ the required nutrients and oxygen levels.

"You will find almost universally that the course of the veins, and the course of the nerves, occupy a common path, are directed to the same muscles, and ramify in the same manner in each of these muscles, and that each vein and nerve pass with the artery between one or other muscle and ramify in them with equal branchings"(Da Vinci, 1983).

So we could then imagine that our body is filled with an organized vascular net with a hierarchical order, as every tree in the forest does with their branches. But where are our "leaves"? Where is the end of our blood vessels? This is one of the fundamental differences comparing our vascular system with other branched structures. It is not a blind-ending but a complexly connected circuit. However, this question was not properly addressed until the 16th century, when William Harvey showed that arteries and veins are functionally connected and allow blood circulation in the body (Aird, 2011). This discovery would become a key milestone in biomedical research and would tear down a quite solid paradigm of the vascular system that stood and convinced researchers for more than 15 centuries: blood vessels were in charge of food and humors distribution that were subsequently consumed and exhausted in every tissue.

However, Harvey inherited the research and discoveries performed in those centuries to build up his own conclusions. He was inspired by the brilliance of Ancient Greeks such as Aristotle, Praxagoras or Erasistratus that believed that the heart was the center of physiology, the core of the soul and the origin of blood vessels. They were even the first to describe blood vessel heterogeneity: Praxagoras was the first to differentiate between arteries and veins. Arteries, originated from the heart, would carry pneuma; and veins, originated from the liver,

would carry blood. While veins were thought to be full of blood, Erasistratus defended that arteries contained only air. Four hundred years later, Galen would embrace some of these ancient doctrines to do his owns observations. Galen's view was focused on nutrition. Specifically, nutrients became blood in the liver, and it was charged with natural spirit to be then transferred by veins to the peripheral tissues. On the other hand, there were also vital spirits, derived from the atmospheric air, which was carried by arteries and would give heat, life and motion to every tissue. We have therefore two open-ended vascular conduits. Unlike Erasistratus, Galen proved that arteries were also filled with blood as veins. Galen defended that this blood goes from the right ventricle (vein blood) to the left ventricle through invisible pores in the interventricular septum. This system would allow distributing natural and vital spirits to every organ and tissue depending on his immediate requirements and being therefore consumed each time.

After Galen, dark and long ages halted any significant scientific improvement in the cardiovascular field. Thus, for more than 1500 years, Galen's physiology system prevailed with modest modifications. As mentioned before, the turning point in the history of medicine was the discovery of blood circulation by the English physician William Harvey. Apart from concluding that arteries and veins contained the same blood, he found that the quantity of blood ejected from the heart was too high to be captured by an open system where blood was constantly consumed in every tissue. Consequently, this blood must be circulating throughout the body and returning to the heart to be pumped in a closed circulatory system (Azizi et al., 2008). Apart from challenging ancient and established ideas, his discoveries would later prompt other researchers to look at other scientific questions in the same manner. Importantly, Harvey's legacy went far beyond the creation of new medical dogmas. His discoveries helped to change the perceptions and plans people made for the urban environment in the 18th century. Blood circulation and blood vessel hierarchy gave new ideas not only for public health but also for planning the city. People would be the circulating blood, which could move and breathe freely along the vascular system, which in this case would be the city. Paris, Washington or Karlsruhe are good examples of circulatory cities designed for moving bodies that were inspired by Havery's inheritance (Sennett, 1994).

What did William Harvey have or do to create such breakthrough paradigm? To understand William Harvey's revolution, we might have to bear in mind that he built on the work of all previous models but importantly he did not have fear in questioning existing and solid dogmas that prevailed for more than 2000 years. "There is no science which does not spring from pre-existing knowledge." Harvey pointed out. As he could take advantage of all

previous observations to create new knowledge, so did I in the work that I present in this doctoral thesis.

INTRODUCTION

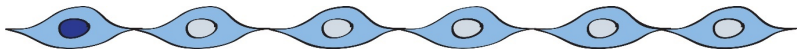

Notch at the center of vascular development

Our body contains an extensive tubular network of blood vessels lined by a monolayer of endothelial cells (ECs) that arose during evolution in order to carry oxygen and nutrients to distant tissues and organs in the body (Carmeliet, 2005). These tubular structures, together with the heart, are the first organs to form and function during mammalian development, which highlights its fundamental role in embryogenesis (Chung and Ferrara, 2011). The first vascular structures are assembled by coalescence of endothelial progenitor cells and *in situ* differentiation, a process known as vasculogenesis, which gives rise to the dorsal aorta, cardinal vein and the primitive vascular plexus (Risau and Flamme, 1995). Later, during the angiogenesis process, the primary vessel network is expanded through a balanced combination of sprouting, proliferation, migration and remodelling. This coordinated formation of new blood vessels from pre-existing ones will form the future adult organism vessel network (Carmeliet and Jain, 2011). After organ development, vessels acquire a quiescent or non-angiogenic state, but retain the potential to be reactivated under certain physiological or pathological stimuli (Figure 1).

The adult vascular system is a very organized and hierarchical vessel network composed of arteries, capillaries and veins. A perfectly branched and closed circuit that contributes to organ physiology and homeostasis throughout the entire life of the organism. Blood vessels also play a very important role in the pathogenesis of many diseases such as cancer, stroke or myocardial infarction (Carmeliet and Jain, 2011). Research in the last decades revealed the existence of complex and coordinated molecular and cellular programs involved in the regulation of angiogenesis and vascular homeostasis.

The angiogenic process is strongly controlled by hypoxia-dependent, tissue-derived pro-angiogenic signals. Vascular endothelial growth factor (VEGF), a ligand which binds to its cognate receptors (VEGFR) in the endothelium, is among the most important factor (Ferrara et al., 2003) . Mice embryos lacking a single *Vegfa* allele die at embryonic day (E) 9.5 due to defects in endothelial cell differentiation and proliferation (Carmeliet et al., 1996; Ferrara et al., 1996). *Vegfr2* null mice cannot undergo vasculogenesis and die between E8.5 and E9.5 (Shalaby et al., 1995). It has been well documented that VEGFR2 signalling through VEGF is the major activator of angiogenesis and induces cell proliferation, survival, sprouting, migration and permeability of ECs (Lohela et al., 2009). Other factors regulate angiogenesis controlling the interaction between the endothelium and the neighboring perivascular cells. This is the case of the Pdgfβ/Pdgfrβ, Angiopoetin1 ligand (ANG1) and its tyrosine kinase receptor TIE2

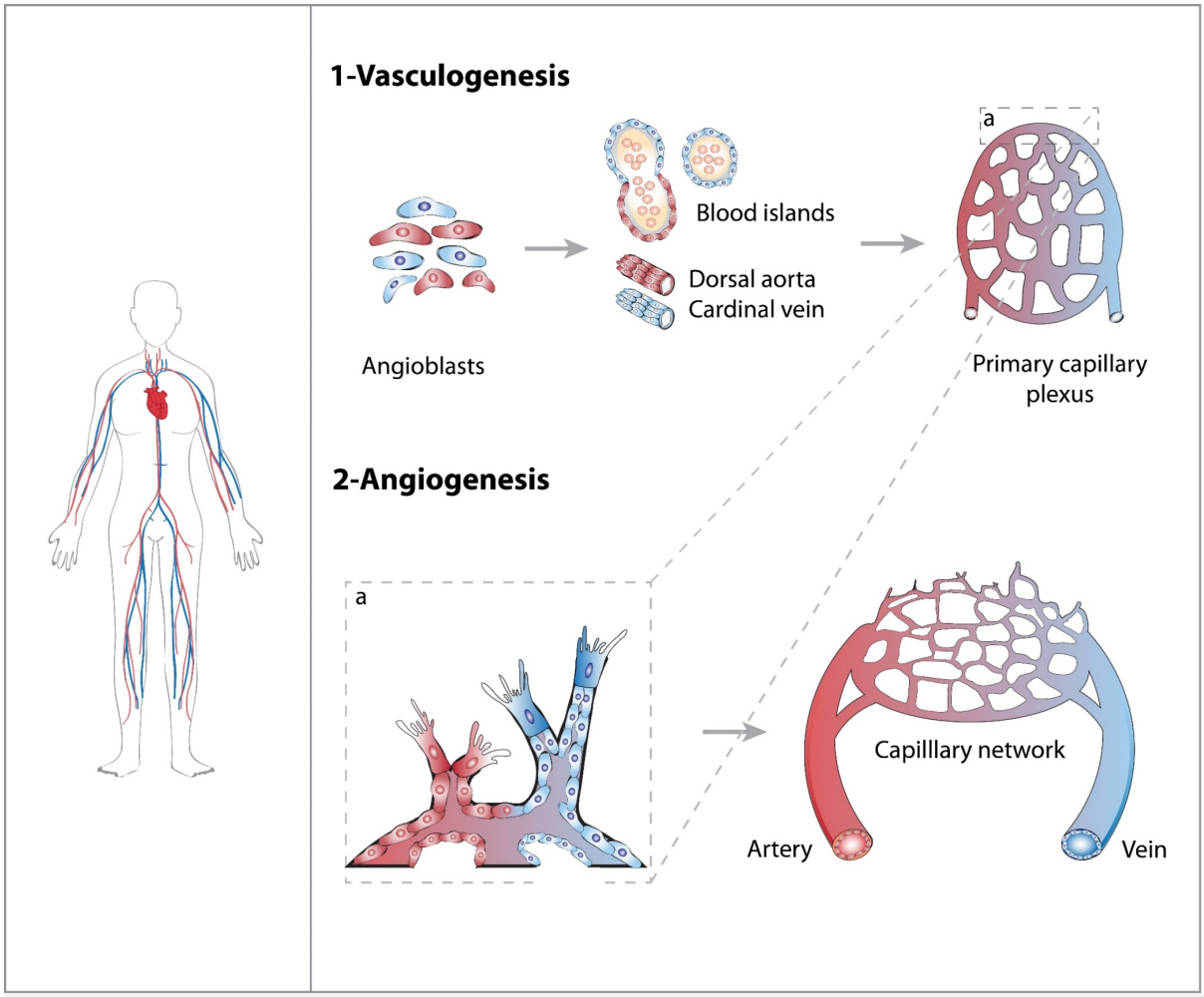

Figure 1: Vascular development. The adult vascular system is mainly formed by vasculogenesis and angiogenesis. **1-** During vasculogenesis, the mesodermal-derived endothelial progenitors - the so-called angioblasts-, assemble to form the dorsal aorta, the cardinal vein and blood islands. These last structures fuse to create a primary capillary plexus. **2-** The expansion of this primitive network and the formation of blood vessels from these pre-existing structures –which is termed as angiogenesis- is achieved by sprouting, proliferation, migration and subsequent remodeling (a). The differentiation and maturation of the forming vascular structures will create a hierarchical blood vessel network composed by arteries, veins and capillaries.

(Armulik et al., 2005; Augustin et al., 2009). Genetic experiments have shown that *Pdfgβ* or *Pdgfrβ* null mutant mice die around birth with severe vascular haemorrhages (Leveen et al., 1994; Soriano, 1994). Mice lacking either *Tie2* or *Ang1* show similar vascular malformations and die at E10.5 and E12.5 respectively (Sato et al., 1995; Suri et al., 1996). The transmembrane ligand Ephrin-B2 expressed on arterial cells and its cognate receptor Ephb-B4 are essential in the early steps of angiogenesis and mutants mice show defective vascular remodelling and arterial-venous development (Herbert et al., 2009; Wang et al., 1998). Besides being regulated by external signals like VEGF, endothelial cells also possess intrinsic signalling pathways that modulate their behaviour. One example is the Notch signalling pathway, which requires cell-to-cell interaction between transmembrane receptors and ligands

and was highly conserved throughout evolution. Notch signalling has been implicated in the regulation of a wide variety of biological processes such as cell fate decision, differentiation, proliferation, apoptosis and homeostasis, not only during development but also in the maintenance of self-renewing tissues (Bray, 2006; Hofmann and Iruela-Arispe, 2007).

In mammals, there are four distinct Notch receptors (Notch1, Notch2, Notch3 and Notch4) that can interact with five different ligands: three of the Delta like family (Dll1, Dll3, Dll4) and two of the Jagged family (Jag1 and Jag2). Both ligands and receptors are transmembrane proteins with large extracellular domains formed by epidermal growth factor (EGF)-like repeats, through which they interact with each other. The activation of the pathway is triggered when a Notch receptor contacts with a transmembrane ligand in the neighbouring cell (Andersson et al., 2011; Kopan and Ilagan, 2009). This binding promotes two proteolytic cleavage events in the Notch receptor. The first cleavage is performed by ADAM-family metalloproteases. The second cleavage, which is mediated by a γ-secretase, releases the Notch intracellular domain (Notch ICD or NICD) of the receptor. Then, the cleaved NICD translocates to the nucleus, where it binds RBPJk and recruits co-activators as Mastermind-like (MAML). This transcriptional complex binds to promoters of canonical Notch target genes to allow their transcriptional activation, including the family of basic helix-loop-helix (bHLH) transcriptional repressors *Hes/Hey* (Hori et al., 2013*)*(Figure 2). The Notch transcriptional program and effects varies greatly between different cell types and cellular contexts, since the effects of this transcriptional machinery are signalling dose-dependent and it interacts with the diverse repertoire of existing transcription factors and chromatin states (Bray, 2006).

In the vasculature, the receptors Notch1 and Notch4, and the ligands Dll1, Dll4 and Jag1 are predominately expressed (Hofmann and Iruela-Arispe, 2007). Targeted disruption of different Notch components leads to embryonic lethality due to vascular development defects, caused by a significant deregulation of endothelial biology. Dll4 has been shown to be the most important Notch ligand for vascular development. Mouse embryos lacking a single *Dll4* allele (Duarte et al., 2004; Krebs et al., 2004) or having endothelial deletion of *Notch1* (Limbourg et al., 2005) die during development with pronounced vascular defects. Full loss-of-function mutants for *Jag1* (Xue et al., 1999) and *Dll1* (Hrabe de Angelis et al., 1997) show milder vascular development defects but die approximately at E10.5 and E12 respectively. *Notch4* mutants are viable with no apparent abnormalities, but double *Notch1, Notch4* loss-of-function mutants show more pronounced vascular development defects than the single *Notch1* mutants, suggesting that Notch4 partially compensates for the loss of Notch1, the most important Notch receptor in endothelial cells (Krebs et al., 2000). The receptors Notch2 and

Notch3 are weakly expressed by ECs and so far, a function for these receptors was not reported in endothelial cells.

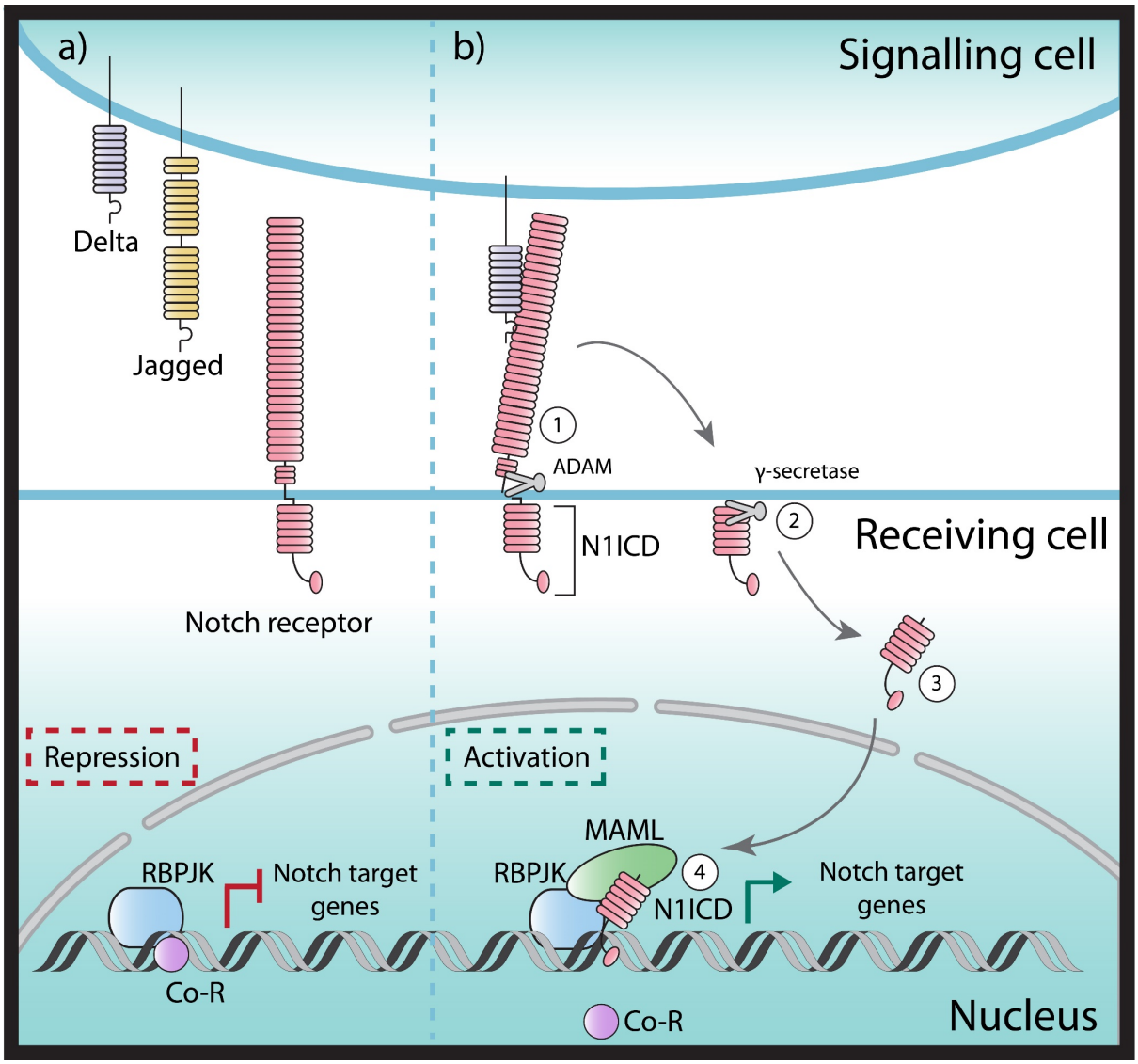

Figure 2 Notch signalling pathway. Notch signalling requires ligand/receptor interaction (typically between a signaling-sending and a receiving cell). Therefore, if the ligand does not bind to the receptor **(a)**, there is not Notch downstream target gene transcription. Once the transmembrane ligand (Jagged or Delta) interacts with the transmembrane Notch receptor in the neighboring cell **(b)**, conformational changes in the Notch extracellular domain allow the cleavage of ADAM metalloproteinases and γ-secretases (1-2), which eventually release the Notch intracellular domain (NICD) (3). Then, the NICD translocates to the nucleus and binds to RBPJk and recruits co-activators such as Mastermind (MAML) to form a transcriptional activation complex (4). This activation complex activates the transcription of downstream Notch targets genes.

It has been shown that Notch signalling components are preferentially expressed by ECs undergoing arterial differentiation, and that the lack of some of the Notch ligands/receptors lead to absence of arterial differentiation during embryonic development

(Duarte et al., 2004; Krebs et al., 2004; Krebs et al., 2000; Lawson et al., 2001; Limbourg et al., 2005). These genetic studies have shown the importance of the Notch signalling pathway for the proper regulation of vascular development and arterial-venous specification.

Role of Notch in arterial-venous specification

After vasculogenesis, the first and primitive capillary plexus is remodelled into a hierarchical network of vessels containing arteries and veins. Arteries are specialized in delivering oxygenated blood to capillaries, that passively distribute it to surrounding organ cells, and veins collect the low oxygen blood, return it to the heart and close the circuit. For a long time, blood flow dynamics was considered to be the only factor driving arterial-venous specification (Adams, 2003). Arteries experience high pulsatile shear stress, high blood flow and contain several circumferential and thick layers of smooth muscle cells (SMCs) together with extracellular matrix. On the other hand, veins experience low shear stress, are covered by significantly less SMCs and also have valves to ensure unidirectionality of blood flow (Adams and Alitalo, 2007).

However, several studies showed that the first steps of arterial-venous differentiation occur before significant differences in blood flow are experienced by ECs. Numerous genes and signalling pathways have been involved in this pre-specification step (Adams, 2003). VEGF has been shown to be required for the development of arteries through the activation of Notch signalling (Lawson et al., 2002; Seo and Kume, 2006). Importantly, Notch ligands and receptors are highly expressed in arteries and almost absent in veins (Leslie et al., 2007; Shutter et al., 2000; Siekmann and Lawson, 2007). Genetic deletion of *Dll4* or *Notch1* leads to loss of arterial markers and widespread expression of venous related genes (Duarte et al., 2004; Gridley, 2010; Krebs et al., 2004; Swift and Weinstein, 2009). Conversely, ectopic activation of Notch signalling represses the expression of venous markers (Carlson et al., 2005; Murphy et al., 2012). The Eph-Ephrin family members expression is regulated by Notch signalling (Lawson et al., 2002) and lack of the arterial-specific Ephrin-B2 ligand also results in lack of arterial development, similar to those observed in Notch mutants (Wang et al., 1998). The relevance of the Notch signalling pathway in arterial development has also been demonstrated by genetic deletion of Notch signalling components in developing coronary vessels. The complete loss of Dll4-Notch signalling also leads to the loss of arterial identity in

coronary ECs and therefore, absence of arteries (D'Amato et al., 2016; Travisano et al., 2019). Moreover, it has been shown that Dll1 is essential to maintain the arterial identity of ECs during mouse fetal development (Sorensen et al., 2009). Altogether, these results highlight the very important role of Notch signalling in controlling arterial blood vessel identity.

Previous models suggested that venous identity was the default program, but it was later shown that it is actively regulated by COUP-TFII, a member of the orphan nuclear receptor super family. COUP-TFII is a vein-specific nuclear receptor that represses Notch signalling and therefore acts upstream in the arterial-venous specification related pathways (Swift and Weinstein, 2009). Absence of this transcription factor leads to the acquisition of arterial identity in venous areas (You et al., 2005).

However, hemodynamic and biomechanical forces such as blood pressure and the type of blood flow also have a pivotal role shaping the cardiovascular system by affecting gene expression. As a result, although arterial-venous differentiation is defined by specific genetic programs, endothelial cells retain a certain degree of plasticity to respond to external signals (Jones et al., 2006). Indeed, Notch is a mechanosensitive pathway (Gordon et al., 2015) and arterial shear stress is able to enhance Notch signalling to suppress endothelial proliferation and trigger the expression of an arterial specific program (Fang et al., 2017).

Recent publications have questioned previously established models, providing deep insight into the process of arterial-venous specification. Studies using mouse retina, zebrafish live imaging and fin regeneration models have suggested that vein-derived ECs and tip cells with high CXCR4/Notch signalling migrate against the flow to be incorporated into the nascent arteries (Hasan et al., 2017; Pitulescu et al., 2017; Xu et al., 2014). The concept of arterial development accomplished by migratory pre-venous cells is supported by the phenotype resulting from deletion of *Cdc42*. Absence of this small GTPase inhibits EC migration and leads to EC accumulation in venous areas (Lavina et al., 2018). In addition, recent single-cell RNA sequencing (scRNA-seq) studies with coronary ECs showed that there are not two independent fates but a continuum of EC identities along the arterial-venous axis. Venous cells go through a gradual switch from a venous programme to a pre-arterial one. Interestingly, ECs with high CXCR4, CX40 and Notch signalling but with low proliferative profile are committed to form coronary arteries. On the contrary, the vein determining transcription factor COUP-TFII suppresses pre-arterial transition by activating cell cycle genes (Su et al., 2018). This idea is supported by early postnatal brain ECs scRNA-seq studies, which have also shown that mitotic ECs express typical venous markers (Sabbagh et al., 2018). In line with these results, new studies have shown that it is not the Notch-dependent arterial differentiation

program but instead the ability of Notch to suppress endothelial metabolism and cell cycle what drives arterial specification (Luo et al., 2020). These studies indicate that arterial-venous pre-specification is tightly linked to the modulation of endothelial cell-cycle, metabolism and migration and it occurs before significant differences in blood flow exist. Blood flow and shear stress may later help to reinforce these pre-genetic programs by providing distinct biophysical factors that further enhance the arteriovenous differences. A better understanding of these molecular and cellular mechanisms is not only important from a basic knowledge point of view, but also because it may allow the improvement and development of therapeutic strategies against artery specific diseases such as atherosclerosis or heart ischemia.

Regulation of sprouting angiogenesis by Notch signalling

The growth of the vascular network is an extremely dynamic process and requires multiple and coordinated steps that include EC proliferation, sprouting and migration. When the surrounding tissue does not have enough oxygen, it secretes pro-angiogenic factors such as VEGF that, by binding to its receptors, activate a fraction of ECs and confer these a motile and invasive phenotype (Lohela et al., 2009). These so-called tip cells acquire long filopodia and lead the sprouting process. Following these invasive and migratory cells, are the stalk cells, the building blocks for the budding sprout. These cells establish a lumen for blood flow and proliferate to sustain the sprout elongation (Eilken and Adams, 2010; Potente and Carmeliet, 2017). Most of the research done uncovering tip/stalk biology has been performed in the postnatal mouse retina as a model for angiogenesis, which is a relatively easy system to genetically manipulate and visualize angiogenic vessels (Pitulescu et al., 2010). The biology of tip and stalk cells is strongly regulated by the VEGF/Notch pathway (Benedito and Hellstrom, 2013). VEGF is one of the most potent pro-angiogenic factors and its absence results in vascular defects not only during development but also in tumour vasculature, impairing tumour growth (Kim et al., 1993). VEGF gradients and concentration finely regulates tip cell migration and stalk cell proliferation respectively (Gerhardt et al., 2003). Mechanistically, VEGF-induced VEGFR2 signalling triggers several phosphorylation cascades, including the downstream MAPK/ERK signalling activation (Shin et al., 2016). In addition, VEGFR2 signalling leads to the transcription of tip cell-enriched genes such as Dll4. Tip cells that express more Dll4, activate in turn Notch signalling in the adjacent cells.

Consequently, this activation maintains the stalk fate in those adjacent cells by suppressing tip cell behaviour (Hellstrom et al., 2007; Lobov et al., 2007; Noguera-Troise et al., 2006; Ridgway et al., 2006). Deletion of just one *Dll4* allele is sufficient to induce excessive sprouting and vessel branching because of increased tip cell formation. This is accompanied by an increase in tip cell markers expression such as *Pdgfβ*, *Unc5b* (Suchting et al., 2007), *Esm1* or *Apln* (del Toro et al., 2010) in the rest of the vasculature. Notch loss-of-function by deleting *Dll4, Notch1* or *Rbpj* leads to pronounced vascular developmental defects that were related with a general increase in EC activity and angiogenesis since EC proliferation and tip cell formation is increased (Benedito et al., 2009; Duarte et al., 2004; Hellstrom et al., 2007; Krebs et al., 2004; Krebs et al., 2000; Limbourg et al., 2005; Lobov et al., 2007; Suchting et al., 2007). Conversely, Notch gain-of-function studies showed that it decreases vascular density and reduced tip cell number and EC sprouting (Hellstrom et al., 2007). Manipulation of Notch signalling in a mosaic manner confirmed the role of Notch signalling in tip cell specification (Hellstrom et al., 2007; Siekmann and Lawson, 2007). Live-imaging and fate-mapping studies in zebrafish and mouse models have shown that tip-cell specification is very dynamic and perhaps oscillatory, since ECs can switch position very fast during angiogenesis. This dynamic process is regulated by VEGF and Notch signalling levels, which drive a continuous shuffling of tip and stalk cells competing for the lead position (Arima et al., 2011; Jakobsson et al., 2010). Since in other developmental systems Notch has been shown to be activated in a oscillatory manner (Kageyama et al., 2010) it may be also involved in the regulation of the observed oscillatory tip-stalk cell fates and dynamics. In addition, BMPs/SMAD1/5 (Aspalter et al., 2015; Mouillesseaux et al., 2016; Moya et al., 2012) and VE-cadherin junctions remodelling (Bentley et al., 2014) have also been shown to be involved in tip-stalk interconversion. Furthermore, tip cells have been shown to polarize against the flow and be the source of arterial development, in the mouse retina and zebrafish (Franco et al., 2015; Hasan et al., 2017)(Figure 3).

The potent effect of Dll4/Notch as a suppressor of sprouting angiogenesis was also shown in pathological conditions. Notch inhibition resulted in decreased of tumour growth due to an excessive but non-productive sprouting angiogenesis (Noguera-Troise et al., 2006; Ridgway et al., 2006).

In addition to Dll4, another Notch ligand was found to have an important role in the tip-stalk cell biology. Jagged1 is a pro-angiogenic regulator mainly expressed in stalk cells and antagonizes Dll4-Notch signalling in Fringe glycosyltransferases (Mfng/Lfng) expressing ECs, including tip cells (Benedito et al., 2009). By glycosylating the Notch receptors, Fringes

polarize the function of the Delta and Jagged ligands (Panin et al., 1997; Yang et al., 2005). Therefore, the relative expression and equilibrium among different Notch ligands and modulators control and reinforce these different EC behaviours between tip cells (Notch signalling sending) and stalk-cells (Notch signalling receiving cells).

For many years, the VEGF/Notch interplay in tip/stalk cell differentiation was thought to rely on the suppression of VEGFR2 transcription by Dll4-Notch activation in stalk cells, which was shown to happen in cultured HUVECs (Phng and Gerhardt, 2009). However, recent studies showed that Notch does not significantly regulate the transcription of *Vegfr2 in vivo* (Benedito et al., 2012; Hogan et al., 2009; Lobov et al., 2007; Pontes-Quero et al., 2019) and that tip cells express similar amounts of Vegfr2 protein than stalk cells (Benedito et al., 2012). These studies also showed that VEGFR3 transcription and protein levels are more tightly regulated by Notch signalling *in vivo*, however this receptor does not bind VEGFA (only VEGFC/D) and its role is more important for lymphangiogenesis, or it requires heterodimerization with VEGFR2 (Tammela et al., 2011). Nonetheless, all available evidence shows that tip cells have higher MAPK/ERK activity, which is strongly activated by VEGF signalling, suggesting that these cells have higher VEGF/Vegfr2 activity, likely because of the higher proximity to the VEGF source. According to this, suppression of MEK/ERK signalling also completely prevents EC sprouting in zebrafish and the mouse retina models (Pontes-Quero et al., 2019; Shin et al., 2016). Since tip cells have higher VEGF/ERK activity and lower Notch activity, they should proliferate more than stalk cells. However, *in vivo* studies have shown that tip cells are in general less proliferative than their neighboring stalk cells. Recent studies have shown that ECs have a bell-shaped dose-response to mitogenic stimuli *in vivo*. Contrary to previous reports, high resolution studies in the retina angiogenesis context have shown that angiogenic ECs proliferate less after Notch inhibition. Although initially ECs subjected to loss of Notch signalling experience a transient increase in the speed of cell-cycle and division, this is followed by a pronounced cell-cycle arrest partially mediated by the cyclin dependent kinase inhibitor *Cdkn1a* (p21) expression. Therefore, physiological Notch signalling does not inhibit angiogenesis, it is instead essential to prevent endothelial cell-cycle arrest. Higher ERK signalling and p21 expression in ECs with low Notch signalling (such as tip cells), arrests the cell-cycle and promote cell sprouting/migration. These studies also show that an adequate Notch signalling balance must be maintained in order for ECs to proliferate and migrate adequately. ECs with either gain or loss of Notch signalling lose their proliferation capacity, even if that occurs at significantly different levels of mitogenic stimulus (Pontes-Quero et al., 2019). These results also highlight that therapeutic pro-angiogenic stimuli, such as the delivery of growth factors after myocardial infarction (Sanganalmath and Bolli, 2013;

Taimeh et al., 2013), will not be enough to effectively stimulate angiogenesis, since vessels elicit cell-cycle checkpoint mechanisms at high levels of stimulation (Figure 3). Understanding these hypermitogenic arrest mechanisms in more detail may shed more light on ways of effectively modulating angiogenesis.

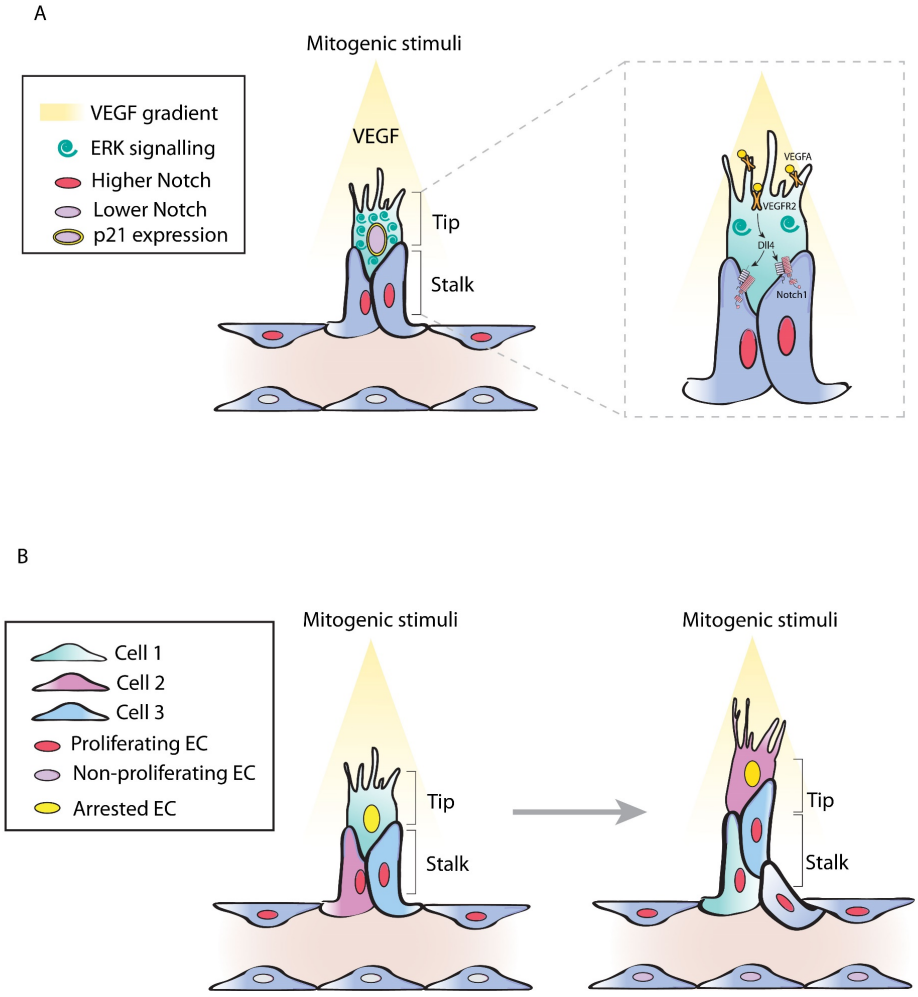

Figure 3: Regulation of angiogenesis by Notch signalling. Hypoxic tissues lead to the secretion of pro-angiogenic growth factors (VEGFA). The gradient of these molecules stimulates a fraction of ECs that become tip cells. These migratory cells have long filopodia and lead the sprouting process to invade the surrounding tissue. These tip cells are followed by stalk cells, which are the building blocks to elongate the sprout. **(A)** By binding to its cognate receptor VEGFR2, the VEGF gradient signalling activates the fraction of ECs that become the leading tip cells. This activation triggers several downstream cascades, including ERK signalling activation in tip cells. These invasive cells also express the cyclin dependent kinase inhibitor p21. Among the plethora of downstream events, VEGFR2 signalling also results on Dll4 expression tip cells, which in turns activates Notch signalling in the adjacent stalk cells and suppresses the tip cell phenotype. Importantly, Notch activation leads to ERK activity inhibition. **(B)** While the tip cells are migratory and invasive arrested cells, the stalk cells proliferate to build the nascent blood vessel. However, this specification of tip/stalk phenotypes is a dynamic process. ECs compete for the tip position and this continuous re-evaluation results in a dynamic exchange among tip and stalk cells during angiogenesis. The tip/stalk dynamic has been shown to be regulated by VEGF and Notch signalling levels.

Role of Notch in vascular maturation and quiescence

After the angiogenic expansion of the blood vessel network, they have to mature to be converted into a functional vascular system. This maturation includes vascular pruning, remodelling, stabilization and cellular differentiation, to culminate with the acquisition of a quiescent state (Adams and Alitalo, 2007; Potente and Carmeliet, 2017). Many signalling pathways required for the development of blood vessels have been related with the maturation process, and the recruitment of endothelial supporting cells, including pericytes and vascular smooth muscle cells (VSMCs), stabilizes nascent blood vessels and secrete important extracellular matrix components. Among others, TGF-β and PDGFR-β regulate proliferation, differentiation and recruitment of murals cells. Loss of TGF-β receptor 2 (*Tgfbr2*), Endoglin, activin A receptor like type 1 (*Acvrl1*) or *Pdgfβ* causes vessel fragility, dysfunction and bleeding due to impaired mural cell development and coverage (Gaengel et al., 2009; Pardali et al., 2010). Mural cell production of ANG1 activates the endothelial receptor TIE2 and stabilizes vessels, promotes pericyte adhesion and tights endothelial junctions (Thomas and Augustin, 2009). Besides the essential role of Notch during vasculogenesis and angiogenesis, it has been shown that Notch signalling it is also required throughout the entire vascular maturation process. In the mouse retina model, it has been shown that Dll4-Notch signalling activity is essential for the maturation of veins and perivenous capillaries, but surprisingly not arteries. Endothelial-specific deletion of *Rbpj* leads to reduced vessel pruning and mural cell recruitment, with an increase in vessel sprouting and proliferation only in the venous areas. Despite the Notch pathway components being expressed in the arterial endothelium throughout life, it is not required for the maintenance of those (Ehling et al., 2013). In line with this study and contrary to what happens in angiogenic ECs, loss of Dll4/Notch signalling in the maturing vascular plexus of the retina leads to cell cycle reentry instead of cell cycle exit, which is likely due to the identified bell-shaped dose-dependent response to mitogenic stimulation (Pontes-Quero et al., 2019). Vessels undergoing maturation are exposed to lower levels of growth factors and a Notch-inhibition induced increase in mitogenic activity in this context triggers cell cycle entry, highlighting how context-dependent is the role of Notch in EC biology. The relevance of the EC interaction with perivascular cells is highlighted by the high expression of Notch3 receptor in arterial VSMCs. *Notch3* knock out mice present dilated arteries with a thinner layer of VSMCs, defects that arise during arterial vessel maturation (Domenga et al., 2004). Similarly, adult endothelial deletion of *Akt* results in reduced Jagged1 expression in ECs and thereby, impaired Notch3 signalling in VSMCs. Loss of endothelial

Jagged1 or Notch3 signalling in SMCs leads to the loss of supporting cells and fragile arteries that result in CADASIL (Joutel, 2011; Joutel et al., 1997; Kerr et al., 2016).

During the process of vascular maturation, there is a progressive switch from an active growth to a quiescence state. Thus, endothelial proliferation and sprouting has to be suppressed. Quiescence is a non-dividing but reversible state that is present in most adult ECs (Potente and Mäkinen, 2017). This state relies on the withdrawal of pro-angiogenic microenvironmental cues but also cell intrinsic and cell-to-cell contact molecular mechanisms. The quiescent phenotype is in general maintained until ECs detect pro-angiogenic signals that can rapidly switch them from a long-term quiescence to an active growth state (Potente and Carmeliet, 2017). In an adult organism, the maintenance of a quiescent and functional vascular network is critical for the structure and function of organ parenchyma, maintaining tissue homeostasis. It is also becoming clear that maintenance of vascular quiescence and homeostasis is not a passive process, and involves the activity of several signalling pathways, most of which were already introduced before as being key regulators of angiogenesis.

Recent evidence has revealed that fully differentiated and quiescent endothelial cells require baseline survival signals to support their viability and function. Indeed, apart from the unquestionable significance of paracrine VEGF as a pro-angiogenic factor, recent studies have shown that autocrine VEGF also has an important role in vascular homeostasis, sustaining endothelial survival and integrity in adult quiescent vessels (Lee et al., 2007). Mechanistically, absence of intracellular VEGF leads to mitochondria fragmentation, suppression of cell metabolism and autophagy, which is mediated by FOXO1 (Domigan et al., 2015). Importantly, autocrine VEGF signalling and consequently EC viability is not affected by pharmacological compounds that inhibit the extracellular VEGF such as bevacizumab. However, if VEGF inhibitors are small enough to enter in the cell, they would impact dramatically the endothelial cell survival (Domigan et al., 2015; Lee et al., 2007), as it has already been shown to occur during chronic treatment with small VEGFR inhibitors (Kasahara et al., 2000). Fibroblast growth factor (FGF) is also important for the maintenance of blood vessel homeostasis. Inhibition of FGF signalling leads to the loss of vascular integrity because of endothelial junction disassembly (Murakami et al., 2008). Among the plethora of mitogenic stimuli and signals involved, VEGF and FGF can ultimately activate the ERK pathway in quiescent ECs. Adult endothelial *Erk2* deletion in an *Erk1* null background results in premature death within 5 weeks due to an increase in endothelial-to-mesenchymal transition and activation of endothelial TGFβ, which finally leads to myocardial fibrosis, renal failure, hypertension and pulmonary haemorrhage. Interestingly, clinical trials using pharmacological

compounds targeting either VEGF/VEGFR2 or the mitogenic-activated kinase (MEK), which is a component of the MAPK pathway, show similarities in the side effects (Banks et al., 2017; Je et al., 2009; Touyz and Herrmann, 2018).

Several studies also showed that the Notch signalling pathway is essential to maintain the quiescence of some organ vessels and their homeostasis. Pharmacological inhibition or genetic deletion of different Notch components such as *Dll4*, *Notch1* or *Rbpj* in the adult and mature endothelium results in enlarged vessels and increased vascular density and in some studies this was linked to an increase in EC proliferation and vascular neoplasms (Cuervo et al., 2016; Dill et al., 2012; Dou et al., 2008; Jabs et al., 2018; Yan et al., 2010). These studies raised important concerns against the use of Notch inhibitors in the clinics and questioned the safety of targeting the Dll4-Notch1 signalling axis. Targeting this signalling pathway was before seen as a very promising approach against cancer, since Dll4 blockade with Dll4-Fc or anti-Dll4 monoclonal antibodies significantly reduced tumor growth, even tumors resistant to anti-VEGF (Noguera-Troise et al., 2007; Ridgway et al., 2006). Now, these more recent studies reveal potential secondary effects of those treatments and raise a red flag in the use of anti-Dll4/Notch for cancer treatment. Some other studies suggested that these anti-Dll4 side-effects are reversible after treatment withdrawal and may have less impact on organ physiology than what was initially proposed (Couch et al., 2016).

The mechanisms triggered by Notch activation that induce EC quiescence are still incompletely understood. Mechanisms identified by overactivation of Notch signalling in cultured cells may also be misleading, since the range of genetic targets activated by Notch signalling is dose-dependent and not easily modelled in gain-of-function assays. Nonetheless, several Notch downstream mechanisms have been suggested to be responsible for inducing EC quiescence by repressing proliferation both *in vitro* and *in vivo*, such as Interleukin-33 (*Il33*), *Cdkn1b* (p27), thrombospondin-1, p21 and PTEN (Noseda et al., 2004; Rostama et al., 2015; Serra et al., 2015; Sundlisaeter et al., 2012). Altogether, these studies point to Notch activation being a pro-quiescence pathway, that is essential to maintain vascular homeostasis (Cuervo et al., 2016; Dill et al., 2012; Dou et al., 2008; Jabs et al., 2018; Yan et al., 2010).

Some other studies have linked the role of Notch in vascular quiescence with shear stress. These studies suggested that vascular quiescence is a blood-flow or shear-stress dependent process, which is mediated by the Notch suppression of cell cycle and the stabilization of cell-to-cell contact mechanisms. These studies proposed that Notch signalling activity is regulated by shear-stress not only during arterial development but also during adult arteries homeostasis (Fang et al., 2017; Mack et al., 2017). Surprisingly, a non-canonical and

transcriptional-independent Notch-mediated mechanism was also proposed to be involved in the endothelial barrier maintenance. Shear stress promotes Dll4-Notch dependent proteolytic cleavages that let the Notch transmembrane domain to complex with other proteins as VE-cadherin or RAC1. This complex allows to control adherent junctions and barrier functions (Polacheck et al., 2017). Either transcriptionally-mediated or not, Notch signalling is an important regulator of blood vessel integrity under flow conditions.

The role of Notch in the adult vasculature after certain pathological insults was also analysed. In the hindlimb ischemia model, *Dll1* haploinsufficieny impairs arterial remodelling and blood flow restoration. Dll1 expression is restricted to arterial endothelium and its upregulation seems to be required for the Notch-dependent arteriogenesis (Limbourg et al., 2007). In line with this, Notch1 and Notch4 have also been shown to be required for proper angiogenesis and blood flow recovery in hindlimb ischemia models (Takeshita et al., 2007). Importantly, although Dll4/Notch signaling has been shown to negatively regulate collateral formations, its inhibition and consequent increase in collaterals does not ameliorate post-ischemic recovery, likely due to defective vessel function (Cristofaro et al., 2013). Therefore, strategies to modulate functional blood flow recovery should be study on detail, discerning between the increase in vessel number vs quality of these vessels. The role of Notch signalling in atherosclerosis has also been evaluated. Some reports have shown that endothelial deletion of *Rbpj* reduces atherosclerosis progression, with decreased secretion of inflammatory factors and leucocyte recruitment. Thus, attenuation of Notch signalling could constitute a potential treatment strategy (Nus et al., 2016). In contrast, only some years later it was also shown that deletion of *Notch1* in ECs leads to increased atherosclerosis in a hypercholesterolemia mouse model, suggesting an atheroprotective role for Notch signalling (Mack et al., 2017). Despite these opposite results, endothelial Notch signalling seems to be clearly involved in the inflammatory response under pathological conditions, such as in the zebrafish regenerating heart (Munch et al., 2017).

Notch maintains the quiescence of some organ vascular beds

As mentioned above, in the last years it has been shown that Notch signalling acts as a gatekeeper of vascular quiescence, but is still not known if its function is specific to some organ vascular beds. Conditional *Rbpj* deletion using MxCre in adult mice showed that the

absence of this transcription factor during two months induces spontaneous reactivation of the endothelium and angiogenesis in several tissues, including adult retina, cornea, liver and lung (Dou et al., 2008). Sporadic and progressive loss of *Notch1* heterozygosity leads to vascular tumors and lethal haemorrhage, mostly in the liver (Liu et al., 2011). In addition, conditional *Notch1* deletion using MxCre resulted in vascular remodelling by intussusceptive angiogenesis in the liver (Dill et al., 2012). The use of an endothelial specific Dll4 blocking antibody in mice, Sprague–Dawley rats and cynomolgus monkeys showed that Dll4/Notch1 signalling blockade induced vascular neoplasms in the liver and skin vasculature (Yan et al., 2010). Specific deletion of *Rbpj* and *Notch1* in adult ECs also confirms that Notch inhibition leads to vascular malformations with sinusoid enlargement in the liver vasculature (Cuervo et al., 2016). A study published during my thesis work also showed that genetic loss of Notch signalling or the use of Dll4 blocking antibodies results in an increase of heart and muscle EC density. Surprisingly, it also leads to heart hypertrophy and failure, deregulating fatty acid transports (Jabs et al., 2018).

These studies suggest that the Notch function is particularly important for the vascular homeostasis of some organs, but did not address if there are differences in the way Notch functions among distinct vascular beds. Several molecular mechanisms were proposed to be downstream of Notch activity in quiescent blood vessels. Notch was shown to repress adult vessels endothelial cell proliferation by downregulation of *Vegfr2* (Dou et al., 2008) or downregulation of *Efnb2* and increased expression of *Ephb4* (Dill et al., 2012) or by repressing several cell cycle genes (Dou et al., 2008; Yan et al., 2010). More recently vascular Notch activity was also shown to induce lipase activity and transendothelial transport of long-chain fatty acids to muscle cells (Jabs et al., 2018). In its absence, heart vessels get denser and cardiac metabolism is also changed. Loss of endothelial *Notch1* using MxCre was also shown to increase neighbouring hepatocyte proliferation (Dill et al., 2012).

Importantly, despite that all of these studies reported an increase in vascular density and malformations in some organs, few have shown an increase in EC proliferation. In fact in one study, the liver vascular defects arising after *Rbpj* deletion were shown to arise without an increase in EC proliferation (Cuervo et al., 2016).

Although these previous studies demonstrate the essential role of Notch in maintaining the quiescence or normal vascular architecture in some organs, especially the liver, the variety of findings and mechanisms proposed do not allow us to obtain a clear understanding of the function of this pathway in maintaining the homeostasis of different organ quiescent blood vessels.

Angiocrine functions of endothelial Notch signalling

Apart from their widely known function delivering oxygen and nutrients, ECs are involved in an extensive variety of physiological processes, ranging from the first steps of organ development to adult organ regeneration and tissue/stem cell homeostasis. Some of these important EC roles are blood flow or oxygen/nutrients delivery independent and rely on the expression and secretion of either stimulatory or inhibitory growth factors, morphogens or chemokines, popularly referred as angiocrine factors. It has been shown that these endothelial secreted factors are able to regulate the homeostasis, self-renewal, growth and differentiation of neighboring cells or resident stem cells (Rafii et al., 2016). Although Aristotle already suggested an essential role of the vascular structures during organogenesis (Crivellato et al., 2007), it was approximately 20 years ago when it was shown that liver sinusoidal ECs were involved in liver bud development in a perfusion-independent manner (Matsumoto et al., 2001). Since then, many studies have listed the genes expressed by ECs, which can code for potential angiocrine factors. Among those signals, Notch was proposed to be such an angiocrine factor for its ability to be transmitted by cell-to-cell contact.

Upon myeloablation, ECs from the bone marrow niche are able to support the self-renewal of the hematopoietic stem cell (HSC) pool through the endothelial expression of the Jagged1 and Jagged2 ligands and subsequent Notch activation in HSCs (Guo et al., 2017; Poulos et al., 2013). In steady state conditions, endothelial expression of Dll1 in the hematopoietic compartment of the bone marrow and spleen regulates monocyte fate, favouring the conversion of $Ly6C^{hi}$ monocytes into $Ly6C^{low}$ monocytes that patrol the endothelium. However, during ischemia, Dll1 upregulation in arterial ECs leads instead to differentiation of $Ly6C^{hi}$ monocytes into macrophages that promote arteriogenesis and allow tissue repair (Gamrekelashvili et al., 2016; Krishnasamy et al., 2017). In contrast to other organs, endothelial Notch signalling in the bone promotes angiogenesis, and its activity leads to the expression and secretion of the angiocrine factor Noggin. This bone morphogenic protein is required for chondrocyte and osteoblast homeostasis (Ramasamy et al., 2014).

Notch activation can also have a detrimental function for the homeostasis or regeneration of the surrounding tissue. Notch activation in sinusoidal liver ECs downregulates important hepatocyte mitogens such as Wnt2, Wnt9b and hepatocyte growth factor (HGF). This leads to impaired hepatocyte turnover not only during organ homeostasis but also in regenerating conditions. Portal hypertension is also regulated by Notch signalling. Mechanically stretched liver sinusoidal ECs upregulate *Cxcl1* via Notch. The secretion of this

angiocrine factor leads to neutrophil recruitment and subsequent formation of neutrophil extracellular traps with microthrombi (Hilscher et al., 2019). Myocardial hypertrophy is enhanced by VEGFR2/Notch signalling in ECs. The activation of the pathway releases the ligands HB-EGF and NRG1 that bind to ErbB receptors in cardiomyocytes (Kivelä et al., 2019). Repetitive lung injury activates pulmonary capillary ECs that result in an upregulation of *Jag1*. This ligand activates Notch signalling in perivascular fibroblasts and consequently enhances fibrosis (Cao et al., 2016).

A comprehensive knowledge of these organ-specific angiocrine functions is required to understand and predict the impact of pharmacological targeting in translational vascular medicine. The promising therapeutic potential of tissue-specific and resident ECs may represent a target for angiocrine-mediated tissue regeneration or for the amelioration of certain conditions, such as fibrosis (Rafii et al., 2016).

Role of Notch on organ-specific endothelial cell heterogeneity

During organ development, ECs undergo consecutive steps of differentiation and specialization until they acquire their final differentiated adult organ-specific vascular state. Though initially plastic, ECs acquire organ-specific features and adapt themselves to their vascular niche demands. Thus, the degree of vascular heterogeneity goes beyond the arterial, capillary and vein differentiation. In each organ or tissue, we can find organ-specific vascular beds, that have specific genetic, morphological and functional features (Aird, 2007, 2012; Augustin and Koh, 2017; Kalucka et al., 2020; Nolan et al., 2013; Rafii et al., 2016).

Anatomical differences between arteries and veins have been established for thousands of years. Arteries are conducts for high and pulsatile blood flow, with thick layers of VSMCs and extracellular matrix, while veins are perfused by low pressure flow and are covered with less VSMCs. Although the discovery of blood circulation by William Harvey in 1628 is one of the biggest milestones in biomedical research, it was not until 1661 when Malpighi observed blood capillaries for the first time. However, only with the discovery of Electron Microscopy 50 years ago, capillary EC started to be described in greater detail (Aird, 2007). While arteries and veins form a continuous monolayer, capillaries can be formed by a continuous, fenestrated or discontinuous single layer of ECs. Continuous ECs form a barrier

that tightly controls inter-endothelial transport. It can be found in the nervous system, skeletal muscle, heart, lung and ovaries. The most specialized continuous capillaries comprise the blood brain barrier (BBB) and the retinal capillaries, and present high expression of tight junctions and solute transporters, which limits paracelullar transport and restricts vascular permeability. This is paramount to its organ-specific function of avoiding the entry of toxins and immunes cells that could damage non-regenerating neurons (Zhao et al., 2015). Fenestrated ECs are characterized by the presence of pores or openings, which can have a diaphragm. These pores transverse the endothelial lining to increase vascular permeability. This endothelium is found in endocrine organs involved in vascular filtration and secretion, such as the kidney and intestine. Discontinuous ECs, commonly named sinusoidal ECs, are found in the liver, spleen, bone marrow and some endocrine organs. Gaps in the ECs and poor or lack of coverage by basement membrane provide high permeability to these ECs (Aird, 2007; Augustin and Koh, 2017; Crivellato et al., 2007)(Figure 4).

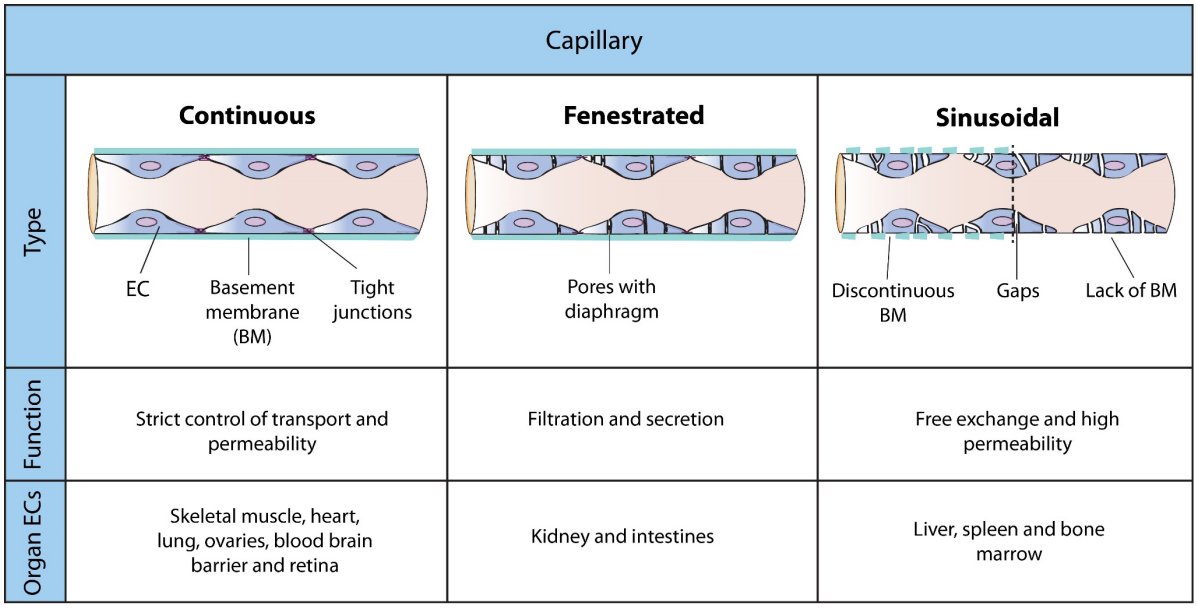

Figure 4: Heterogeneous capillary morphology and function. Capillary ECs can be classified as continuous, fenestrated or sinusoidal. Continuous capillaries are characterized by a continuous monolayer of ECs surrounded by a basement membrane (BM). They function as strict barrier for transport and permeability. The most specialized continuous capillaries are found in the brain and retina, where the transport has to be limited and controlled between the circulation and the neighboring tissue. High concentration of tight junctions is found in the EC boundaries. Fenestrated capillaries display pores or openings, which are called as fenestrae (latin for “windows”) and they can contain a diaphragm. These intracellular pores provide discontinuity to the EC layer to enhance the exchange between the blood flow and the surrounding tissue. Sinusoidal capillaries are characterized by gaps in their irregular EC blood vessel coverage. In addition, they have either a poor or lack of basement membrane. They are able to maximize the exchange and allow free transport.

EC heterogeneity allows proper and organ-specific functions. These functional specializations are reflected not only by their different morphologies, but also by their expression profiles. For example, organs that are very demanding on energy, as the heart, have ECs specialized in nutrients transfer with high expression of CD36 (Coppiello et al., 2015). In addition, there is functional heterogeneity among the same organ vascular bed. As an example, postcapillary venules are highly specialized in leukocyte trafficking (Aird, 2007)

How do these ECs get specialized into such a diverse network? One of the main hypotheses is that this complex palette of heterogeneous endothelium, results from time- and niche-specific microenvironmental inputs. During organ development, the endothelium of distinct organs is exposed to different biochemical and biomechanical forces. It is believed that the specificity of organ signals (paracrine signals, shear stress, growth factors, oxygen levels, biomechanical forces) is what makes ECs different across distinct organs. When endothelial cells are taken from their particular microenvironment, such as after tissue dissociation and *in vitro* culture, part of their site-specific features are lost but some of these are retained, supporting the evidence that those heterogeneous phenotypes are maintained by strong epigenetic programmes once differentiation is completed (Aird, 2005, 2007). As an example of a tissue-specific signal that maintains EC specialization, VEGF is required to maintain capillary fenestration in pancreatic islets, thyroid, adrenal cortex, pituitary, villi of small intestine and epididymal adipose tissue (Kamba et al., 2006). The transcription factors MEOX2 and TFC15 , which are specifically expressed in heart ECs, programme the endothelium as efficient transporters of fatty acids to the adjacent myocardium (Coppiello et al., 2015). *Gata4* expression is essential for the development of sinusoidal ECs, and lack of this transcription factor leads to the transformation into continuous capillaries, which ultimately results in embryonic lethality (Géraud et al., 2017). In addition, it has been shown that lack of Notch signalling in liver sinusoidal ECs increased membranous "holes" (Cuervo et al., 2016). On the contrary, Notch activation in liver sinusoidal ECs results in decreased sinusoids and increased expression of genes related with the continuous phenotype/structure of ECs (Duan et al., 2018). These findings suggest that Notch is also involved in maintaining organ-specific endothelial specialization and structure.

The remarkable heterogeneity of organ capillary ECs leads to differences in vessel structure and function. This heterogeneity arises from the great variety of organ specific mechanisms of blood vessel specification, development and maturation. Given the highly conserved role of Notch in regulating cell differentiation and fate, it may be also involved in the regulation of vascular organotypicity.

Zonal and single-cell Notch vascular heterogeneity

The development of techniques for EC purification, isolation and profiling have allowed the study of vascular heterogeneity, revealing the enrichment in the expression of specific clusters of transcription factors, chemokines, angriocrine and adhesion molecules by organ-specific ECs in homeostatic and regenerating conditions (Nolan et al., 2013). However, during my thesis work, the development of single-cell RNA sequencing has allowed a much higher resolution in the profiling of cellular heterogeneity and the discovery of endothelial-specific populations that would have remained masked by bulk transcriptional profiling techniques. Recent scRNA-seq studies have allowed the comparative analysis of the transcriptome of most ECs within most adult organ vascular beds (Dobie et al., 2019; Goveia et al., 2020; Guo et al., 2019; Kalucka et al., 2020; Karaiskos et al., 2018; Khan et al., 2019; Menon et al., 2020; Ramachandran et al., 2019; Sabbagh et al., 2018; Tikhonova et al., 2019; Vanlandewijck et al., 2018). By profiling single ECs from 11 different organs, Kalucka et al., have identified specialized EC clusters and a remarkable organ-related endothelial heterogeneity. The endothelium of arteries, veins and lymphatic vessels across different organs share many common markers and have less organ-specialization than interconnecting capillary ECs. Capillary ECs adapt more to the organ features and demands. Interestingly, these studies have also shown, that an arterial or venous endothelial cell is more similar to its organ-related capillary neighbour than another arterial or venous cell from a distinct organ. This indicates that the organ and context in which an endothelial cell develops and matures is the major contributor for its molecular heterogeneity.

As mentioned above, apart from discerning among the well-known vascular populations such as arteries, veins or capillaries, they have uncovered small but specialized tissue-specific EC populations that have remained invisible by immunohistochemistry or bulk sequencing techniques. Although these EC phenotypes found in different organs express common capillary genes, they also express unique tissue-specific markers and have specialized biological functions. In intestines, they found an EC population which expresses genes related with fatty acid and glycerol uptake and metabolism. In brain, it was uncovered a subcluster of choroid plexus capillary ECs with enriched expression of *Plvap* and the tip cell marker *Esm1.* In different tissues such as heart, brain, muscle and spleen it was found an EC population with increased expression of interferon signalling genes. Unexpectedly, in different quiescent tissue they found EC clusters (0.6%-11.1% from total ECs) expressing angiogenesis and proliferation-related genes. In heart, skeletal muscle, kidney and testicular

tissues, this EC cluster expresses tip-cell enriched genes such as *Apln, Col4a2* and *Trp53i11.* The specialized EC population in liver and spleen (1.4% and 0.6% respectively) expresses typical proliferation markers (*Ccdc34, Cdkn1a, Pcna, Stmn1*). These scRNA-seq data might have uncovered an infrequent but important migratory or proliferative EC population in adult quiescent blood vessels (Kalucka et al., 2020).

At the beginning, most trajectory bioinformatics analyses of single-cell experiments were used to study the differentiation of different cell types during development. In the case of the vascular system, it was elegantly shown that venous cells go through a gradual switch from a venous programme to a pre-arterial one during heart development (Su et al., 2018). However, these analyses have also allowed to uncover the spatial profile of the different adult EC populations and reconstruct the transcriptional basis of the gradual changes in gene expression, the so-called zonation, in different tissue-specific vasculatures. Trajectory bioinformatics analysis have revealed that there is a continuum of EC identities along the arterial-venous axis, allowing the spatial location of these EC clusters (Halpern et al., 2018; Sabbagh et al., 2018; Vanlandewijck et al., 2018).

One of the clearest examples of tissue-specific zonation is the liver organ. By combining single molecule *in situ* hybridization and scRNA-seq, a recent study spatially reconstructed the hepatocyte zonation (Halpern et al., 2017). A follow up study from the same group uncovered at high resolution the endothelial spatial gene expression along the hepatic sinusoid by coupling paired-cell sequencing with the previous results obtained from hepatocytes scRNA-seq (Halpern et al., 2018). Interestingly, the spatial zonation of liver ECs genes showed that Notch signalling is periportally zonated in liver sinusoidal ECs. The ligand *Dll4* and the Notch target *Efnb2* are highly expressed in the oxygenated portal nodes, which comprise the arteries, portal veins and bile ducts. Then, the expression progressively decreases continuously alongside the arteriovenous axis towards the central vein (Halpern et al., 2018).

Understanding Notch intravascular heterogeneity in different organs will uncover the role of this signalling pathway in the homeostasis of distinct vascular beds or different populations of ECs, which might differ among tissues. While some studies suggest that Notch is expendable in retina artery maturation and quiescence (Ehling et al., 2013), others claim that is essential for the maintenance of adult aorta (Mack et al., 2017). As we have discussed, several studies in adult endothelium have shown that Notch seems crucial to maintain EC quiescence only in some organ vascular beds (Cuervo et al., 2016; Dill et al., 2012; Dou et al., 2008; Jabs et al., 2018; Yan et al., 2010). So are these results a vascular bed type specific

consequence or mostly organ specific? If we establish a fixed black-and-white pattern for high Notch in arteries and low Notch in veins, what happens with adult capillaries from different organs? Importantly, all 4 vertebrate Notch receptors can be activated by 4 different ligands (Nandagopal et al., 2018). In principle, depending on the biological context, different ligands are required and could be used to activate distinct set of genes. Ligands could have from opposing roles (on muscle differentiation or angiogenesis e.g) (Benedito et al., 2009; Cappellari et al., 2013) to almost interchangeably functions (on T cell differentiation e.g) (Mohtashami et al., 2010). Therefore, different Notch signalling components may be important to regulate the homeostasis of different vascular beds or EC populations in different organs. More importantly, we have to bear in mind that Notch signalling is a cell-to-cell communication signalling pathway, and therefore diverse parenchymal signalling in different organs could play a role in the heterogeneous organ specific EC phenotype. Hence, it is essential to understand and map Notch signalling pathway in the different organ-specific vasculatures and vascular bed types, but also in the surrounding tissue. Having a spatial gene expression map at single cell resolution will facilitate the identification of ECs behaviours not only in homeostatic conditions but also during pathological processes, such as angiogenesis in cancer, where it has been demonstrated the relevance of Notch signalling activation (Gridley, 2010). Those EC phenotypes might be future targets for regeneration processes or anti-angiogenic therapies.

OBJECTIVES

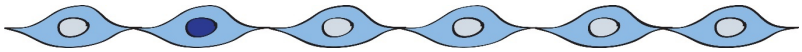

Pharmacological compounds targeting distinct members of the Notch signalling pathway have been used in the clinics but their effect on the homeostasis of different types of blood vessels is unknown. The main aim of the doctoral was to identify and understand the molecular mechanisms controlled by distinct Notch signalling members in different quiescent vascular beds. Therefore, the main objectives of this study were:

- To determine the role of Notch signalling for the homeostasis of distinct organ vascular beds.
- To identify the molecular mechanisms driving the observed organ-specific vascular function.
- To dissect the contribution of different Notch signalling pathway members for the organ-specific regulation of vascular quiescence.
- To understand the role of Notch in the regulation of the endothelial cell cycle and single-cell clonal dynamics.
- Generation of a new genetic tool to significantly increase the ease, efficiency and reliability of conditional genetics.

MATERIALS AND METHODS

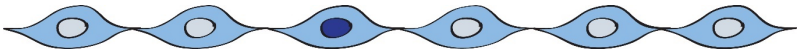

Mice

The following mouse lines were used and interbred when multiple alleles/transgenes were combined in the mouse: *Tg(Cdh5-CreERT2)*(Wang et al., 2010), *Tg(iSuRe-Cre)*(Fernandez-Chacon et al., 2019), *Dll4*$^{flox/flox}$ (Koch et al., 2008), *Notch1*$^{flox/flox}$ (Radtke et al., 1999), *Rbpj*$^{flox/flox}$ (Han et al., 2002), *Myc*$^{flox/flox}$ (de Alboran et al., 2001), *Tg(Ubc-CreERT2)*(Ruzankina et al., 2007), *Gt(ROSA)26-CreERT2* (Schonhuber et al., 2014), *Gt(ROSA)26*$^{LSL-EYFP}$ (Srinivas et al., 2001), *Kdr*$^{flox/flox}$ (Haigh et al., 2003), *Mycn*$^{flox/flox}$ (Knoepfler et al., 2002) ,*Cdkn1a(p21)*^{KO} (Brugarolas et al., 1995), *iChr-Mosaic* (Pontes-Quero et al., 2017) and *iMb-Mosaic* (Pontes-Quero et al., 2017). To induce CreERT2 activity in adult mice, 20 mg or 10 mg tamoxifen (Sigma-Aldrich, T5648) (Sigma-Aldrich, P0130) were first dissolved in 140 µl absolute ethanol and after 860 µl corn oil (20 mg/ml or 10 mg/ml tamoxifen). This solution was given by intraperitoneal injection (200 µl, total dose of 1 or 2 mg tamoxifen respectively) to adult mice (8-12 weeks). Dosing and dissection schedules for individual experiments were the following: for *Dll4, Myc, iChr2 and iMb2* inducible loss-of-function experiments, 1 mg tamoxifen was injected for 3 consecutive days and dissection was done 7, 14 or 21 days after first injection. For *Rbpj, Notch1* inducible loss-of-function experiments, 2 mg tamoxifen was injected for 5 consecutive days and dissection was done 14 days after first injection. To activate recombination in pups containing CreERT2 alleles, tamoxifen was injected at the indicated stages at a dose of 40 µg/g body weight. All mouse lines are detailed in Table 1.

Experiments involving animals were conducted in accordance with official guidelines and laws, following protocols approved by local animal ethics committees and authorities (Comunidad Autónoma de Madrid and Universidad Autónoma de Madrid - CAM-PROEX 177/14 and CAM-PROEX 167/17). Male and female mice were used for the analysis and maintained under specific pathogen-free conditions.

Genotyping

DNA samples were obtained from biopsies of the tail of adult mice. Genomic DNA extraction was performed incubating the samples with 500 µl of 50 mM NaOH at 95ºC for 10

minutes and equilibrating with 50 µl of 1M Tris-HCl pH8. Primers listed in Table 1 were used to genotype the mice.

Name	Expected size fragment	Genotyping Oligonucleotides
PAC-Cdh5-CreERT2 mice	*Mut band: ~550bp*	Cdh5 Trans F: GGAGGCTGGAAAGTAGAGCA
		CreM R: TCCCTGAACATGTCCATCAG
Dll4 flox /flox mice	*WT band: ~400bp* *Mut band: ~500bp*	Dll4 lox F : GTGCTGGGACTGTAGCCACT
		Dll4 lox R: TGTTAGGGATGTCGCTCTCC
iSuRe-Cre mice	*WT band:140bp* *Mut band:260bp*	Sv40 pA F: CCCCCTGAACCTGAAACATA
		AVT MTomato R: CCTTGCTCACCATGGTCTTG
		Chr17 R: GTGTCTGTACCAGGTTGGTTTG
		Chr17 R: GCTCTGCATGTTGCAAGAAA
ROSA26 LSL-EYFP mice	*WT band:250bp* *KI band:350bp*	GCACTTGCTCTCCCAAAGTC
		GGGCGTACTTGGCATATGAT
		CTTTAAGCCTGCCCAGAAGA
		GCGAAGAGTTTGTCCTCAACC
KDR flox /flox mice	*WT band: 200bp* *Mut band: 220bp*	KDR lox F: GCCTGCAGGTTCTGGTTTG
		KDR lox R: GCTGTGACATCTGGGTAGAG
Rbpj flox/flox mice	*WT band: 200bp* *Mut band: 350bp*	Rbpj lox F: ATAATTTGCCAAGCCAAAGC
		Rbpj lox R: GCTCCCCACTGTTGTGAACT
N-myc flox/flox mice	*WT band: 200bp* *Mut band: 220bp*	N-Myc lox F: GTCGCGCTAGAAGAGCTGAGAT
		N-Myc lox R: CACAGCTCTGGAAGGTGGGAGAAAGTTGAAGCGTCTCC
Ubc-CreERT2 mice	*Mut band: 700bp*	Cre1 BSW F: CGGTCGATGCAACGAGTGATGAGG
		Cre2 BSW R: CCAGAGACGGAAATCCATCGCTCG
Notch1 flox/flox mice	*WT band: 445bp* *Mut band: 500bp*	Notch1 lox F: CTGAGGCCTAGAGCCTTGAA
		Notch1 lox R: TGTGGGACCCAGAAGTTAGG
Rosa26-CreERT2 mice	*Mut band: ~450bp*	R26 CAG F: GTTCGGCTTCTGGCGTGT
		CrERT2 R: CGATCCCTGAACATGTCCATC
Myc flox/flox mice	*WT band: 315bp* *Mut band: ~370bp*	Myc lox F: GACAGGGATGTGACCGATTC
		Myc lox R: GCTCAGTCTCCGGCTATCAC
p21 KO mice	*WT band: 760bp* *KO band: 600bp*	p21f_2B9: ACCCAGCAAAGCCTTGATTCT
		NeoF_8B6: CCTTCTATCGCCTTCTTGACGA
		p21r_3B2: CAGGTCGGACATCACCAGGAT
iMb-Control-Mosaic mice ***iChr-Control-Mosaic mice***	*WT band:250bp* *Mut band:350bp*	Rosa26 RR711: GCACTTGCTCTCCCAAAGTC
		Rosa26 RR713: CTTTAAGCCTGCCCAGAAGA
		CAG PCR F: CGGGGTCATTAGTTCATAGCC
		CAG PCR R: CACCTCGACCATGGTAATAGC

Table 1: Mouse lines and genotyping PCR primers.

Recombinant DNA and ES cell culture

The basic elements of the *iSuRe-Cre* DNA constructs were obtained from varied sources and assembled by standard DNA cloning (Pontes-Quero et al., 2017). The Int-Cre

sequence was obtained from plasmid p210 pCMV-CREM (Kaczmarczyk and Green, 2001), a gift from Jeffrey Green (Addgene plasmid #8395).

Mouse ES cells on the G4 background (George et al., 2007) were cultured in standard ES cell culture medium (DMEM containing Glutamax (31966-047, Gibco), 15% FBS (tested for germline transmission), 1 x NEAA (Hyclone, SH3023801), 0,1% ß-mercaptoethanol (Sigma, M7522), 1 x Pen/Strep (Lonza, DE17-602E) and LIF) in dishes covered with a feeder layer of mouse embryonic fibroblasts (MEFs). For classical gene targeting with the large *iSuRe-Cre* plasmid, 25ug of linearized DNA was used to electroporate 5 million ES cells. Selection in 200ug/ml G418 (Geneticin) was performed for 6 days, after which individual colonies were picked for storage, PCR and Southern blot screening. Selected positive clones were expanded and used for microinjection in host blastocysts of the C57Bl/6J strain. Chimeras with a high percentage of agouti coat color were then crossed with mice to obtain germline transmission of the targeted insertion. PCR with ROSA26 5'homology arm flanking primers (Table 2), allowed us to identify ES cell clones with precise homologous recombination and insertion of the *iSuRe-Cre* construct in the *ROSA* locus. After identification of clones with precise gene targeting, we performed PCR with the iSuRe-Cre F and iSuRe-Cre R primers (Table 2) to detect ES cell clones containing the MbTomato-2A-Int-Cre transgene sequence. Selected ES cell clones were expanded for further analysis and mouse generation.

Immunofluorescence on cryosections

For immunostaining of organ and embryo cryosections, tissues were fixed for 2 hours in a solution of PFA 4% in PBS at 4ºC. After washing the tissue in PBS three times for 10 minutes each wash, organs were stored overnight in 30% sucrose (Sigma) in PBS. Then, organs were embedded in OCT™ (Sakura) and frozen at -80C. Cryosections of organs (35μm) were cut on a cryostat (Leica). Sections were washed three times 10 minutes each in PBS and blocked/permeabilized in PBS with 10% Donkey Serum (Milipore), 10% Fetal Bovine Serum (FBS), and 1% Triton. Primary antibodies were diluted in blocking/permeabilization buffer and incubated overnight at 4ºC. This step was followed by three washes in PBS of 10 minutes each and incubation for 2 hours with conjugated secondary antibodies (1:200, Jackson Laboratories) and DAPI in PBS at room temperature. After three washes in PBS, sections were mounted with Fluoromount-G (SouthernBiotech). All antibodies used are listed

in Table 3. To detect Ki67 or c-Myc in the same section as ERG, rabbit anti-Ki67 or anti-cMyc plus a Fab fragment CY3 secondary antibody was used, which is compatible with the use after of rabbit anti-ERG-Alexa647.

Primer Name	Genotyping Oligonucleotides	Expected size fragment	Purpose
Rosa26 GT Accu F	TCAGAGAGCCTCGGCTAGGTAGGG	*1.200bp*	To detect gene targeting in Rosa26 locus
INS GT Accu R	ACTCCAGGACGGAGTCAGTGAGGA		
MTomato F	CCGCTACCTGGTGGAGTTCA	*350bp*	To detect Tg(iSuRe-Cre) allele
Cre R	TCCCTGAACATGTCCATCAG		
Sv40 pA F	CCCCCTGAACCTGAAACATA	*260bp Mutant band 104bp Wt band*	To detect Tg(iSuRe-Cre) allele and distinguish heterozygous from homozygous
MTomato R	CCTTGCTCACCATGGTCTTG		
Chr17 F	GCTCTGCATGTTGCAAGAAA		
Chr17 R	GTGTCTGTACCAGGTTGGTTTG		
Notch1 floxed F	CTG ACT TAG TAG GGG GAA AAC	*500bp*	To detect the Notch1 floxed allele
Notch1 floxed R	AGT GGT CCA GGG TGT GAG TGT		
Control Dll4 Wt F	GTGCTGGGACTGTAGCCACT	*430bp*	To have an internal PCR control for the Mycn, Rbpj and Notch1 floxed PCRs
Control Dll4 Wt R	TGTTAGGGATGTCGCTCTCC		
Myc floxed F	TTTTCTTTCCGATTGCTGAC	*450bp*	To detect the Myc floxed allele
Myc floxed R	TAAGAAGTTGCTATTTTGGC		
Mycn floxed F	GTCGCGCTAGTAAGAGCTGAGATC	*260bp*	To detect the Mycn floxed allele
Mycn floxed R	CACAGCTCTGGAAGGTGGGAGAAAGTT GAAGCGTCTCC		
Rbpj floxed F	ATAATTTGCCAAGCCAAAGC	*350bp*	To detect the Rbpj floxed allele
Rbpj floxed R	GCTCCCCACTGTTGTGAACT		
Control Jag1 F	TGAACTCAGGACAGTGCTCT	*389bp*	To have an internal PCR control for the Myc floxed PCR
Control Jag1 R	GTTTCAGTGTCTGCCATTGC		

Table 2: PCR primers information

Vibratome immunofluorescence and 3D imaging

For immunostaining of vibratome sections, tissues were fixed for 2 hours in a solution of PFA 4% in PBS at 4ºC. After washing the tissue in PBS three times for 10 minutes each wash, organs were embedded in 6% agarose low melting gel (Invitrogen). Then, organ sections (100 μm) were cut on a vibratome. Sections were permeabilized in PBS with 1%

Triton and 0.5% Tween20 for 1 hour. Then, sections were blocked in a solution of 1%Triton, 10% Donkey Serum and 10% FBS for 1 hour. Primary antibodies were diluted in blocking buffer and incubated overnight at 4ºC. This step was followed by 6 washes with %1Triton in PBS for 15 minutes each wash and incubation for 2 hours with conjugated secondary antibodies (1:200, Jackson Laboratories) and DAPI in PBS at room temperature. After three washes in PBS for 15 minutes each wash, sections were mounted with Fluoromount-G (SouthernBiotech All antibodies used are listed in Table 3. To detect Ki67 or c-Myc in the same section as ERG, rabbit anti-Ki67 or anti-cMyc plus a Fab fragment CY3 secondary antibody (1:200) was used, which is compatible with the use after of rabbit anti-ERG-Alexa647.

Immunofluorescence on paraffin sections

To detect the short-lived, and difficult to detect, cleaved/activated N1ICD epitope, and the lowly expressed Jag1 ligand, we used the TSA amplification kit (NEL774) procedure in paraffin sections after antigen retrieval. Briefly, sections were dewaxed and rehydrated followed by antigen retrieval in sub-boiling sodium citrate buffer (10mM, PH=6.0) for 30min. The slides were cooled down at RT for 30min, followed by incubation for 30 minutes in 3% H_2O_2 in methanol to quench the endogenous peroxidase activity. Next, slides were rinsed in ddH_2O and washed in PBS 3x5min, followed by blocking in 3% BSA, 200mM MgCl2, 0.3%Tween20, 5% Donkey Serum in PBS for 1h, and incubation in the same solution with the primary antibody overnight at 4ºC. Next, the slides were washed and incubated for 2h in anti-rabbit-HRP secondary antibody at RT, after washing, the signal was amplified using the TSA fluorescein kit (NEL774). Sections were mounted with Fluoromount-G (SouthernBiotech). All antibodies used are listed in Table 3.

Immunofluorescence on mouse retinas

For immunostaining of mouse retinas, eyes from mouse pups were dissected and fixed for 1 hour in a solution of PFA4% in PBS. After washing the tissue in PBS twice, retinas were

microdissected and processed for immunostaining. The blocking/permeabilization buffer contains 0.3% Triton (Sigma), 3% FBS, 3% Donkey Serum (Millipore) and antibody washes were 30 minutes each. Primary antibody was diluted in blocking solution and incubated for 2 hours at room temperature or overnight, followed by three washes in PBS and incubation for 1 to 2 hours with conjugated secondary antibodies at room temperature. After three washes in PBS, cells were mounted with Fluoromount-G (SouthernBiotech). All antibodies used are listed in Table 3.

ANTIBODIES	DILUTION (IF or WB)	SOURCE	IDENTIFIER
Anti-GFP/YFP/Cerulean	1 to 200 (IF)	Acris Antibodies	Cat# R1091P
Anti-Dsred	1 to 400 (IF)	Clontech	Cat# 632496
Anti-HA -647	1 to 200 (IF)	Cell Signaling Technology	Cat# 3444S
Anti-ERG	1 to 400 (IF)	Abcam	Cat# ab110639
Anti-ERG-AF-647	1 to 200 (IF)	Abcam	Cat# ab196149
Anti-Ki67	1 to 200 (IF)	Thermo Fisher	Cat# RM-9106-S0
Anti-Endomucin	1 to 200 (IF)	Santa Cruz Biotechnology	Cat# SC-53941
Anti-CD31	1 to 200 (IF)	BD Biosciences	Cat# 553370
Anti-p21	1 to 100 (IF)	Santa Cruz Biotechnology	Cat# SC-397-G
Anti-P-ERK	1 to 100 (IF) 1 to 1000 (WB)	Cell Signaling Technology	Cat# 4370S
Anti-Myc	1 to 200 (IF)	Millipore	Cat# 06-340
Anti-cleaved N1ICD	1 to 200 (IF)	Cell Signaling Technology	Cat# 4147
Anti-Dll4	1 to 200 (IF)	R&D system	Cat# AF1389
Anti-alpha/beta-Tubulin	1 to 5000 (WB)	Cell Signaling Technology	Cat# 2148
Anti-PhiYFP	1 to 200 (IF)	Axxora	Cat# EVN-AB605
Anti-Jagged1	1 to 100 (IF)	Cell Signaling Technology	Cat# 2620
Anti-VEGFR2	1 to 200 (IF)	BD Pharmingen	Cat# 550549
Anti-CD34	1 to 200 (IF)	BD Biosciences	Cat# 560238
Anti-53BP1	1 to 500 (IF)	Abcam	Cat# ab36823
Anti-CD45	1 to 200 (IF)	TonboBio	Cat# 35-0454-U100
Anti-Runx1	1 to 200 (IF)	Abcam	Cat# ab92336
Anti-Caspase 3	1 to 50 (IF)	Cell Signaling Technology	Cat# 9661S
Alexa fluor-conjugated antibodies (488, 546, 594,633,647)	1 to 400 (IF)	Life Technologies	N/A

Table 3: Antibodies list

Image acquisition and analysis

Organs sections with immunostaining were imaged at high resolution with a Leica SP5, SP8 or SP8 Navigator confocal microscopes. 10x, 20x or 40x objectives were used for confocal scanning. Individual fields or tiles of large areas were acquired in cryosections and paraffin sections. Large Z-volumes of the vibratome samples were image for 3D representations. Fiji/ImageJ was used to threshold, select and quantify objects in confocal micrographs. Quantifications for each parameter are specified here below.

For quantification of vascular parameters, random vascular areas were selected from 2 or more different animals. For N1ICD quantifications in different vascular beds, positive endothelial nuclei (N1ICD+DAPI+Endomucin+) were divided by the total number of endothelial nuclei counted on sections (DAPI+Endomucin+). For N1ICD quantification in liver portal area and central area, 350 μm x 350 μm pictures with a portal or central vein in its center were selected. Endothelial cell density (EC number/ mm^2) was measured as the number of ERG+ cells relative to the total vascular area included in each field. The total ERG+ (EC nuclei) objects in IsolectinB4 or MbTomato+ or MbYFP+ surface area was also quantified. For vessel width quantifications, the diameter of random capillaries was measured. The frequencies of Ki67+ and p21+ were manually quantified as the ratio of double positive cells –Ki67+ERG+ or p21+ERG+ - to the total number of ERG+ cells per field. Liver central and portal vein were distinguished by CD34 staining and the diameter was measured. For hepatocyte proliferation, Ki67+ERG- cells with a distinguishable hepatocyte DAPI morphology were counted as proliferating hepatocytes. Total number of proliferating hepatocytes was divided by the total vascular area. For nuclei EC size quantifications, images were automatically thresholded for the endothelial nuclei marker ERG+, and the ImageJ plugging Analyze Particles was used to detect the endothelial nuclei perimeter and measure its area. In Portal Vein and Central Vein analysis, the shape descriptor map from BioVoxxel Toolbox ImageJ plugin was used to quantify endothelial nuclei area. Quantification of PCR and Western gel bands intensity was done with Image J by calculating the mean grey value of each band and subtracting it from the background mean grey value. Indicated relative ratios represent the ratio between control and floxed PCR bands when comparing control samples (with no inducible genetic deletion) with MbTomato negative and MbTomato positive samples. To identify and quantify two binucleated ECs we used a semi-automatic customed Fiji macro that identifies whether two or more nuclei are more than 8.5 μm closed. To quantify p-ERK+ cells frequency and intensity we used an automatic Fiji macro that among DAPI+ cells distinguish p-ERK+ positive signal

from the background. For immune cell quantification, total Runx1+CD45+ cells were relativized to the total area. For hepatocyte senescence, p21+ERG- cells with a distinguishable hepatocyte DAPI morphology were counted as senescent hepatocytes. Total number was divided by the total vascular area. Apoptotic cells were measured as the Active Caspase relative to the total area. For quantifications of endothelial clonal dynamic in the liver after *Dll4* deletion, dual color-code clones were identified on large 3D sections. As dual color-code ECs are infrequent among all the single color-code (no other dual color-code in the proximity), cells within the same clone were assumed to proceed from the same progenitor cell.

Western blot analysis

For the analysis of protein expression, liver organs were transferred to a reagent tube and frozen in liquid nitrogen. On the day of the immunoblotting the tissue was lysed with lysis buffer [(Tris-HCl pH=8 20mM, EDTA 1mM, DTT 1mM, Triton X-100 1% and NaCl 150mM, containing protease inhibitors (P-8340 Sigma) and phosphatase inhibitors (Calbiochem 524629) and orthovanadate-Na 1 mM)] and homogenized with a cylindrical glass pestle.. Tissue/ cell debris was removed by centrifugation, and the supernatant was diluted in loading buffer and analysed by SDS–PAGE and immunoblotting. Membranes were blocked with BSA and incubated with primary antibodies listed in Table 3.

Endothelial cell isolation and RNA/DNA extraction

To isolate and profile quiescent ECs with full loss of Dll4, 1 mg tamoxifen was injected for 3 consecutive days to *Tg(Cdh5-CreERT2)*; *Dll4*$^{flox/flox}$ *(Koch et al., 2008; Wang et al., 2010)*. To analyze loss of *Notch1* and *Rbpj*, 2 mg tamoxifen was injected for 5 consecutive days to *Tg(Cdh5-CreERT2)*(Wang et al., 2010); *Tg(iSuRe-Cre)*(Fernandez-Chacon et al., 2019); Notch1flox/flox (Radtke et al., 1999) mice and Tg(Cdh5-CreERT2)(Wang et al., 2010); Tg(iSuRe-Cre)(Fernandez-Chacon et al., 2019); Rbpjflox/flox (Han et al., 2002) mice. As

controls, tamoxifen injected C57BL/6J mice and Tg(Cdh5-CreERT2)(Wang et al., 2010); Tg(iSuRe-Cre) (Fernandez-Chacon et al., 2019); mice were used. At day 14, heart, lung, liver and brain organs were dissected, minced and digested with 2.5 mg/ml of Collagenase (Thermofisher) type I, 2.5 mg/ml Dispase II (Thermofisher) and 50 ng/ml of DNAseI (Roche) at 37ºC for 30 minutes to create a single cell suspension. Cells were filtered through a 70 μm filter to remove non-dissociated tissue. Erythroid cells were removed from cells suspensions with a Blood Lysis Buffer (0.15 M NH4Cl, 0.01M KHCO3 and 0.01 M EDTA in distilled water) incubated for 10 minutes on ice. Cells suspensions were blocked with in DPBS no Ca2+ or Mg2+, containing 3% Dialyzed FBS (Termofisher). For endothelial cell analysis, cells were incubated at 4ºC for 30 minutes with APC conjugated rat anti-mouse CD31 (1:200, BD Pharmigen, 551262). DAPI (5 mg/ml) was added to the cells immediately before Fluorescence Activated Cell Sorting (FACS). FACs was performed using a FACS Aria Cell Sorter (BD Biosciences) and Synergy4L machines. For the isolation of endothelial cells from the dissociated tissues, viable cells were selected by DAPI negative fluorescence. All viable cells were interrogated by examining FSC and SSC to select by size and complexity, and by comparing FSC-H and FSC-W repeated with SSC-H and SSC-W in order to discern single cells. An additional channel lacking any endogenous or fluorescent label was also acquired to detect and exclude autofluorescence. Cells were selected by their APC and/or endogenous MbTomato positive signal and YFP gated with a negative control sample.

For qRT-PCR and Next Generation Sequencing experiments, approximately 10000-20000 cells for each group of DAPI negative APC-CD31+ ECs (for Dll4 loss of function and control), DAPI negative APC-CD31+/MbTomato+ ECs (for Notch1 or Rbpj loss of function and control) and CD31+YFP+ were sorted directly to buffer RLT (RNAeasy Micro kit - Qiagen). RNA was extracted according to the manufacturer instructions and stored at -80C.

For DNA isolation, a minimum of 42.000 cells per sample, were sorted and spin down for 10 minutes at 350g, and resuspended in 50 μl of lysis buffer prepared as follows: 25 μl of DirectPCR (Cell) Lysis Reagent for PCR (VIAGEN Cat #301-C) and 25 μl of distilled water and a final concentration of 0,4 mg/ml of proteinase K. Cells were incubated 55ºC overnight and then the proteinase was inactivated at 85ºC for 45 minutes.

For proteomic analysis, approximately 3000000 cells DAPI negative APC-CD31+ ECs per group were sorted directly to blocking buffer (DBPS no Ca2+ or Mg2+, containing 3% Dialyzed FBS). Cells were spin down for 10 minutes at 350g and stored ad -80ºC.

qRT-PCR and competitive PCR

For quantitative real time PCR (RT-qPCR), 1-2 μl of sorted liver EC RNA was retrotranscribed with the High Capacity cDNA Reverse Transcription Kit with RNase Inhibitor (Thermo fisher, 4368814). cDNA was preamplified with Taqman PreAmp Master Mix containing a Taqman Assay-based pre-amplification pool containing a mix of the following Taqman assays (*Cdh5* (Mm00486938_m1), *Kdr* (Mm01222421_m1), *Rbpj*(Mm01217627_g1) *and Notch1*(Mm00435245_m1). Preamplified cDNA was used for RT-qPCR with the same gene specific Taqman Assays and Taqman Universal Master Mix in a AB7900 thermocycler (Applied Biosystems).

Semi-quantitative and competitive PCR was performed with 1 μl of DNA from the different samples using the primers mentioned in Table 2. Groups of 3 or 4 primers were used per PCR reaction. Some of the PCRs served as control of DNA input, and the others corresponded to the different floxed genes sequences.

Next Generation Sequencing – RNA-seq

Next Generation Sequencing (NGS) experiments were performed in the Genomics Unit of the CNIC. They were performed in different years, and therefore we had to use different protocols and kits.

For *Dll4*^{iDEC} ECs samples, 1 ng of total RNA was used to amplify the cDNA using the SMART-Seq v4 Ultra Low Input RNA Kit (Clontech-Takara) following manufacturer´s instructions. Then, 1 ng of amplified cDNA was used to generate barcoded libraries using the Nextera XT DNA library preparation kit (Illumina). Basically, cDNA is fragmented and adapters are added in a single reaction followed by an amplification and clean up. The size of the libraries was checked using the Agilent 2100 Bioanalyzer High Sensitivity DNA chip and their concentration was determined using the Qubit® fluorometer (ThermoFisher Scientific). Libraries were sequenced on a HiSeq2500 (Illumina) to generate 50 bases single end reads. FastQ files for each sample were obtained using CASAVA v1.8 software (Illumina).

For *Rbpj*^{iDEC} and *Notch1*^{iDEC} ECs samples, between 400 and 3000 pg of total RNA were used to generate barcoded RNA-seq libraries using the NEBNext Single Cell/Low Input RNA Library Prep Kit for Illumina (New England Biolabs) according to manufacturer's instructions. First cDNA strand synthesis was performed, then cDNA was amplified by PCR followed by fragmentation. Next, ends of cDNA were repaired and adenylated. The NEBNext adaptor was then ligated followed by second strand removal, uracile excision from the adaptor and PCR amplification. The size of the libraries was checked using the Agilent 2100 Bioanalyzer and the concentration was determined using the Qubit® fluorometer (Life Technologies). Libraries were sequenced on a HiSeq2500 (Illumina) to generate 60 bases single reads. FastQ files for each sample were obtained using bcl2fastq 2.20 Software software (Illumina).

RNA-seq data analysis

RNA-seq data analysis was performed by the Bioinformatics Unit of CNIC. The number of reads per sample was between 12 and 42 million. Reads were processed with a pipeline that used FastQC (Babraham Insitute- http://www.bioinformatics.babraham.ac.uk/projects/fastqc/) to evaluate their quality, and cutadapt (Martin, 2011) to trim sequencing reads, eliminating Illumina and SMARTer adaptor remains, and to discard reads that were shorter than 30 bp; more than 93% of the reads were kept for any of the samples. Resulting reads were mapped against mouse transcriptome GRCm38.76 and GRCm38.91, and gene expression levels were estimated with RSEM (Li and Dewey, 2011). The percentage of aligned reads was above 83% for most samples. Expression count matrices were then processed with an analysis pipeline that used Bioconductor package limma (Ritchie et al., 2015) for normalization (using TMM method) and differential expression testing, taking into account only those genes expressed with at least 1 count per million (CPM) in at least two samples (the number of samples for the condition with less replicates), and using a random variable to define blocks of samples obtained from the same animal. Seven pairwise contrasts were performed: Heart_KovsWT, Lung_KovsWT, Liver_KovsWT, Brain_KovsWT, Dll4LOFvsWT, RbpjLOFvsWT and RbpjLOFvsWT. Changes in gene expression were considered significant if associated to Benjamini and Hochberg adjusted p-value < 0.05.

Complementary enrichment analyses with GSEA (Subramanian et al., 2005) were performed for each contrast, using the whole collection of genes detected as expressed (12,872 genes) to identify gene sets that had a tendency to be more expressed in either of the conditions being compared. Gene sets, representing pathways or functional categories from the Hallmark, KEGG, Reactome and Biocarta databases, and GO collections from the Biological Process, Molecular Function and Cellular Component ontologies were retrieved from MsigDB (Liberzon et al., 2011). Enriched gene sets with FDR < 0.05% were considered of interest.

For scRNA-seq results, published datasets (Kalucka et al., 2020) available at https://www.vibcancer.be/software-tools/ec-atlas, were used to analyze single cells from the adult mouse liver. To determine the average gene expression of *Dll4, Dll1, Jag1, Notch1, Notch4, Hey1, Efnb2*, *Mfng* and *Lfng* clusters were categorized as described in the publication (capillary, capillary venous, vein, large artery, proliferating, lymphatic). Data analysis was done using Python 2.7 with Seaborn (https://seaborn.pydata.org) and Pandas libraries (https://pandas.pydata.org/).

Liver endothelial cell proteomics

Preparation of protein extracts and on-filter tryptic digestion

Cells were boiled for 10 min in lysis buffer (4% SDS, 50 mM Tris-HCl pH 8.5) supplemented with 50 mM iodoacetamide (Sigma-Aldrich) to block reduced Cys residues (Martinez-Acedo et al., 2012). After centrifugation at 13,000 rpm the supernatants were collected and protein concentration was determined by the RC/DC Protein Assay (Bio-Rad Laboratories).

Samples were subjected to tryptic digestion using the FASILOX method (Bonzon-Kulichenko et al., 2020), a modification of the filter-aided sample preparation (FASP) technology (Expedeon) (Wisniewski et al., 2009) for the study of Cys oxidation. Briefly, the protein extracts (100 µg) were diluted in Urea Sample Solution (USS, 8 M urea in 100 mM Tris-HCl at pH 8.5) and loaded onto the filters. After centrifugation and a washing step with USS, the oxidized Cys residues were reduced with 50 mM DTT (GE Healthcare) in USS for 1 h at room temperature. Then the samples were centrifuged, washed with USS and

subsequently alkylated with 50 mM S-methyl methanethiosulfonate (MMTS) (Thermo Fisher Scientific) in USS for 1 h at room temperature. Thereafter the filters were washed three times with USS and three times with ABC Buffer (50 mM NH4HCO3 at pH 8.8). Proteins were digested using sequencing grade trypsin (Promega) in 1:40 (w/w) trypsin: sample ratio at 37 ºC overnight with gentle agitation.

Multiplexed stable isotope labeling of tryptic peptides

The resulting tryptic peptides were recovered by centrifugation at 10,000 rpm for 5 min after addition of 40 μl of trypsin digestion buffer, after which 50 μl of 500 mM NaCl were added and the filters centrifuged for 15 min at 13,000 rpm. Trifluoroacetic acid was added to a final concentration of 1% and the peptides were desalted on C18 Oasis HLB extraction cartridges (Waters Corporation, Milford, MA, USA) and dried-down. The eluted, cleaned-up peptides were subjected to stable isotope labeling using isobaric tags for relative and absolute quantitation (iTRAQ) 8-plex (AB Sciex) according to the manufacturer's protocol. The six differentially tagged samples were then pooled and desalted on Waters Oasis HLB C18 cartridges.

Peptide fractionation

For peptide fractionation, the labeled sample was separated into five fractions using the high pH reversed-phase peptide fractionation kit (Thermo Fisher Scientific) according to the manufacturer's instructions. Bound peptides were eluted with: 1) 12.5% (v/v) ACN; 2) 15% (v/v) ACN; 3) 17.5% (v/v) ACN; 4) 20% (v/v) ACN; and 5) 50% ACN. The fractions obtained were vacuum-dried and stored at -20 ºC for later use.

Liquid chromatography coupled to tandem mass spectrometry

The tryptic peptide mixtures were subjected to nanoscale liquid chromatography coupled to tandem mass spectrometry (LC-MS/MS). High-resolution analysis of samples was performed on an EASY-nLC 1000 liquid chromatograph (Thermo Fisher Scientific) coupled to a Q Exactive HF (Thermo Fisher Scientific) mass spectrometer. Peptides were suspended in 0.1% formic acid, loaded onto a C18 RP nano-precolumn (Acclaim PepMap100, 75 µm internal diameter, 3 µm particle size and 2 cm length, Thermo Fisher Scientific), and separated on an analytical C18 nano-column (EASY-Spray column PepMap RSLC C18, 75 µm internal

diameter, 3 µm particle size and 50 cm length, Thermo Fisher Scientific) in a continuous gradient: 8-27% B for 240 min, 31-100% B for 2 min, 100% B for 7 min, 100-2% B for 2 min and 2% B for 30 min (where A is 0.1% formic acid in HPLC-grade water and B is 90% ACN, 0.1% formic acid in HPLC-grade water).

Full MS spectra were acquired over the 400-1500 mass-to-charge (m/z) range with 120000 resolution, 2 x 105 automatic gain control and 50 ms maximum injection time. Data-dependent MS/MS acquisition was performed at 5 x 104 automatic gain control and 120 ms injection time, with 2 Da isolation window and 30 s dynamic exclusion. Higher-energy collisional dissociation of peptides was induced with 31% normalized collision energy and analyzed with 35,000 resolution in the orbitrap.

Protein identification based on database searching

Proteins were identified in the raw files using the SEQUEST HT algorithm integrated in Proteome Discoverer 2.1 (Thermo Fisher Scientific). MS/MS scans were matched against the mouse (UniProtKB 2017-07 release) protein database supplemented with pig trypsin and human keratin sequences. For database searching, parameters were as follows: trypsin digestion with maximum 2 missed cleavage allowed, precursor mass tolerance of 800 ppm, and a fragment mass tolerance of 0.02 Da. The N-terminal and lysine iTRAQ 8-plex modifications were chosen as fixed modifications, whereas methionine oxidation, Cys carbamidomethylation, and Cys methylthiolation were chosen as variable modifications. SEQUEST results were analyzed with the probability ratio (pRatio) method (Martinez-Bartolome et al., 2008). The false discovery rate (FDR) was calculated based on the results obtained by database searching against the corresponded inverted database using the refined method (Bonzon-Kulichenko et al., 2015; Navarro and Vazquez, 2009). Quantitative information was extracted from the intensity of iTRAQ reporter ions showing in the low-mass region of the MS/MS spectra (Garcia-Marques et al., 2016).

Statistical analysis of proteomics data

For comparative analysis of protein abundance changes, we applied the SanXoT software package (Trevisan-Herraz et al., 2019), designed for the statistical analysis of high-throughput, quantitative proteomics experiments and based on the Weighted Scan-Peptide-Protein (WSPP) statistical model (Navarro et al., 2014) . As input, WSPP uses a list of quantifications in the form of log2-ratios (each cell sample versus the mean of the three WT

cell samples) with their statistical weights. From these, WSPP generates the standardized forms of the original variables by computing the quantitative values expressed in units of standard deviation around the means (Zq). Known artifact proteins such (keratin contaminants and trypsin) were excluded from the data sets after the analysis.

For the study of coordinated protein alterations, we used the Systems Biology Triangle (SBT) model, which estimates functional category averages (Zc) from protein values by performing the protein-to- category integration, as described (Garcia-Marques et al., 2016) . The protein category database was built up using annotations from the Gene Ontology (GO) database.

Statistical analysis

Two groups of samples with a Gaussian distribution were compared by unpaired two-tailed Student *t*-test. Comparisons among more than two groups were made by ANOVA followed by the Turkey pairwise comparison. Graphs represent mean +/- SD as indicated, and differences were considered significant at $p < 0.05$. All calculations were done in Excel and final datapoints analysed and represented with GraphPad Prism. No randomization or blinding was used, and animals or tissues were selected for analysis based on their genotype, the detected Cre-dependent recombination frequency, and quality of multiplex immunostaining. The sample size was chosen according to the observed statistical variation and published protocols.

Data availability

All other data supporting the findings of this study are available from the corresponding author upon request. This includes additional raw data such as unprocessed original pictures and independent replicates, which are not displayed in the thesis, but are included in the data analysis in the form of graphs.

RESULTS

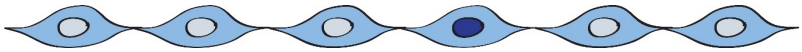

Chapter I:

The role of Notch signalling members in the regulation of organ-specific vascular homeostasis

Notch signalling is active in quiescent endothelial cells of several organs

Although previous studies have shown the expression of the Notch ligands and receptors in the endothelial compartment during angiogenesis or in quiescent vessels of a few organs (Aird, 2007; Claxton and Fruttiger, 2004; Del Monte et al., 2007; Favre et al., 2003; Hofmann and Iruela-Arispe, 2007; Jabs et al., 2018; Limbourg et al., 2005; Nolan et al., 2013; Phng and Gerhardt, 2009; Villa et al., 2001) none of them analysed in a quantitative and comparative manner their organ-specific endothelial expression and signalling heterogeneity. In order to quantitatively characterize the expression of all Notch signalling components in adult quiescent endothelial cells, and in an organ-specific fashion, we sought to analyse by bulk RNA-seq the transcriptome of endothelial cells (ECs; CD31+) isolated by FACS from several vascular beds such as heart, lung, liver and brain endothelium (Figure 5A,B). Heart and lung samples were analysed in biological triplicates and brain and liver samples were analysed in biological duplicates based on a preliminary clustering analysis test. Consistent with the previous studies describing transcriptional vascular heterogeneity by microarrays (Nolan et al., 2013), an unsupervised hierarchical clustering analysis of the differentially expressed genes (DEGs) confirmed that the EC replicates derived from each organ clustered together and several genes were expressed in the endothelium in an organ-specific manner. Gene Ontology (GO) enrichment analysis revealed categories related with the organ or its specific functions (Figure 5C). As examples, liver ECs were distinguished by the expression of genes having a role as immunoregulators given their exposure to antigens derived from the gastrointestinal tract and brain ECs by the expression of transmembrane transporters specific to the blood-brain-barrier functions. As expected, some of these functions have already been described in the literature (Shetty et al., 2018; Sweeney et al., 2019). Overall, these results, obtained with wild type samples, provide a resource for the comparative expression of endothelial genes across different organs and demonstrate the accuracy of our cell labelling, isolation and gene expression profiling techniques. Having confirmed our gene expression dataset, we next evaluated the expression of Notch signalling components in different vascular beds. We found that all Notch ligands, receptors, co-factors and modulators are expressed in all the characterized vascular beds: heart, lung, liver and brain ECs (Figure 5D). This analysis also revealed that Dll4 and Notch1 are the ligand/receptor combination most expressed in ECs of all organs analysed. This data is consistent with previous studies showing that Dll4 and Notch1 are the most important ligand and receptor pair for activation of Notch signalling and vascular development (Duarte et al., 2004; Krebs et al., 2004). Given the bulk RNA-seq

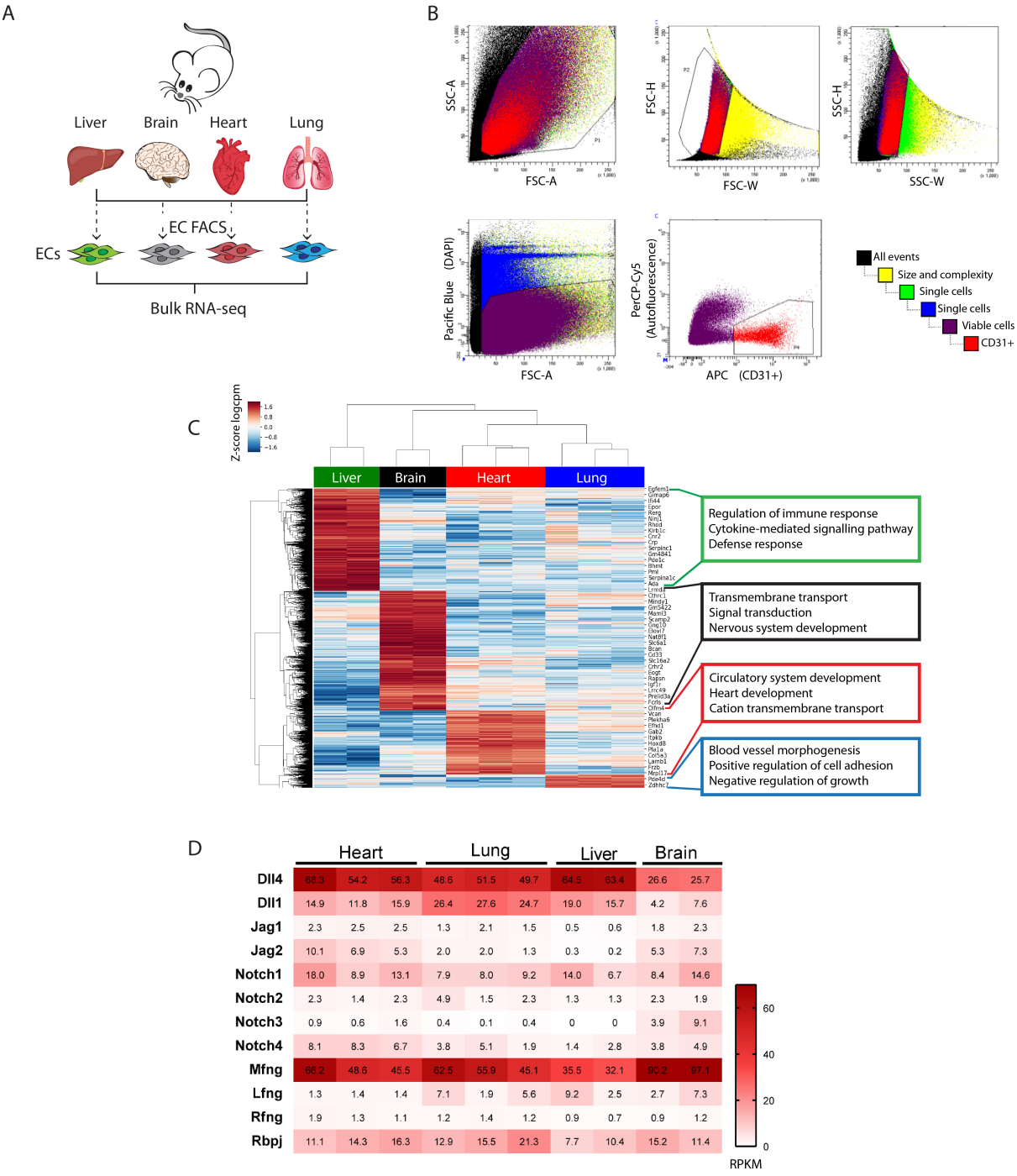

Figure 5: ECs from different vascular beds have a tissue-specific gene expression profile. **(A)** Schematic representation to illustrate the bulk RNA-seq experiment performed with adult ECs isolated by FACS from heart, lung, liver and brain. **(B)** Representative FACS plots to show the EC gating strategy. The detectors, dyes and fluorophores are indicated in the X and Y-axes. **(C)** Unsupervised hierarchical clustering with a list of differentially expressed genes in different organ ECs. Z-score logcpm: Z-score of the logarithmic counts per million. Bars red color indicates upregulation and blue color downregulation. Gene Ontology enrichment analysis (right boxes) reveals enriched gene sets. **(D)** Heatmap with Notch pathway members RNA-seq RPKM (Reads per kilo base per million mapped reads) from different vascular beds points to Dll4/Notch1 as the main ligand/receptor.

results, we next generated *Dll4 floxed Cdh5(PAC)-CreERT2* mice, allowing us to conditionally delete *Dll4* only in the adult vasculature (Cdh5+) and analyse the consequence of the loss of Dll4/Notch signalling specifically in quiescent ECs (Figure 6A). The tamoxifen-driven endothelial deletion of *Dll4* in adult mice (*Dll4*^{iDEC}) was very efficient and resulted in the absence of Dll4 ligand (protein) expression in the large majority of organ ECs evaluated (Figure 6B). We next sought to determine the level of Notch1 signalling activity in the different vascular beds with or without Dll4 expression. The cleaved Notch1 intracellular domain epitope (N1ICD, V1744) is generated only upon Notch activation and has been detected in ECs during developmental angiogenesis (Del Monte et al., 2007), *in vitro* (Mack et al., 2017) and in the adult heart (Jabs et al., 2018) by tyramide-amplification based immunohistochemistry in paraffin sections. Using this method, we found that Notch1 signalling is active in ECs of all organs analysed (heart, lung, liver and brain). Deletion of *Dll4* significantly reduced the activation of Notch1 in most vascular beds (Figure 7A, B). Taken together, our results show that Notch1 signalling is active in the quiescent adult endothelium of several organs and that Dll4 is its major functional ligand, even though quiescent ECs also strongly express other Notch ligands.

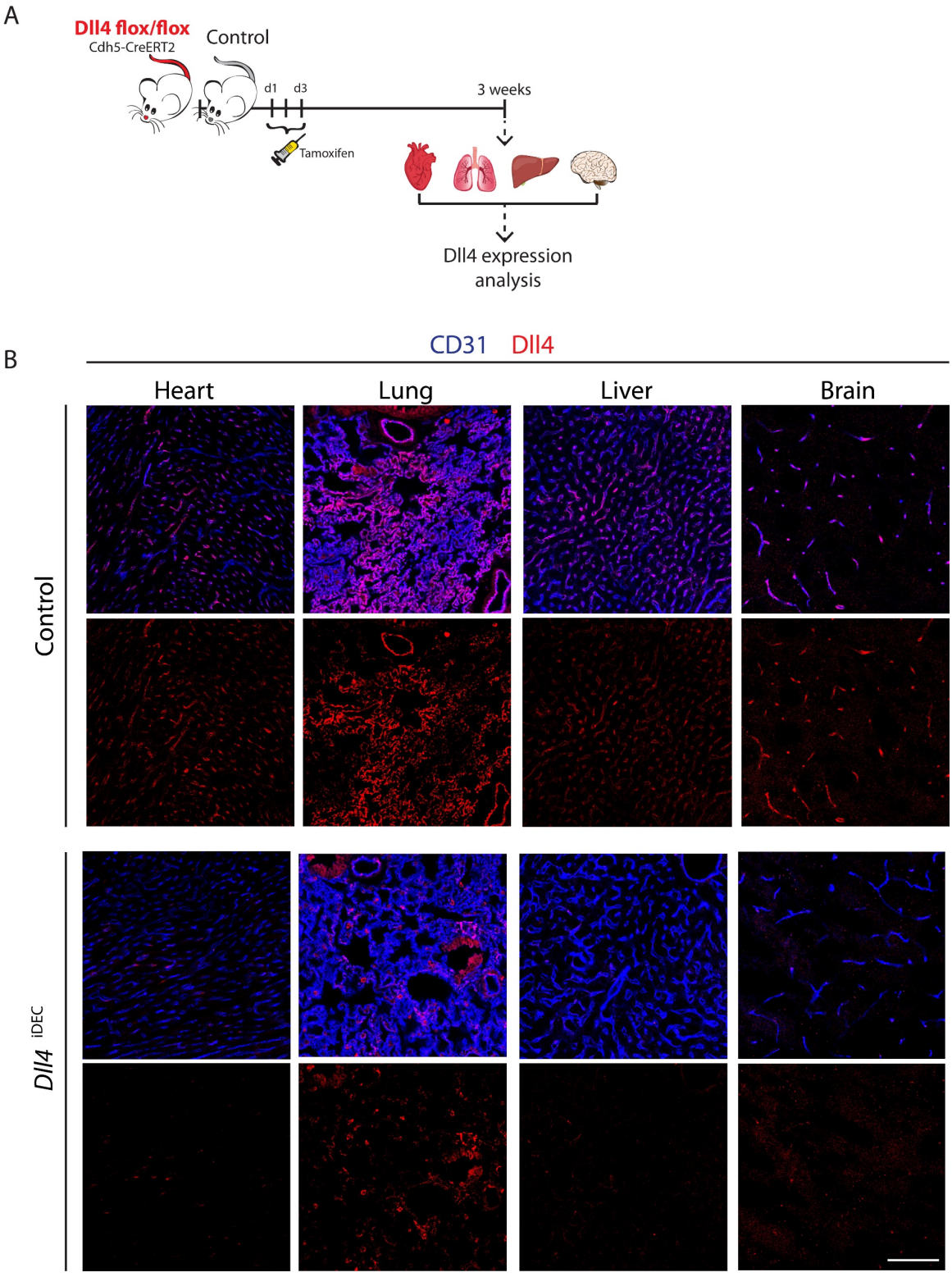

Figure 6: The ligand Dll4 is expressed in heart, lung, liver and brain endothelium. (A) Experimental layout for the inducible deletion of Dll4 (*Dll4*^{iDEC}) in Cdh5+ ECs. *Cdh5(PAC)-CreERT2 Dll4* floxed adult mice received three intraperitoneal injections of tamoxifen as did age-matched control mice. 3 weeks after the first tamoxifen injection, mice were sacrificed and heart, lung, liver, brain were evaluated for Dll4 expression. **(B)** Confocal micrographs showing that Dll4 is specifically expressed in heart, lung, liver and brain quiescent endothelium (CD31+). Tamoxifen-driven *Dll4* deletion efficiently abrogates Dll4 protein in most ECs of all organs analysed. Scale bars, 100 μm

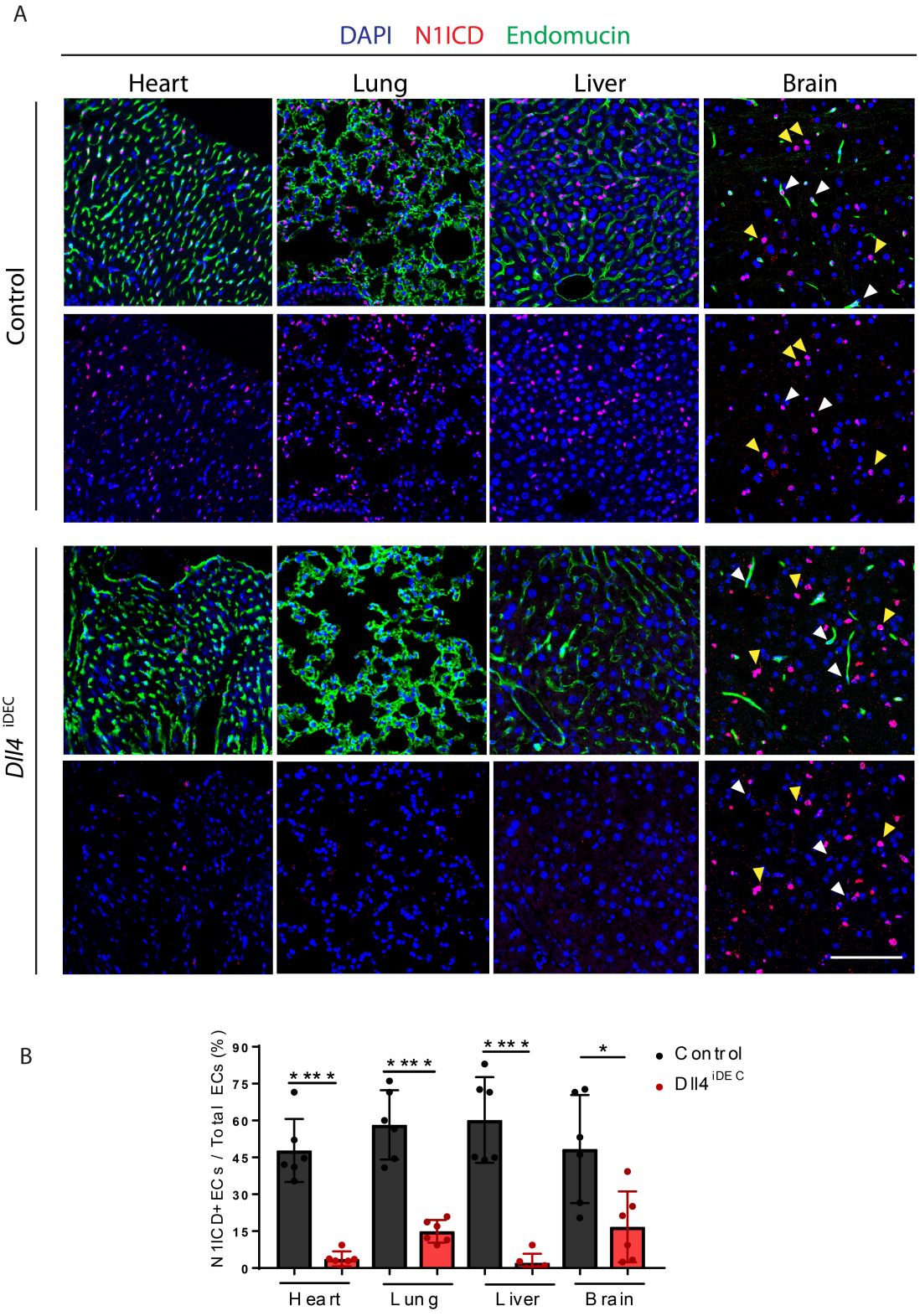

Figure 7: Dll4/Notch1 signalling is active in heart, lung, liver and brain endothelium. (A-B) Confocal micrographs showing that Notch1 signaling is active (N1ICD+) in heart, lung, liver and brain quiescent endothelium (DAPI+Endomucin+). Quantification chart of Notch1 activation frequency in quiescent ECs (N1ICD+DAPI+Endomucin+) shows that *Dll4* deletion significantly reduces Notch1 activity in all quiescent vascular beds. In brain micrographs, white arrowheads indicate ECs and yellow arrowheads non-ECs. Note that whereas N1ICD is maintained in non-ECs, most N1ICD signal disappears from the ECs in *Dll4*^{iDEC} brains (n=3 animals per group). Scale bars, 100 μm. Error bars indicate SD. *$p < 0.05$. ****$p < 0.0001$.

Dll4 deletion leads to cell cycle entry and hyperproliferation of liver and heart ECs

To understand the role of Dll4/Notch1 signalling in the homeostasis of the quiescent endothelium, we analysed the vasculature of several organs in control and *Dll4*^{iDEC} mice 3 weeks after tamoxifen injection (Figure 8A). Despite the relatively short window of treatment, *Dll4*^{iDEC} mice displayed an increase in heart weight and size (Figure 8B,C), together with a strikingly affected liver when compared to control mice. Gross examination of the liver showed a remarkable change in the normal liver morphology. While some regions of the liver parenchyma were discoloured, other areas seemed to have vascular congestion. Hematoxylin and eosin (H&E) staining revealed histopathological changes and sinusoidal dilation as previously described (Figure 8D)(Yan et al., 2010). In agreement with previous studies (Cuervo et al., 2016; Dill et al., 2012; Dou et al., 2008; Jabs et al., 2018; Yan et al., 2010), we found an increase in blood vessel density and capillary enlargement both in the heart and the liver. However, this increase was specific to these organs, and it was not observed in the brain (Figure 9A,B). We could not quantify the capillary width in the lung because of the high EC density in this organ, but no major differences were observed. To obtain detailed insight into the endothelial structure in *Dll4*^{iDEC} mice, we developed a thick vibratome section immunofluorescence protocol that enabled us to perform 3D imaging of large organ volumes. Further supporting the increase in blood vessel density seen on thin sections, 3D imaging of vibratome sections revealed the expansion of the endothelial compartment in heart and liver of *Dll4*^{iDEC} mice with the consequent reduction of the neighbouring parenchymal space (Figure 9C). We did not observe any morphological change in the brain endothelium. Unfortunately, due to technical difficulties in processing the lung samples in the vibratome, we were not able to obtain 3D images of this organ.

The current view in the vascular biology field is that the Dll4/Notch signalling pathway in general inhibits endothelial sprouting and proliferation (Phng and Gerhardt, 2009; Potente et al., 2011). More recently, we have shown that this depends on the mitogenic context, such that when angiogenesis is active, Notch activity sustains EC proliferation, whereas in more quiescent ECs it supresses EC proliferation (Pontes-Quero et al., 2019). However, this study was performed during retina blood vessel development and there is less consensus on the role of Notch signalling pathway in the quiescent endothelium of distinct organs. While some studies have reported that the increase in blood vessel density after Notch inhibition in quiescent ECs is associated to an increase in endothelial proliferation (Dill et al., 2012; Dou

et al., 2008; Yan et al., 2010), others suggest that the vascular phenotypes observed are not due to an increase in proliferation (Cuervo et al., 2016; Jabs et al., 2018). In addition, the few reports supporting that Notch signalling acts as an EC proliferation inhibitor in quiescent ECs, mostly rely on gene expression and vascular surface density data (Cuervo et al., 2016; Dou et al., 2008; Yan et al., 2010) and have relatively poor resolution. To address whether homeostatic endothelial Notch signalling in fact inhibits EC proliferation in the adult vasculature, we analysed the total number of ECs (nuclei ERG+ cells) and the expression of the cell cycle marker Ki67 in the nuclei of ECs (ERG+ cells) in control and *Dll4*^{iDEC} mice (Figure 10A). Ki67 labels all cells in cycle (G1/S/G2/M) and is quantitatively superior to S-phase (EdU) or mitosis (PH3) markers. In the absence of *Dll4*, we observed a significant increase in the number of ERG+ ECs in heart and liver, but not in lung or brain ECs (Figure 10B). This 2-fold increase in cell number was associated with a 9- and 13-fold increase in the proportion of proliferating ECs (Ki67+ERG+/ERG+) in heart and liver vessels, respectively (Figure 10C). These findings indicate that despite the Dll4/Notch signalling pathway being active in the ECs of all organs analysed, only in some of these (heart and liver) does it play an essential role in the maintenance of vascular quiescence.

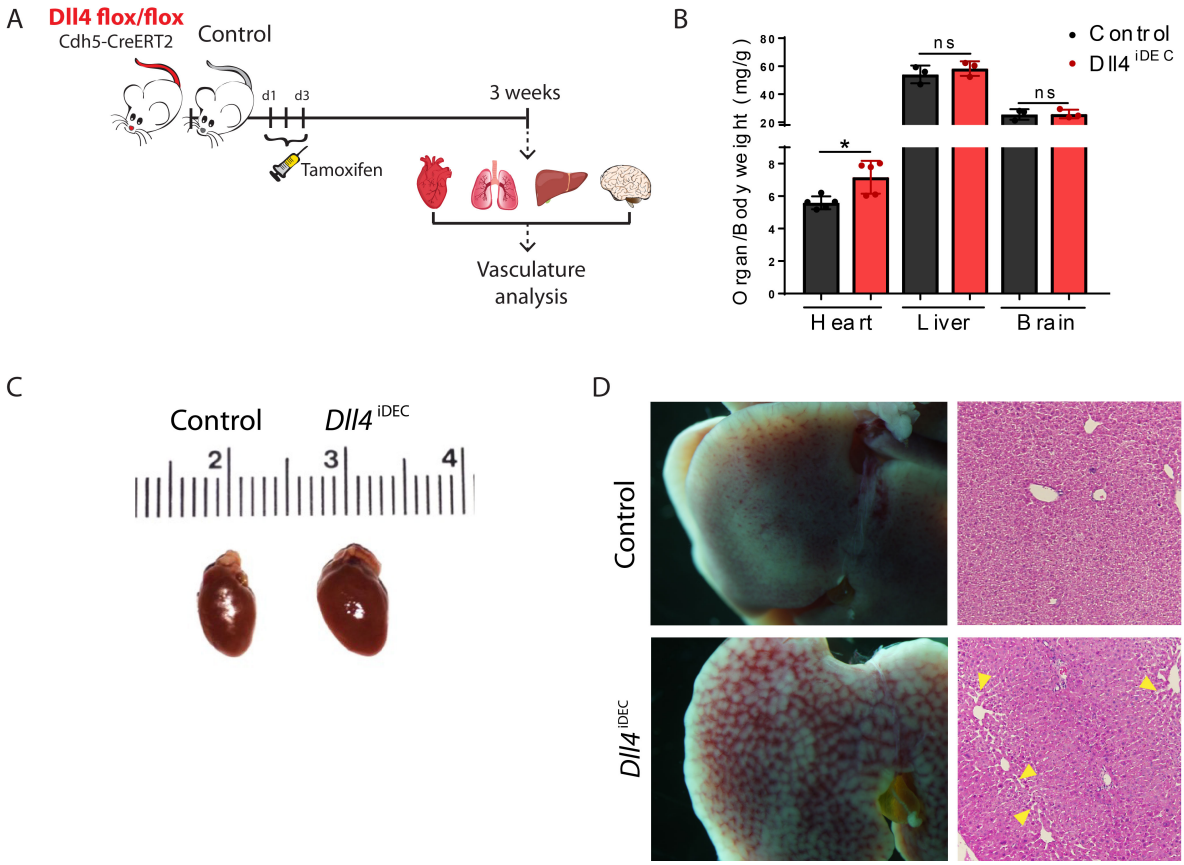

Figure 8: Deletion of *Dll4* in quiescent endothelium strongly affects heart and liver homeostasis. (A) Experimental layout for the inducible deletion of *Dll4* (*Dll4*^{iDEC}) in Cdh5+ ECs. *Cdh5(PAC)-CreERT2 Dll4* floxed adult mice received three intraperitoneal injections of tamoxifen as did age-matched control mice. 3 weeks after the first tamoxifen injection, mice were sacrificed and heart, lung, liver, brain were evaluated. **(B)** Hearts from *Dll4*^{iDEC} mice have an increase in weight (n=3-5 animals per group). **(C)** Representative image of the increase in heart size in *Dll4*^{iDEC} mice compared with control hearts. **(D)** Livers from control and *Dll4*^{iDEC} mice (left panel) showing gross morphological changes in mutants. Representative H&E images of liver sections from control and *Dll4*^{iDEC} mice (right panel). Arrowheads indicate enlarged vessels and sinusoidal dilation in mutants. Error bars indicate SD. *p < 0.05. ns, non-significant.

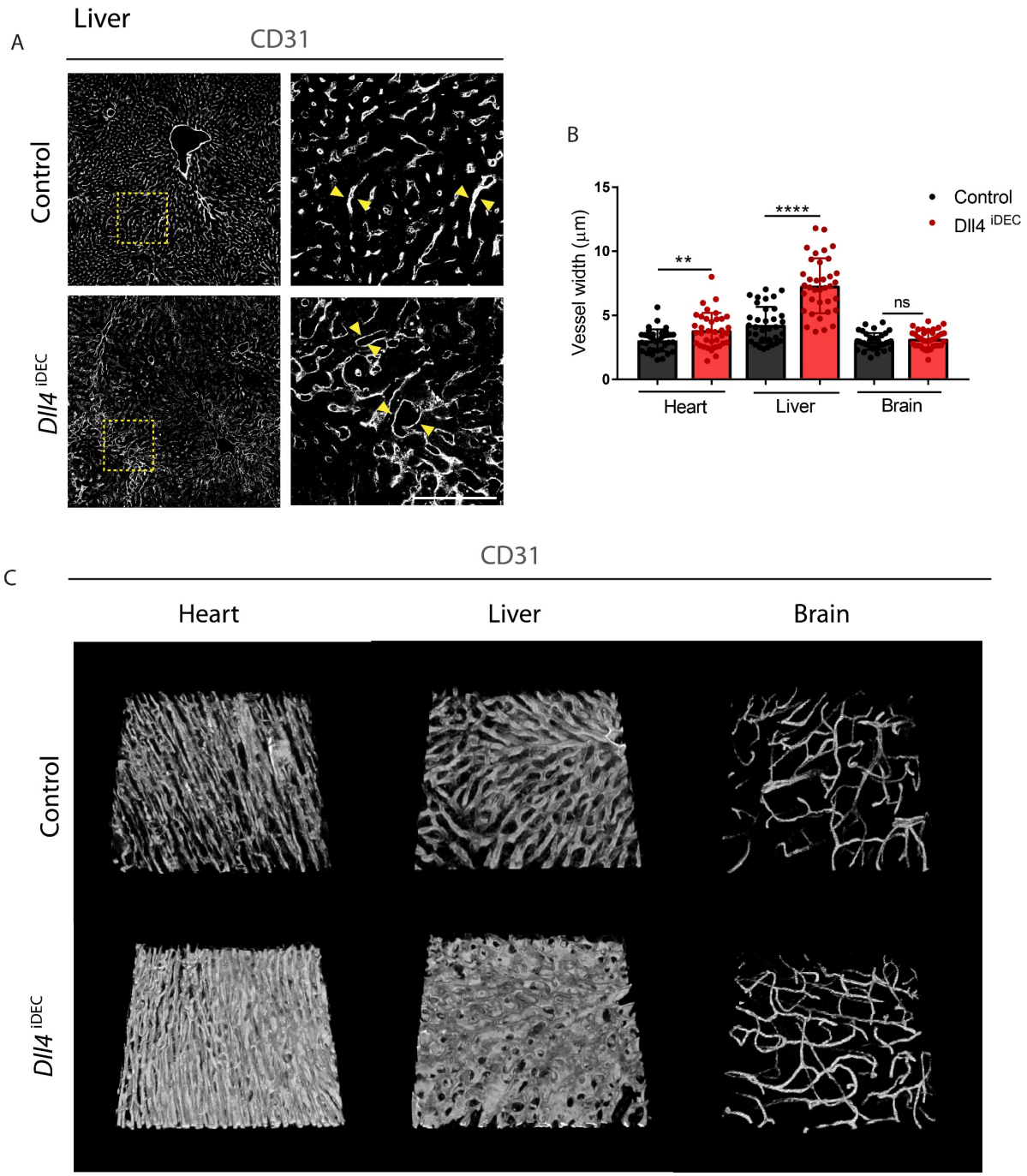

Figure 9: Deletion of *Dll4* leads to an increase in heart and liver vessel density but not in brain. (A) Confocal micrographs of liver sections showing dilated endothelium (CD31+) in *Dll4*^{iDEC} mice. Yellow dotted rectangle within left panel is to highlight the location of high-magnification images in right panel. Arrowheads in right panel show the increase in vessel width (larger lumen). **(B)** Quantification of vessel width in *Dll4*^{iDEC} and control mice shows a significant increase in heart and liver but not in brain (n=3 animals per group). **(C)** 3D reconstruction images from thick vibratome sections clearly show the increase in vessel density due to the expansion of the endothelial compartment (CD31+) in *Dll4*^{iDEC} heart and liver but not in brain. Parenchymal space is also reduced in *Dll4*^{iDEC} mutant hearts and livers. Scale bars, 100 μm. Error bars indicate SD. **p < 0.01. ****p < 0.0001. ns, non-significant.

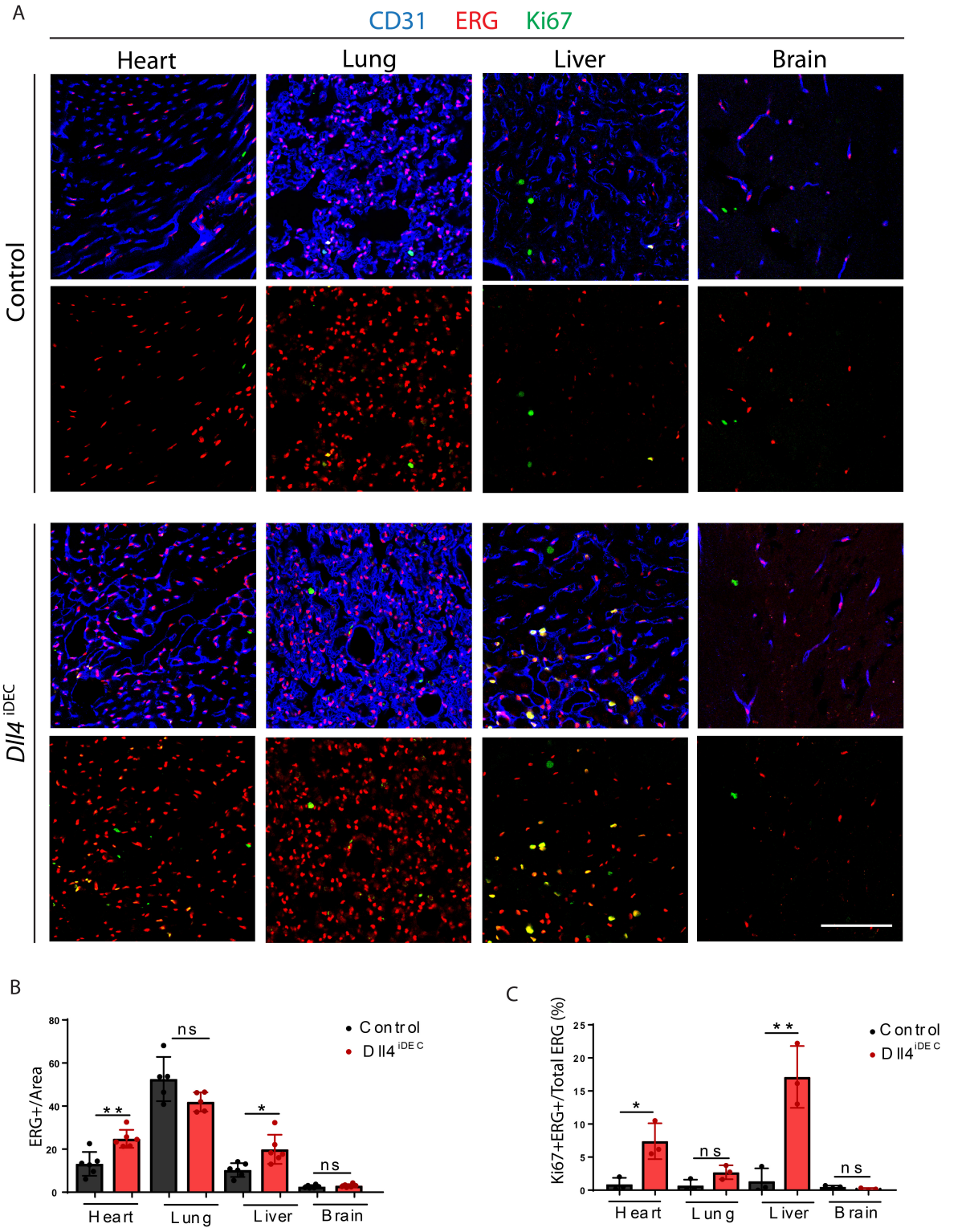

Figure 10: *Dll4*^{iDEC} mutants have an increase in EC density and proliferation only in the heart and liver, but not in lung and brain. **(A-C)** Confocal micrographs of heart, lung, liver and brain sections showing that deletion of *Dll4* results in an increase in EC density (ERG+ cells) and EC proliferation (Ki67+ERG+ cells) in heart and liver, but not in lung and brain, as depicted in charts B and C (n=3 animals per group). Scale bars, 100 μm. Error bars indicate SD. *p < 0.05. **p < 0.01. ns, non-significant.

Transcriptomic analysis after the loss of Dll4/Notch signalling in quiescent ECs of several organs

The data above suggests that Notch signalling is crucial to sustain the quiescence of the endothelium in an organ-specific manner. This is in accordance with the concept of vascular heterogeneity and organotipicity and may be explained by the different gene expression profile, microenvironment and functions of each organ vascular bed. To further understand the molecular mechanisms regulated by Dll4/Notch signalling in each of these vascular beds, we performed bulk RNA-seq of heart, lung, liver and brain ECs from *Dll4*^{iDEC} mice after 2 weeks of *Dll4* deletion (Figure 11A). Although we previously corroborated the absence of Dll4 protein and the concomitant reduction in the activation of the Notch pathway by N1ICD V1744 immunostaining, we now confirmed also at the transcriptomic level that *Dll4* was efficiently deleted and that the Notch canonical targets were downregulated in most organ ECs, with exception of the lung endothelium, in which deletion was not complete (Figure 11B, C). By performing gene set enrichment analysis (GSEA) we found that liver ECs had the most significant upregulation of genes and number of gene sets related with cell proliferation and metabolism (E2F targets, G2M Checkpoint, Myc and oxidative phosphorylation targets) (Figure 11D). As an example, we can see that Myc targets are strongly upregulated in liver ECs after *Dll4* deletion but not as much in heart, lung or brain ECs (Figure 11E). These transcriptomic results in general correlate with the significant increase in EC proliferation observed in livers from *Dll4*^{iDEC} mice and the absence of a proliferative response in the lung endothelium (Figure 10C). However, it is interesting to see that even though the brain and heart endothelium show a significant upregulation of cell cycle and metabolism genes, they differ significantly in their vascular phenotype and proliferative response after *Dll4* deletion (Figure 9 and Figure 10).

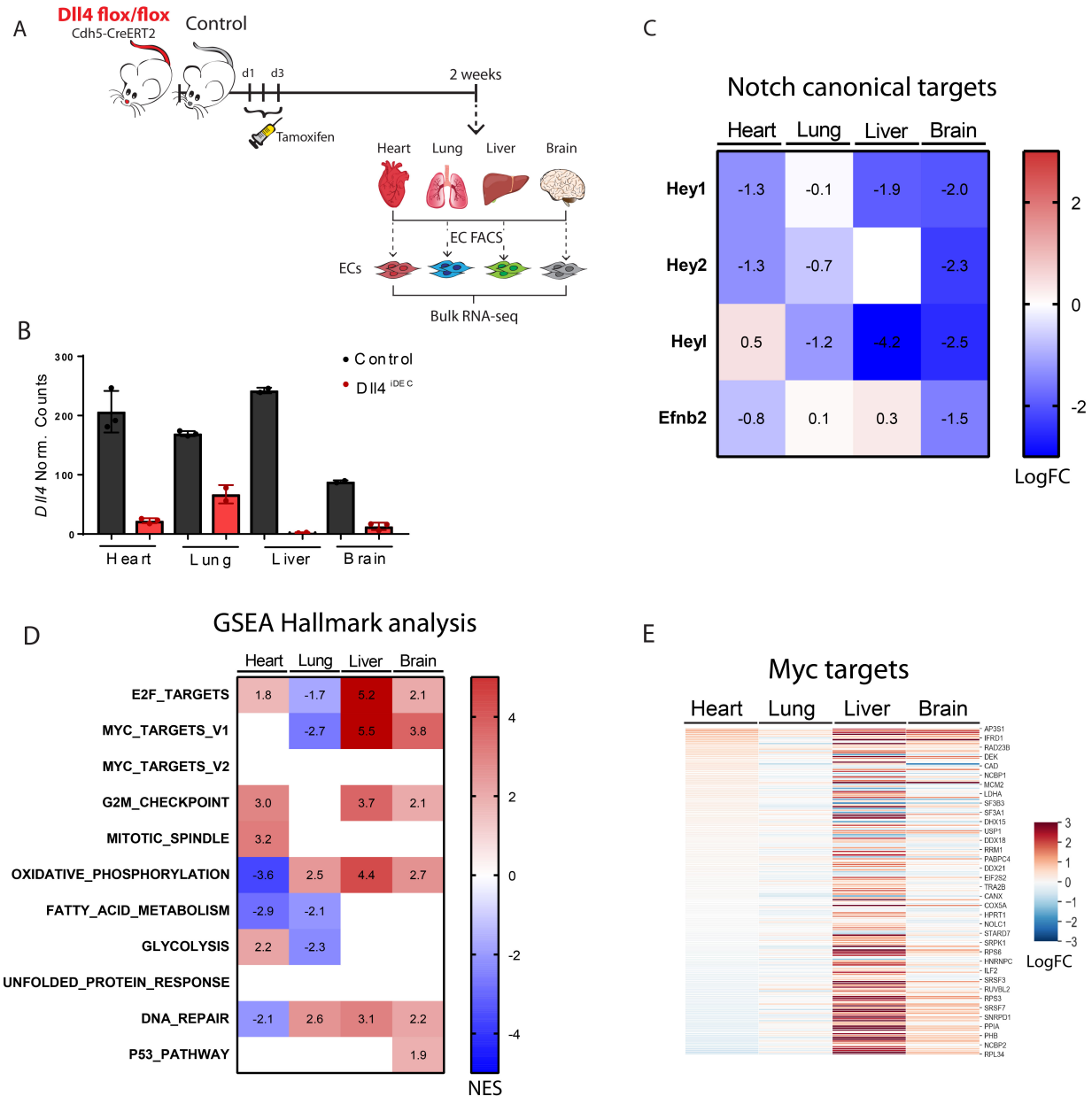

Figure 11: Cell cycle and metabolic pathways are specifically activated in liver ECs after loss of *Dll4*. **(A)** Schematic representation to illustrate the bulk RNA-seq experiment performed with adult ECs isolated by FACS from *Dll4*^{iDEC} and control heart, lung, liver and brain. *Cdh5(PAC)-CreERT2 Dll4* floxed adult mice received three intraperitoneal injections of tamoxifen as did age-matched control mice. 2 weeks after the first tamoxifen injection, mice were sacrificed and heart, lung, liver and brain tissues were used for the experiment. **(B)** *Dll4* expression (normalized counts) in *Dll4*^{iDEC} and control ECs. **(C)** LogFC heatmap showing that most Notch canonical target genes are downregulated after *Dll4* deletion. **(D)** Heatmap with the Normalized Enrichment Score (NES) from significant hallmark analysis (FDR q-val<0.05) by GSEA in *Dll4*^{iDEC} heart, lung, liver and brain ECs compared to control. *Dll4*^{iDEC} liver ECs present a more pronounced enrichment of gene sets related to cell cycle and metabolism. **(E)** LogFC heatmap showing a strong upregulation of Myc targets (from MSigDB Hallmark collection) in *Dll4*^{iDEC} liver ECs compared to the other organ ECs. LogFC: Logarithmic Fold Change. Heatmap red color indicates upregulation and blue color downregulation.

Differentially expressed proteins after the loss of Dll4/Notch signalling in liver ECs

To further characterize the molecular mechanisms deregulated by *Dll4* deletion in liver ECs, we performed a proteomic analysis by liquid chromatography coupled to tandem mass spectrometry (LC-MS/MS) with 3 million of liver ECs per sample isolated by FACS from *Dll4*^{iDEC} and control mice (Figure 12A). We found a significant deregulation of 109 proteins such as ribosomal proteins (*Rpl*), mini chromosome maintenance complexes (*Mcm*) or fatty acid binding proteins (*Fabp*) (Figure 12B). Similarly to the RNA-seq results, GSEA obtained from LC-MS/MS also revealed a significant upregulation of proteins related with cell proliferation and metabolism (Figure 12C). We also discovered an enrichment in processes that were not observed in the RNA-seq GSEA. Among those, we found a deregulation in genes related with fatty acid metabolism, which is in line with previous reports (Jabs et al., 2018). Interestingly, Myc target genes were upregulated and appeared as the gene set with the highest enrichment score (Figure 12C,D). Myc is the most relevant regulator of cell proliferation in most cell types, including in ECs (Kress et al., 2015; Meyer and Penn, 2008). Although at the RNA level we detected a significant increase in *Myc* expression in *Dll4*^{iDEC} liver ECs (Figure 12E), Myc protein was not detected in our proteomic assay. However, we validated its upregulation after *Dll4* deletion in liver ECs by immunostaining control and *Dll4*^{iDEC} livers for Myc (Figure 12F). In addition, a significant enrichment in ribosome and translation processes, together with a significant upregulation of proteins whose expression is regulated by the Myc/Max heterodimer complex corroborated Myc activation (Fisher et al., 1993; Kress et al., 2015) (Figure 12G). Thus, our results suggest that the Myc pathway is one of the most tightly and specifically repressed by the Notch signalling pathway in liver ECs in order to maintain their quiescence and vascular homeostasis.

The results above suggest that after *Dll4* deletion, the endothelium of only some organs, such as heart and liver, reactivates and proliferates abnormally. Although we have identified Myc pathway as a direct Notch driver of EC proliferation in *Dll4*^{iDEC} liver ECs, the non-proliferating phenotype of lung and brain ECs or the milderer hiperproliferation in heart ECs remains poorly understood. To address these different phenotypes, we performed an in-depth analysis of our RNA-seq.

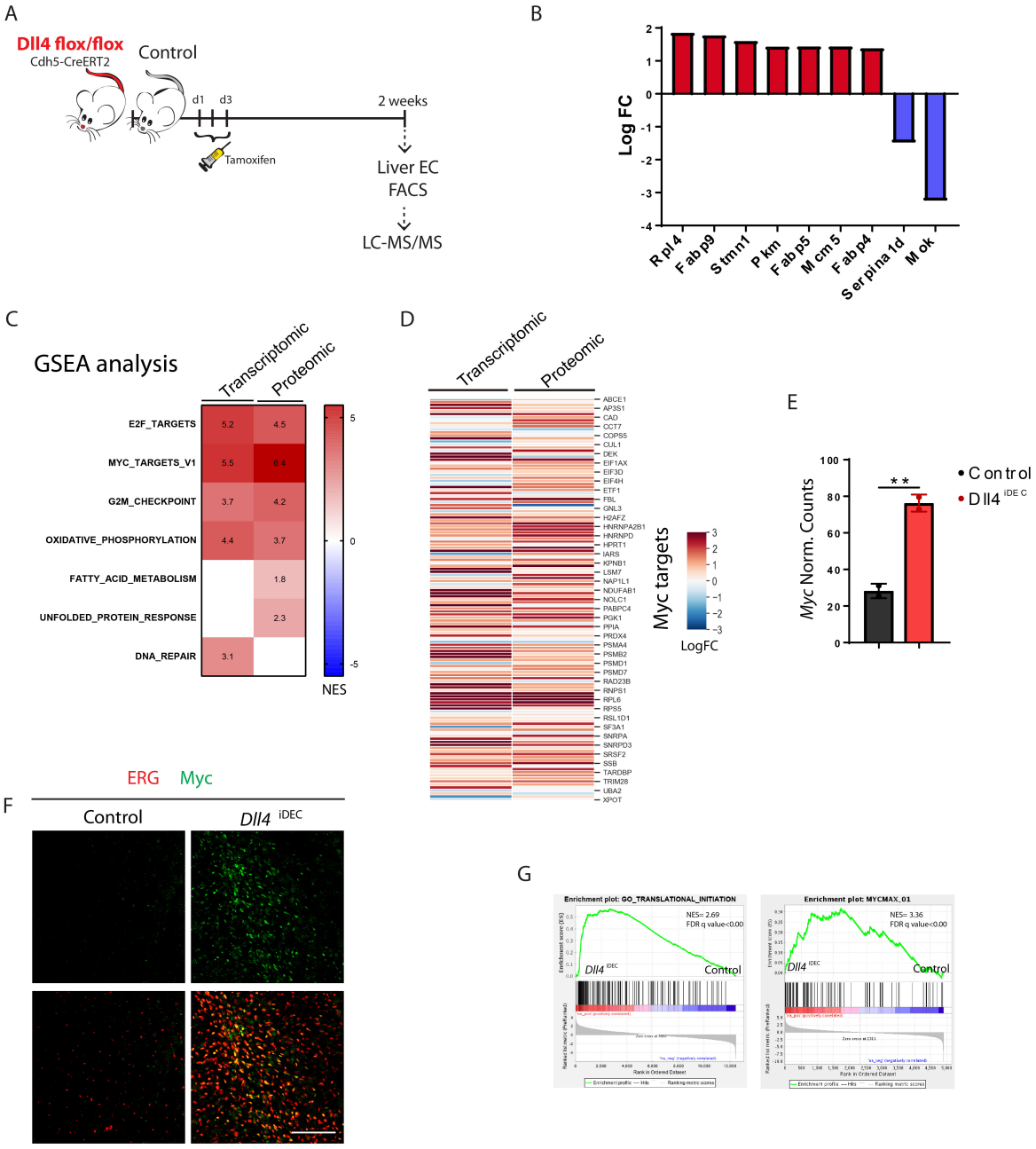

Figure 12: Transcriptomic and proteomic analysis point to Myc protein as tightly repressed Dll4/Notch signalling target specifically in liver quiescent ECs. (A) Schematic representation to illustrate the LC-MS/MS experiment performed with adult ECs isolated by FACS from *Dll4*^{iDEC} and control livers. *Cdh5(PAC)-CreERT2 Dll4* floxed adult mice received three intraperitoneal injections of tamoxifen as did age-matched control mice. 2 weeks after the first tamoxifen injection, mice were sacrificed and liver tissues were used for the experiment. **(B)** List of some of the most statistically up- and downregulated proteins (from a total of 109) after *Dll4* deletion in liver quiescent ECs for 2 weeks. **(C)** Transcriptomic and proteomic GSEA Hallmark analysis show correlation in cell cycle signatures enrichment. Myc pathway is the most upregulated pathway at proteomic and transcriptomic level. NES: Normalized Enrichment Score. **(D)** LogFC heatmap showing a strong upregulation at the transcriptomic and proteomic level of Myc targets (from MSigDB Hallmark collection) in *Dll4*^{iDEC} liver ECs. **(E)** *Myc* expression (normalized counts) in *Dll4*^{iDEC} and control ECs. **(F)** Confocal micrographs of liver sections showing that Myc protein is upregulated in ECs (ERG+ cells) after *Dll4* deletion. **(G)** GSEA GO transcriptomic and transcription factor proteomic analysis in *Dll4*^{iDEC} liver ECs reveal a significant enrichment in translation processes and Myc/Max related proteins. NES: Normalized Enrichment Score. Scale bars, 100 μm. Heatmap red color indicates upregulation and blue color downregulation. LogFC: Logarithmic Fold Change. Error bars indicate SD. $^{**}p < 0.01$

Possible genetic compensation mechanisms in lung and brain ECs after loss of Dll4/Notch signalling

GO enrichment analysis of wild type ECs from different organs, revealed that the expression of negative regulators of endothelial growth are specifically enriched in lung ECs (Figure 5C). Lung ECs had a clear enrichment of genes like *Acvrl1* (*Alk1*) and *Fgfr3* that have been described to stabilize the quiescent endothelium before (Murakami et al., 2008; Roman and Hinck, 2017) and whose expression did not change after *Dll4* deletion (Figure 13A). Lung ECs also showed an enrichment in cell adhesion genes (Figure 5C), which are essential key players in vessel stabilization (Carmeliet and Jain, 2011). This enrichment was clearly not observed in any other organ ECs (Figure 13B). The brain endothelium is also known to have tight cellular junctions due to the BBB. In contrast to the lung and brain, the liver endothelium is known to be discontinuous, and has a lower expression of cell adhesion genes, and these are particularly downregulated after *Dll4* deletion, which may partially explain the hyperproliferative response of liver ECs. In $Dll4^{iDEC}$ heart ECs, where the increase in endothelial proliferation was milder, we also found that cell adhesion genes were significantly enriched after *Dll4* deletion (Figure 13C). The different expression levels of cell adhesion-related genes might partially explain the different degree of proliferative response in heart and liver *Dll4* deficient ECs. A combination of an increase in cell cycle signatures (Figure 11D) and downregulation of cell adhesion genes (Figure 13C) may explain the different organ-specific responses in cell proliferation. Interestingly, we also observed an enrichment in the expression of the p53 tumor suppressor pathway related genes (Horn and Vousden, 2007) specifically in $Dll4^{iDEC}$ brain ECs (Figure 13D). This suggests a potential p53-related compensatory mechanism in brain ECs, which may block or counteract the effect of *Dll4* deletion and the observed upregulation of the cell cycle and metabolic genes in this vasculature.

Other possible explanation for the differential phenotypic compensation in Dll4 mutant vascular beds, could be related with the differential expression of other Notch ligands in some organ vascular beds. Gene expression analysis of the different Notch signalling components revealed a strong upregulation of the *Dll1* ligand in $Dll4^{iDEC}$ lung ECs but not in $Dll4^{iDEC}$ ECs of other organs (Figure 13E), suggesting the existence of a possible lung-endothelium-specific compensatory mechanism among these homologous Notch ligands. In line with this, GSEA analysis showed a significant enrichment in positive effectors and regulators (such as *Dll1, Notch1, Notch4, Lfng and Mfng*) of the Notch signalling pathway in lung ECs (Figure 13F).

Both *Lfng* and *Mfng* positively modulate Notch signalling activity by favouring Delta-ligand-mediated signalling while inhibiting signalling mediated by Jagged ligands (Benedito et al., 2009; Panin et al., 1997; Yang et al., 2005). Although we previously observed a significant downregulation of N1ICD immunostaining in *Dll4*^{iDEC} lung ECs (Figure 7), a method that only detects the cells with highest Notch activity, we hypothesize that this genetic compensation, and the residual basal/non-detectable higher Notch activity might be able to support the quiescence of *Dll4*^{iDEC} lung ECs.

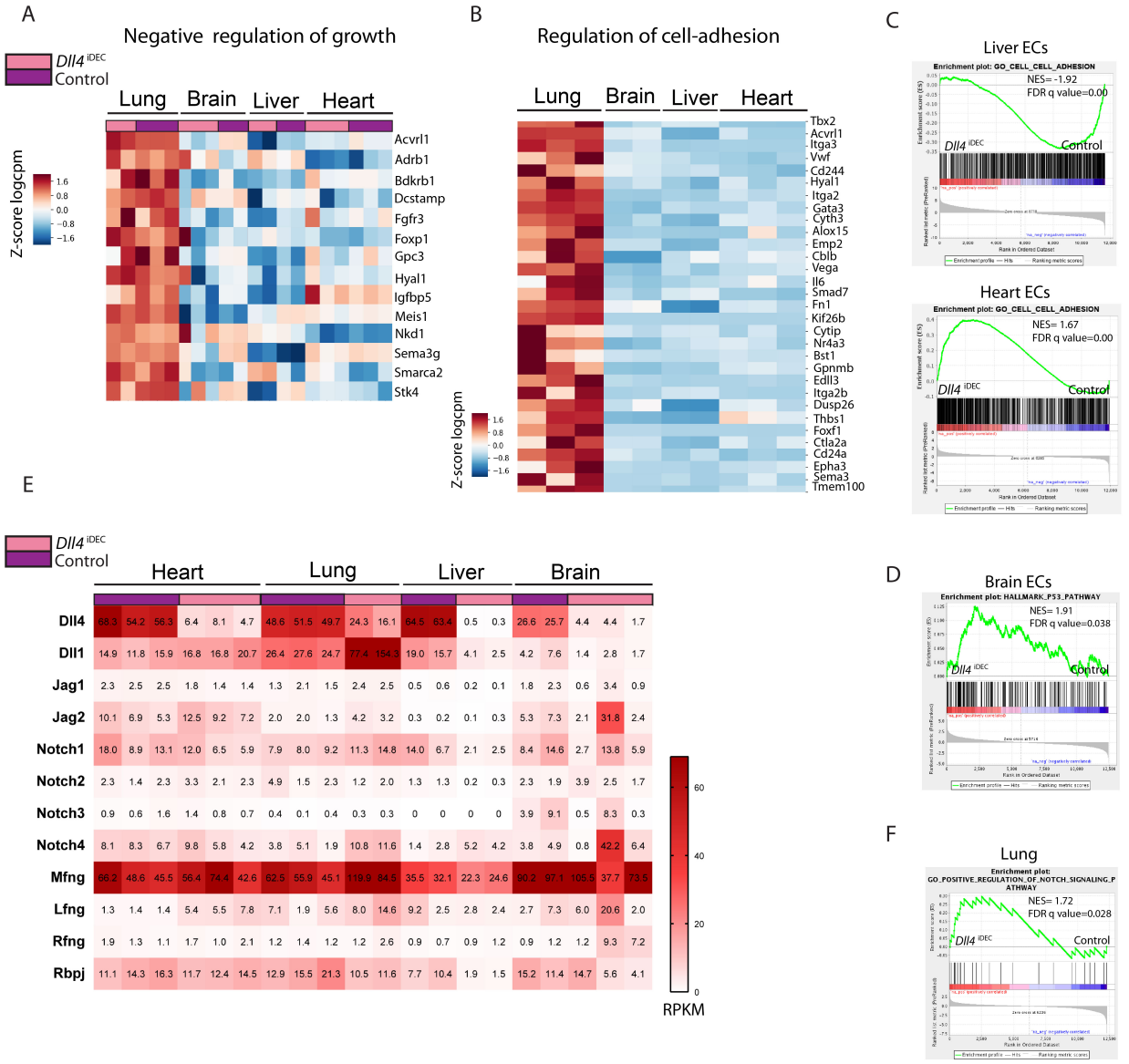

Figure 13: Genetic compensation mechanisms in lung and brain ECs after loss of Dll4/Notch1 signalling. **(A)** Heatmap showing that genes commonly known as negative regulators of cell growth are enriched in lung ECs compared to other organ ECs. **(B)** Heatmap showing that genes commonly known as regulators of cell-adhesion are enriched in lung ECs compared to other organ ECs. **(C)** GSEA GO analysis show that contrary to negative enrichment in *Dll4*^{iDEC} liver ECs, cell-cell adhesion related genes are positively enriched in *Dll4*^{iDEC} heart ECs. **(D)** p53 pathway related genes are significantly enriched in *Dll4*^{iDEC} brain ECs. **(E)** Heatmap showing the relative expression of all Notch pathway genes and the significant upregulation of *Dll1*, *Notch1*, *Notch4*, *Lfng* and *Mfng* in the lung ECs of *Dll4*^{iDEC} mutants. **(F)** GSEA analysis shows positive regulation of Notch signalling GO term in *Dll4*^{iDEC} lung ECs despite the loss of *Dll4* expression. Z-score logcpm: Z-score of the logarithmic counts per million. Red color indicates upregulation and blue color downregulation. NES: Normalized Enrichment Score.

Myc is essential for the proliferation of liver ECs after the loss of Dll4/Notch signalling

Given the strong upregulation of transcripts and proteins related with the Myc pathway observed in the livers of *Dll4*^{iDEC} liver ECs (Figure 12C-G), we next tested if Myc was indeed a key driver of EC proliferation in these mutants. In order to achieve this, we had to generate mice carrying 4 floxed alleles (*Dll4*$^{f/f}$/*Myc*$^{f/f}$) and the *Cdh5-CreERT2* allele. However, in contrast to Dll4, Myc protein cannot be detected by immunostaining in most quiescent ECs, and with this approach we could not safely confirm the simultaneous deletion of *Dll4* and *Myc* in the analysed liver ECs. The use of indirect gene deletion validation approaches with other samples, such as RT-qPCR or western blot of FACS sorted cells, do not indicate the deletion of genes in the tissues analysed by confocal microscopy, and only represent the average gene deletion efficiency, without *in situ* information of its cellular heterogeneity. This is a very common problem in conditional genetic experiments and motivated us to generate the new *iSuRe-Cre* genetic tool (Fernandez-Chacon et al., 2019). The use and validation of this new genetic tool was a very important part of my thesis. In Chapter II I will mention in detail its technical development, particularities and main advantages over other conventional Cre-reporter alleles, which unlike the *iSuRe-Cre* allele, do not effectively report cells with full deletion of floxed genes. By using the *iSuRe-Cre* allele I could effectively induce multiple genetic deletions in the adult endothelium, since all reporter expressing cells (MbTomato+) also express Cre (MbTomato-2A-Cre), which we have shown to induce full deletion of all tested floxed allele (see Chapter II for details). The analysis of the liver vasculature 2 weeks after inducing double genetic deletion in *Dll4*$^{f/f}$/*Myc*$^{f/f}$ *Cdh5-CreERT2 iSure-Cre* mice revealed that contrary to *Dll4*^{iDEC} liver ECs, ECs with dual loss of *Dll4* and *Myc* (*Dll4*^{iDEC} *Myc*^{iDEC}) do not proliferate, as we did not observe an increase in the number of ECs (nuclei ERG+ cells) or proliferating cells (Ki67+ERG+ cells) (Figure 14). These results indicate that the suppression of the Myc function by the Dll4/Notch signalling pathway in liver ECs is key to maintain their quiescence. These results also show that suppressors of Myc pathway activity may be used to counteract the adverse endothelial effects of pan-Notch inhibitors in therapeutic settings (Yan et al., 2010).

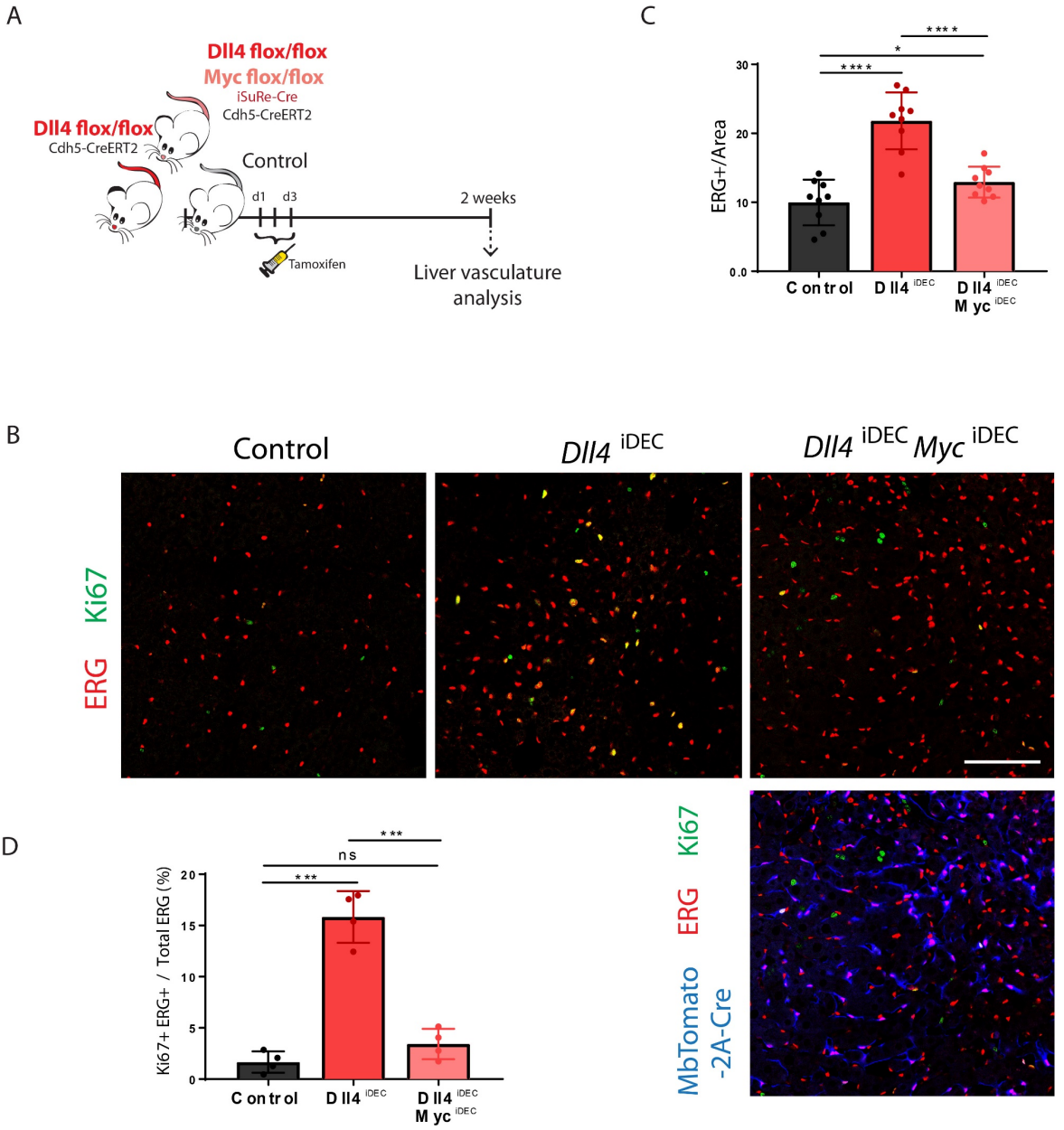

Figure 14: The increase in liver EC proliferation in the absence of Dll4/Notch signalling can be suppressed by *Myc* deletion. (A) Experimental layout for the double inducible deletion of *Dll4* and *Myc* (*Dll4*^{iDEC} *Myc*^{iDEC}) in Cdh5+ ECs. *Cdh5(PAC)-CreERT2 Dll4* floxed and *Myc* floxed adult mice received three intraperitoneal injections of tamoxifen as did age-matched *Dll4*^{iDEC} and control mice. 2 weeks after the first tamoxifen injection, mice were sacrificed and the liver was evaluated. **(B-D)** Confocal micrographs of liver sections showing that double deletion of *Dll4* and *Myc* in ECs results in a significant rescue of EC density (ERG+ cells) and proliferation (Ki67+ERG+ cells) to control conditions, as depicted in chart C and D (n=4 and n=2 animals per group respectively). For EC proliferation, only ERG+ MbTomato+ (ECs with reliable gene deletion) have been used for quantification. Scale bars, 100 µm. Error bars indicate SD. *p < 0.01. ***p<0.0001. ****p < 0.0001. ns, non-significant.

Deletion of *Rbpj* and *Notch1* in quiescent blood vessels does not phenocopy Dll4 deletion

Despite the high expression levels of *Dll4* and its role as a major activator of the Notch pathway in the quiescent vasculature of the heart, lung, liver and brain ECs (Figure 5D, 7) all other Notch ligands are expressed in quiescent ECs (Figure 5D) and could partially compensate for the loss of Dll4. In addition, only heart and liver quiescent ECs became hyperproliferative after the loss of Dll4/Notch signalling, raising questions about genetic compensation by other Notch ligands. Previous studies have also shown that Jagged1 is very relevant for blood vessel development (Benedito et al., 2009), even though a function for this ligand has not been shown in quiescent vessels. Indeed, *Jag1* mRNA is 120 times less expressed than *Dll4* in quiescent ECs (Figure 5D). However, we have found Jag1 protein levels to be relatively high in quiescent ECs by immunostaining (Figure 15A). We have also observed upregulation of *Dll1* in *Dll4*^{iDEC} lung ECs (Figure 13E). These results led us to hypothesize that perhaps the Dll4 function could be partially compensated by other Notch ligands, and that deletion of *Notch1* or *Rbpj* could result in a stronger loss of Notch signalling and the consequent hyperproliferative EC phenotype, not only in the liver and heart but also in the lung and brain vessels.

To evaluate the effect of a more pronounced cell-autonomous loss of Notch signaling, we used two mouse models: one allowing full deletion of *Notch1* and the other *Rbpj*. Because none of these floxed genes are easy to delete, and they code for proteins not easily detectable by immunostaining, we used mice carrying the *iSuRe-Cre* allele, in combination with the *Cdh5-CreERT2* and *Notch1/Rbpj* floxed alleles (Figure 15B). After tamoxifen induction, almost all quiescent ECs (Cdh5+) recombined and expressed the iSure-Cre allele (MbTomato-2A-Cre+) (Figure 15C). To specifically confirm the intended floxed gene deletion in this model system, we extracted mRNA from Tomato-2A-Cre+ liver ECs (Cdh5+, CD31+, Tomato+) isolated by FACS from the two mouse models. RT-qPCR results showed very efficient deletion of both genes in Tomato+ ECs (Figure 15D). As it will be shown later, the residual expression of *Rbpj* and *Notch1* is not due to incomplete deletion of these genes in some Tomato+ cells, but related with the nature of the FACS and RT-qPCR assay.

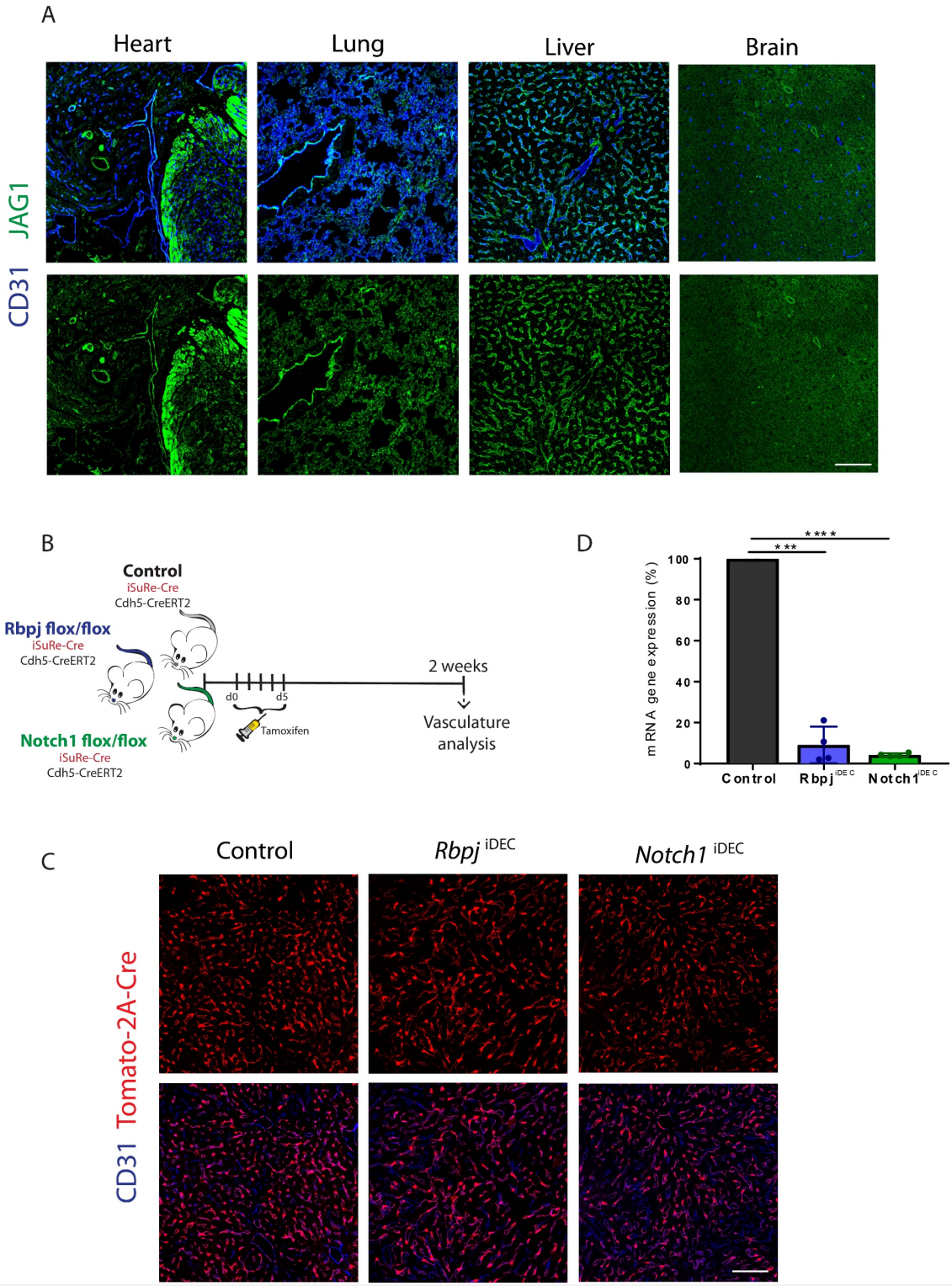

Figure 15: Mouse models to study Notch1 and Rbpj loss-of-function. **(A)** Confocal micrographs of heart, lung, liver and brain sections showing that Jagged1 protein is expressed in vessels of these organs. **(B)** Experimental layout for the inducible deletion of *Rbpj* (*Rbpj*^{iDEC}) and *Notch1* (*Notch1*^{iDEC}) in Cdh5+ ECs. *Cdh5(PAC)-CreERT2 iSuRe-Cre Rbpj* floxed and *Notch1* floxed adult mice received five intraperitoneal injections of tamoxifen as did age-matched control mice. 2 weeks after the first tamoxifen injection, mice were sacrificed. **(C)** MbTomato-2A-Cre from the *iSuRe-Cre* allele is expressed in most quiescent liver endothelium (CD31+) from mutant and control mice. **(D)** Deletion of *Notch1* and *Rbpj* is achieved in MbTomato+ cells as shown by RT-qPCR gene expression analysis. (n=4 animals per group respectively). Note: residual expression is due the nature of FACS and RT-qPCR assay. Scale bars, 100 µm. ***p<0.0001. ****p < 0.0001.

A first gross analysis of the liver vascular phenotype with vascular surface markers (CD31) in *Rbpj*^{iDEC} and *Notch1*^{iDEC} mutants, revealed an increase in vascular density and vessel width as in *Dll4*^{iDEC} mutants (Figure 16A,B), which is consistent with previous publications (Cuervo et al., 2016; Dill et al., 2012; Dou et al., 2008; Jabs et al., 2018; Yan et al., 2010). Unlike other organs, the liver receives blood rich in oxygen from two sources: the hepatic artery and the portal vein. They are physically located close to each other and are molecularly and functionally related (Kalucka et al., 2020; MacParland et al., 2018). Although it is named as a "vein", the portal vein not only provides oxygen rich blood to the liver, but it also expresses common arterial markers as the hepatic artery, such as the Notch ligands. The blood inflow provided by the hepatic artery and portal vein is channelled through the capillaries and it is finally drained by the central veins, which are the real veins of the liver (Halpern et al., 2018). We have seen that deletion of any of the Notch signalling components led to a reduction in the portal vein (CD34+) diameter but not the central veins diameter (Figure 16C-E). This result relates with the artery calibre reduction described in Notch mutants during early vascular development (Benedito et al., 2008; Duarte et al., 2004; Gale et al., 2004; Krebs et al., 2004; Krebs et al., 2000), even though mechanistically it should be very different, since deletion of Rbpj from already established retina arteries does not affect their calibre (Ehling et al., 2013).

Importantly, and in contrast to *Dll4*^{iDEC} mutant livers, the increase in vascular (CD31) density in *Rbpj*^{iDEC} and *Notch1*^{iDEC} mutant livers was not associated with an increase in EC number (ERG+) or its proliferation (Figure 17A-C). Although *Rbpj*^{iDEC} ECs remained non-proliferative, we found a significant increase in the adjacent hepatocyte proliferation (Figure 17D), suggesting that these mutant cells may secrete factors that promote hepatocyte proliferation. Previous research has already uncovered the role of liver ECs supporting hepatocyte development and liver regeneration by angiocrine factors in a blood perfusion independent fashion. Indeed, Notch activation in ECs has been shown to be disadvantageous for hepatocyte proliferation (Duan et al., 2018). Therefore, our findings support the view that activation of ECs, not necessarily their proliferation, may release important angiocrine signals that later drive parenchymal cell proliferation (Rafii et al., 2016).

Contrary to the generalized view in the vascular biology field, these results indicate that deletion of different Notch signalling components such as *Dll4*, *Rbpj* and *Notch1* does not result in the same vascular response and phenotype.

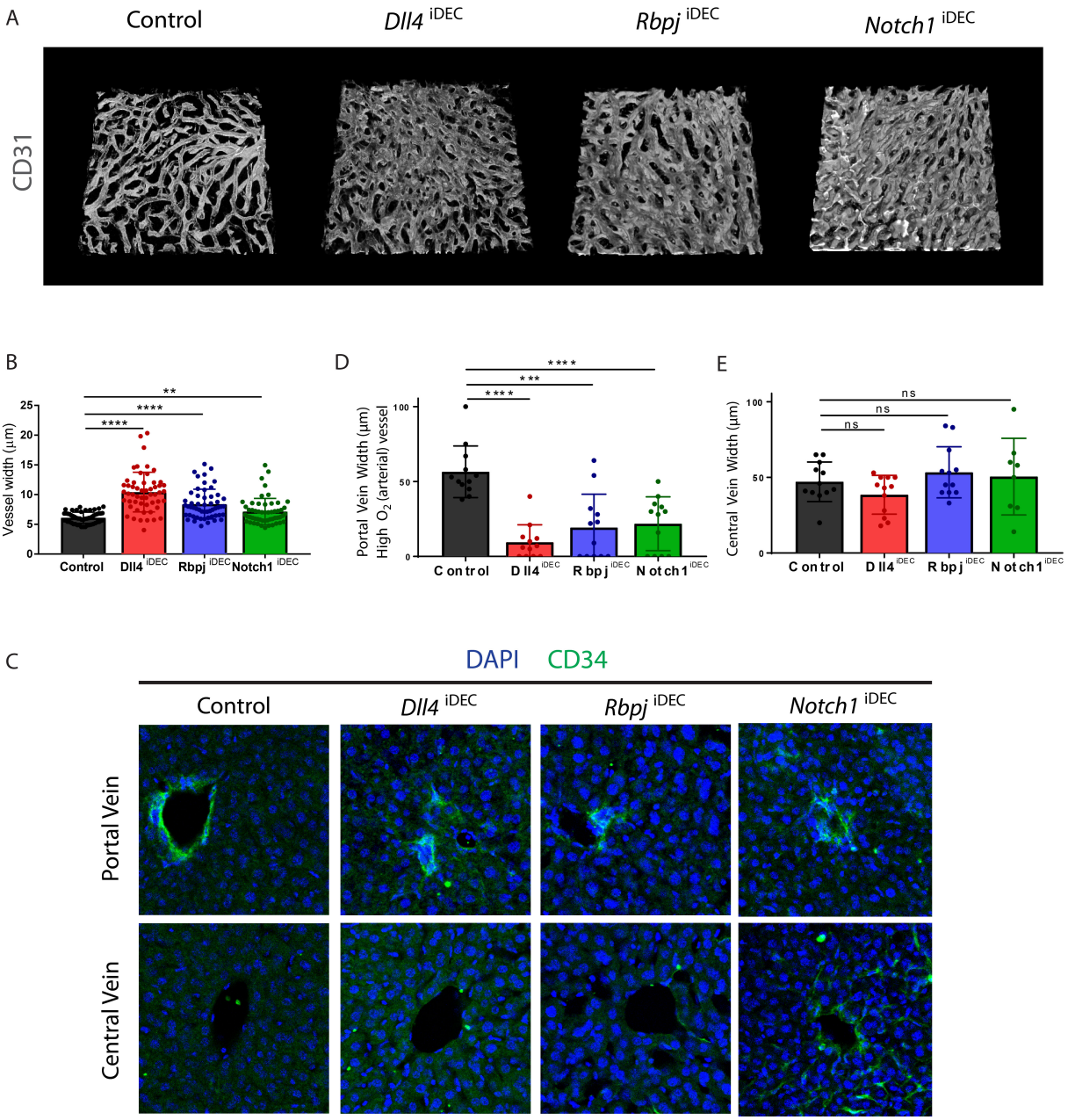

Figure 16: All Notch loss-of-function mutant livers show enlarged capillaries. (A) 3D reconstruction images from thick vibratome sections show the increase in vessel density (CD31+) in *Dll4*^{iDEC}, *Rbpj*^{iDEC} and *Notch1*^{iDEC} mutant livers. Parenchymal space is also reduced in all mutants. **(B)** Quantification of liver vessel width (CD31+) in *Dll4*^{iDEC}, *Rbpj*^{iDEC} and *Notch1*^{iDEC} mutant livers shows a significant increase compared with control mice. (n=3 animals per group). **(C-E)** Confocal micrographs of liver sections show that all Notch loss-of-function mutants have a significant decrease in portal vein diameter (CD34+) but not in central vein, as depicted in charts D and E (n=3 animals per group). Scale bars, 100 µm. Error bars indicate SD. $^{**}p < 0.01$. $^{***}p < 0.001$. $^{****}p < 0.0001$. ns, non-significant.

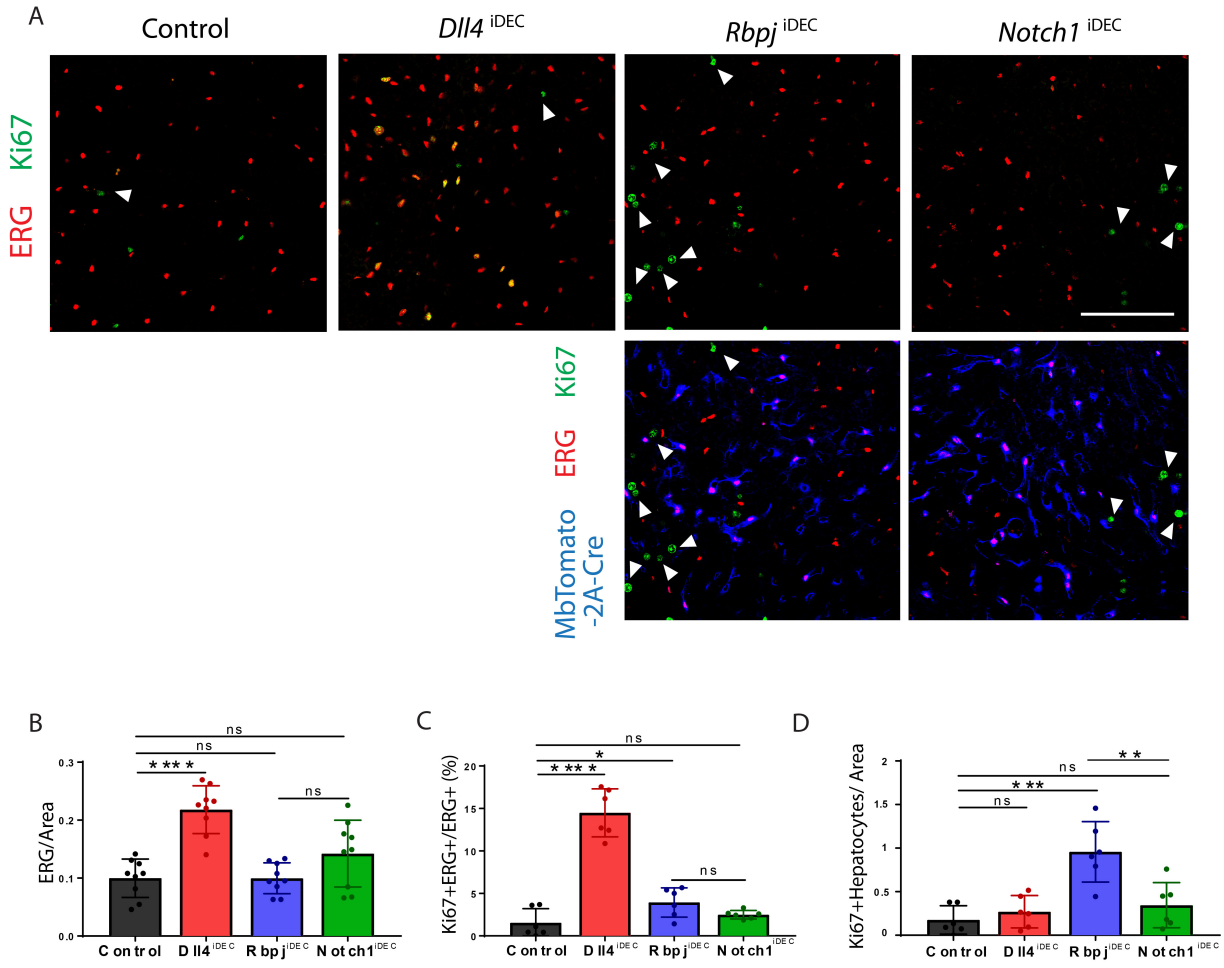

Figure 17: In contrast to loss of Dll4, loss of Rbpj and Notch1 does not increase EC proliferation. (A-D) Confocal micrographs of liver sections show that there is an increase in EC density (ERG+) and proliferation (Ki67+ERG+) only in *Dll4*^{iDEC} livers and not in *Rbpj*^{iDEC} and *Notch1*^{iDEC} mutant livers. However, there is increased hepatocyte proliferation (Ki67+ERG-Hepatocyte DAPI+ - white arrowheads) in *Rbpj*^{iDEC}. Quantification of the mentioned parameters is represented in charts B,C and D. In *Rbpj*^{iDEC} and *Notch1*^{iDEC} mutants only liver sections with more than 70% of *iSuRe-Cre* allele recombination have been considered for quantification. For EC proliferation, only ERG+ MbTomato+ (ECs with reliable gene deletion) have been used for quantification (n=3-4 animals per group). Scale bars, 100 µm. Error bars indicate SD. *p < 0.05. ***p < 0.001. ****p < 0.0001. ns, non-significant.

Transcriptional differences after the loss of *Notch1* and *Rbpj*

To identify transcriptional profile that could explain the phenotypic differences identified in *Dll4*^{iDEC} and *Notch1*^{iDEC} *or* *Rbpj*^{iDEC} mutants, we performed bulk RNA-seq of liver ECs (Cdh5+,CD31+, MbTomato+) isolated by FACS from control, *Rbpj*^{iDEC} and *Notch1*^{iDEC} mice after 2 weeks of *Rbpj* and *Notch1* deletion respectively (Figure 18A). Obtained results were compared and analysed with the previous bulk RNA-seq results from *Dll4*^{iDEC} liver mutants (Figure 18B). To verify the reliability of our different full loss-of-function models we first checked *Notch1* and *Rbpj* gene deletion efficiency in *iSuRe-Cre* expressing cells (Tomato-2A-Cre+). As expected, we observed the nearly complete absence of *Notch1* and *Rbpj* transcripts (Figure 18C) and as a consequence downregulation of the canonical Notch targets (Figure 18D). Despite the absence of EC proliferation differences (Ki67) in *Notch1/Rbpj*^{iDEC} mutants, GSEA analysis revealed a significant enrichment in gene sets related to cell proliferation and an activated cell status such as E2F targets, Myc targets, oxidative phosphorylation and G2M checkpoint, particularly in *Rbpj*^{iDEC} mutants (Figure 18E). These results indicate that *Rbpj*^{iDEC} mutant ECs, and to a lesser extent *Notch1*^{iDEC} mutant ECs, are also transcriptionally activated towards a proliferative and biosynthetic mode, but in contrast to *Dll4*^{iDEC} ECs they are unable to do so.

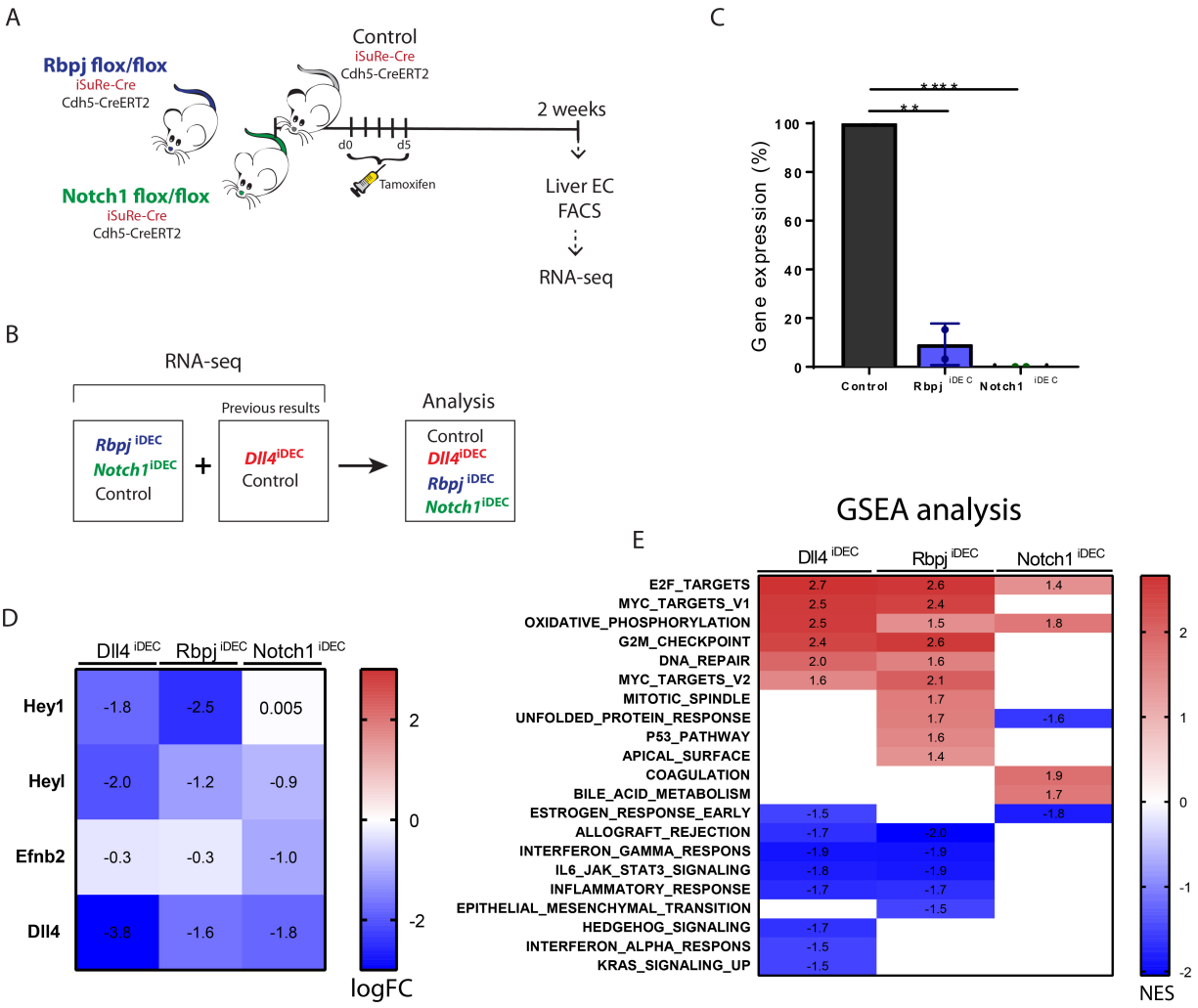

Figure 18: Bulk RNA-seq analysis reveals an upregulation of genes related to cell cycle and active metabolism in all Notch loss-of-function mutants. (A) Schematic representation to illustrate the bulk RNA-seq experiment performed with adult ECs isolated by FACS from *Rbpj*^{iDEC} , *Notch1*^{iDEC} and control liver tissues. *Cdh5(PAC)-CreERT2 iSuRe-Cre Rbpj* floxed and *Notch1* floxed adult mice received five intraperitoneal injections of tamoxifen as did age-matched control mice. 2 weeks after the first tamoxifen injection, mice were sacrificed and liver tissues were used for the experiment. **(B)** Experimental layout for the bulk RNA-seq analysis from *Dll4*^{iDEC}, *Rbpj*^{iDEC}, *Notch1*^{iDEC} and control liver ECs. **(C)** *Rbpj* and *Notch1* were efficiently deleted in liver quiescent ECs as shown by their RNA-seq transcript counts. **(D)** Common canonical Notch target genes are downregulated in all Notch mutants. Note the distinct degrees of downregulation in different mutants/targets. LogFC: Logarithmic Fold Change. **(E)** Heatmap with the normalized enrichment score (NES) from significant hallmark analysis by GSEA in *Dll4*^{iDEC}, *Rbpj*^{iDEC} and *Notch1*^{iDEC} mutants compared with control livers. *Dll4*^{iDEC} and *Rbpj*^{iDEC} GSEA analysis is very similar. Red color indicates upregulation and blue color downregulation. Error bars indicate SD. $^{**}p < 0.01$. $^{****}p < 0.0001$.

Loss of Notch signalling increases nuclei size and the number of binucleated cells

Interestingly, we found that the activated status of *Dll4/Notch1/Rbpj*^{iDEC} mutant ECs was accompanied by an increase in the nuclei size when compared to control livers (Figure 19A,B). A delicate balance between cell growth and division must be established. Before cell division, there is an increase in biosynthetic activities that is accompanied by an increase in cell and nuclei size (Gregory, 2005). Indeed, an increase in EC size was also shown after *Rbpj* deletion during vessel remodelling (Ehling et al., 2013).

RNA-seq GO analysis revealed that *Rbpj*^{iDEC} liver ECs are significantly enriched in genes related to cell division processes, such as chromosome segregation or attachment of spindle microtubules to kinetochores (Figure 20A). As an example, *psrc1, ska1* and *bub1* cell division genes were strongly upregulated (Figure 20B). *Psrc1* is essential for normal progression through mitosis, *ska1* is required for proper chromosome segregation and *bub1* is a key player in the establishment of mitotic spindle checkpoint and chromosome congression (Bolanos-Garcia and Blundell, 2011; Hsieh et al., 2008; Sivakumar et al., 2014). Interestingly, analysis of isolated MbTomato-2A-Cre+ ECs in *Rbpj*^{iDEC} and *Notch1*^{iDEC} livers revealed many ECs with two nuclei, indicating that many ECs reentered the cell cycle but were unable to complete the cell division process (Figure 20C). We then quantified these binucleated cell events in *Dll4*^{iDEC}, *Rbpj*^{iDEC}, *Notch1*^{iDEC} and control liver sections immunostained for ERG/MbTomato. Binucleated ECs were detected in all the mutants, but were more frequent in *Rbpj*^{iDEC} livers (Figure 20D,E).

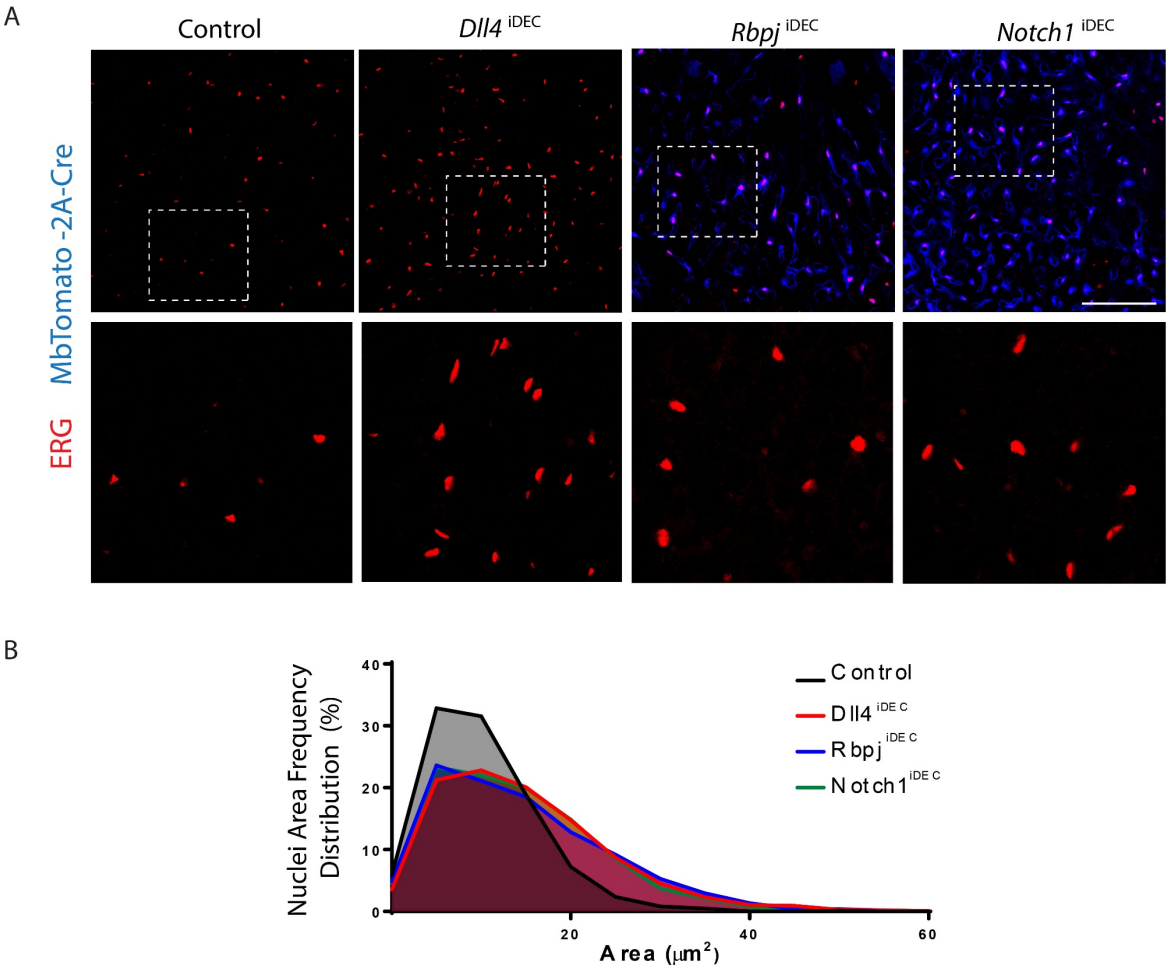

Figure 19: Notch loss-of-function leads to increased EC nuclei size. (A-B) Confocal micrographs of liver sections showing that ECs in *Dll4*^{iDEC}, *Rbpj*^{iDEC} and *Notch1*^{iDEC} mutant livers have a larger nuclei size compared with control liver ECs, as depicted in the frequency distribution chart in B (n=3 animals per group). Top panel indicates the original area shown in the bottom panel. Scale bars, 100 μm.

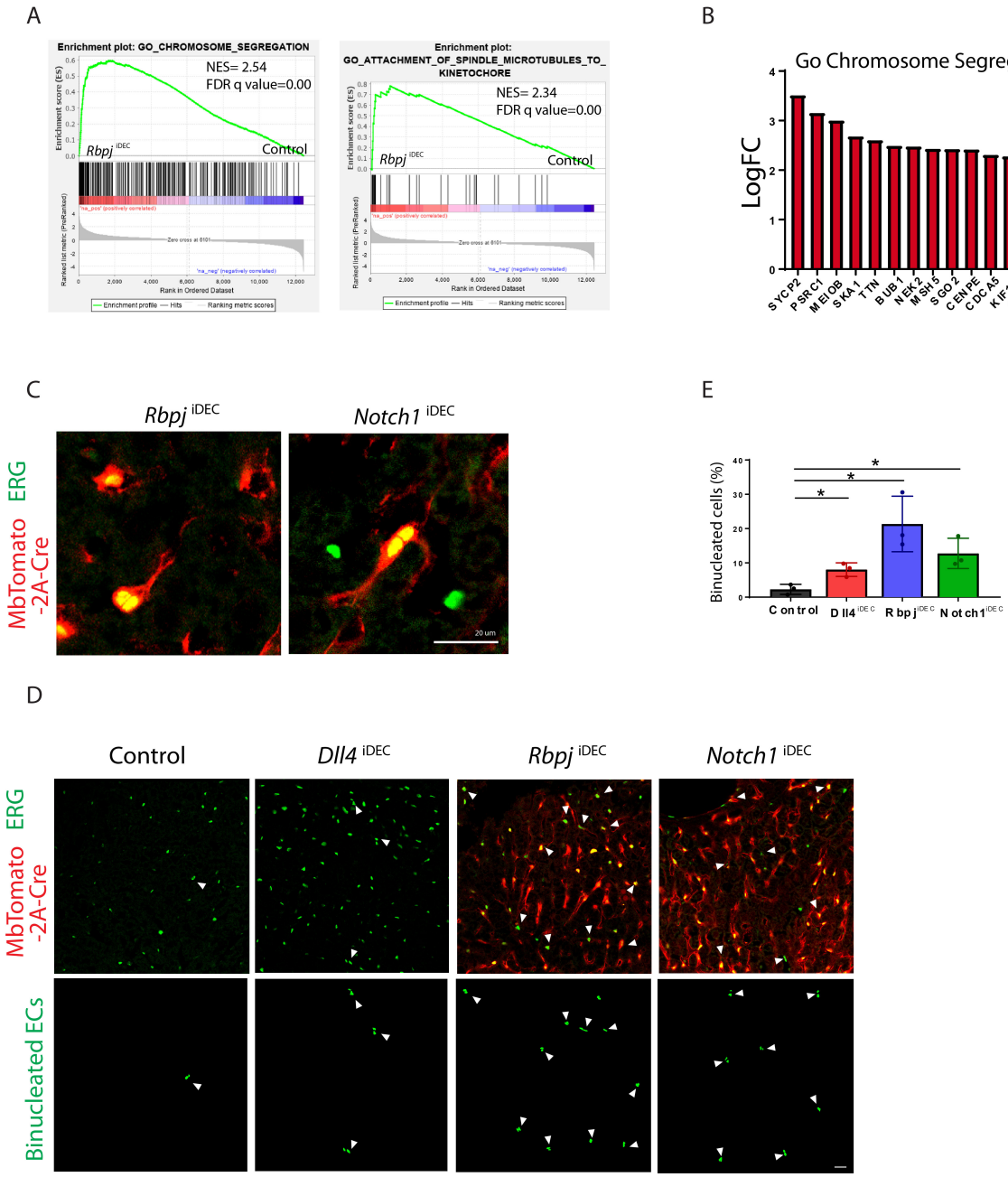

Figure 20: *Rbpj*^{iDEC} and *Notch1*^{iDEC} liver ECs cannot complete cell division. (A) GSEA analysis in *Rbpj*^{iDEC} liver ECs show a significant positive enrichment in chromosome segregation or attachment of spindle microtubules to kinetochores GO terms. **(B)** List of the 15 most upregulated genes in *Rbpj*^{iDEC} liver ECs from GSEA analysis in A. LogFC: Logarithmic Fold Change. **(C)** Confocal micrographs of liver sections showing that in *Rbpj*^{iDEC} and *Notch1*^{iDEC} mutants there are ECs that do not complete cell division and remain in a binucleated stage. **(D)** Representative images from confocal micrographs analysis of liver section showing the binucleated cells identified in *Dll4*^{iDEC}, *Rbpj*^{iDEC} and *Notch1*^{iDEC}. Top figures automatic Fiji analysis results in the bottom mask images that represent the binucleated cells. White arrowheads point the binucleated cells. **(E)** Quantification of ECs that do not complete cell division (ERG+ nuclei closer more than 8.5 µm – binucleated cells) in *Dll4*^{iDEC}, *Rbpj*^{iDEC}, *Notch1*^{iDEC} and control livers (n=3 animals per group). Scale bars, 20 µm. Error bars indicate SD. *p < 0.05.

High-ERK activation after the loss of *Notch1* and *Rbpj*

Recent studies have shown that high mitogenic stimulation induced by Notch inhibition, arrests the proliferation of angiogenic vessels. This is a result of a bell-shaped dose-dependent response to VEGF and MAPK/ERK activity regulated in part by Notch (Pontes-Quero et al., 2019). This cell cycle arrest was detected only in ECs closer to the VEGF source, and not in mature or quiescent ECs. Given the observed differences between the *Dll4*^{iDEC} and *Notch1*/*Rbpj*^{iDEC} mutants, we hypothesized that *Dll4* deletion may result in an incomplete inactivation of the Notch signalling pathway and a more moderate activation of MAPK/ERK activity, as opposed to the full inactivation of the pathway through the deletion of the downstream co-factor *Rbpj* or the main receptor *Notch1*. This different doses of loss of Notch signalling could trigger different levels of mitogenic stimulation, which may lead to different proliferative outcomes. To test this hypothesis, we performed immunostaining for phosphorylated-ERK (p-ERK) in *Dll4*^{iDEC}, *Rbpj*^{iDEC}, *Notch1*^{iDEC} and control liver sections. While *Dll4*^{iDEC} liver ECs had a relatively mild increase of p-ERK compared to control conditions, we observed a significant increase in the frequency and intensity of p-ERK signals in *Rbpj*^{iDEC} and *Notch1*^{iDEC} liver ECs (Figure 21A-D). This increase in p-ERK levels was also validated by western blot analysis of whole liver lysate (Figure 21E). We also observed that liver ECs that could not complete cell division were p-ERK+ (Figure 22A), which supported our hypothesis that high mitogenic stimulation after a more pronounced loss of Notch signalling - *Rbpj*^{iDEC} and *Notch1*^{iDEC} mutants - could trigger hypermitogenic arrest of liver capillaries. Interestingly, deletion of any of the Notch components did not affect p-ERK levels in liver portal veins endothelium (Figure 22B). These results suggest that *Dll4* deletion leads to a partial loss of Notch signalling that would be sufficient to activate EC proliferation through a moderate increase in p-ERK levels. On the contrary, *Notch1* and *Rbpj* deletion would lead to a more pronounced loss of Notch signalling that triggers a much higher level of P-ERK and mitogenic stimulation that arrests endothelial cell proliferation. These results would be in line with the bell-shape dose-dependent response to mitogenic stimuli observed in retina ECs during development (Pontes-Quero et al., 2019).

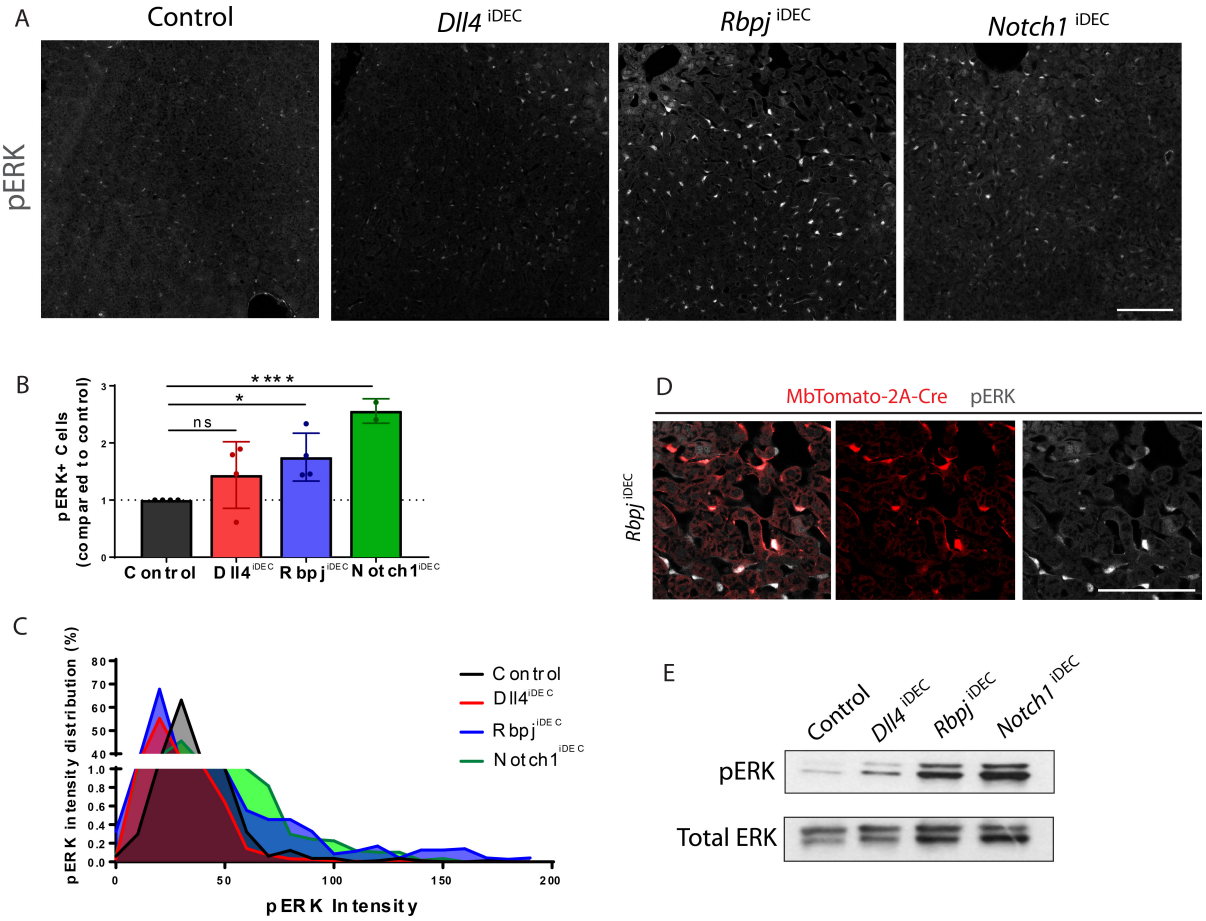

Figure 21: Quiescent ECs with high ERK signalling do not proliferate. (A-D) Confocal micrographs of liver sections show that deletion of *Rbpj* and *Notch* highly increase p-ERK expression frequency and intensity levels compared with *Dll4*^{iDEC} and control mice as depicted in chart B and C. The increase in p-ERK occurs specifically in ECs as shown by its localization with the EC-specific expression of MbTomato as shown in D (n=2 animals per group). **(E)** Whole liver Western Blot analysis show increased levels of p-ERK in *Rbpj*^{iDEC} and *Notch1*^{iDEC} mutants compared with control and *Dll4*^{iDEC} mice. Scale bars, 100 µm. Error bars indicate SD. *p < 0.01. ****p < 0.0001. ns, non-significant.

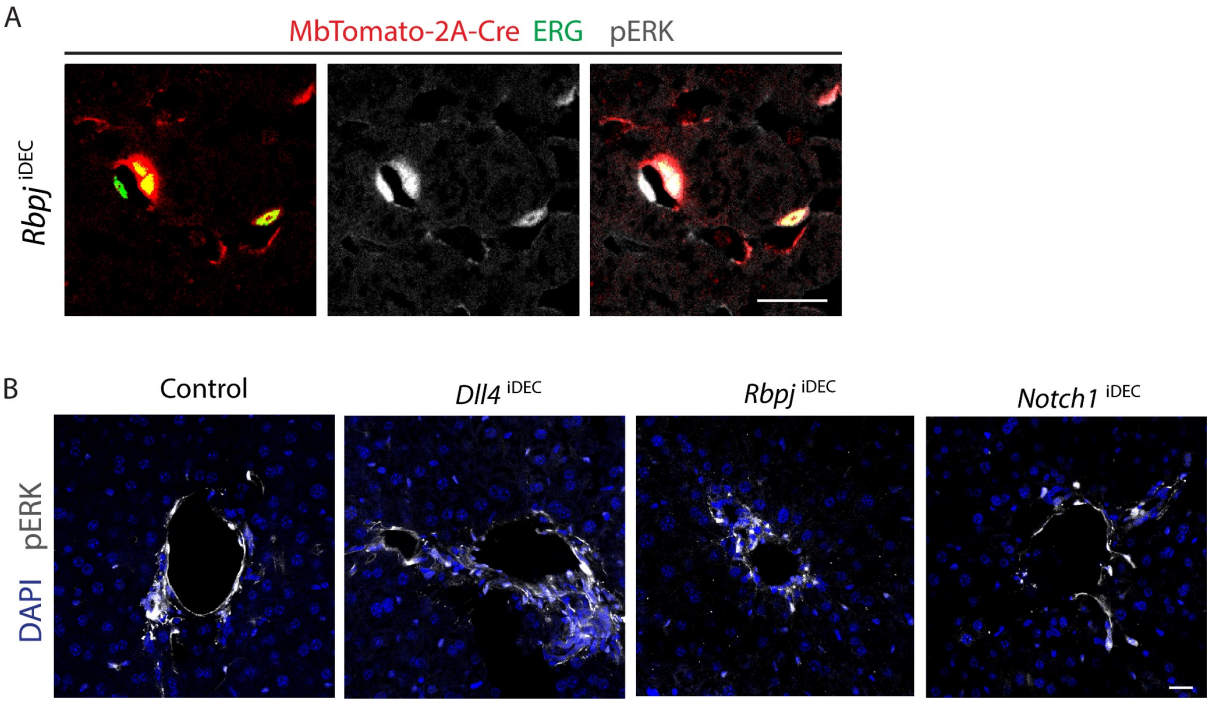

Figure 22: Quiescent ECs with high ERK signalling do not divide. (A) Representative confocal microcraphs of *Rbpj*^{iDEC} liver showing that ECs that cannot complete cell-division are p-ERK+.**(B)** Confocal micrographs of portal vein in liver sections showing ERK activity. Scale bar, 20 µm

Despite the enrichment in gene sets related to the regulation of cell cycle and metabolism, we also observed a significant enrichment in gene sets such as DNA repair and the p53 pathway in *Rbpj*^{iDEC} mutants (Figure 18E, 23A). DNA repair mechanisms driven by DNA damage and the p53 pathway are closely related mechanisms. Cellular stress signals such as DNA damage, MAPK/oncogene activation or ribosome biogenesis stress are different cues that can ultimately activate the tumour suppressor p53, the “guardian of the genome” and a key player in the inhibition of tumour development (Horn and Vousden, 2007). By halting cell cycle progression, p53 allows DNA repair mechanisms to correct the DNA lesions (Williams and Schumacher, 2016). *Rbpj*^{iDEC} mutants also showed upregulation of 53BP1 immunostaining signals. 53BP1 is an important regulator and marker of DNA damage responses (Panier and Boulton, 2014). Interestingly, 53BP1+ signal was upregulated in both endothelial and non-endothelial cells (Figure 23B), which may be related with the increase in hepatocytes proliferation mentioned above (Figure 17D). Given the strong upregulation of p-ERK in *Rbpj*^{iDEC} and *Notch1*^{iDEC} liver ECs, we next investigated whether such a high mitogenic stimulation could not only prevent endothelial cell proliferation but also trigger cell cycle arrest

mechanisms. In response to some forms of DNA damage, p53 is activated and leads to the transcription of one of its first described target genes: *cdkn1a*, which encodes the cyclin-dependent kinase inhibitor p21 protein. p21 binds cyclin and Cdk complexes and blocks proliferation (el-Deiry, 1994; Levine, 1997).

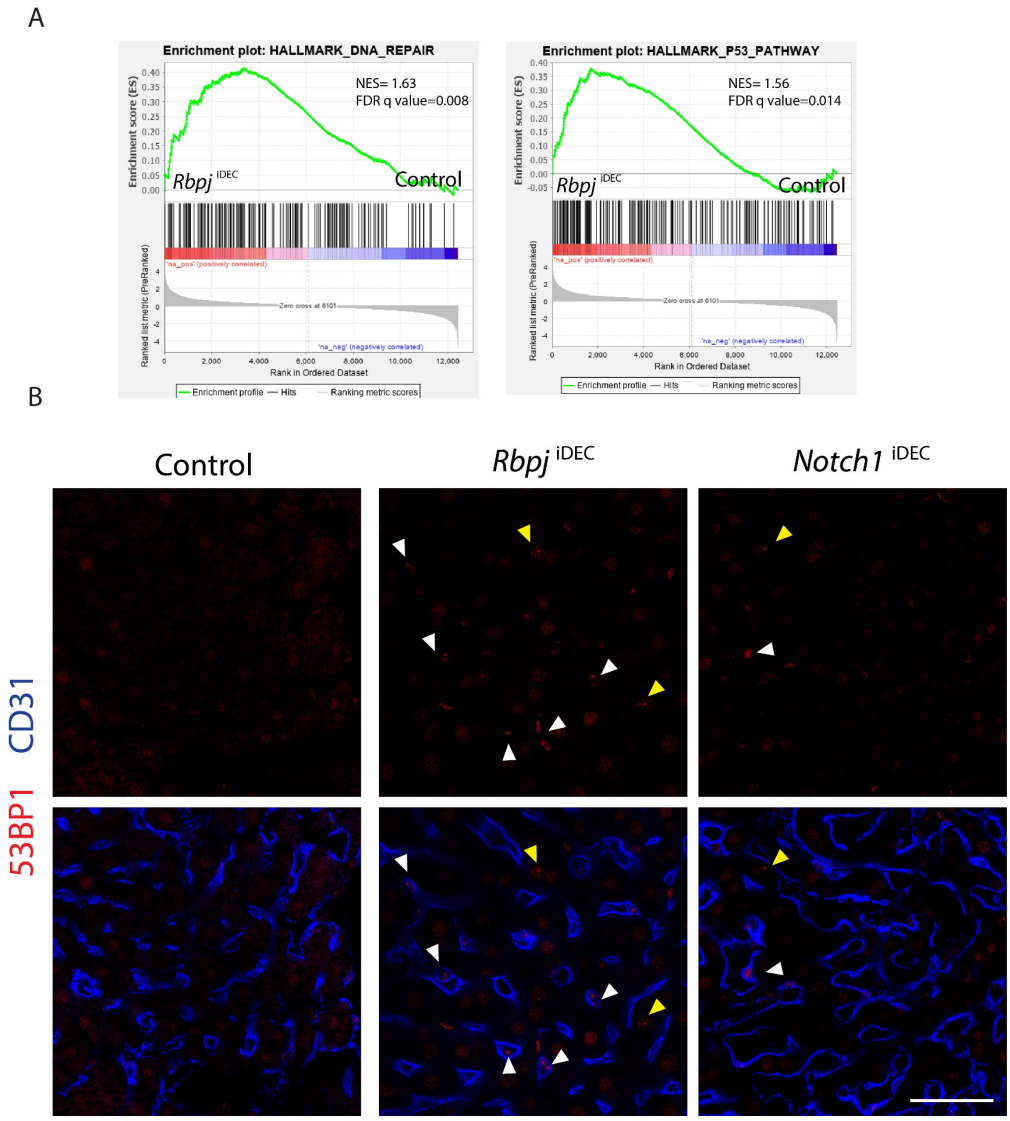

Figure 23: High mitogenic stimulation triggers DNA repair and p53 pathways. (A) GSEA Hallmark analysis in *Rbpj*^{iDEC} liver ECs reveal a significant and positive enrichment in DNA repair and p53 related pathways. NES: Normalized Enrichment Score. **(B)** Confocal micrographs of liver sections showing the presence of DNA damage (53BP1+) in endothelial (white arrowheads) and non-endothelial cells (yellow arrowheads). Arrowheads indicate DNA damage (53BP1+ staining). Scale bar, 20 µm.

In addition, we have recently described that during retina vascular development ECs with high ERK signalling strongly upregulate p21 and exit the cell cycle during development (Pontes-Quero et al., 2019). Consistent with these observations, we found that *cdkn1a* (p21) expression was strongly upregulated in the *Dll4*^{iDEC} and *Rbpj*^{iDEC} liver ECs, but surprisingly not in *Notch1*^{iDEC}liver ECs (Figure 24A). When we analysed p21 expression at the protein level (Figure 24B), we found that the frequency of p21+ ECs was around 70% and 50% in *Rbpj*^{iDEC} and *Notch1*^{iDEC} liver ECs, respectively. Although p21 transcription is strongly upregulated in *Dll4*^{iDEC} liver endothelium, we did not observe more than 20% of liver ECs with high p21 protein expression (Figure 24C).This discrepancy may be due to p21 post-transcriptional protein stability regulation (Deng et al., 2018; Liu et al., 2019; Scoumanne et al., 2011). The higher frequency of p21+ ECs in *Rbpj*^{iDEC} and *Notch1*^{iDEC} livers correlates with their activated but non-proliferative phenotype, the higher frequency of binucleated cells and higher p-ERK levels (Figure 17A-D, 18E, 20C-E, 21A-E, 24B,C). In agreement with these observations, in *Rbpj*^{iDEC} and *Notch1*^{iDEC} livers 50% of binucleated cells are p21+ (Figure 25A,B).

To determine the cell cycle status of p21+ cells, we performed co-immunostaining for Ki67, and the EC nuclei marker ERG in *Dll4*^{iDEC} livers (Figure 26A). We found that most Ki67+ERG+ ECs are not p21+ and that most p21+ERG+ ECs are not Ki67+. Nonetheless, there is a minor fraction of p21+/Ki67+/ERG+ ECs (3.5%) that expresses both proteins and may represent cells that are being arrested and terminating their cell cycle (Figure 26B). This result is consistent with a model in which an abnormally high mitogenic stimulation leads to p21 upregulation and cell cycle arrest, which is significantly more frequent in liver ECs with loss of *Rbpj* or *Notch1*.

After these results, we questioned if a similar increase in mitogenic stimuli (p-ERK) and p21 expression could explain why we did not observe an increase in lung and brain EC proliferation after *Dll4* deletion. Similar to liver ECs, we observed a significant increase in the frequency of p21+ ECs (0% control vs 7% mutant) in *Dll4*^{iDEC} heart endothelium, which is proliferative (Figure 10). However, contrary to our hypothesis, we did not observe any increase in the frequency of p21+ cells in brain and lung ECs (Figure 26C,D). The RNA-seq data also showed only a 2-fold upregulation of *cdkn1a* (p21) in heart, lung and brain *Dll4*^{iDEC} ECs compared to the 16-fold upregulation observed in liver ECs (Figure 26E).

Overall, these results indicate that deletion of the *Rbpj* co-transcription factor and the *Notch1* receptor leads to a more pronounced loss of Notch signalling and higher mitogenic stimuli, which induces p21 and cell cycle arrest. While mild mitogenic stimulation after *Dll4* deletion induces cell cycle reentry and proliferation, excessive mitogenic stimulation after the

loss of Rbpj drives an abnormal increase in MAPK, upregulation of p53 pathway related-genes, DNA damage, p21 and cell cycle arrest.

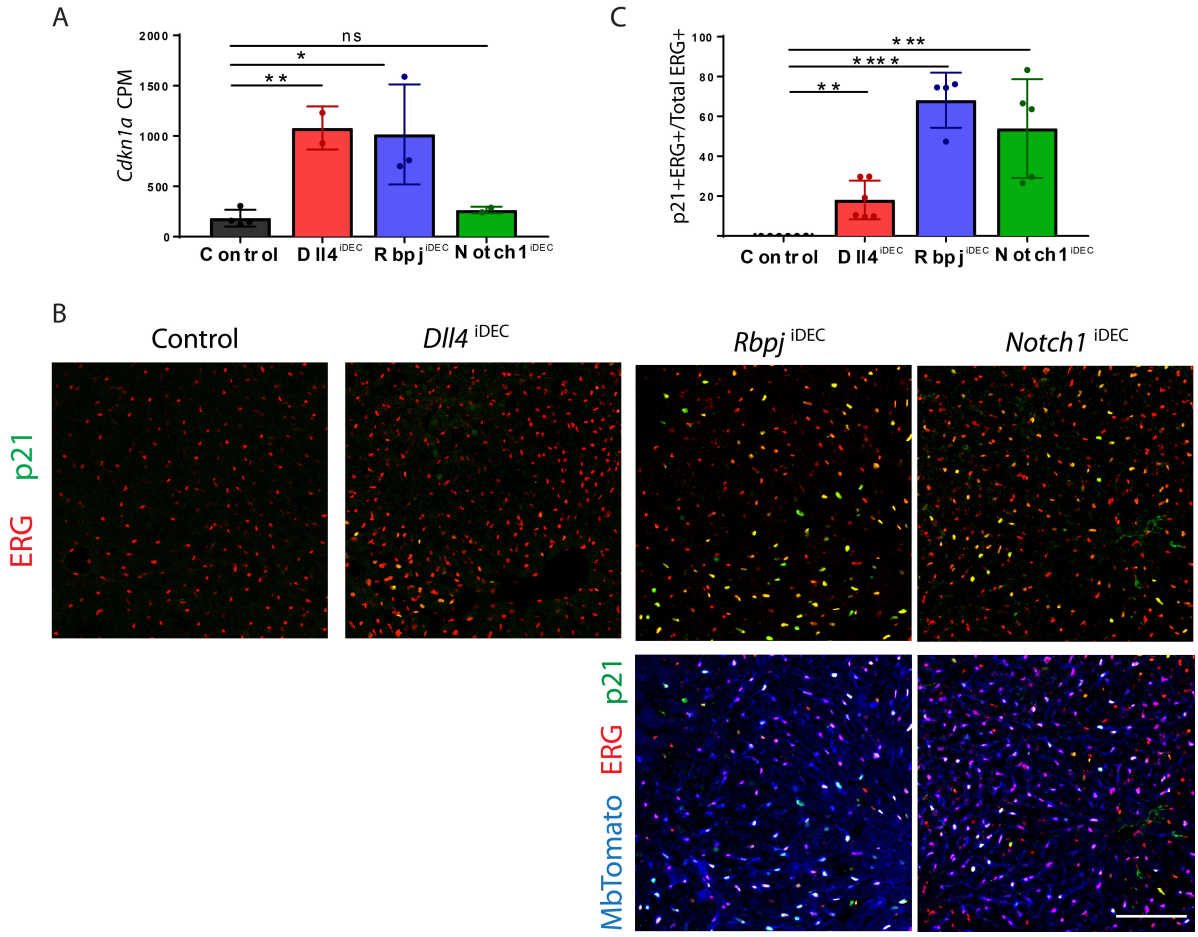

Figure 24: p21 is upregulated in cells with loss of Dll4/Notch1 signalling. (A) *Cdkn1a* (p21) expression (counts per million) in *Dll4*^{iDEC}, *Rbpj*^{iDEC} and *Notch1*^{iDEC} mutants (n=2-3 animals per group). **(B-C)** Confocal micrographs of liver sections showing a significant upregulation of p21 protein in *Dll4*^{iDEC}, *Rbpj*^{iDEC}, *Notch1*^{iDEC} ECs (p21+ERG+ cells). In *Rbpj*^{iDEC} and *Notch1*^{iDEC} mutants only ERG+ MbTomato+ (ECs with reliable gene deletion) have been considered for quantification (n=3 animals per group). Scale bar, 100 µm. Error bars indicate SD. *p < 0.05, **p < 0.01. ***p < 0.001. ****p < 0.0001 ns, non-significant.

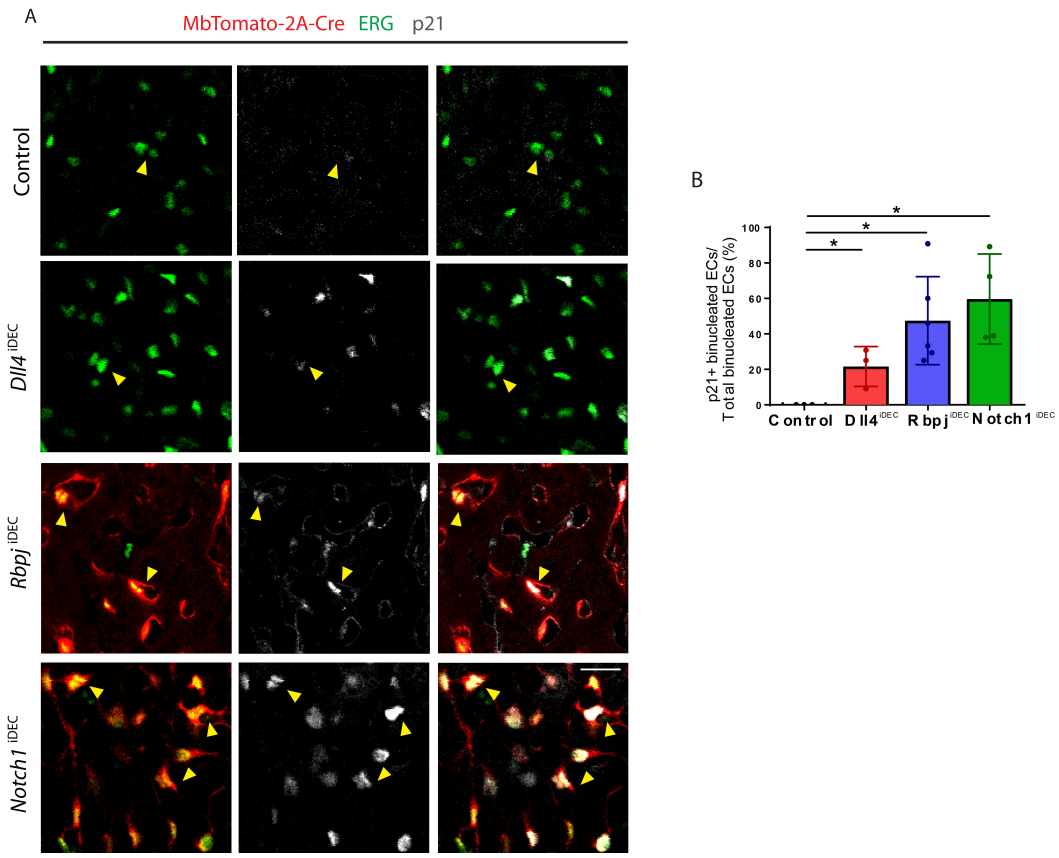

Figure 25: Binucleated ECs in *Rbpj*^{iDEC} and *Notch1*^{iDEC} livers are p21+. (A-B) Confocal micrographs of liver sections showing that binucleated *Rbpj*^{iDEC} and *Notch1*^{iDEC} ECs are p21+ (n=3 animals per group) as shown in chart B. Yellow arrowheads indicate p21+ binucleated EC events. Scale bar, 20 µm. Error bars indicate SD. *$p < 0.05$. ns, non-significant.

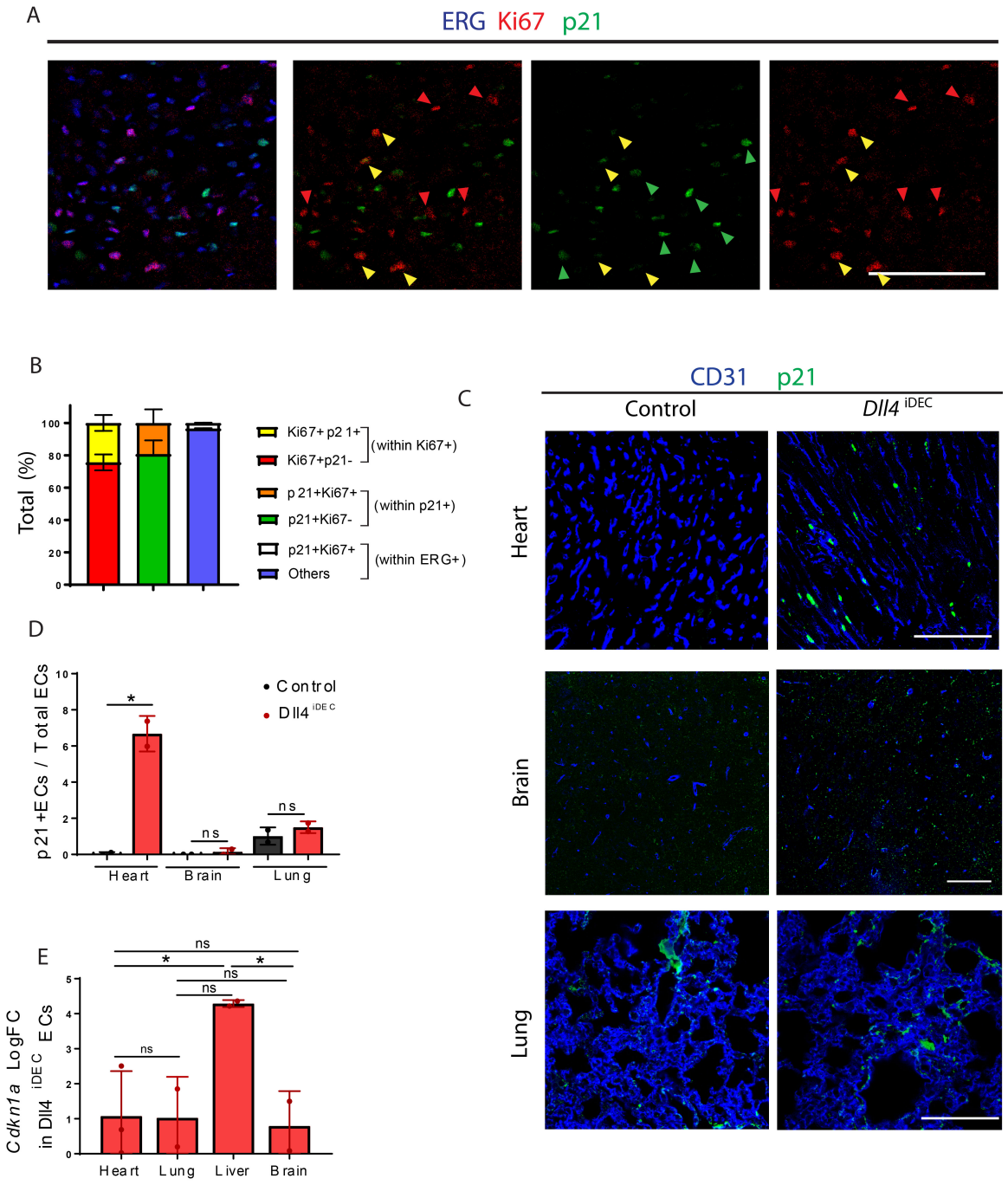

Figure 26: p21 labels mostly Ki67- cells. **(A-B)** Confocal micrographs of *Dll4*^{iDEC} liver sections show that only a small fraction of proliferating ECs (Ki67+ERG+) also expresses p21 protein (p21+Ki67+ERG), as depicted in chart B (n=3 animals per group). **(C-D)** *Dll4*^{iDEC} and control sections from heart, brain and lung show an upregulation of p21 expression in heart ECs (CD31+) but not in brain and lung, as depicted in chart D (n=2 animals per group). **(E)** *Cdkn1a* (p21) mRNA is strongly upregulated in *Dll4*^{iDEC} liver ECs (16-fold) compared to other vascular beds. LogFC: Logarithmic Fold Change. Scale bar, 100 µm. Error bars indicate SD. *p < 0.05. ns, non-significant.

Notch signalling prevents EC senescence

As we mentioned above, the expression of p21 has shown to be triggered by different pathways, including DNA-damage and p53, and it also labels cells that undergo senescence (Munoz-Espin and Serrano, 2014). Senescence is defined by an irreversible and stable cell cycle arrest, which has been shown to occur during normal embryonic development and upon cellular damage or aging. Therefore, we next investigated whether Notch was preventing endothelial senescence. In *Dll4*^{iDEC} and *Rbpj*^{iDEC} liver ECs, GSEA analysis of the Reactome pathway database showed us a significant enrichment in cellular senescence related genes. Although positively enriched in *Notch1*^{iDEC} liver ECs, it was not statistically significant (Figure 27A). We also confirmed the upregulation of other cell cycle inhibitors and senescence markers such as *cdkn1b* (p27), *cdkn1c* (p57*)* or *cdkn2a* (p16) (Figure 27B). Besides the arrest in cell cycle, senescent cells also have other features, such as a bigger size and higher biosynthetic or secretory activity (Hernandez-Segura et al., 2018). It is well documented the senescence-associated secretory phenotype (SASP) as a pro-inflammatory transcriptional programme that mediates the secretion of cytokines/chemokines by senescent cells. Interestingly, we observed the upregulation of already established SASP-related factors in liver ECs with loss of Notch signalling components (Figure 27C). This secretory response was heterogeneous among the different Notch mutants. The gene *Mif* was upregulated in all mutants. *Mif* codes for macrophage migration inhibitory factor (MIF) which is a chemokine with an important role in monocyte/leukocyte recruitment and arrest. Under inflammatory processes, absence of MIF leads to reduced leukocyte-EC interactions (Cheng et al., 2010; Tillmann et al., 2013). In line with this observation, we found an increase in the frequency of Runx1+CD45+ cells, presumably monocytes/leukocytes, in mutant livers (Figure 28A-C).

Moreover, it has been described that SASP can induce secondary senescence in neighbouring cells. Indeed, we observed an increase in p21+ hepatocytes in all Notch mutants compared to control conditions, where we do not detect p21 expression (Figure 29A,B). Previous research in keratinocytes has shown that while prolonged SASP exposure drives cell-intrinsic senescence arrest, transient exposure leads to an increase in the regenerative capacity that is accompanied by the expression of stem cell markers such as CD34, Lgr6, Prom1 and Nestin (Ritschka et al., 2017). Particularly, we have seen that the transmembrane phosphoglycoprotein CD34 is specifically expressed in the liver portal vein endothelium, which carries oxygen-rich blood and has relatively high Dll4/Notch activity. However, we observed that after *Notch1* deletion, CD34 expression was upregulated in capillaries of *Notch1*^{iDEC} livers

(Figure 29C), instead of being restricted to portal veins. Unexpectedly, *Dll4*^{iDEC} and *Rbpj*^{iDEC} mutants do not show the same upregulation (Figure 29D). Interestingly, it was recently shown *in vitro* that CD34 also labels tip cells, which also have high ERK activity and express p21 (Pontes-Quero et al., 2019). These cells also have a lower proliferation profile (Siemerink et al., 2012).

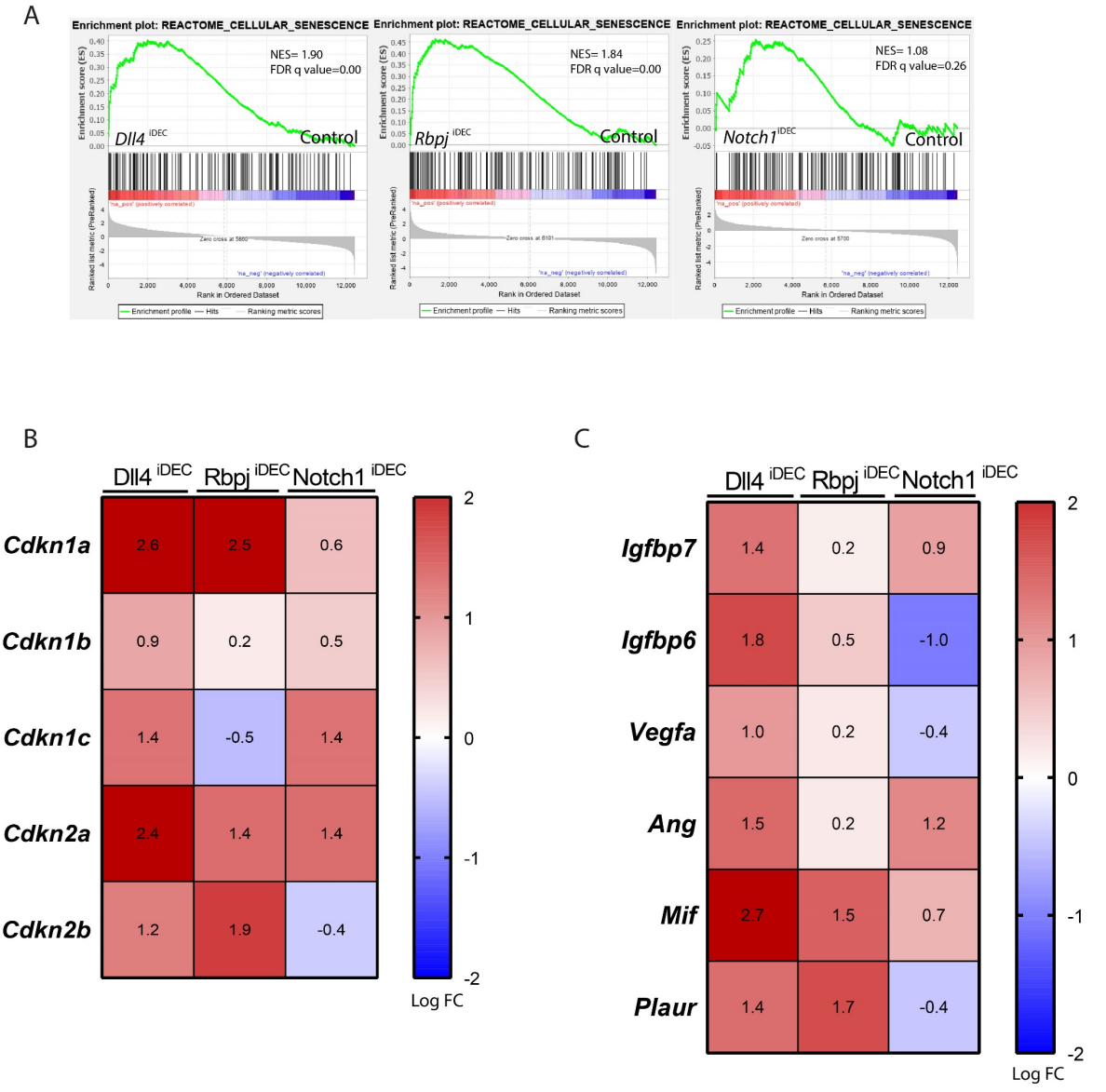

Figure 27: RNA-seq analysis suggests Notch signalling suppresses endothelial senescence. **(A)** Cellular senescence related genes are positively enriched in all Notch mutants as shown by GSEA Reactome analysis. The analysis is statistically significant only in *Dll4*^{iDEC} and *Rbpj*^{iDEC} liver ECs. NES: Normalized Enrichment Score. **(B)** Heatmap showing the upregulation of different cell cycle inhibitors as depicted by the positive Logarithmic Fold Change (LogFC). **(C)** Heatmap showing the logFC of different SASP factors in *Dll4*^{iDEC}, *Rbpj*^{iDEC}, *Notch1*^{iDEC} livers. Red color indicates upregulation and blue color downregulation.

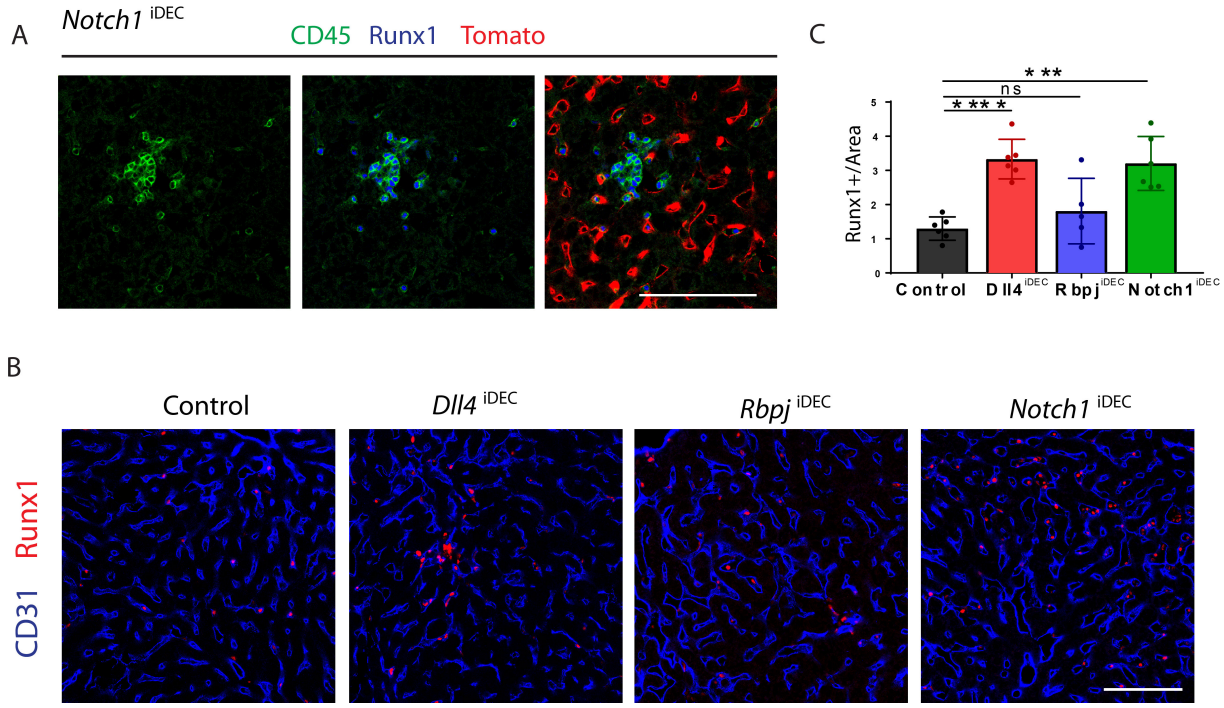

Figure 28: Increased number of immune cells after loss of endothelial Notch signalling. (A-C) Representative confocal micrographs of liver sections showing that Notch loss-of-function results in increased localization of immune cells (CD45+Runx1+) in the liver, specifically more pronounced in *Dll4*^{iDEC} and *Notch1*^{iDEC} mutants, as depicted in chart C (n=2-3 animals per group). Scale bar, 100 µm. Error bars indicate SD. ***p < 0.001. ****p < 0.0001 ns, non-significant.

It has also been shown *in vitro* that cells become larger and flat when they become senescent given their higher biosynthetic activity (Hernandez-Segura et al., 2018; Munoz-Espin and Serrano, 2014). As mentioned above, we also observed an increase in nuclei size in all Notch mutants compared to control livers (Figure 19A,B). We also saw that the vasculature of Notch mutants occupies significant more space (Figure 16A), even though the number of ECs do not change significantly (Figure 17A,B), particularly in *Notch1*^{iDEC} and *Rbpj*^{iDEC} mutant livers. This indicates that each endothelial cell in these mutants must be significantly larger.

Altogether, these results suggest that Notch signalling pathway prevent ECs from becoming senescent. When the Notch function is reduced (Dll4) or completely lost (Rbpj), excessive mitogenic stimuli drives endothelial cell senescence in a cell autonomous manner. The senescence-associated secretory phenotype may also induce secondary senescence of surrounding hepatocytes by paracrine factors.

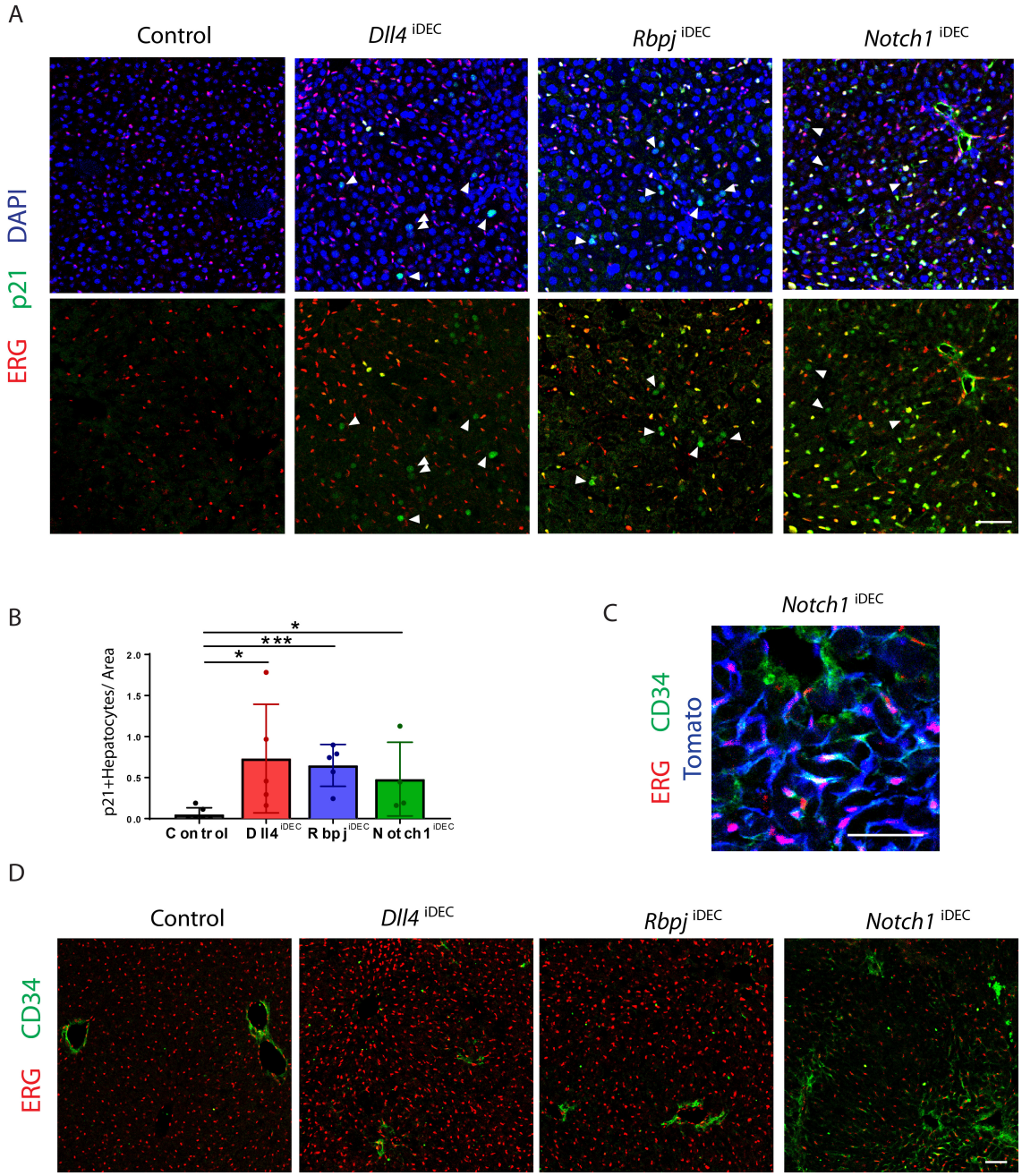

Figure 29: Endothelial Notch loss-of-function results in increased hepatocyte senescence. **(A-B)** Confocal micrographs of liver sections showing a common upregulation of p21 in hepatocytes compared to control liver. Arrowheads indicate p21+ hepatocytes (n=3 animals per group). **(C)** Representative confocal micrographs of liver sections showing that *Notch1* deletion results in increased CD34 expression in liver capillaries. **(D)** Contrary to the restricted expression of CD34 in portal veins of *Dll4*^{iDEC}, *Rbpj*^{iDEC} and control livers, CD34 expression in *Notch1*^{iDEC} is present throughout the endothelium. Scale bar, 50 µm. Error bars indicate SD. **p < 0.01. ****p < 0.0001. ns, non-significant.

p21 induces EC senescence and prevents apoptosis after the loss of *Rbpj*

To determine the functional link between Notch signalling and p21 function in the regulation of liver EC quiescence/senescence, we investigated whether the lack of EC proliferation in *Rbpj* mutants could be rescued by p21 deletion. To test this hypothesis, we compared *Rbpj*^{iDEC} with *Rbpj*^{iDEC} *p21*^{KO} mice. In our experiments we also included *Cdh5-CreERT2 iSuRe-Cre* control mice and *p21*^{KO} mice (Figure 30A). After 2 weeks of genetic deletion, we observed that the vascular abnormalities and enlargement of sinusoids presented in *Rbpj*^{iDEC} livers were also present in *Rbpj*^{iDEC} *p21*^{KO} mice. Surprisingly, we also noted that the architecture of *p21*^{KO} vasculature was also affected (Figure 30B). In the absence of p21, we observed only a mild increase in the number of liver ECs (ERG+) (Figure 31A,B).This shows that the loss of the cell cycle inhibitor p21 does not significantly impact the generation of ECs, even after the loss of *Rbpj* for 2 weeks. Surprisingly, in contrast to the modest increase in EC number, lack of p21 in *Rbpj*^{iDEC} liver ECs led to a substantial increase in the frequency of Ki67+ ECs, but only after the loss of *Rbpj* (Figure 31A,C). These results confirm that p21 upregulation after the loss of *Rbpj* (70% of ECs become p21+) not only marks hypermitogenic cells, but also partially prevents the increase in proliferation that is normally seen in *Dll4*^{iDEC} livers but not in *Rbpj*^{iDEC} livers (Figure 31C).

The 2-fold increase in proliferating Ki67+/ERG+ ECs in *Rbpj*^{iDEC}*p21*^{KO} livers (vs *Rbpj*^{iDEC} livers), did not correlate with the 1.2-fold increase in total EC number. These results suggest that the p21 absence in ECs could be triggering other biological processes that would prevent the increase in EC number. In particular, previous reports have shown the ability of p21 to inhibit apoptosis (Abbas and Dutta, 2009; Georgakilas et al., 2017). Loss of p21 may also induce apoptosis in hyperactivated cells. Indeed, we detected high levels of the apoptosis marker caspase-3 expression in *Rbpj*^{iDEC} *p21*^{KO} livers (Figure 31D,E). This very significant increase in EC apoptosis after the loss of p21, may explain the relatively mild increase in EC number in *Rbpj*^{iDEC} *p21*^{KO} livers. These results also suggest that hypermitogenic *Rbp*^{iDEC} ECs activate anti-apoptosis pathways and may be more sensitive to compounds targeting these pathways, such as senolytics (Childs et al., 2017)

These results also confirm the direct link between Notch signalling and p21 in liver quiescent ECs. The crosstalk between these pathways finely tunes the dose-dependent switch that determines whether an EC proliferates, remains quiescence, arrest, becomes senescent or ultimately dies.

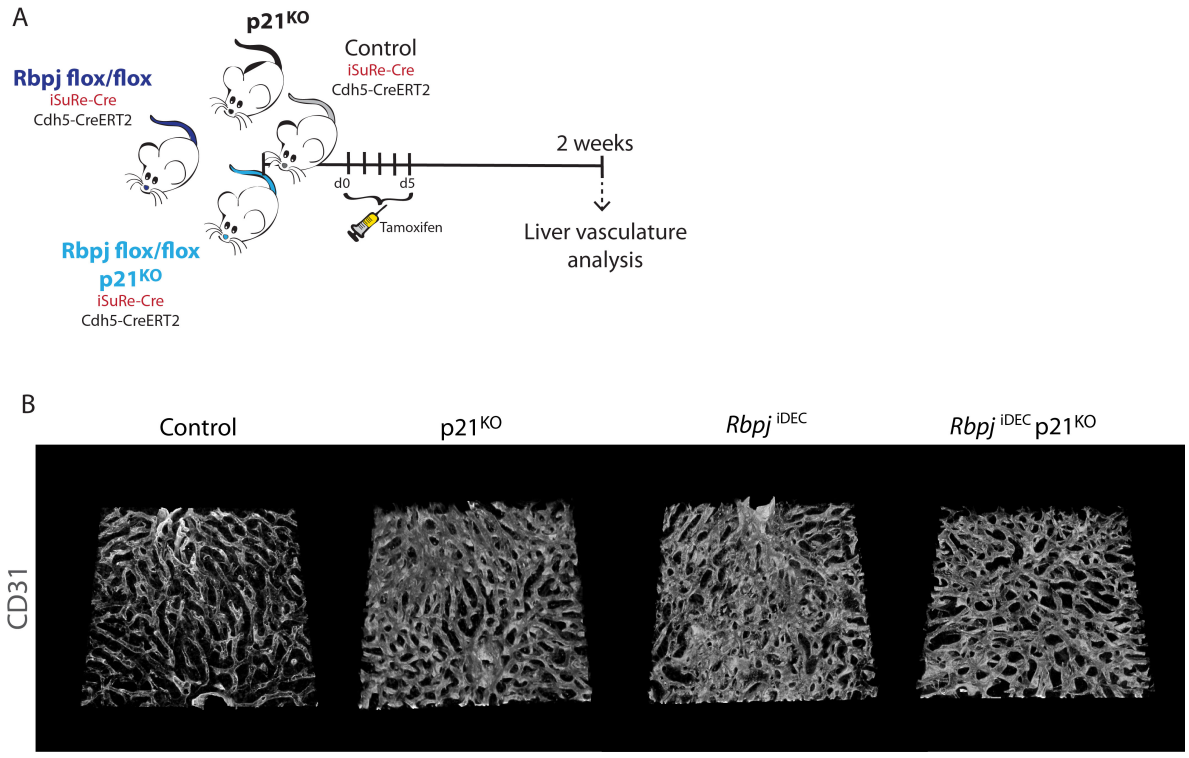

Figure 30: Absence of p21 does not ameliorate the sinusoidal vascular dilation observed after *Rbpj* deletion. **(A)** Experimental layout for the inducible deletion of *Rbpj* in a p21^{KO} background (*Rbpj*^{iDEC} p21^{KO}) in Cdh5+ ECs. *Cdh5(PAC)-CreERT2 iSuRe-Cre Rbpj* floxed p21^{KO} adult mice received five intraperitoneal injections of tamoxifen as did age-matched control mice. 2 weeks after the first tamoxifen injection, mice were sacrificed and the liver was evaluated. **(B)** 3D projection of thick vibratome sections show the expansion and dilation of the endothelial compartment (CD31+) in *Rbpj*^{iDEC} p21^{KO} mutant livers. p21^{KO} vascular pattern is also slightly affected compared to control.

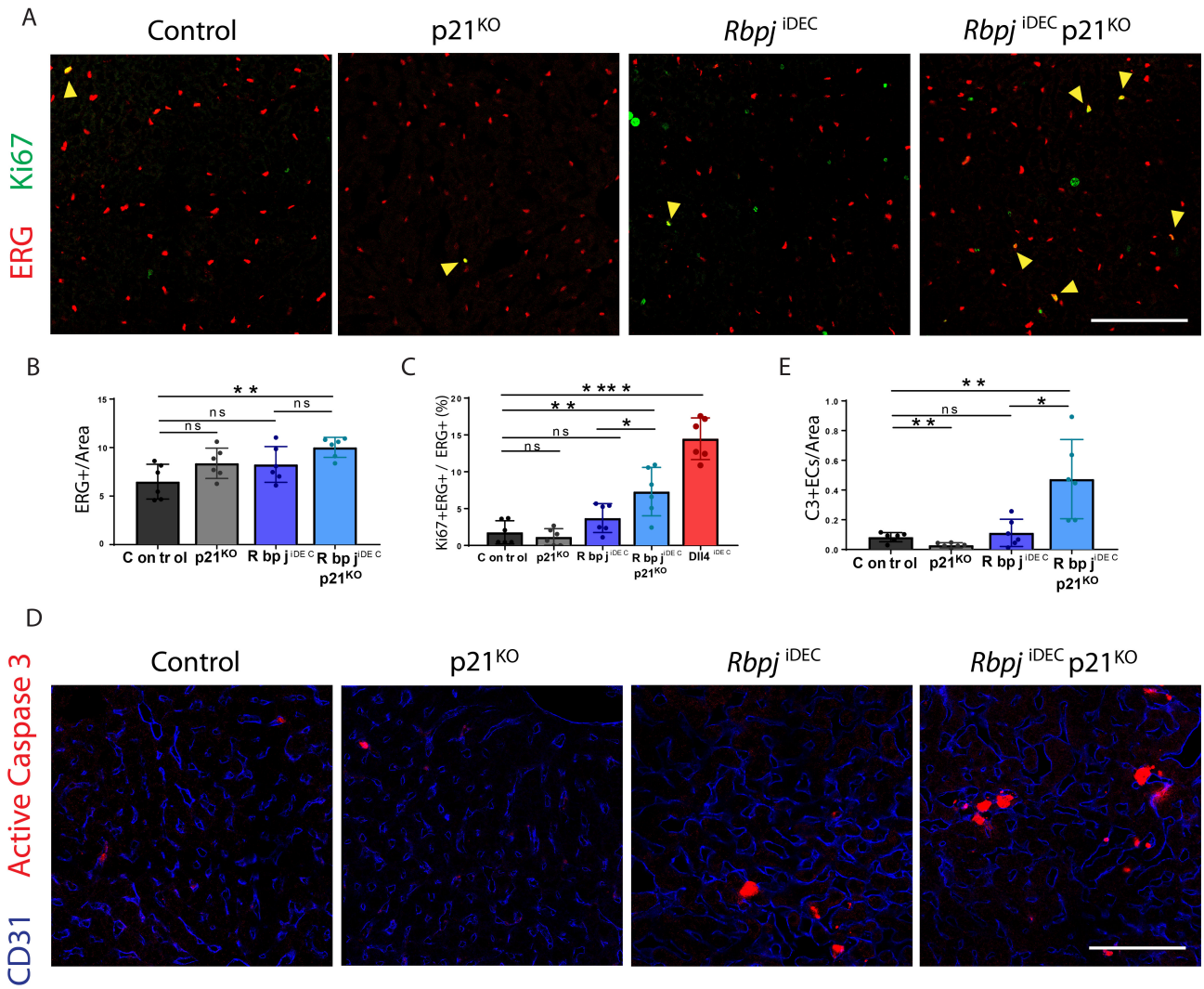

Figure 31: p21 represses EC proliferation and apoptosis after loss of Rbpj. (A-C) Confocal micrographs of liver sections showing that while the absence of p21 in a *Rbpj*^{iDEC} background results in a modest increase in EC density (ERG+), EC proliferation (Ki67+ERG+) is significantly increased compared with p21KO, *Rbpj*^{iDEC} and control mice. For EC proliferation, only ERG+ MbTomato+ (ECs with reliable gene deletion) have been used for quantification (n=3 animals per group). *Dll4*^{iDEC} EC proliferation is also included for group comparison. **(D-E)** Confocal micrographs of liver sections showing that the absence of p21 in a *Rbpj*^{iDEC} background results in a significant increase in apoptosis (Active Caspase 3+) (n=3 animals per group). Scale bars, 100 µm. Error bars indicate SD. *p < 0.05. **p < 0.01. ****p < 0.0001. ns, non-significant.

Temporal course of *Dll4*^{iDEC} liver phenotype

To better elucidate the role of *Dll4* in EC proliferation in the quiescent vasculature, we next aimed to examine the effects of *Dll4* deficiency over time. Thus, we evaluated *Dll4*^{iDEC} liver vasculature 1, 2 and 3 weeks after tamoxifen-induced deletion (Figure 32A). 3D imaging of CD31 vascular staining in thick vibratome sections revealed that the vascular abnormalities and enlargement of capillaries only occur between the first and second week after *Dll4* deletion (Figure 32B-a). At the 1 week post-*Dll4*-deletion timepoint we observed an increase in filopodia tip-like structures that are no longer present or detectable 2/3 weeks after deletion (Figure 32B-b, yellow arrowheads). These results are in partial accordance with the excessive tip cell formation and filopodia protrusion observed after *Dll4* deletion during retina vascular development or tumor angiogenesis (Hellstrom et al., 2007; Lobov et al., 2007; Noguera-Troise et al., 2006; Ridgway et al., 2006). Moreover, to visualize EC density and proliferation, we stained liver sections with the nuclear marker ERG and the cell cycle marker Ki67. At the 1 week post-*Dll4*-deletion timepoint there was already an increase in the frequency of EC proliferation (18%) compared to control conditions (1.4%) (Figure 33A,B-1week) despite no significant changes in the total number of ECs. This suggests that the cell cycle entry and consequent division process after the loss of Dll4 signalling in quiescent ECs is very slow or infrequent. Remarkably, at this same timepoint, we observed a substantial increase in hepatocyte proliferation (33A,C). This peak in hepatocyte proliferation at 1 week, declined at 2 weeks post-*Dll4*-deletion (Figure 33A,C - 2 weeks), which corresponds to a timeframe when the number of total ECs increases significantly, due to the prior increase in EC proliferation (Figure 33A,B - 2 weeks). While the EC number and frequency of proliferation stabilizes 3 weeks after *Dll4* deletion, hepatocyte proliferation returns to basal levels (Figure 33A-C - 3 weeks). This is in agreement with the already described chronologically biphasic contribution of liver ECs to liver regeneration. By releasing angiocrine factors, activated liver ECs stimulate adjacent hepatic proliferation in the early phases. Later, the regenerating liver requires blood supply and the liver ECs start to divide to meet that demand, but the hepatocytes no longer proliferate (Ding et al., 2010).

At the same time there is a gradual increase in EC number in *Dll4*^{iDEC} livers, the nuclei size also increases (Figure 33D), suggesting that these cells become progressively larger given their higher biosynthesis rate.

Collectively, this data suggests that cell cycle reentry and subsequent cell division from a previously quiescent state, is a relatively slow process. Contrary to the rapid increase –

24/48h- in EC number after loss of Dll4-Notch signalling during retina vascular development (Pontes-Quero et al., 2019), in the quiescent liver vasculature the increase in EC numbers only occurs 2 weeks after inducing *Dll4* deletion.

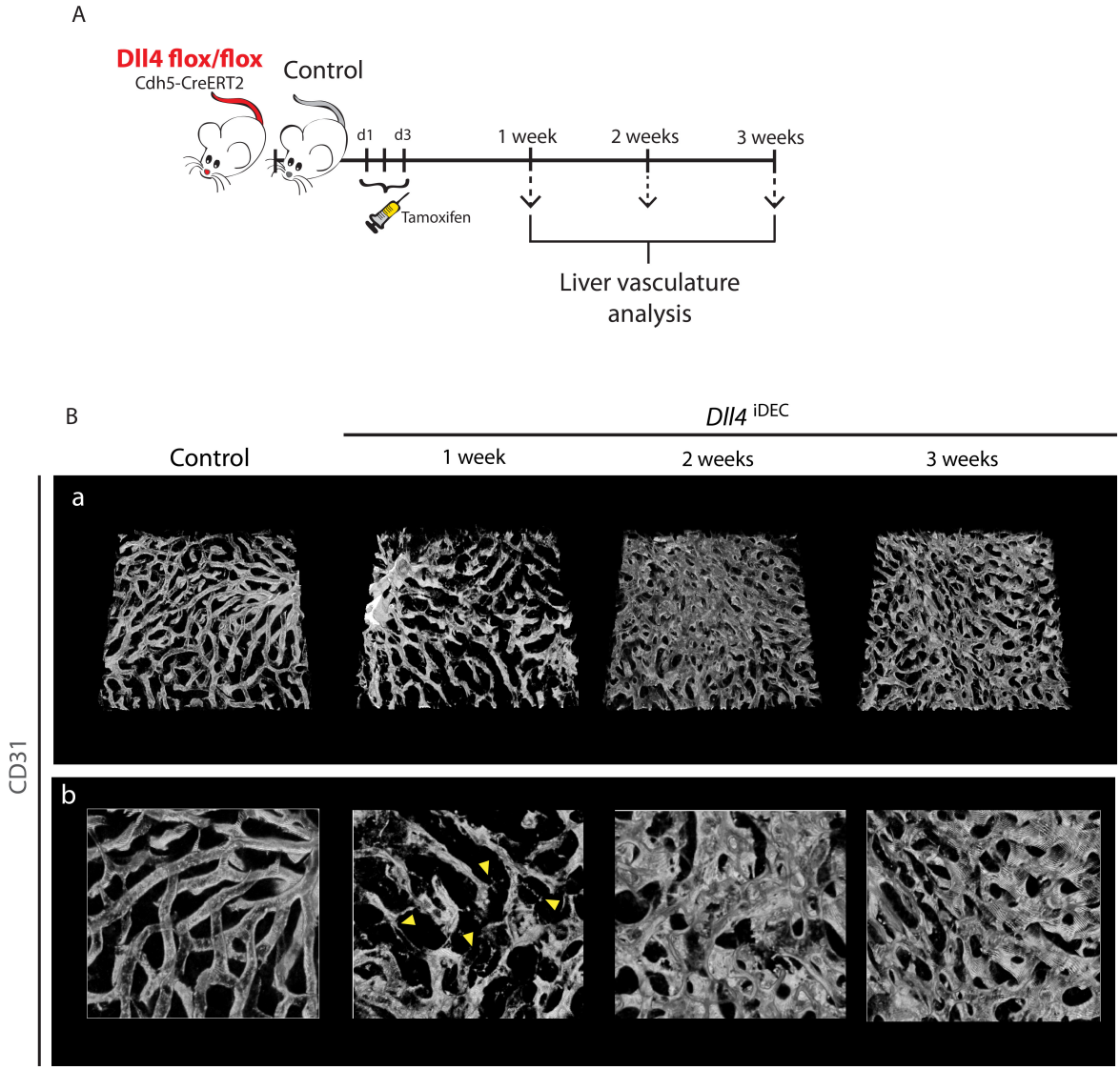

Figure 32: Time course of Dll4 deficiency effects in liver vessels. **(A)** Experimental layout for the inducible deletion of Dll4 (*Dll4*^{iDEC}) in Cdh5+ ECs. *Cdh5(PAC)-CreERT2 Dll4* floxed adult mice received three intraperitoneal injections of tamoxifen as did age-matched control mice. 1, 2 and 3 weeks after the first tamoxifen injection, mice were sacrificed and the liver was evaluated. **(B)** 3D projection of confocal images from thick vibratome sections show that the vascular malformations and capillary enlargement arise between the first and second week post-*Dll4*-deletion (a). Higher magnification pictures in panel (b) shows that 1 week after Dll4 deficiency we can observe filipodia tip-like structures (arrowheads) that are not present or visible at later stages.

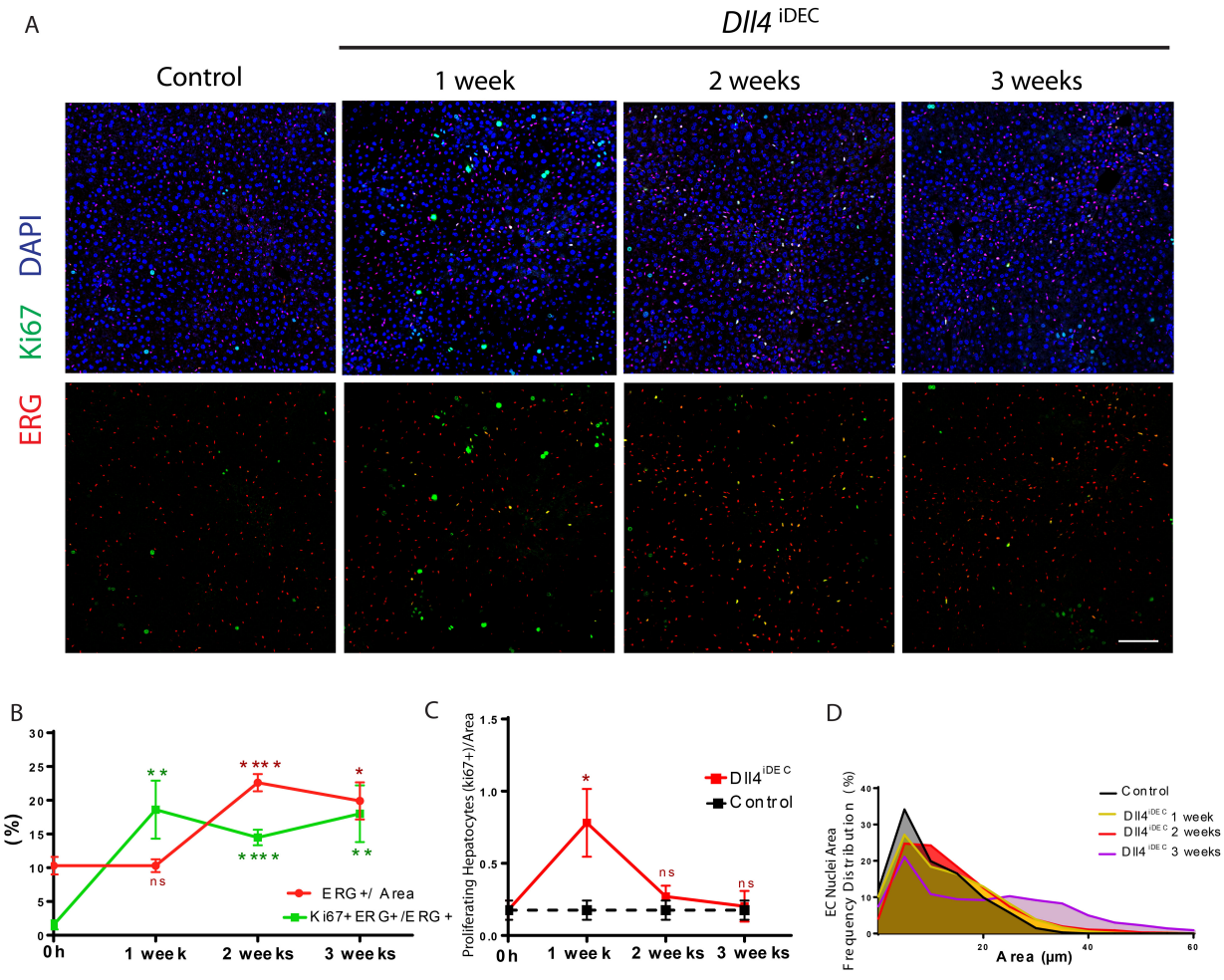

Figure 33: Endothelial and hepatocyte proliferation are dynamically coupled in time. **(A-C)** Confocal micrographs of liver sections showing EC (ERG+ cells) and hepatocyte proliferation (ERG- cells) in time. Whereas the absence of Dll4 results in an increase in EC (Ki67+ERG+) and hepatocyte proliferation (Ki67+ERG- hepatocyte DAPI+) 1 week after deletion, a significant increase in EC density only occurs 2 weeks after. Hepatocyte proliferation declines 2 weeks after Dll4 deficiency, but EC proliferation and density are steadily maintained. Quantifications of the mentioned parameters are depicted in B and C. Each time point is compared to control conditions (n=3 animals per group). **(D)** Nuclei area distribution shows that after *Dll4* deletion, there is an increase in the number of ECs with larger size in time, particularly at 3 weeks. (n=3 animals per group). Scale bars, 100 µm. Error bars indicate SEM. *p < 0.05. **p < 0.01. ****p < 0.0001. ns, non-significant.

Heterogeneous and zonal response of liver vessels to *Dll4* deletion

The gradual increase in EC proliferation and density after full loss of Dll4 signalling does not occur equally throughout the entire liver endothelium. EC density and proliferation were significantly higher in the zone around the central veins (CV), when compared to the portal veins (PV) zone (Figure 34A-E). This liver vasculature proliferation zonation correlates also with the zonation in the nuclei size of those ECs compared to their neighbouring ECs from PV zone (Figure 34C). Interestingly, the increase in hepatocyte proliferation observed in *Dll4*^{iDEC} livers was located more in the less proliferative PV areas and not CVs (Figure 34D). We have also found that the p21-expressing ECs in *Dll4*^{iDEC} livers are located mostly in the most proliferative and dense CV zone (Figure 34F-G), suggesting that the cell cycle arrest occurs mostly in highly mitogenic environments.

Microscopy imaging of thin or thick liver sections with CD31 immunostainings confirmed that while the PV capillaries were not apparently affected by *Dll4* deletion, the vascular malformations and enlarged sinusoids observed in *Dll4*^{iDEC} livers were only presented in the capillaries connecting CV (Figure 35A,B). In the CVs zone we also found increased apoptosis by active caspase-3 staining (Figure 35C,D).

Taken together, these observations suggest there is a heterogeneous and zonal response of liver vessels to *Dll4* deletion with the capillaries around CVs being the most sensitive/reactive to the loss of Dll4 signalling.

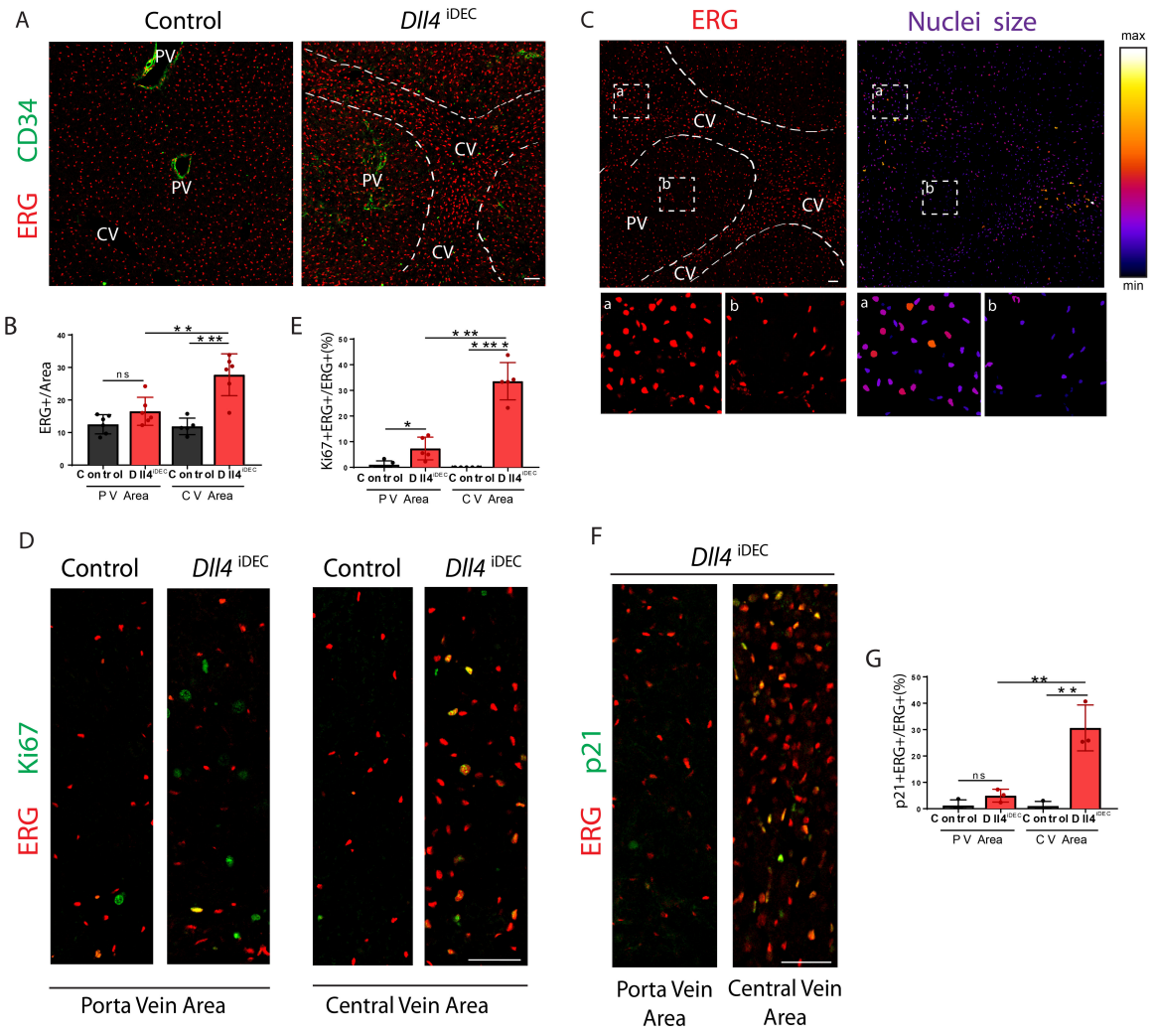

Figure 34: Spatial heterogeneity in the proliferation of liver vessels after *Dll4* deletion. (A-B) Confocal micrographs of liver sections showing that EC density in *Dll4*^{iDEC} liver is higher in the endothelium connecting the central veins (CV) rather than the endothelium surrounding portal veins (PV), that are distinguished by CD34+ staining. White dotted lines highlight the denser area. Quantification of the above-mentioned parameters is depicted in B (n=3 animals per group). **(C)** Representative images from confocal micrographs analysis of *Dll4*^{iDEC} liver section showing the increase in nuclei size specifically in CV connecting sinusoids. White dotted lines highlight the denser area. Larger nuclei are brighter colored in the images at right. Higher magnification pictures in panels (a) and (b) show differences in nuclei size between CV and PV areas respectively. **(D-E)** Confocal micrographs of liver sections showing that EC proliferation (Ki67+ERG+) in *Dll4*^{iDEC} liver is higher in the endothelium connecting the CV rather than the endothelium surrounding PV, as depicted in chart E (n=3 animals per group). **(F-G)** Confocal micrographs of liver sections showing that p21 expression (p21+ERG+) in *Dll4*^{iDEC} liver is also higher in the endothelium connecting the CV rather than the endothelium surrounding PV, as depicted in chart G (n=3 animals per group). Scale bar, 50 µm. Error bars indicate SD. *p < 0.05. **p < 0.01. ***p < 0.001. ****p < 0.0001. ns, non-significant.

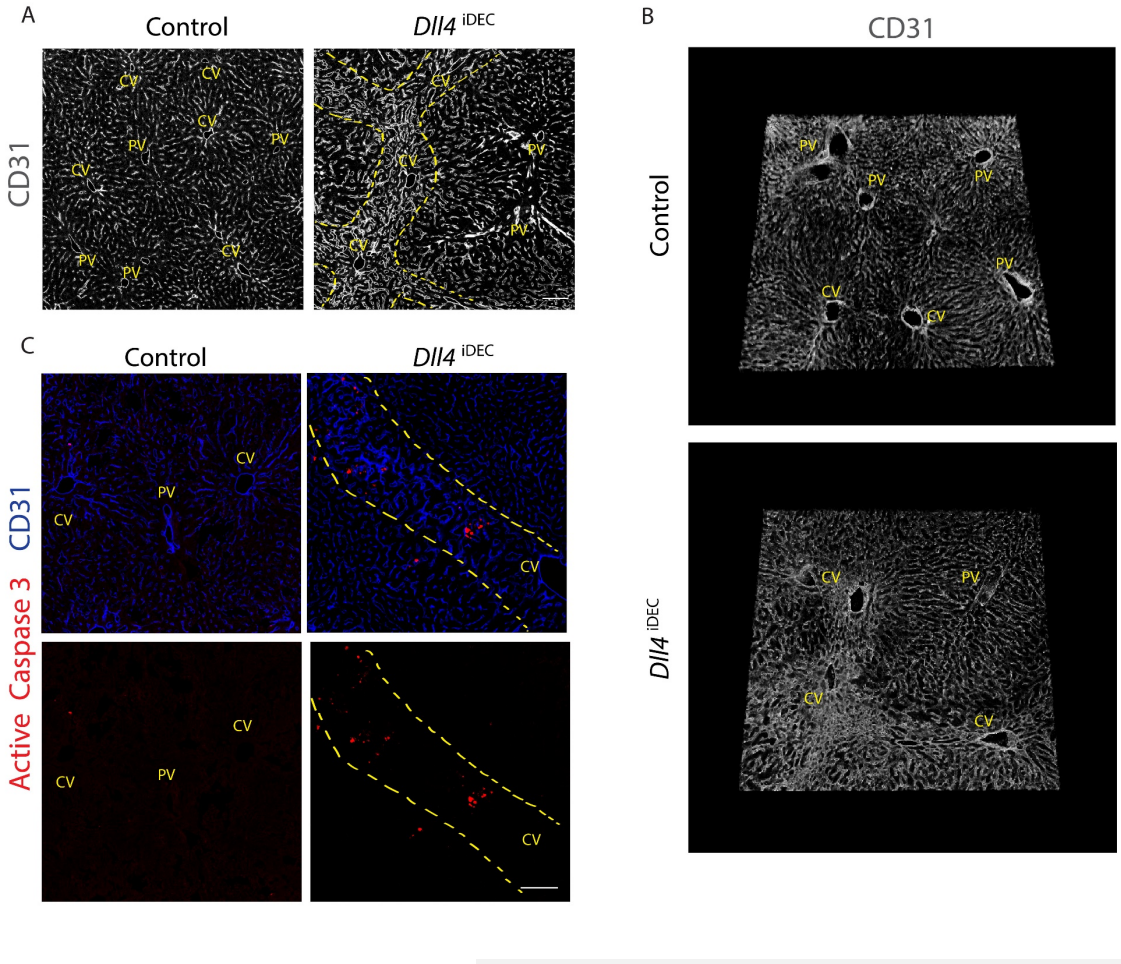

Figure 35: Vascular malformations after *Dll4* deletion are localized in ECs surrounding central veins but not portal veins. (A-B) Confocal micrographs of large liver sections with CD31+ immunostaining and 3D reconstruction images from vibratome sections show that the vascular malformations observed in *Dll4*^{iDEC} livers are located in CV connecting sinusoids, but not in PV surrounding ECs. **(C-D)** Confocal micrographs of liver sections with C3+ staining showing that there is increased apoptosis as depicted in chart D (Active Caspase 3)(n=3 animals per group). Scale bar, 100 µm. Error bars indicate SD. *p < 0.05. ns, non-significant.

The expression of Notch signalling members is spatially zonated in the liver endothelium

Recent scRNA-seq studies have reported that apart from the already known hepatocyte transcriptional zonation, liver ECs also present a zonated gene expression pattern

(Halpern et al., 2018). Given the higher sensitivity and reactivity to *Dll4* deletion of CV zone capillaries, we initially expected a higher expression or activity of the Notch signalling members in these vessels. However, it is known that Notch signalling components are mostly expressed in well oxygenated arteries and capillaries and less in perivenous capillaries (Gridley, 2010; Swift and Weinstein, 2009). Indeed, Dll4 ligand was highly expressed in oxygen-rich PV areas and surrounding capillaries (Figure 36A-a) and weakly expressed in capillaries surrounding the CVs, and completely absent from CVs (Figure 36A-b). Immunostaining against the active form of the receptor (N1ICD, V1744), that only detects ECs with the highest levels of Notch signalling, confirmed that Notch signalling activation is much more frequent in PV zone capillaries (Figure 36A-a-b,B,C), correlating with the observed Dll4 ligand expression pattern. As expected, the N1ICD activation we detected in control liver ECs was abolished in both *Dll4*^{iDEC} PV and CV surrounding capillaries (Figure 36B,C). Indeed, scRNA-seq studies (published during the course of this thesis) corroborated our results. Expression of *Dll4* and the Notch target *Efnb2* is zonated, with expression levels highest in periportal areas and lowest closest to the CVs (Halpern et al., 2018). To analyse the expression of other Notch signalling components in the entire liver vasculature, with single cell resolution, we analysed the raw data published recently (Kalucka et al., 2020). Consistent with our Dll4 immunostainings and with previous scRNA-seq publications, the highest expression of *Dll4* was found in the portal-periportal areas and capillaries and its expression was very low in central veins or venous capillaries. Surprisingly, liver venous vessels express both *Dll1* and *Jag1* ligands at relatively high levels (Figure 37A). In contrast to the heterogeneous ligand distribution in the liver vasculature, Notch receptors were homogenously expressed throughout the entire liver vasculature, including veins. Similarly to our bulk RNA-seq analysis, we found *Notch1* to be the main receptor to be expressed in the liver endothelium, with *Notch4* being less expressed (Figure 37B). We also analysed the expression of canonical Notch signalling target genes, with single-cell resolution. Similar to the *Dll4* expression pattern observed, both *Hey1* and *Efbn2* expression was zonated, being highly expressed in the portal veins and periportal capillaries, known to have higher Dll4/Notch signalling activities (Figure 37C). These results suggest that even though *Dll1*, *Jagged1* and Notch receptors are expressed in venous vessels, they induce relatively low Notch signalling activity when compared to Dll4, presumably because these vessels also highly express the Notch receptor modifiers Fringe proteins, particularly *Lfng* and *Mfng* (Figure 1D). Interestingly, *Lfng* expression is zonated unlike *Mfng* (Figure 37D).

This Notch members expression and signalling zonation could explain the heterogeneous and zonal EC phenotypes observed in *Dll4*^{iDEC} liver ECs. However, both

periportal and perivenous liver vessels express *Dll1* and *Jagged1*, and they do not seem to compensate for the loss of Dll4 in CVs capillaries. They may compensate for its loss in PV capillaries and arterial vessels.

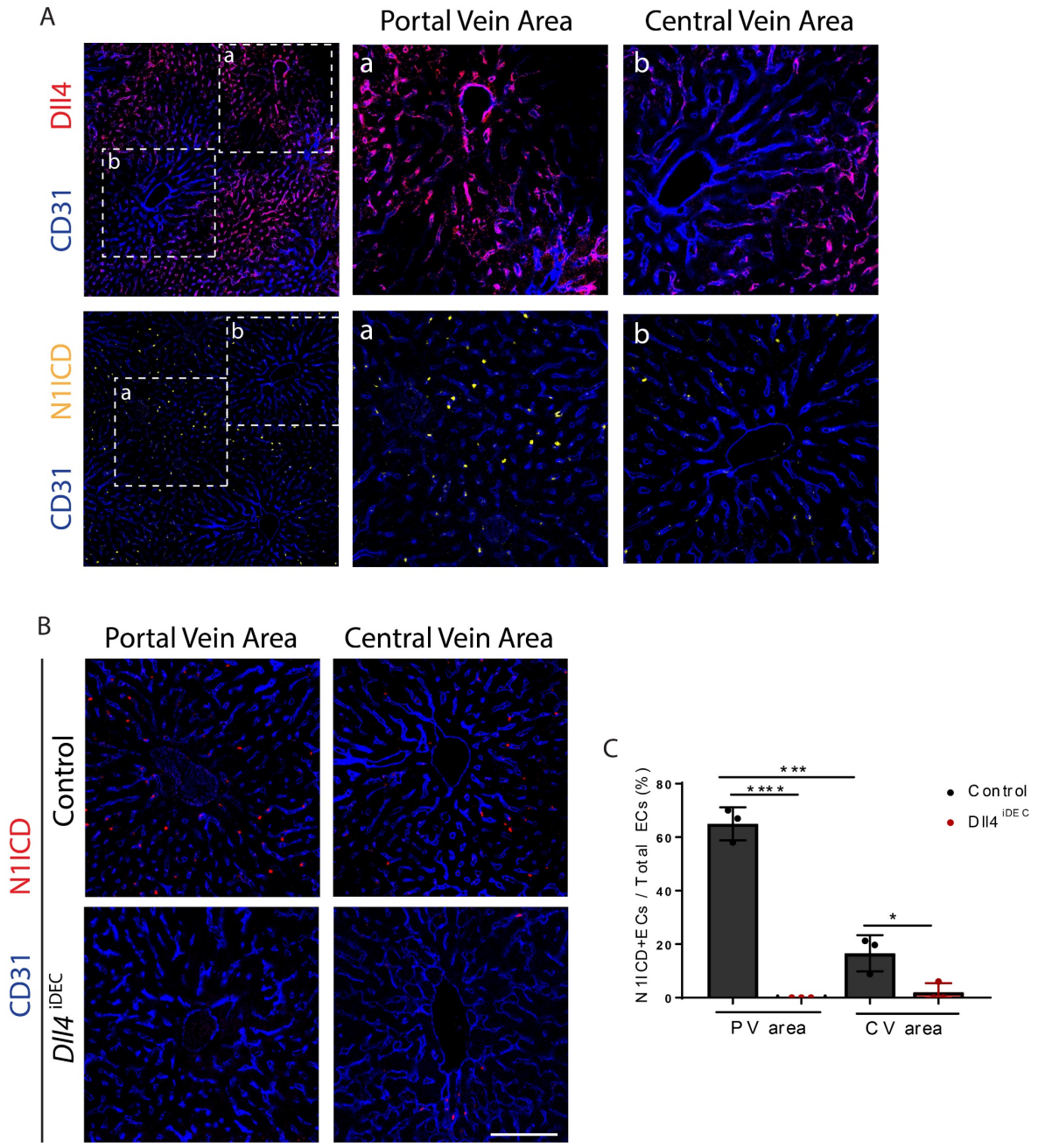

Figure 36: Dll4/Notch1 expression and signalling is periportally zonated in liver quiescent ECs. (A) Confocal micrographs of liver sections show that Dll4 and activated N1ICD (V1744) are mostly present in PV areas (a) and are not detectable or weaker in CV areas (b). **(B-C)** Confocal micrographs of liver sections show that liver ECs lose N1ICD activation after *Dll4* deletion as depicted in chart C (n=3 animals per group). Scale bar, 100 µm. Error bars indicate SD. *p < 0.05. ***p < 0.001. ****p < 0.0001.

The genetic compensation of *Dll4* deletion by Dll1 and Jagged1 could also explain the differences observed between *Dll4*^{iDEC} *and Rbpj*^{iDEC} *or Notch1*^{iDEC} livers. Consistent with this, we have found that contrary to the restricted zonation in p21 expression in the CV zone of *Dll4*^{iDEC} livers, in *Rbpj*^{iDEC} livers p21 is expressed both in PV and CV zones, supporting the hypothesis that Dll4 functions can be compensated by other Notch ligands, unlike the Rbpj or Notch1 functions (Figure37E).

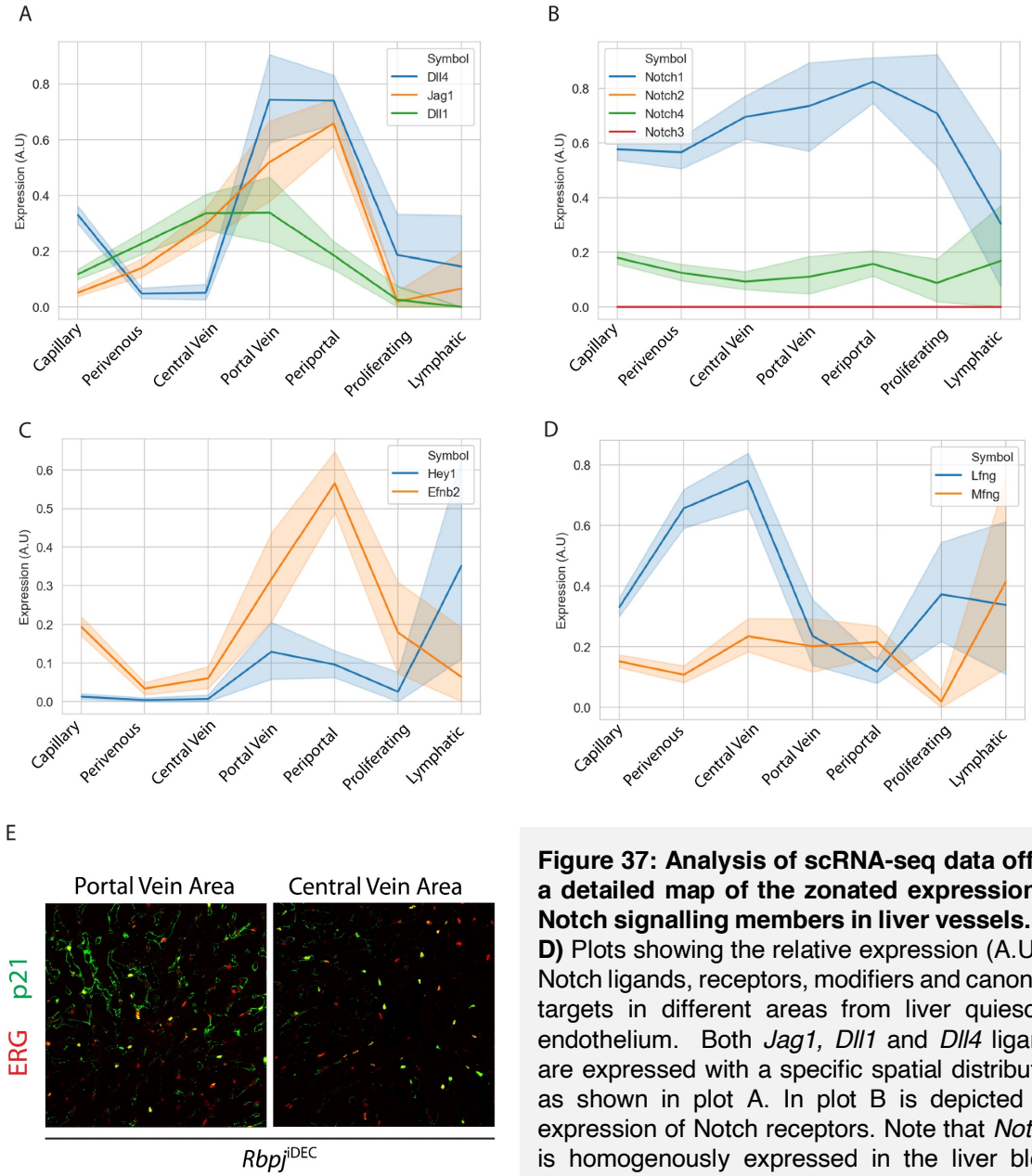

Figure 37: Analysis of scRNA-seq data offers a detailed map of the zonated expression of Notch signalling members in liver vessels. (A-D) Plots showing the relative expression (A.U) of Notch ligands, receptors, modifiers and canonical targets in different areas from liver quiescent endothelium. Both *Jag1, Dll1* and *Dll4* ligands are expressed with a specific spatial distribution as shown in plot A. In plot B is depicted the expression of Notch receptors. Note that *Notch1* is homogenously expressed in the liver blood vasculature. Plot C shows that Notch target genes are highly expressed only in portal and periportal capillaries compared with other areas. Plot D shows that *Lfng* is zonated, being highly expressed in venous vessels. **(E)** Representative confocal micrographs of liver sections show that p21 is expressed in both CV and PV areas after *Rbpj* deletion in liver ECs.

Multispectral clonal analysis reveals that only a very small fraction of liver ECs have the potential to proliferate and expand over time

Our previous analysis of *Dll4*^{iDEC} livers suggested that 2 weeks after *Dll4* deletion, ECs more than double in number when compared to control liver ECs (Figure 17A,B). Nonetheless, our more detailed temporal analysis of *Dll4*^{iDEC} liver ECs revealed that this increase in EC number only occurred between the first and the second week post-Dll4 deletion, and it stabilizes 3 weeks after deletion (Figure 33A,B). Given the zonal proliferation of liver ECs (Figure 34), it may be that there is also a significant difference in the way single ECs proliferate in the liver. The previous zonal data only offer us an estimate of the average EC number and proliferation differences and does not allow us to establish the precise spatio-temporal dynamics of EC proliferation. In addition, even if given percentage of the endothelium was found to be Ki67+, it does not give us an idea of which of these cells is actually dividing and proliferating, and how many times each cell proliferates over time.

Inducible fluorescent genetic mosaics are powerful tools to study the biology of single cells, their organization in the tissue, their clonal expansion or the migration over time. Inspired by the Brainbow technology, our laboratory developed the optimized ifgMosaic technology (Pontes-Quero et al., 2017) that consists in several new mosaic mouse lines and enables the induction of genetic mosaics with higher cellular/clonal resolution *in vivo* (Garcia-Gonzalez et al., 2020). The ifgMosaic technology is based on the stochastic Cre-dependent recombination of mutually exclusive and different Loxp sites in two alleles, the iMb-Mosaic allele and the iChr-Mosaic allele. Stochastic and combinatorial recombination of these two alleles generates only one outcome of 15 possible in each cell. Each cell expresses either a nuclear (iChr2-Mosaic), or a membrane (iMb2-Mosaic), or a combination of both nuclear and membrane fluorescent reporters, which allows the distinction of up to 15 different colour-coded clones (9 dual labelled and 6 single labelled) with high single cell or clonal resolution. Importantly, the probability of obtaining a given dual colour code is so low, that any given dual colour clone in a given tissue area and timepoint corresponds to the progeny of a single pre-existing recombined cell. For this reason, and in order to better understand the dynamics of EC proliferation in *Dll4*^{iDEC} liver ECs, we combined these mice with *Cdh5(PAC)-CreERT2* and *Dll4 floxed* mice (Figure 38A,B). Fate mapping of single *Dll4*^{iDEC} liver ECs 2 weeks after tamoxifen induction revealed that the most frequent clone sizes (Figure 38C, D) ranged between 1 cell (66% of clones) (Figure 38E, yellow arrow) to 3 cells per clone (7%) (Figure 38E, white arrow). Unexpectedly, by analysing large sections, we found a rare type of highly proliferative clones (1.3%) that were formed by

25 to 80 cells (Figure 38F). Interestingly, these big clones were located very close to CVs, the vascular area with a higher proliferation rate and EC density.

These findings clearly show that after *Dll4* deletion, only a relatively minor fraction (32%) of quiescent cells enter cell cycle (Ki67+), and among these, only a very small fraction of cells proliferate significantly more than their immediate neighbours. This analysis uncovered a specific liver endothelial subpopulation that has a high proliferation potential, locates in areas close to the CV, and its high proliferation potential is negatively regulated by Dll4/Notch signalling.

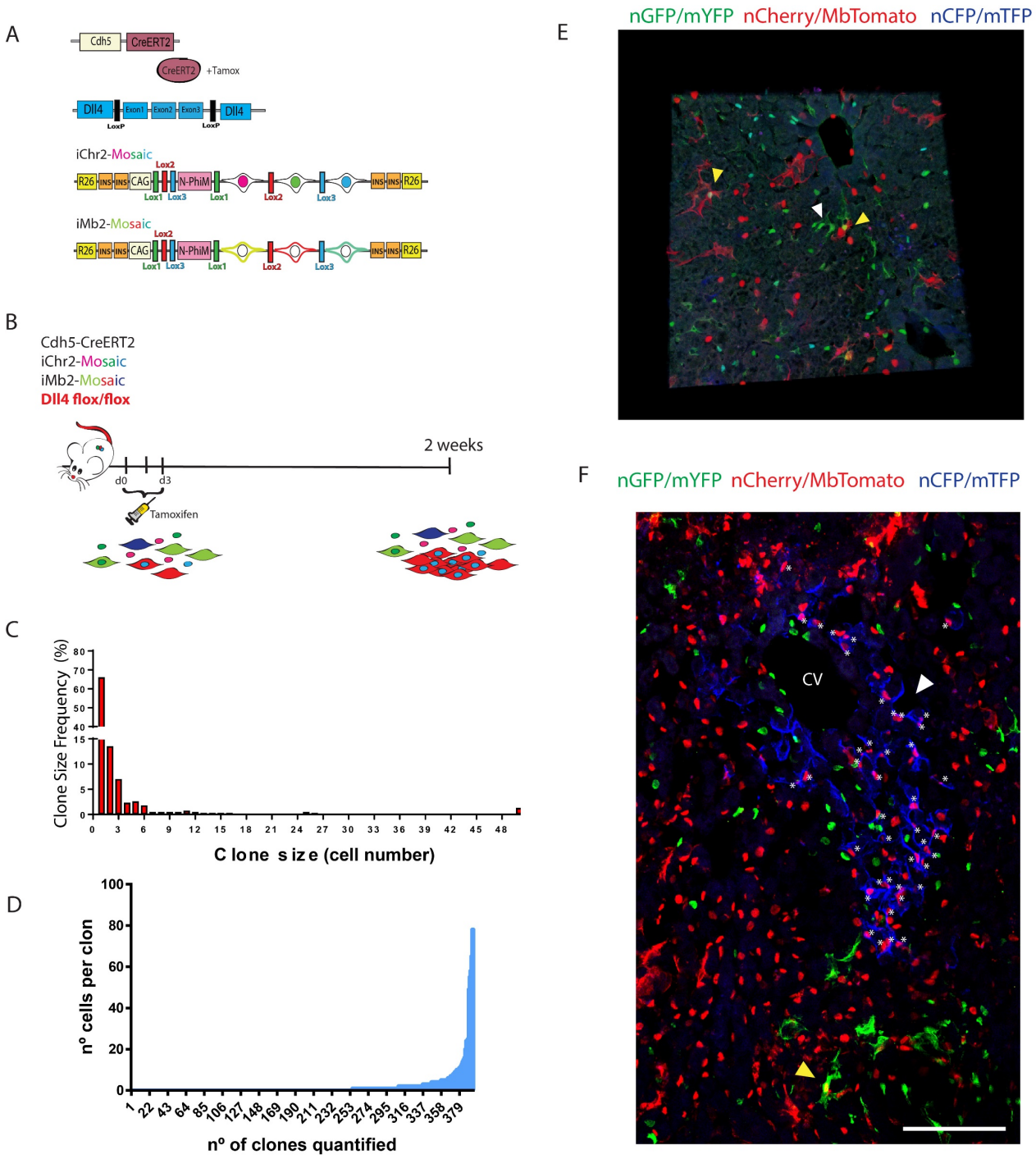

Figure 38: Fate mapping of liver ECs with Dll4 deficiency reveals a population with a hyperproliferative potential. (A) Schematic representation to illustrate the alleles and transgenes used for the study. **(B)** Experimental layout to fate map single ECs with *Dll4* deletion. *Cdh5(PAC)-CreERT2 iChr2-Mosaic iMb2-Mosaic Dll4* floxed adult mice received three intraperitoneal injections of tamoxifen. 2 weeks after the first tamoxifen injection, mice were sacrificed and the liver was evaluated. **(C-D)** Distribution charts showing the clone size frequency and the number of dual-labelled clones quantified 2 weeks after inducing *Dll4* deletion. **(E)** 3D reconstruction images from vibratome sections show the multispectral mosaic of ECs obtained with this strategy. As an example, yellow arrowheads indicate 1 cell-clone and white arrowhead indicates 3 cell-clone. **(F)** Confocal micrograph of large liver sections shows a rare population found around the CVs. Yellow arrowhead indicates 1 cell-clone and white arrowhead indicates 42 cell clone. Each cell of the clone is mark with a white asterisk. Scale bar, 100 µm.

Chapter II:

iSuRe-Cre: a genetic tool to reliably induce and report Cre-dependent genetic modifications

Design and testing of *iSuRe-Cre* constructs

The Cre/LoxP technology has several limitations that are mainly related to the weak and often variable expression of promoters in transgenes containing the Cre or CreERT2 coding sequences, which frequently do not induce the deletion of all different types of floxed alleles in the cells where they are expressed. In our laboratory, we have observed that while the *Dll4* floxed gene is completely deleted in quiescent ECs after tamoxifen induction, other genes such as *Myc*, *Rbpj* or *Notch1* are much more difficult to delete, limiting the efficiency and reliability of conditional mouse genetic studies, particularly in quiescent ECs, that weakly express the promoters (such as the Cdh5 promoter) that are used to drive CreERT2 expression specifically in ECs. To overcome these technical problems, we sought to develop a new DNA construct that would be easy to induce by Cre/CreERT2-mediated recombination, and that would subsequently enable strong and sustained co-expression of a fluorescent reporter and a constitutively active Cre (Figure 39A). We reasoned that this simple construct (*iSuRe-Cre*), when inserted in the genome of ES cells or mice, would significantly increase the efficiency and reliability of conditional genetic modifications in reporter expressing cells. The *iSuRe-Cre* construct contains the ubiquitous and strong CAG promoter followed by a very short (1.1kb), and therefore easy to recombine (Pontes-Quero et al., 2017; Zheng et al., 2000), LoxP-flanked (floxed) DNA sequence. This sequence has the *N-PhiM* reporter gene, which encodes a non-cytotoxic and non-fluorescent mutated PhiYFP protein (Evrogen) having a nuclear localization signal (Cai et al., 2013; Pontes-Quero et al., 2017), and a transcription stop signal. After recombination/deletion of the floxed cassette by Cre or CreERT2, the *iSuRe-Cre* construct enables the strong co-expression of a bright membrane-localized fluorescent reporter (MbTomato) and a constitutively active and permanently expressed Cre protein. These two proteins are separated by the viral 2A peptide to guarantee equimolar expression (Trichas et al., 2008) and complete correlation between the MbTomato reporter expression and Cre activity (Figure 39B). The iSuRe-Cre DNA elements were finally inserted in a modified ROSA26 gene-targeting vector (Muzumdar et al., 2007; Soriano, 1999), containing four chicken β-globin HS4 insulator sequences, to reduce genomic interference and silencing from neighbouring genomic regions (Chung et al., 1993). The assembled plasmid was used to generate several independent embryonic stem (ES) cell lines and we proceeded to generate mice using selected clones.

Despite the use of insulators, transgenic alleles can be silenced in some cell types (Martin and Whitelaw, 1996), reducing their usefulness as research tools. Therefore, we

analysed expression of N-PhiM (reporter of transgene promoter activity) and MbTomato (reporter of transgene recombination and Cre expression) in most embryonic and adult tissues of *iSuRe-Cre* mice. This analysis revealed that the *iSuRe-Cre* allele was not silenced, it did not self-recombine in the embryo or in most organs and cell types, and it only recombined in the presence of tamoxifen (Figure 39C). We next evaluated the relative inducibility rate of the *iSuRe-Cre* allele by combining it with *Cdh5-CreERT2* and other available Cre reporter alleles, such as the *Gt(ROSA)26Sor-LoxP-STOP-LoxP-EYFP* allele (abbreviated here as $ROSA26^{LSL\text{-}EYFP}$) (Srinivas et al., 2001). At any recombination frequency, all MbTomato+ cells were EYFP+, demonstrating the high recombination efficiency in MbTomato-2A-Cre+ cells. At low induction frequency, many YFP+ cells did not recombine the iSuRe-Cre allele, but all Tomato-2A-Cre+ cells recombined the R26-YFP alelle as expected (Figure 39D-F). In addition, inclusion of the stronger CAG promoter, the brighter fluorescent protein (Tomato), and the WPRE element results in higher reporter expression in each recombined cell, making it easier to detect and distinguish from background tissue autofluorescence than the other commonly used ROSA26 reporter allele ($ROSA26^{LSL\text{-}EYFP}$), as determined by FACS (Srinivas et al., 2001) (Figure 39G).

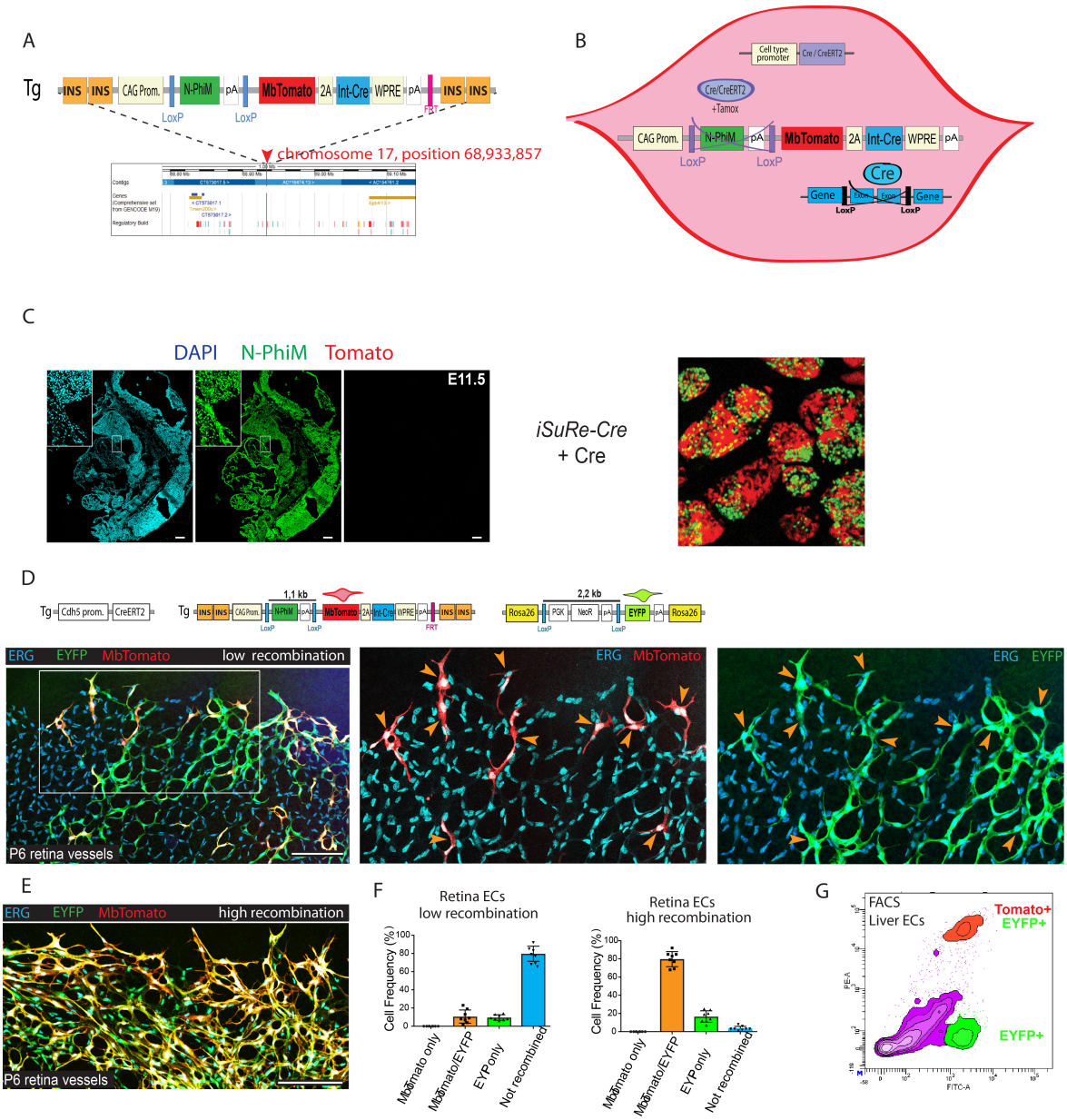

Figure 39: An Inducible Super Reporter of Cre (*iSuRe-Cre*) transgene for efficient gene deletion. (A) Schematic design of *iSuRe-Cre* DNA construct used to produce both transgenic ES cells and mice. DNA sequencing shows the transgene integration site in the genome. The new *iSuRe-Cre* genetic tool enables stronger (CAG promoter driven) and constitutive co-expression of a reporter (MbTomato) and Cre, which is expected to increase the correlation between reporter expression and gene deletion. Loxp, short DNA sequences recognized and recombined by Cre; N-PhiM, nuclear-localized and mutated PhiYFP; pA, Sv40polyadenylation sequence; 2A, self-cleaved viral 2A peptide to guarantee equimolar expression but separate localization of the reporter and Cre. WPRE, Woodchuck hepatitis virus posttranscriptional regulatory element to enhance expression. **(B)** Schematic *iSuRe-Cre* working model. Any tissue-specific Cre or inducible CreERT can recombine the *iSuRe-Cre* transgene to enable a constitutive co-expression of a membrane fluorescence reporter (MbTomato) and a constitutive Cre. **(C)** Analysis of *iSuRe-Cre* expression in the absence of Cre activity reveals its expression (N-PhiM+) in most cells of mouse embryos. The allele does not self-recombine in embryos (MbTomato-negative). Only in the presence of Cre, the *iSuRe-Cre* is recombined (MbTomato-positive). White dotted rectangle within this area is to highlight where the zoomed photos are located. **(D-E)** Confocal micrographs of postnatal day (P) 6 retina vessels from animals with the alleles depicted above the panels and induced with tamoxifen from P1 to P3. All endothelial cells (ECs; nuclei, ERG+) expressing MbTomato-2A-Int-Cre also recombined the reporter allele ROSA26LSL-YFP. **(F)** Quantification of the different recombination events/reporters in retinal vessels with low and high frequencies of tamoxifen-induced CreERT2 recombination (n=4 full retinas per group). **(G)** FACS analysis of liver ECs from tamoxifen-induced adult animals with the genotype indicated in d. All induced MbTomato+ cells also recombined the reporter allele ROSA26LSL-YFP. The MbTomato reporter from the iSuRe-Cre allele is easier to separate from baseline autofluorescence. Scale bars, 150 µm.

iSuRe-Cre reliably reports cells with full gene deletion

Having confirmed the *iSuRe-Cre* allele as a *bona fide* recombination reporter, we next sought to determine if it would also allow us to achieve higher efficiencies of CreERT2-inducible gene deletion. In contrast to the very short (1.1kb), inter-loxP genetic distance in the *iSuRe-Cre* allele, the floxed alleles of many other genes have significantly larger genetic distances and require two allelic recombination events for full gene loss-of-function. To determine the robustness of the *iSuRe-Cre* allele in inducing genetic deletions, we generated mice containing the *Cdh5-CreERT2* and *iSuRe-Cre* transgenes and two *Kdr* floxed (*Kdr* ^{flox}) alleles (Haigh et al., 2003), where the LoxP sites are 4.7kb apart. *Kdr* is an essential gene for EC differentiation, proliferation, migration, and survival (Carmeliet et al., 1996; Koch and Claesson-Welsh, 2012). The results show that when *Kdr*$^{flox/flox}$ *Cdh5-CreERT2*$^{Tg/Wt}$ mice contain the *iSuRe-Cre* allele, there is a significant decrease in the number of ECs (ERG+ nuclei), particularly in retinas with higher induction of the *iSuRe-Cre* allele (Figure 40A-C). These results also show that full *Kdr* recombination and loss-of-function cannot be consistently achieved with tamoxifen-inducible conditional genetics unless the *iSuRe-Cre* allele is present. As with any tamoxifen induction experiment, there was some littermate variability in the degree of recombination of the *Kdr*^{flox} and *iSuRe-Cre* alleles. However, the mutants with almost complete expression of the *MbTomato-2A-Int-Cre* cassette could be safely selected for phenotypic and statistical analysis (Figure 40D). In animals containing the *ROSA26*$^{LSL\text{-}YFP}$ reporter allele, the number of retina ECs at P6 was significantly higher, even in tissues with very high reporter recombination rates (Figure 40E, F). Importantly, the vascular phenotype obtained at high *ROSA26*$^{LSL\text{-}YFP}$ reporter recombination rates was not representative of the real full gene loss-of-function phenotype, reflecting the poor correlation between the recombination of a conventional Cre-reporter (i.e. *ROSA26*$^{LSL\text{-}YFP}$) and deletion of the gene of interest. In addition, the detected endpoint frequency of YFP+ cells was on average significantly higher than the frequency of Tomato+ (iSuRe-Cre+) cells in P6 retina vessels (Figure 40F). This is in agreement with the fact that *Kdr* is an essential gene for EC proliferation and survival (Carmeliet et al., 1996; Koch and Claesson-Welsh, 2012), therefore the initially (P1 to P3) recombined mutant cells are strongly outcompeted by the remaining *Kdr* wildtype cells over time, resulting on average in a relatively lower frequency of Tomato+ cells, because these efficiently delete *Kdr*, unlike the YFP + cells (Figure 41A-B). Importantly, retinas with around 50-60% *iSuRe-Cre*/Tomato+ cells at P6 (Figure 40B), showed more severe vascular defects than retinas with 80-95% *ROSA26*$^{LSL\text{-}YFP}$/YFP+ cells (Figure 40E).

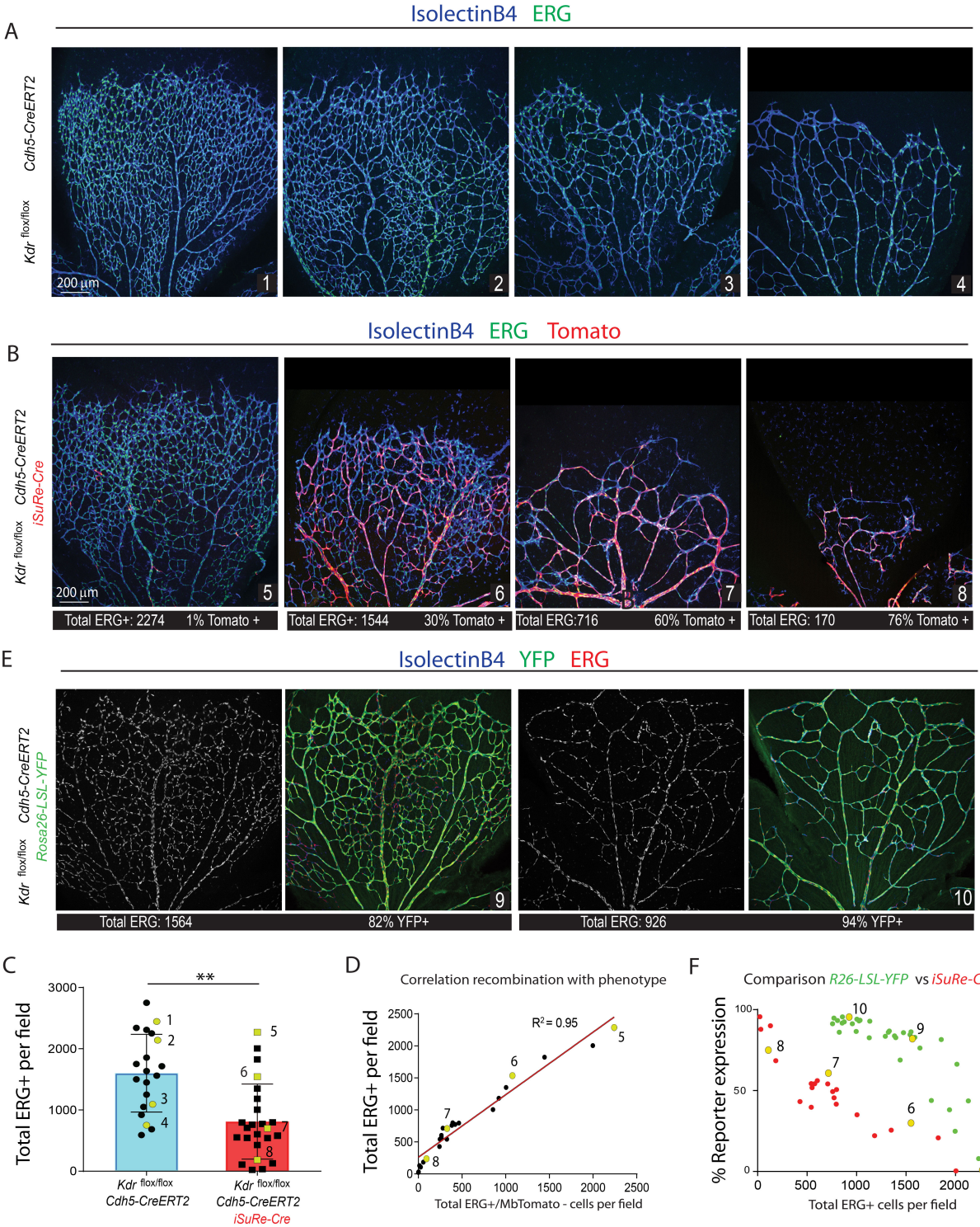
A
IsolectinB4 ERG
Cdh5-CreERT2
Kdr flox/flox
200 µm
1
2
3
4
B
IsolectinB4 ERG Tomato
Cdh5-CreERT2
iSuRe-Cre
Kdr flox/flox
200 µm
5
6
7
8
Total ERG+: 2274 1% Tomato +
Total ERG+: 1544 30% Tomato +
Total ERG:716 60% Tomato +
Total ERG: 170 76% Tomato +
E
IsolectinB4 YFP ERG
Cdh5-CreERT2
Rosa26-LSL-YFP
Kdr flox/flox
9
10
Total ERG: 1564 82% YFP+
Total ERG: 926 94% YFP+
C
Total ERG+ per field
3000
2000
1000
0
**
Kdr flox/flox
Cdh5-CreERT2
Kdr flox/flox
Cdh5-CreERT2
iSuRe-Cre
D
Correlation recombination with phenotype
Total ERG+ per field
R² = 0.95
Total ERG+/MbTomato - cells per field
F
Comparison R26-LSL-YFP vs iSuRe-Cre
% Reporter expression
Total ERG+ cells per field

Figure 40: The *iSuRe-Cre* allele report and significantly increases the efficiency of inducible genetic modifications. (A–C) Representative confocal micrographs of P6 retina vessels labelled with IsolectinB4 (endothelial surface) and anti-ERG antibody (endothelial nuclei), obtained from animals with the genotype indicated to the left and induced with high-dose tamoxifen from P1 to P3. Images represent the observed phenotypic variability; EC number for each image is depicted in chart C (yellow dots). 20 vs 24 retina microscopic fields were analysed (n =5 vs n =6 animals per group). **(D)** Linear regression showing the high correlation (r2) between total Erg + EC number (phenotype) and the number of Erg + /MbTomato- cells. **(E-F)** Representative confocal micrographs of P6 retina vessels from animals with the genotype indicated to the left and induced with high-dose tamoxifen from P1 to P3. Images represent the phenotypic variability of animals with the same genotype. EC number and reporter expression frequency is indicated below the figures. A comparison of EC number and reporter expression frequency is depicted in chart for 24 vs 34 retina microscopic fields (n = 6 animals per group). Yellow dots in chart f represent the values for images in B and E. Scale bars 200 µm. Error bars indicate SD. **p<0.001. ***p<0.0001

Besides the gene *Kdr*, we also examined the efficiency of the *iSuRe-Cre* allele in deleting the genes *Rbpj*, *Mycn* and *Notch1*. Cells expressing MbTomato had very efficient deletion of these genes. Importantly, a significant fraction of cells expressing a conventional Rosa26 Cre reporter (YFP+), had no deletion of these genes (Figure 41C).

To analyse the efficiency of the *iSuRe-Cre* allele in the recombination of genes, in other cell types and organs, we interbred this mouse line with the ubiquitously expressed *Rosa26-CreERT2* (Schonhuber et al., 2014*)* and *Ubc-CreERT2* lines (Ruzankina et al., 2007)*,* and induced recombination of the genes *Rbpj* and *Notch1* with tamoxifen. In cells with *iSuRe-Cre* allele induction (MbTomato+), the *Rbpj* and *Notch1* genetic deletion was highly efficient (Figure 41D, E).

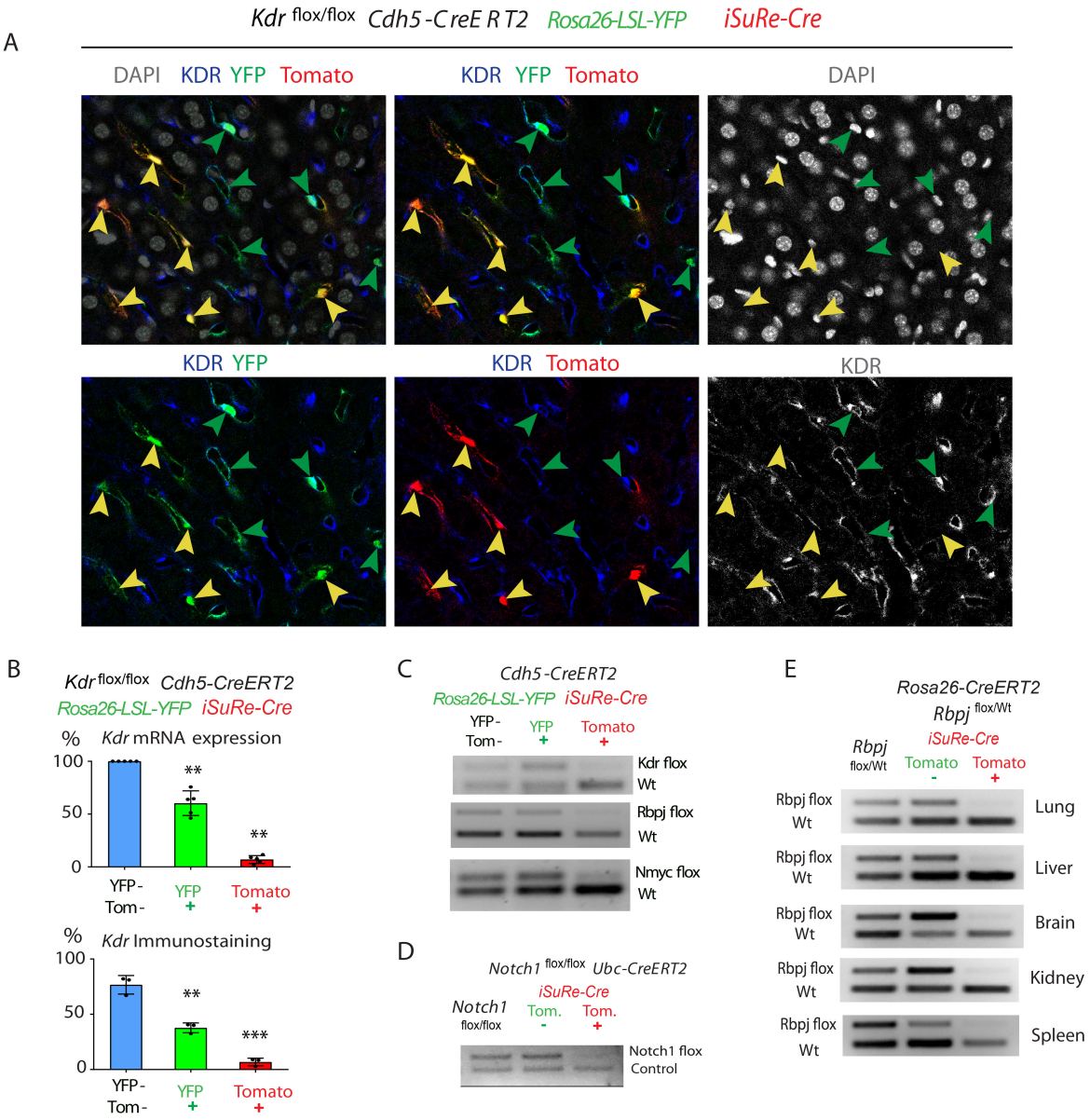

Figure 41: MbTomato fluorescent reporter reliable labels cells with full gene deletion. (A) 4-channel confocal micrographs showing Kdr immunostaining signals in YFP+ and Tomato+ cells of animals with the indicated genotype. DAPI staining was used to identify the nuclei of endothelial cells and segment objects during quantification. iSuRe-Cre Tomato+ cells (yellow arrowheads) recombined the Rosa26-LSL-YFP+ allele, express YFP, and deleted the gene *Kdr*. In contrast, a significant fraction of YFP+ cells (green arrowheads), still express Kdr. Note that endothelial cells have a very elongated shape, and mutant (Kdr-) cells are surrounded by wildtype (Kdr+) cells. Only the stronger Kdr signals in the cell cytoplasm (overlapping with DAPI+ nuclei) was used for the quantifications. **(B)** qRT-PCR analysis of *Kdr* mRNA levels from FACs-sorted liver ECs (n=5 animals), or immunostaining analysis of liver sections animals (n=3) with the indicated genotype. **(C)** Semi-quantitative competitive PCR showing the efficiency of *Kdr, Rbpj* and *Nmyc* deletion in FACS-sorted cells of adult mice with the indicated genotypes and induced with tamoxifen. Note that some cross-contamination of samples and DNA may occur during tissue dissociation and FACS of mutant and wild-type cells. **(D)** Semi-quantitative competitive PCR for the *Notch1* floxed allele and a control genomic sequence showing the efficiency of the *Ubc-CreERT2* induced *Notch1* deletion in Tomato+ and Tomato- cells of the liver. **(E)** Semi-quantitative competitive PCR showing the efficiency of *Rbpj* gene inducible deletion in the Tomato– and Tomato+ cells of several distinct organs from *Rosa26-CreERT2* mice induced with tamoxifen. Error bars indicate SD. **p<0.00. ***p<0.0001.

iSuRe-Cre enables deletion of multiple genes and epistasis analysis

As mentioned above, a common strategy for understanding and validating genetic redundancy or gene interaction networks is to induce the deletion of two or more genes in the same tissue and analyse if deletion of one gene aggravates or rescues the phenotype caused by the other. This is a fundamental method for understanding how genes interact to regulate a given biological process.

As an example, we present data for the simultaneous deletion of the genes *Dll4/Kdr* and *Myc/Mycn/Rbpj* in ECs expressing *Cdh5-CreERT2*, after inducing animals with tamoxifen. This implies the deletion of 4 or 6 floxed alleles in each cell to achieve cell-autonomous multiple gene loss-of-function and in this way perform epistasis analysis. Dll4 and Kdr are expressed by most liver ECs, and their presence in ECs could be detected by immunostaining (Figure 42A). In animals containing the *Cdh5-CreERT2* and *iSuRe-Cre* alleles and injected three times with tamoxifen, we observed deletion of *Dll4* in most liver ECs, but not of *Kdr* (Figure 42B,C). This result shows how recombination efficiency differs among different floxed genes. Importantly, MbTomato+ ECs had complete deletion of both *Dll4* and *Kdr*, whereas most MbTomato negative cells maintained *Kdr* expression, even after three high-dose tamoxifen injections (Figure 42B,C).

We next analysed multiple gene deletion efficiency in *Myc/Mycn/Rbpj*$^{flox/flox}$, *Tg(Cdh5-CreERT2), iSuRe-Cre* mice induced with a single 1mg injection of tamoxifen (Figure 42D,E). Technically, it is much more difficult to confirm the simultaneous deletion of more than 2 genes in single cells by direct immunostaining, due to the lack of compatible commercial antibodies to distinguish all epitopes of the encoded proteins in combination with other tissue or reporter markers. We therefore extracted DNA from FACS-sorted MbTomato+ and MbTomato- ECs (CD31+) isolated from the induced animals and assessed gene deletion by semi-quantitative PCR. Only MbTomato-2A-Int-Cre+ cells had deletion of all 3 genes (Figure 42D-F). The *iSuRe-Cre* allele enabled us to achieve high efficiency in multiple gene deletion and safely correlate the expression of the single and easy-to-detect MbTomato reporter with the deletion of 3 genes (6 floxed alleles), which encode proteins that could not be detected by tissue immunostaining.

Altogether, these results have shown that the *iSuRe-Cre* allele provides certainty that these cells have completely recombined multiple floxed alleles. This genetic tool increases the ease, efficiency, and reliability of conditional mutagenesis and gene function analysis.

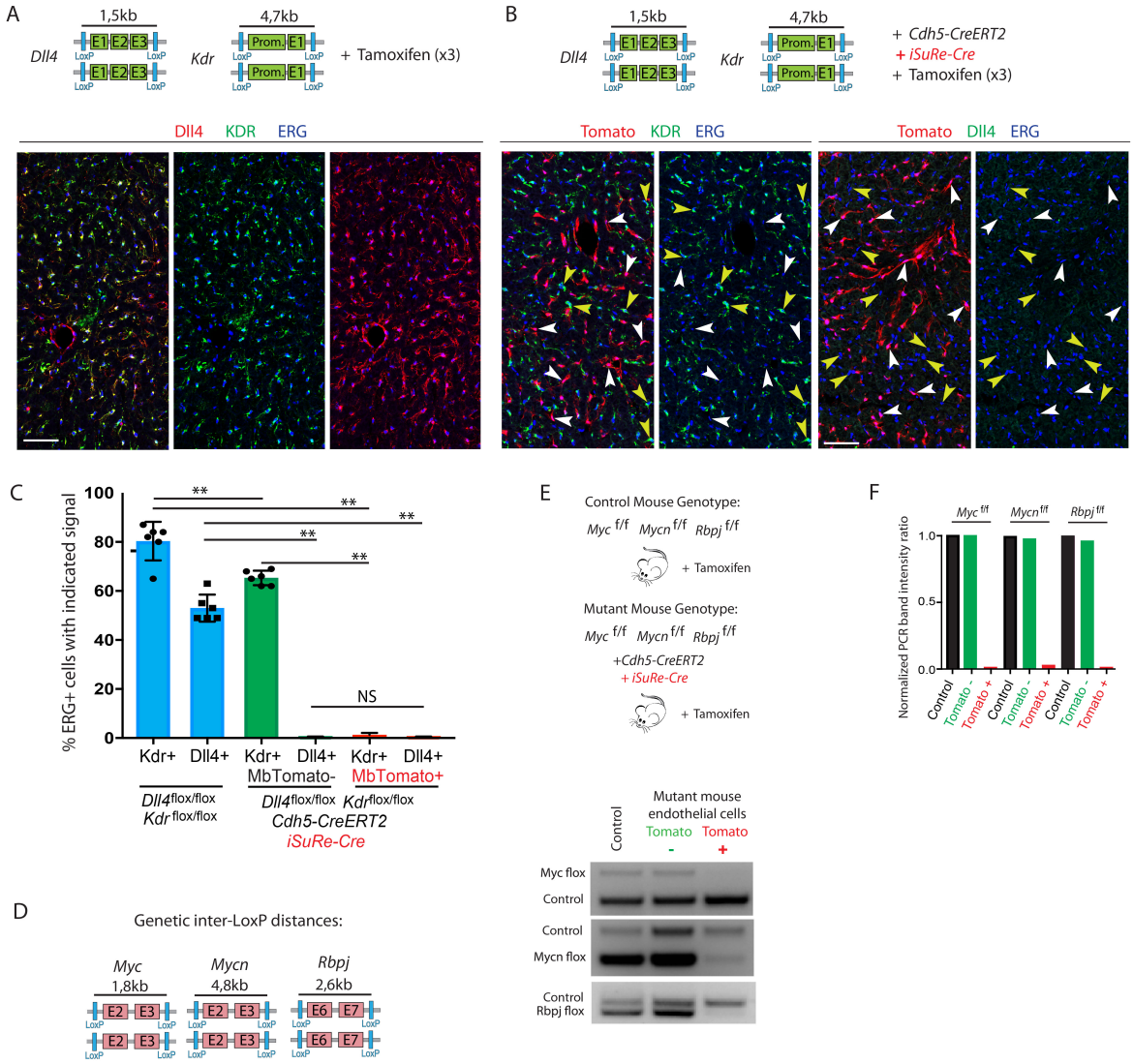

Figure 42: The *iSuRe-Cre* allele enables multiple gene deletions in single cells or tissues. (A) The schemes illustrate the *Dll4* and *Kdr* floxed alleles, showing inter-LoxP-site genetic distance, which is significantly larger in the Kdr allele. All four alleles must be deleted to achieve full dual gene loss-of-function. Kdr and Dll4 proteins are expressed in most liver ECs (ERG+, nuclei) of *Dll4* flox/flox *Kdr* flox/flox animals injected with tamoxifen on 3 consecutive days. **(B)** Adult mice carrying in addition the *Cdh5-CreERT2* and *iSuRe-Cre* alleles and treated with the same high-dose tamoxifen for 3 consecutive days show very pronounced deletion of *Dll4*, but not *Kdr*, in liver MbTomato-/ERG+ ECs (yellow arrowheads). However, MbTomato+ cells (white arrowheads) have complete deletion of both genes. **(C)** Quantification of the immunostaining signals for ERG, Dll4, Kdr, and MbTomato in large liver sections of the indicated animals. **(D)** Illustration of the *Myc*, *Mycn* and *Rbpj*-floxed alleles showing the genetic distances between the LoxP sites.**(E)** Genotypes of control and mutant adult mice injected once with 1mg of tamoxifen and used for gene-deletion quantification by PCR. The control PCR band provides a DNA input quantitative control for the PCR, since it corresponds to a wild-type genomic sequence, present in all DNA samples. Animals containing the *Cdh5-CreERT2* and *iSuRe-Cre* alleles have deletion of the six floxed alleles only in FACS-sorted MbTomato+ cells, as detected by semi-quantitative competitive PCR. Weak Mycn and Rbpj-floxed bands in the MbTomato+ sample PCR may result from incomplete gene deletion or contamination of this sample with MbTomato-negative cells, or their DNA, during the FACS protocol. **(F)** Image J quantification of the relative intensity of the floxed and control PCR gel bands shown in E, providing an estimate of the degree of the indicated floxed gene deletion. Scale bars 65 µm. Error bars indicate SD. **p < 0.001. ns, non significant

DISCUSSION

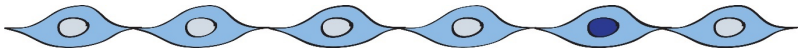

For many years, the prevailing view was that Dll4/Notch blockade led to increase EC proliferation in different context, such as vessel development or tumour growth (Benedito et al., 2012; Duarte et al., 2004; Hellstrom et al., 2007; Krebs et al., 2004; Limbourg et al., 2005; Noguera-Troise et al., 2006; Ridgway et al., 2006). Indeed, pharmacological compounds targeting distinct members of the Notch pathway were used in clinics to promote non-functional angiogenesis and therefore reduce tumour burden (Ileana Dumbrava et al., 2018). Unfortunately, these compounds caused undesired side effects due to the pleotropic roles of Notch (Milano et al., 2004; Wong et al., 2004). Later, neutralizing anti-Dll4 antibodies were generated to circumvent the indiscriminate Notch blockade and specifically target endothelial cells. These blocking antibodies efficiently deregulated angiogenesis and inhibited tumour growth, while apparently no affecting the rest of the vasculature, emerging as an attractive approach for cancer therapy (Noguera-Troise et al., 2006; Ridgway et al., 2006). However, this dream was torn down when chronic Dll4 blockade was shown to cause pathological activation of quiescence vasculature (Yan et al., 2010). Interestingly, the side effects of anti-Dll4 treatment only occurred in the liver and subcutaneous vasculature, and other quiescent vascular beds remained unaltered. At that time, most vascular biology knowledge was obtained from developmental research, and few studies were focusing on studying the apparently inert quiescent vasculature. However, it started to become clear that the differentiated quiescent endothelium also required survival signals to maintain vascular homeostasis. Later, by deleting Notch signalling components such as *Rbpj* and *Notch1*, some studies also suggested that liver quiescent ECs were sensitive to Notch inhibition (Cuervo et al., 2016; Dill et al., 2012; Dou et al., 2008). Nevertheless, there was no consensus on the rest of vascular beds. This discrepancy and the lack of clear analysis set the starting point of this doctoral thesis that we will discuss in the following sections.

Although Dll4/Notch1 signalling is active in different organ-specific ECs, only in some vascular beds its activity is essential to maintain EC quiescence

Previous studies inferred the relevance of Notch signalling in the quiescent endothelium based on an increase in vascular surface density after Notch loss-of-function

(Cuervo et al., 2016; Dill et al., 2012; Dou et al., 2008). However, there was no research supporting Notch activation or Notch signalling component expression in different quiescent vascular beds. In this work, we have shown that the four Notch ligands and receptors are expressed in the quiescent endothelium of heart, lung, liver and brain tissues. Due to their higher mRNA expression, Dll4 and Notch1 seemed to be the key ligand and receptor, which is in agreement with previous research during development (Duarte et al., 2004; Krebs et al., 2004). This hypothesis was confirmed, as we could observed that Notch signalling pathway was mostly activated by the Dll4 ligand in all these organ-specific vascular beds. In line with the heart hypertrophy described after *Rbpj* inhibition (Jabs et al., 2018) and the liver sensitivity to Notch loss-of-function (Cuervo et al., 2016; Dill et al., 2012; Dou et al., 2008; Yan et al., 2010), we observed that after endothelial specific *Dll4* deletion, heart and liver vascular homeostasis was strongly impaired. The publications describing heart and liver sensitivity to Notch loss-of-function also agreed in the endothelial dilation and the increase in vessel density that we have observed in these organs (Cuervo et al., 2016; Dill et al., 2012; Dou et al., 2008; Jabs et al., 2018; Yan et al., 2010). We did not observe any change in brain endothelium, which is consistent with previous publications (Jabs et al., 2018). Contrary to previous studies that described spontaneous angiogenesis in lung endothelium (Dou et al., 2008), we did not observe it. This could be explained by the non-EC specific deletion of *Rbpj*, which by affecting other cell types, could lead to non EC-specific results. In addition, gene deletion was not checked in these mouse models, so they could be evaluating the result of partial deletion of *Rbpj*. Remarkably, although Notch activation is significantly decreased in lung and brain endothelium after *Dll4* deletion, these vascular beds do not react as it happens in heart and liver. We therefore discard the possible hypothesis of Notch pathway not being partially activated by Dll4 in the quiescent vascular beds that do not react after its loss-of-function. Importantly, none of the studies that highlighted the pathological activation of the quiescent endothelium after Notch inhibition have clearly shown either activation of the endothelium (by any marker) or aberrant EC proliferation. The use of endothelial nuclear and cell cycle markers has allowed us to see that the increase in endothelial width and density observed in heart and liver is accompanied by an increase in the endothelial cell number and proliferation.

Myc is a Notch downstream target in liver quiescent ECs that controls proliferation

The different sensitivities to Notch inhibition in different vascular beds did not catch us off guard. Despite the lack of consensus, several reports had already suggested that Notch inhibition affected only to some tissue-specific blood vessels (Cuervo et al., 2016; Dill et al., 2012; Dou et al., 2008; Jabs et al., 2018; Yan et al., 2010). In addition, the heterogeneous consequence after global endothelial Notch loss-of-function is supported by the concept of vascular heterogeneity. Nowadays we know that vascular heterogeneity goes beyond the anatomical classification of arteries, veins and capillaries. ECs from different vascular beds are structurally and functionally different, which is supported by a unique gene expression profile (Aird, 2012; Kalucka et al., 2020; Nolan et al., 2013). Therefore, we could infer that Notch signalling pathway is not only essential in some EC types, but also in some organ-specific vascular beds.

To identify the mechanisms that could be driving these different proliferative behaviours after Dll4/Notch1 inhibition, we performed bulk RNA-seq from heart, lung, liver and brain adult *Dll4*^{iDEC} ECs isolated by FACS. Interestingly, we could observe that liver ECs have the strongest upregulation of genes related with cell cycle and metabolism compared with other vascular ECs. In heart *Dll4*^{iDEC} ECs there was a milder upregulation of cell cycle and metabolism genes, which reflected the lower increase in EC proliferation we observed *in vivo*. The proteomic analysis supported the transcriptomic results and pointed to Myc pathway as the main driver of these proliferative differences, which was confirmed by double genetic deletion of *Dll4* and *Myc* in liver ECs. Interestingly, Myc is considered one the most important regulators of cell proliferation and metabolism (Kress et al., 2015; Meyer and Penn, 2008). Indeed, it was recently shown that FOXO1 promotes quiescence in ECs by repressing Myc (Wilhelm et al., 2016) and that Myc is required for aortic EC regeneration (McDonald et al., 2018).

Myc protein and Notch signalling relation has been extensively explored. Notch directly regulates *Myc* expression in Hematopoietic Stem Cells (HSCs) and induces proliferation and self-renewal by binding to *Myc* proximal promoter sequences (Weng et al., 2006). Importantly, 50% of patients with T cell lymphoblastic leukemia (T-ALL) have an activating mutation in *Notch1*, which induces the aberrant expression of *Myc* and consequently leads to leukemic growth (Palomero et al., 2006). So then, how is *Notch1* and *Myc* expression regulated in the

endothelium? We hypothesize a possible different regulation of those signalling pathways specifically in ECs. Unfortunately, in this doctoral thesis we have not been able to decipher the mechanisms downstream of Notch that negatively regulates *Myc*. Remarkably, our laboratory has recently shown that it is not the Notch-dependent arterial differentiation program, but its ability to inhibit endothelial metabolism and cell cycle by supressing Myc what drives arterial development (Luo et al., 2020). Therefore, there is supporting evidence to believe that while Notch signalling activates *Myc* in HSCs, in ECs it suppresses it. However, they have observed *in vitro* that the regulation of *Myc* by Notch signalling in ECs might not be a direct mechanism (Luo et al., 2020).

Why do not some organs proliferate after *Dll4* deletion?

Some organ ECs in *Dll4*^{iDEC} mice did not proliferate after Notch inhibition, even though *Dll4* was deleted and Notch activity was decreased in all organs. One of our working hypotheses is that each vascular bed has a Notch dependent scenario and that we should consider other signalling ligands. As an example, we have clearly pointed to a potential Notch compensatory mechanism that could be supporting lung ECs quiescence. Besides our descriptive observation based on transcriptomic results, we agree that the phenotypic observation of double deletion of *Dll1* and *Dll4* in lung endothelium would be of great interest. Unfortunately, we cannot exclude that basal Notch activity after *Dll4* deletion (either by remaining *Dll4* expression or signalling from other ligands through Notch1 receptor) could maintain the EC quiescence in lung *Dll4*^{iDEC} tissue. Despite we observed downregulation of the ligand (both at the protein and mRNA level) and downregulation of Notch activity (with active N1ICD immunostaining and mRNA Notch targets levels), we cannot ignore that the level of downregulation is not as pronounced as it happens in the liver endothelium. However, in brain ECs we have similar levels of Notch canonical target genes downregulation compared with liver endothelium and it does not reactivate after *Dll4* deletion. Moreover, Notch pathway is a cell-to-cell communication signalling pathway and we cannot discard parenchymal signalling from packed adjacent cells (such as cardiomyocytes in heart or epithelial cells in the lung) to the neighbouring endothelium, as it has been shown during heart development (D'Amato et al., 2016). Notch ligand-receptor interaction between different cell types does not occur in the liver as it has been shown by scRNA-seq techniques (Halpern et al., 2018). Future

whole organ scRNA-seq techniques will allow to address the potential contribution of non-ECs signalling to the endothelium.

It is already established that while quiescent endothelial cells need to stabilize through barrier molecules, cell-to-cell connections and pericytes recruitment; angiogenic ECs need to lose their connections to migrate and proliferate (Carmeliet and Jain, 2011). We observed an enrichment in cell-to-cell adhesion genes both in control lung ECs and heart *Dll4*^{iDEC} ECs that might regulate from controlled proliferation in heart *Dll4*^{iDEC} ECs to quiescence maintenance in *Dll4* deficient lung endothelium. These proliferative differences based on cell-to-cell adhesion molecules would be consistent with a higher sensitivity to mitogenic stimulation in liver endothelium, where we observed a downregulation in cell-to-cell adhesion related genes.

Another hypothesis is that different vascular beds might rely on different mechanisms to support their quiescent. Therefore, while Notch signalling would be an essential driver of quiescence only in some organ vascular beds - such as heart and liver ECs -, additional signalling pathways and genes would be responsible of regulating quiescence in other tissue-specific ECs. As an example, we can highlight the enrichment in negative regulators of growth both in control and in *Dll4*^{iDEC} lung ECs, which is not observed in any other vascular beds. Interestingly, we can find another example of tissue-specificity in the liver endothelium. This specialized endothelium is a discontinuous barrier with lack of basement membrane (Aird, 2012; Poisson et al., 2017) and it could be more prone to mitogenic stimulation following Notch inhibition rather than other vascular bed. In addition, it has been shown that pericyte density differs among different organ capillary beds (Gerhardt and Betsholtz, 2003), being the highest density found in vessels from neural tissue such as retina or brain, which are also characterized by a continuous endothelium with increased tight junctions. These compact connections together with a higher density of pericytes protect from vessel degeneration and might protect from Notch loss-of-function stimuli. This protection facing mitogenic stimulation could be also performed by the significant upregulation of p53 targets expression we observed in *Dll4*^{iDEC} brain ECs.

Yet, further studies are required to complete this heterogeneous landscape. For a long time, epigenetic regulation has also been related to vascular function (Yan and Marsden, 2015). Indeed, epigenetic regulation of Notch has been shown to occur in the transition from the proliferative developing lung endothelium to its quiescent state. These epigenetic changes acquired during quiescence might be different among vascular beds, adding another layer of complexity (Schlereth et al., 2018). During the course of this thesis, single-cell biology techniques have been developed and have allowed to dissect the heterogeneity of ECs within

the same tissue. The profiling of the complex mosaic of ECs in every organ/tissue will allow to discover with unprecedented resolution the heterogeneity within the same vascular beds and uncover specific features that could have remained masked by bulk techniques. Indeed, whether adult ECs from different organs have the potential to reactivate under homeostatic and pathological conditions or some tissue-specific ECs have lost this ability during development will be uncover soon. Importantly, recent papers have shown that only in some vascular beds there are specific EC clusters with proliferating capacities, such as in the liver and spleen organs (Kalucka et al., 2020). This might also explain why some organs do proliferate after *Dll4* deletion and others do not.

Deletion of different Notch pathway components does matter: let's forget about an equal Notch loss-of-function response

In order to avoid cell-to-cell signalling from other ligands in the absence of Dll4 (or from reduced Dll4 as it could happen in lung ECs), we decided to evaluate full Notch loss-of-function in a cell-autonomous manner. For this reason, we sought to delete the co-factor *Rbpj* or the receptor *Notch1* in the quiescent endothelium. As expected, the changes in the liver vascular morphology observed by CD31+ staining were consistent with our *Dll4*^{iDEC} phenotype and with all existing publications (Cuervo et al., 2016; Dill et al., 2012; Dou et al., 2008; Jabs et al., 2018; Yan et al., 2010). Surprisingly, immunostainings for the nuclear endothelial transcription factor ERG and the cell cycle marker Ki67 revealed that despite observing enlargement of sinusoids in all Notch mutants, those vascular abnormalities occurred independently of EC proliferation in *Rbpj*^{iDEC} and *Notch1*^{iDEC} livers. Due to the increased area of endothelial membrane surface markers (such as CD31) and most probably by extrapolating results from developmental research, previous studies concluded that Notch inhibition by either *Dll4*, *Rbpj* or *Notch1* deletion in quiescence endothelium led to increased EC proliferation, even without addressing that possibility. Indeed, only in one study where *Rbpj* was deleted in the adult endothelium they did not observed an increase in endothelial proliferation, which is in line with our observations (Cuervo et al., 2016). Importantly, we also observed an increase in the nuclei size of all these mutants compared to control liver, indicating that the sinusoidal dilation might be due to an increase in the size of each endothelial cell. However, it has also been shown that Notch signalling regulates the expression of vasoactive genes such as *Nts* and *Adm* during vessel remodelling (Lobov et al., 2011). Interestingly, this regulation can occur

independently of vessel proliferation, as it was demonstrated after VEGF injection in the retina vitreous (Ubezio et al., 2016). Therefore, it might be possible that inhibition of Notch signalling by deleting *Dll4*, *Rbpj* or *Notch1* could also regulate blood vessel dilation independently of EC proliferation. Nonetheless, studies during tumour development have shown a decreased expression in genes involved in vasodilation after *Dll4* deletion (Patenaude et al., 2014) and other reports have described vessel enlargement by using different Notch gain of function models (Li et al., 2007; Uyttendaele et al., 2001). This controversy highlights the need of a better comprehension of Notch signalling pathway and vessel dilation in different endothelial context.

Importantly, although these experiments were mostly conceived to analyse the vascular phenotypes in lung and brain tissues, we still need to address that part of the project.

The present study has rejected a consolidated view in the vascular biology field: deleting the endothelial specific ligand *Dll4*, the main Notch receptor *Notch1*, or the downstream co-factor *Rbpj* does not lead to the common and expected proliferative response. Furthermore, it questions previous research in different cell types and context, where the effect of Notch specific components should be revisited and addressed in detail.

Notch signalling regulates p-ERK signalling to balance EC quiescence, proliferation and cell cycle-arrest

Unexpectedly, the non-proliferating *Rbpj*^{iDEC} and *Notch1*^{iDEC} liver ECs had a significant upregulation of cell cycle related genes together with a massive increase in p-ERK levels compared with *Dll4*^{iDEC} and control liver ECs. In our laboratory we have recently shown that high mitogenic stimulation induced by Notch inhibition arrests EC proliferation during angiogenesis (Pontes-Quero et al., 2019). Then, we hypothesized that the excessive mitogenic stimulation triggered by *Rbpj* or *Notch1* deletion could pause or prevent uncontrolled EC proliferation, as suggested by the increase in binucleated ECs. So then why Dll4 deficiency does not lead to the same break that stops EC proliferation? We hypothesized that due to the presence of other signalling ligands, *Dll4* deletion leads only to partial Notch signalling downregulation with subsequent mild mitogenic stimulation (intermediate p-ERK). This mild mitogenic stimuli is sufficient to activate the quiescence endothelium and allow

controlled cell cycle progression. This is in agreement with results from the laboratory (Pontes-Quero et al., 2019) observed during retina development, where it was shown that in areas that are far from the high VEGF angiogenic front (which decreases the mitogenic signalling driven by VEGF), *Dll4* deletion induced a mild increase in p-ERK signalling that led to cell cycle reentry of mature endothelium. Nevertheless, *Dll4* deletion in high mitogenic stimulated areas did not allow EC expansion and promoted cell cycle exit. During retina development, Dll4 inhibition in VEGF-driven mitogenic stimulated areas would recapitulate the high mitogenic stimulation we observed after *Rbpj* deletion in quiescence endothelium. *Rbpj* is the master integrator factor that conveys the huge variety of possible ligand-receptor interactions and ultimately activates Notch signalling downstream gene transcription. Consequently, deletion of this bottleneck would lead to full loss of Notch, as no ligand or receptor could signal anymore. *Notch1* deletion would be closed to *Rbpj*^{iDEC} phenotype: most of previous results point to Notch1 as the main receptor in ECs (James et al., 2014; Limbourg et al., 2005), so no other receptors could maintain basal mitogenic stimulation and continuous EC proliferation. *In vitro* studies have suggested that the duration and magnitude of MAPK/ERK signalling define whether a cell remains in a quiescent state, re-enters cell cycle or undergoes cell cycle arrest. However, whether transient MAPK/ERK leads to proliferation or cell cycle arrest seems to depend on the cell type and context. While in PC12 cells sustained MAPK/ERK activation leads to cell differentiation or cycle-arrest, in fibroblasts high ERK is associated to proliferation (Marshall, 1995). We have confirmed in the liver quiescent endothelium that whereas mild mitogenic stimuli leads to proliferation from previously quiescent ECs, high p-ERK signalling does not allow endothelial cell cycle reentry with subsequent division.

We do not know in which phase of the cell cycle these high-mitogenic-stimulated cells experience the p21 mediated cell cycle arrest, but the presence of binucleated ECs indicate us that at least a fraction of ECs does enter mitosis with no successful cell division. Detailed analysis of these mutants at earlier time points would indicate if indeed a fraction of ECs is in an active cell cycle phase.

We fully agree that apart from the different pERK levels detected, we were not able to further support this theory with any set of Notch gene targets that are differentially regulated and reflect this partial versus total loss-of-function. Unfortunately, one of the caveats of doing RNA-seq with quiescent ECs is that most Notch targets are lowly expressed, rendering our Notch target genes analysis more difficult. Thus, further experiments such as quadruple ligand or receptor deletion that should mimic *Rbpj* deletion would be required to validate this theory.

High mitogenic stimuli after *Rbpj* and *Notch1* deletion in liver quiescent ECs leads to cell cycle exit by p21 expression

Transcriptomic analysis of *Rbpj*^{iDEC} liver ECs revealed an enrichment in DNA repair mechanisms and p53 pathway related genes. These results, together with the presence of DNA damage markers, led us to focus on p21 protein. The cyclin-dependent kinase inhibitor (CDKI) p21, which is encoded by the *cdkn1a* gene (el-Deiry, 1994; Levine, 1997), is a p53 target and inhibits cell proliferation. The link between p21 and Notch has already been discussed in *vitro* and *in vivo* with no clear consensus on the role and regulation of p21 by Notch signalling (Dou et al., 2008; Noseda et al., 2004; Rangarajan et al., 2001). In our laboratory we have recently seen that retina ECs with high p-ERK during development upregulate p21 expression and consequently exit the cell cycle (Pontes-Quero et al., 2019). We detected higher p21 levels in *Rbpj*^{iDEC} and *Notch1*^{iDEC} compared with *Dll4*^{iDEC} and control liver ECs, which was consistent with the non-proliferative phenotype in a high mitogenic stimulation scenario. Indeed, *in vitro* studies have shown that sustained increase in p-ERK signalling leads to growth arrest through p21 induction (Balmanno and Cook, 1999; Pumiglia and Decker, 1997). Altogether, these findings suggest that in quiescence liver endothelium, Notch signalling pathway is able to titrate ERK signalling. The resultant different increase in p-ERK levels is able to drive from controlled EC quiescence, to sustained proliferation or cell cycle arrest (Figure 43).

Finally, recent studies have suggested Notch-independent Rbpj functions (Castel et al., 2013; Diaz-Trelles et al., 2016). Nonetheless, due to the similar but gradual response between *Notch1* and *Rbpj* deletion, we agree that the results we observe in *Rbpj*^{iDEC} liver ECs are canonical Notch signalling-dependent.

Liver EC senescence is prevented by Notch signalling pathway

It has been suggested that the hypermitogenic stimulation with the consequent inhibition of CDKs can result in cellular senescence (Blagosklonny, 2003). Indeed, following

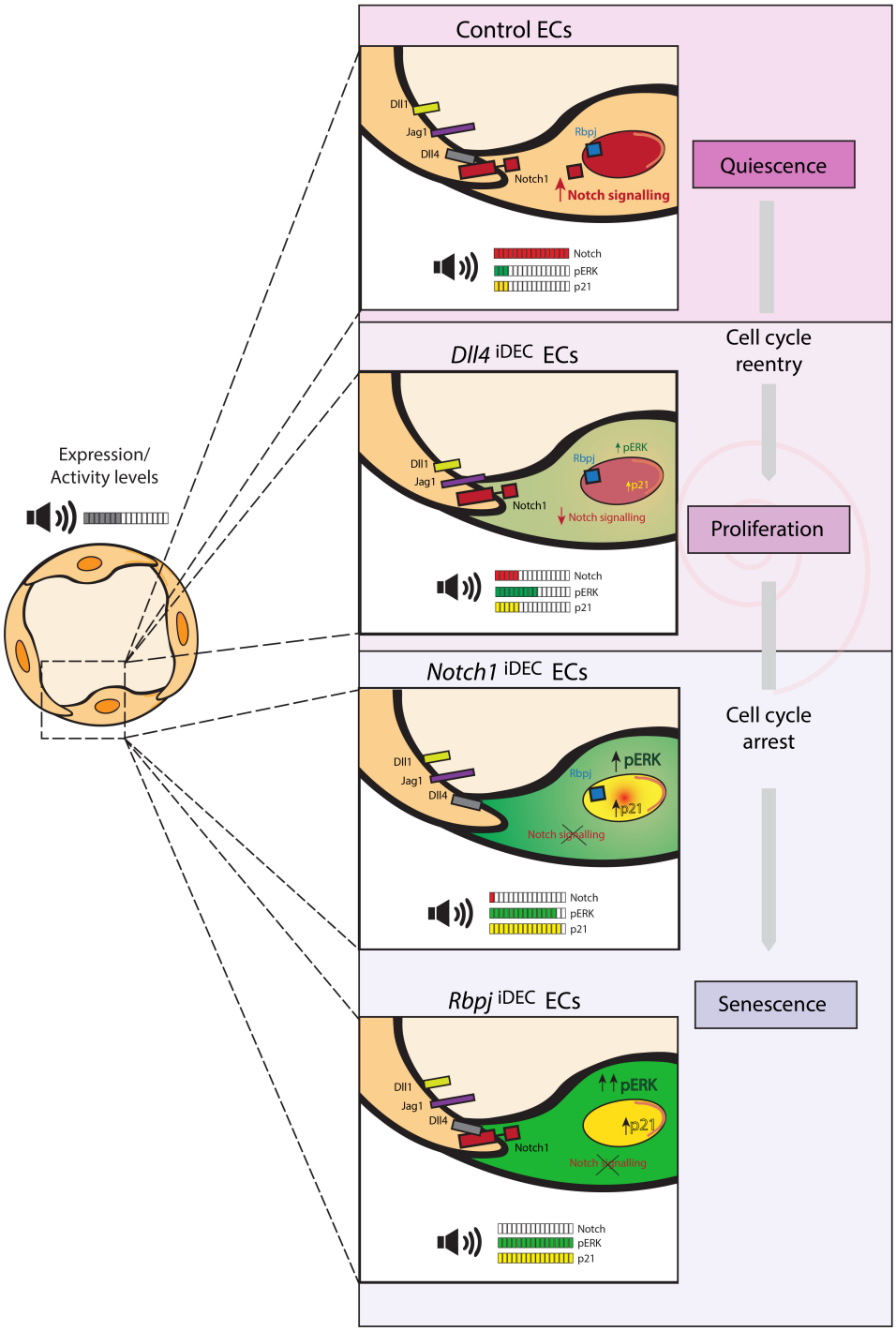

Figure 43: Working model of Notch signalling in quiescent liver ECs. Proposed dose-response model regulated by Notch, ERK and p21. In control homeostatic conditions, adult liver ECs are quiescent, since they have high Notch signalling (red dark recolor) and therefore low ERK signalling (green color). The deletion of the ligand *Dll4* leads to partial downregulation of Notch signalling. This downregulation is sufficient to activate intermediate levels of ERK signaling, which leads to cell cycle reentry and EC hyperproliferation. This abnormal activation of the endothelium leads to the expression of the cell cycle arrest protein p21 only in a fraction of these proliferative ECs. Deletion of the main receptor *Notch1* or the co-factor *Rbpj* leads to a strong Notch signalling downregulation, which is completely abrogated in the *Rbpj*^{iDEC} liver ECs. Such a complete downregulation induces a strong upregulation of p-ERK that leads to high p21 expression. This p21 expression results in cell cycle arrest and endothelial senescence. The expression or activity level of Notch, ERK and p21 is indicated by the volume level bars in the different Notch mutants. Color intensity in the cartoon also indicates the observed strength of signal.

high p-ERK stimulation we have observed p21 upregulation, which specifically labels cells that undergo senescence (Munoz-Espin and Serrano, 2014). By exploring our RNA-seq data and by using immunohistological techniques we have been able to confirm the presence of additional cellular senescence markers. As expected, we found the most number and strongest senescent hallmarks in *Rbpj*^{iDEC} liver ECs, which is where we have observed higher mitogenic stimuli. Supporting the strongest cell cycle arrest, by GSEA transcriptomic analysis we observed a significant enrichment in p53 related genes only in *Rbpj*^{iDEC} mutants but not in *Dll4*^{iDEC} or Notch1^{iDEC} liver ECs. Although our significant enrichment in p53 pathway related genes could give a clue in the p53-dependent p21 expression, GSEA hallmarks analysis uses gene sets that are generated by computational methodology from multiple sets with coherent and redundant expression (Liberzon et al., 2015). Therefore, we cannot affirm the link between p21 expression after Notch inhibition through p53 protein. Indeed several CDK genes (*cdkn*) such as p21 also have p53-independent growth arrest functions (Abbas and Dutta, 2009) and several reports have suggested that MAPK/ERK signalling induces p21 independently of p53 (Hong et al., 2009; Woods et al., 1997). Further experiments exploring the connection between Notch and p53 in the quiescent endothelial context are required.

Our study has shed light on the potential role of Notch signalling preventing quiescent ECs to become senescent. Indeed, the association between Notch and senescence has been a controversial debate for a long time. While culture of ECs *in vitro* has shown that Notch signalling is upregulated in p21+ senescent ECs (Venkatesh et al., 2011) and Notch1 activity in tumour ECs *in vivo* leads to senescence-like phenotype (Wieland et al., 2017), other authors have shown that Notch activation in ECs downregulates p21 expression and reduces cell senescence (Noseda et al., 2004; Yoshida et al., 2014). Our laboratory has recently shown that increased p-ERK signalling leads to p21 expression and cell cycle arrest in angiogenic vessels (Pontes-Quero et al., 2019). Apart from the cell-autonomous role in EC senescence, Notch has been shown to be involved in the modulation of the senescence-associated secretory phenotype (SASP) in fibroblasts (Hoare et al., 2016). Although we agree that some experiments such as the classical senescence-associated b-galactosidase immunostaining are missing in our study, our results show that gradual Notch loss-of-function leads to progressive cell senescent-like phenotype.

Furthermore, our rescue experiment by deleting *Rbpj* in liver ECs in a p21^{KO} background confirms the functional link between Notch signalling and p21-mediated cell cycle arrest in quiescent liver ECs. Although the number of proliferating liver ECs in *Rbpj*^{iDEC} p21^{KO} mice increased almost by 2-fold, we also wondered why we did not observe a more

pronounced increase in EC proliferation as we found by an almost 10-fold in *Dll4*^{iDEC} liver ECs. Compensatory functions have been described for different *cdkn* genes (Otto and Sicinski, 2017; Tateishi et al., 2012). Thus, we think that other CDKIs might be either blocking excessive EC proliferation from development - in the p21^{KO} background - or decelerating cell cycle after mitogenic stimulation - driven by *Rbpj* deletion -. This is consistent with previous research performed in control adult livers. While single absence of p21 or p27 does not disrupt hepatocyte quiescence, double knock out leads to increased proliferation (Kwon et al., 2002). CDKI compensatory studies within the *cdkn1* family have been performed during development. Only in double p27/p57 and triple p21/p27/p57 global KO cell proliferation and apoptosis were increased, suggesting that mice lacking a single CDKI are viable because of compensatory mechanisms (Tateishi et al., 2012). We then could hypothesize that although in a homeostatic environment p21 is not essential to prevent proliferation and inhibit apoptosis, under stress conditions such as high mitogenic stimulation after Notch inhibition, p21 expression in quiescent ECs is required to inhibit EC proliferation and prevent from apoptosis. Further experiments by deleting *Rbpj* in quiescent ECs in a double or triple *cdkn1* KO background would support our hypothesis.

Lastly, our study raises safety concerns on the use of Notch inhibitors in clinics. Those treatments include from monoclonal antibodies against the Notch ligands and receptors to gamma-secretase inhibitors. Despite showing efficacy, all of them have shown toxicity (Ileana Dumbrava et al., 2018). Thus, this study could shed light on the understanding of the side effects observed in patients - especially those arising from the endothelium -, which could range from hyperpoliferation of heart and liver endothelium to endothelial senescence of different vascular beds. While continuous proliferation could result on vascular malformations, circulatory defects, heart hypertrophy and failure; endothelial senescence could even aggravate cancer treatment, as it has been shown to promote metastasis (Wieland et al., 2017). Therefore, understanding the consequences of inhibiting different Notch signalling components in the vascular system would benefit to all Notch signalling-based therapies.

Temporal proliferation analysis of *Dll4*^{iDEC} liver ECs

Contrary to the rapid increase in EC number and proliferation after Dll4/Notch inhibition during angiogenesis (Pontes-Quero et al., 2019), our analysis revealed that cell cycle reentry

is a slow process in a quiescent environment. Although at the 1 week post-*Dll4*-deletion timepoint ECs have already re-entered cell cycle, these cells have not exited, as we do not observe an increase in EC number. At this time point we do not observe the sinusoidal dilation we described in *Dll4*^{iDEC} livers at the 2 and 3 weeks post-*Dll4*-deletion timepoint, but we observed an increase in filopodia tip-like structures, which we did not observe at later stages. The appearance of filopodia structures is consistent with the already described role of Dll4 as a negative regulator of vascular sprouting and branching during vascular network formation (Suchting et al., 2007). Nevertheless, these tip-like cells disappear later on, maybe due to excessive vascular density, which reduces perivascular space for filopodia extension.

Notch gain-of-function studies have shown that Notch activation negatively affects hepatocyte proliferation in homeostatic and regenerating conditions through the downregulation of important angiocrine molecules (Duan et al., 2018). Interestingly, we observed that *Dll4* deficiency in quiescent ECs not only leads to endothelial proliferation, but also to hepatocyte proliferation, most probably by upregulation of important hepatocyte mitogens. Unfortunately, we were not able to identify any specific change in the angiocrine profile, as our RNA-seq was performed two weeks after *Dll4* deletion, moment that hepatocyte proliferation has already decreased. We also discard cell-to-cell signalling to the hepatocytes, as they do not express Notch1 receptors (Halpern et al., 2018). In addition, we have seen a biphasic dynamic in hepatocyte-EC proliferation that perfectly coincides with the kinetics of liver EC expansion and hepatocyte proliferation described during liver regeneration (Ding et al., 2010). These results are also in agreement with the enhanced hepatocyte proliferation we observed when EC are reactivated in *Rbpj*^{iDEC} and *Notch1*^{iDEC} mutants but there is not active EC proliferation. These results suggest that when ECs sustain hepatocyte proliferation, they do not promote their own cell-division, as it happen in regenerating conditions (Ding et al., 2010). We wonder whether Notch based therapies should be considered to ameliorate liver regeneration in clinics.

Liver EC zonation: Notch signalling and EC proliferation in *Dll4*^{iDEC} livers

Our temporal analysis also revealed a heterogeneous proliferation and EC density in *Dll4*^{iDEC} livers. ECs around central veins areas (CV) were more sensitive to *Dll4* deletion and hyperproliferated more compared to their neighboring ECs located in the portal vein (PV)

areas. Moreover, the sinusoidal dilation we observed was present in those proliferating areas and not in the PV regions. Collectively, these results suggested that Dll4/Notch signalling might be behind this heterogeneous response. Surprisingly, immunostaining of liver sections and scRNA-seq analysis showed that the anti-proliferative effect of Dll4/Notch signalling is stronger in the areas where Dll4 is less expressed and there is less activation of the Notch pathway. These counterintuitive results might be explained by the presence of other ligands such as Jag1 and Dll1. Previous research has uncovered the parallel and non-compensating functions of different Notch ligands. In different cell types and context, it has been shown that ligands could have from opposing roles to interchangeably functions, which could be consequence of pulsatile or sustained Notch activation (Benedito et al., 2009; Cappellari et al., 2013; Mohtashami et al., 2010; Nandagopal et al., 2018). Then, deletion of the most potent signalling ligand *Dll4* would allow Dll1 and Jag1 to signal in all liver ECs. It is still unclear for us how Dll1 and Jagged1 spatial expression patterns and ligand-specific functions would permit EC cell cycle reentry in *Dll4* deficient venous ECs but not in periarterial ECs. In addition, in our *Dll4*^{iDEC} livers ECs we do not detect Notch activation through Notch1 (N1ICD staining). Yet, it remains unexplored whether these levels are so low that we cannot detect it by immunostaining, or we have Notch activation through Notch4. Nonetheless, the high increase in p-ERK levels we observed after Notch1 deletion does not support the possibility of a strong signalling activation by Dll1 and Jag1 through Notch4.

However, we cannot reject the hypothesis of Notch signalling being dispensable for EC proliferation in peri-arterial areas (closed to PV). Ehling and colleagues already described that Dll4-Notch signalling was essential to promote quiescence in veins and peri-venous ECs during vessel remodelling. However, contrary to the essential role of Notch in artery formation (D'Amato et al., 2016; Su et al., 2018; Travisano et al., 2019), its activity is no longer required in formed arteries (Ehling et al., 2013). These results showed during vessel remodelling could be conserved in blood vessel quiescence, supporting our results of a non-proliferating arterial area after Dll4/Notch inhibition. As previously discussed, it has been widely accepted that during arterial-venous specification the proliferating cells arise from vein areas (Pitulescu et al., 2017; Su et al., 2018; Xu et al., 2014). In addition, our laboratory has recently shown that Notch regulates arterialization by supressing cell cycle (Luo et al., 2020). Indeed, recent scRNA-seq studies of whole human liver have shown that periportal ECs have an enrichment in cell cycle-arrest genes compared to the central venous ECs. On the contrary, central venous ECs have an enrichment in genes related to ERK2 pathway compared to periportal ECs (MacParland et al., 2018). Therefore, it might be possible that proliferation in ECs in PV areas is tightly controlled either by Notch and/or other signalling pathways that control cell cycle-

arrest, and ECs in CV closed areas are more sensitive to mitogenic stimulation and ERK signalling. However, we still think that ligand distribution (by Jag1 and Dll1) in the liver endothelium might take a role in this heterogeneous proliferation after *Dll4* deletion as we observed p21 upregulation both in CV and PV areas after *Rbpj* deletion, indicating that the non-proliferating areas in Dll4 mutants are indeed reactivated in Rbpj and Notch1 mutants.

There is a specific liver EC population with the potential to proliferate and expand over time

To understand the spatio-temporal dynamics of EC proliferation in *Dll4*^{iDEC} livers, we used the inducible fluorescent genetic mosaics generated in the laboratory (Pontes-Quero et al., 2017) - *Dual ifgMosaics* mice – which allowed us to uncover that not all quiescent ECs have the same potential to reentry cell cycle and proliferate over time. There is a rare and specific EC population (1.3%), which is located next to the CVs and can generate more than 50 cells in only two weeks after *Dll4* deficiency.

While some studies in our laboratory have elegantly shown that retina and heart vessels are formed by a mosaic of ECs during development (Pontes-Quero et al., 2017), some reports have suggested that post-natal vasculogenesis or angiogenesis can arise from single cells. The development of *in vivo* lineage tracing and single-cell techniques have allowed to observe clonal expansion of resident ECs under pathological conditions. Two of the few studies that have clearly shown this scenario *in vivo* so far are the clonal expansion of lymph node ECs under inflammatory conditions or during cerebral cavernous malformation development (Malinverno et al., 2019; Mondor et al., 2016). In addition, scRNA-seq from aortas have recently shown a potential endothelial progenitor population (Lukowski et al., 2019).

Therefore, consistent with previous publications, we have demonstrated that after *Dll4* deletion there is a clonal division of ECs closed to central vein. These ECs can generate up to 79 cell-clones. However, while the majority of quiescence ECs do not proliferate (66%), most proliferative ECs only divide once or twice, generating 2-4 cells per clone (25%). Nevertheless, the presence of these “special” ECs with a clonal expansion ability (1.3%) and negatively regulated by Dll4/Notch raises the question of the presence of an EC stem cell

system. As we have not investigated that possibility, we cannot discard that we have targeted the endothelial specific deletion of *Dll4* in a stem cell-like population, which is able to clonally expand over time. Our results are in agreement with a recent study in the regenerating adult intra-renal aorta, where it was shown that resident quiescent ECs in large vessels were able to reenter cell cycle. Interestingly, some of them had an enhanced proliferative capacity, forming larger clones (McDonald et al., 2018).

Importantly, our results are also in line with very recent scRNA-seq studies which have shown that there is a subset of ECs that expresses typical proliferation markers in the adult liver and spleen (1.4% and 0.6% respectively) but not in other organs (Kalucka et al., 2020). This EC cluster with proliferation markers might represent the population we have uncovered. In addition, a very recent study found in the portal veins a CD157+ endothelial progenitor population that is able to contribute to vascular homeostasis and regeneration (Wakabayashi et al., 2018).

On the importance of reliable gene deletion experiments

In conditional genetics, fluorescent Cre-reporter-expressing cells are usually considered mutant cells, even though a variable fraction of them may escape the desired gene deletion, especially if this gives them a competitive advantage (Zhang et al., 2018). Many Cre transgenes are sensitive to epigenetic regulation, which causes variegation or weak expression in a fraction of cells (Heffner et al., 2012). We have shown several examples in which weak Cre or CreERT2 expression/activity may be enough to recombine a floxed reporter allele localized in the permissive Rosa26 locus; however, this weak activity is insufficient to fully delete other genes that require higher or longer-lasting Cre expression, which can be provided by the *iSuRe-Cre* allele. This work also shows that a conventional Cre reporter allele, only accurately reports recombination of itself, not of other reporters or other floxed genes. In contrast to conventional Cre reporters, the *iSuRe-Cre* allele accurately reports cells with recombination/deletion of any other tested reporter or floxed gene, greatly decreasing the rate of false positives.

As our results have clearly shown, the use of the new *iSuRe-Cre* allele allows the analysis of phenotypes produced by multiple gene deletions, with high cellular resolution and genetic reliability in live or fixed tissues.

In summary, we propose use of the *iSuRe-Cre* mouse line instead of conventional Cre activity reporters, which we and others (Liu et al., 2013; Schmidt-Supprian and Rajewsky, 2007) have demonstrated are not bona fide reporters of the recombination/deletion of other genes (Figure 44). This new genetic tool will significantly increase the ease, efficiency and reliability of conditional genetic modifications in the mouse, the most widely used model organism in biomedical research (Fernandez-Chacon et al., 2019).

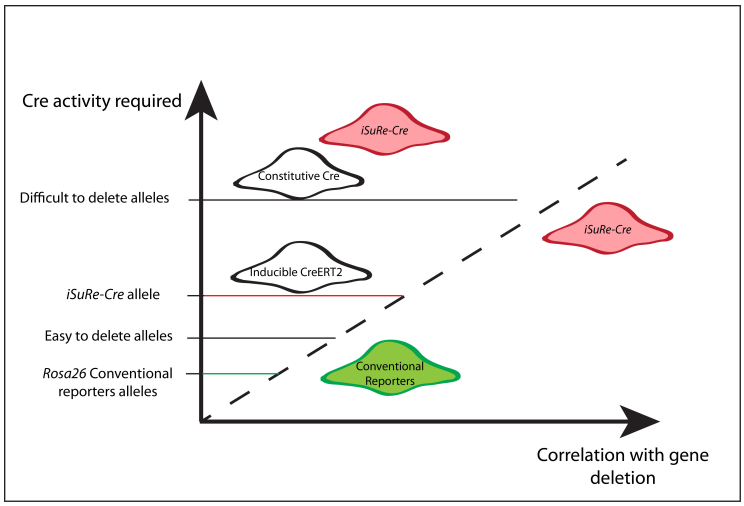

Figure 44: Illustrative chart comparing the most used genetic strategies in biomedical research and the developed *iSuRe-Cre*. In the Y axis the position of the cells represent the Cre activity achieved with most Cre/CreERT2 lines and the *iSuRe-Cre* allele. Different levels of Cre activity are required to delete different floxed alleles. In The X axis is represented the correlation with gene deletion of conventional Cre reporter compared to our new allele *iSuRe-Cre*. Only the iSuRe-Cre can ensure the deletion of most genes in reporter-expressing cells

Concluding remarks and outlook

Understanding the maintenance of the quiescent vascular network is highly relevant for human health. In serious life-threatening conditions, the modulation and control of the EC quiescence phenotype have been shown to be crucial. While the induction of angiogenesis may be advantageous in cardiovascular diseases such as heart and brain ischemia, hypovascular-related dementia, neurodegeneration and wound healing; its inhibition would be beneficial in inflammatory disorders, diabetes and cancer (Carmeliet, 2003; Carmeliet and

Jain, 2011). Many risk factors of cardiovascular diseases are associated with endothelial dysfunction, which also occurs during human ageing (Widlansky et al., 2003). Importantly, now that we face the major global health crisis of our time, emerging evidence is suggesting that ECs are key players in the initiation and propagation of COVID-19 (Ackermann et al., 2020; Teuwen et al., 2020; Varga et al., 2020). Therefore, a better comprehension of the signalling pathways that control and maintain EC homeostasis, proliferation and aged-related senescence would benefit most therapeutic treatments. Importantly, the understanding of these complex and heterogeneous ECs across different organ vascular beds will allow to target tissue-specific ECs, providing more accuracy and less undesired side effects in these therapies. I hope that the findings presented in this doctoral thesis have done its bit to get us a little bit closer to that future (but possible) horizon.

CONCLUSIONS

CONCLUSIONES

1-Dll4/Notch1 signalling is active in quiescent ECs from heart, lung, liver and brain.

2-Global loss of Dll4 in the adult endothelium causes the reentry in cell cycle and hyperproliferation of otherwise quiescent heart and liver ECs, but not brain and lung ECs.

3-Dll4/Notch1 maintains liver endothelial quiescence by supressing the Myc signalling pathway.

4- In contrast to the loss of Dll4, ECs with loss of Rbpj or Notch1 do not proliferate more.

5- Loss of distinct Notch signalling members in quiescent liver ECs, results in distinct and Notch-dose dependent ERK activation, being highest after the loss of Rbpj.

6-Excessive mitogenic stimulus induced by High-ERK activity in Notch1 and Rbpj-deficient liver endothelium induces p21-mediated cell cycle arrest.

7- By negatively regulating ERK activity and p21 expression, Notch signalling induces endothelial quiescence and prevents endothelial proliferation, senescence and apoptosis.

8- The expression and function of Dll4/Notch signalling in liver ECs is zonated: Dll4/Notch genes are less expressed in perivenous ECs and more expressed in periportal ECs, but their anti-proliferative function is stronger in perivenous areas.

9- Single cell and multispectral clonal analysis revealed that Dll4/Notch1 signalling negatively regulates the clonal expansion of a rare population of ECs located around liver central veins.

10- *iSuRe-Cre* is a genetic tool to reliably induce and report Cre-dependent genetic modifications.

1-La señalización de Dll4/Notch1 está activa en las células ECs quiescentes del corazón, pulmón, hígado y cerebro.

2-La pérdida de Dll4 en el todo el compartimiento endotelial causa la reentrada en ciclo celular y la hiperproliferación de las ECs del corazón e hígado previamente quiescentes, pero no de las ECs del pulmón y cerebro.

3-La señalización de Dll4/Notch1 mantiene la quiescencia del endotelio del hígado suprimiendo la vía de señalización de Myc.

4-Al contrario que con la pérdida de Dll4, las células ECs quiescentes del hígado con una pérdida de función de Rbpj o Notch1 no proliferan.

5-La pérdida de distintos miembros de la vía de señalización de Notch en las ECs quiescentes del hígado resulta en una activación de ERK diferente y dependiente de la dosis de Notch, que es mayor después de la pérdida de Rbpj.

6-En el endotelio del hígado deficiente para Notch1 y Rbpj, un estímulo mitogénico excesivo causado por una actividad alta de ERK induce un arresto celular mediado por p21.

7-La señalización de Notch induce la quiescencia endotelial y previene la proliferación, la senescencia y la apoptosis endotelial regulando negativamente la actividad de ERK y la expresión de p21,

8-La expresión y la función de la señalización de Dll4/Notch en las células endoteliales de hígado está zonificada: los genes regulados por Dll4/Notch están menos expresados en las ECs cerca de la vena central y están más expresados en las ECs cerca de la vena portal, pero su función anti-proliferativa es más fuerte en áreas cerca de la vena central.

9-El análisis unicelular y multiespectral clonal ha revelado que la señalización de Dll4/Notch1 regula de manera negativa la expansión clonal de una población poco frecuente que se encuentra alrededor de las venas centrales del hígado.

10- *iSuRe-Cre* es una herramienta genética que induce e indica de manera segura las modificaciones genéticas dependientes de Cre.

BIBLIOGRAPHY

Abbas, T., and Dutta, A. (2009). p21 in cancer: intricate networks and multiple activities. Nat Rev Cancer *9*, 400-414.

Ackermann, M., Verleden, S.E., Kuehnel, M., Haverich, A., Welte, T., Laenger, F., Vanstapel, A., Werlein, C., Stark, H., Tzankov, A.*, et al.* (2020). Pulmonary Vascular Endothelialitis, Thrombosis, and Angiogenesis in Covid-19. N Engl J Med *383*, 120-128.

Adams, R.H. (2003). Molecular control of arterial-venous blood vessel identity. J Anat *202*, 105-112.

Adams, R.H., and Alitalo, K. (2007). Molecular regulation of angiogenesis and lymphangiogenesis. Nat Rev Mol Cell Biol *8*, 464-478.

Aird, W.C. (2007). Phenotypic heterogeneity of the endothelium: I. Structure, function, and mechanisms. Circ Res *100*, 158-173.

Aird, W.C. (2011). Discovery of the cardiovascular system: from Galen to William Harvey. J Thromb Haemost *9 Suppl 1*, 118-129.

Aird, W.C. (2012). Endothelial cell heterogeneity. Cold Spring Harb Perspect Med *2*, a006429.

Andersson, E.R., Sandberg, R., and Lendahl, U. (2011). Notch signaling: simplicity in design, versatility in function. Development *138*, 3593-3612.

Arima, S., Nishiyama, K., Ko, T., Arima, Y., Hakozaki, Y., Sugihara, K., Koseki, H., Uchijima, Y., Kurihara, Y., and Kurihara, H. (2011). Angiogenic morphogenesis driven by dynamic and heterogeneous collective endothelial cell movement. Development *138*, 4763-4776.

Armulik, A., Abramsson, A., and Betsholtz, C. (2005). Endothelial/pericyte interactions. Circ Res *97*, 512-523.

Aspalter, I.M., Gordon, E., Dubrac, A., Ragab, A., Narloch, J., Vizan, P., Geudens, I., Collins, R.T., Franco, C.A., Abrahams, C.L.*, et al.* (2015). Alk1 and Alk5 inhibition by Nrp1 controls vascular sprouting downstream of Notch. Nat Commun *6*, 7264.

Augustin, H.G., and Koh, G.Y. (2017). Organotypic vasculature: From descriptive heterogeneity to functional pathophysiology. Science *357*.

Augustin, H.G., Koh, G.Y., Thurston, G., and Alitalo, K. (2009). Control of vascular morphogenesis and homeostasis through the angiopoietin-Tie system. Nat Rev Mol Cell Biol *10*, 165-177.

Azizi, M.H., Nayernouri, T., and Azizi, F. (2008). A brief history of the discovery of the circulation of blood in the human body. Arch Iran Med *11*, 345-350.

Balmanno, K., and Cook, S.J. (1999). Sustained MAP kinase activation is required for the expression of cyclin D1, p21Cip1 and a subset of AP-1 proteins in CCL39 cells. Oncogene *18*, 3085-3097.

Banks, M., Crowell, K., Proctor, A., and Jensen, B.C. (2017). Cardiovascular Effects of the MEK Inhibitor, Trametinib: A Case Report, Literature Review, and Consideration of Mechanism. Cardiovasc Toxicol *17*, 487-493.

Benedito, R., and Hellstrom, M. (2013). Notch as a hub for signaling in angiogenesis. Exp Cell Res *319*, 1281-1288.

Benedito, R., Roca, C., Sorensen, I., Adams, S., Gossler, A., Fruttiger, M., and Adams, R.H. (2009). The notch ligands Dll4 and Jagged1 have opposing effects on angiogenesis. Cell *137*, 1124-1135.

Benedito, R., Rocha, S.F., Woeste, M., Zamykal, M., Radtke, F., Casanovas, O., Duarte, A., Pytowski, B., and Adams, R.H. (2012). Notch-dependent VEGFR3 upregulation allows angiogenesis without VEGF-VEGFR2 signalling. Nature *484*, 110-114.

Benedito, R., Trindade, A., Hirashima, M., Henrique, D., da Costa, L.L., Rossant, J., Gill, P.S., and Duarte, A. (2008). Loss of Notch signalling induced by Dll4 causes arterial calibre reduction by increasing endothelial cell response to angiogenic stimuli. BMC Dev Biol *8*, 117.

Bentley, K., Franco, C.A., Philippides, A., Blanco, R., Dierkes, M., Gebala, V., Stanchi, F., Jones, M., Aspalter, I.M., Cagna, G.*, et al.* (2014). The role of differential VE-cadherin dynamics in cell rearrangement during angiogenesis. Nat Cell Biol *16*, 309-321.

Blagosklonny, M.V. (2003). Cell senescence and hypermitogenic arrest. EMBO Rep *4*, 358-362.

Bolanos-Garcia, V.M., and Blundell, T.L. (2011). BUB1 and BUBR1: multifaceted kinases of the cell cycle. Trends Biochem Sci *36*, 141-150.

Bonzon-Kulichenko, E., Camafeita, E., Lopez, J.A., Gomez-Serrano, M., Jorge, I., Calvo, E., Nunez, E., Trevisan-Herraz, M., Bagwan, N., Barcena, J.A.*, et al.* (2020). Improved integrative analysis of the thiol redox proteome using filter-aided sample preparation. J Proteomics *214*, 103624.

Bonzon-Kulichenko, E., Garcia-Marques, F., Trevisan-Herraz, M., and Vazquez, J. (2015). Revisiting peptide identification by high-accuracy mass spectrometry: problems associated with the use of narrow mass precursor windows. J Proteome Res *14*, 700-710.

Bray, S.J. (2006). Notch signalling: a simple pathway becomes complex. Nat Rev Mol Cell Biol *7*, 678-689.

Brugarolas, J., Chandrasekaran, C., Gordon, J.I., Beach, D., Jacks, T., and Hannon, G.J. (1995). Radiation-induced cell cycle arrest compromised by p21 deficiency. Nature *377*, 552-557.

Cai, D., Cohen, K.B., Luo, T., Lichtman, J.W., and Sanes, J.R. (2013). Improved tools for the Brainbow toolbox. Nature methods *10*, 540-547.

Cappellari, O., Benedetti, S., Innocenzi, A., Tedesco, F.S., Moreno-Fortuny, A., Ugarte, G., Lampugnani, M.G., Messina, G., and Cossu, G. (2013). Dll4 and PDGF-BB convert committed skeletal myoblasts to pericytes without erasing their myogenic memory. Dev Cell *24*, 586-599.

Carlson, T.R., Yan, Y., Wu, X., Lam, M.T., Tang, G.L., Beverly, L.J., Messina, L.M., Capobianco, A.J., Werb, Z., and Wang, R. (2005). Endothelial expression of constitutively active Notch4 elicits reversible arteriovenous malformations in adult mice. Proc Natl Acad Sci U S A *102*, 9884-9889.

Carmeliet, P. (2003). Angiogenesis in health and disease. Nat Med *9*, 653-660.

Carmeliet, P. (2005). Angiogenesis in life, disease and medicine. Nature *438*, 932-936.

Carmeliet, P., Ferreira, V., Breier, G., Pollefeyt, S., Kieckens, L., Gertsenstein, M., Fahrig, M., Vandenhoeck, A., Harpal, K., Eberhardt, C.*, et al.* (1996). Abnormal blood vessel development and lethality in embryos lacking a single VEGF allele. Nature *380*, 435-439.

Carmeliet, P., and Jain, R.K. (2011). Molecular mechanisms and clinical applications of angiogenesis. Nature *473*, 298-307.

Castel, D., Mourikis, P., Bartels, S.J., Brinkman, A.B., Tajbakhsh, S., and Stunnenberg, H.G. (2013). Dynamic binding of RBPJ is determined by Notch signaling status. Genes Dev *27*, 1059-1071.

Cheng, Q., McKeown, S.J., Santos, L., Santiago, F.S., Khachigian, L.M., Morand, E.F., and Hickey, M.J. (2010). Macrophage migration inhibitory factor increases leukocyte-endothelial interactions in human endothelial cells via promotion of expression of adhesion molecules. J Immunol *185*, 1238-1247.

Childs, B.G., Gluscevic, M., Baker, D.J., Laberge, R.M., Marquess, D., Dananberg, J., and van Deursen, J.M. (2017). Senescent cells: an emerging target for diseases of ageing. Nat Rev Drug Discov *16*, 718-735.

Chung, A.S., and Ferrara, N. (2011). Developmental and pathological angiogenesis. Annu Rev Cell Dev Biol *27*, 563-584.

Chung, J.H., Whiteley, M., and Felsenfeld, G. (1993). A 5' element of the chicken beta-globin domain serves as an insulator in human erythroid cells and protects against position effect in Drosophila. Cell *74*, 505-514.

Claxton, S., and Fruttiger, M. (2004). Periodic Delta-like 4 expression in developing retinal arteries. Gene Expr Patterns *5*, 123-127.

Couch, J.A., Zhang, G., Beyer, J.C., de Zafra, C.L., Gupta, P., Kamath, A.V., Lewin-Koh, N., Tarrant, J., Allamneni, K.P., Cain, G.*, et al.* (2016). Balancing Efficacy and Safety of an Anti-DLL4 Antibody through Pharmacokinetic Modulation. Clin Cancer Res *22*, 1469-1479.

Cristofaro, B., Shi, Y., Faria, M., Suchting, S., Leroyer, A.S., Trindade, A., Duarte, A., Zovein, A.C., Iruela-Arispe, M.L., Nih, L.R.*, et al.* (2013). Dll4-Notch signaling determines the formation of native arterial collateral networks and arterial function in mouse ischemia models. Development *140*, 1720-1729.

Cuervo, H., Nielsen, C.M., Simonetto, D.A., Ferrell, L., Shah, V.H., and Wang, R.A. (2016). Endothelial notch signaling is essential to prevent hepatic vascular malformations in mice. Hepatology *64*, 1302-1316.

D'Amato, G., Luxan, G., del Monte-Nieto, G., Martinez-Poveda, B., Torroja, C., Walter, W., Bochter, M.S., Benedito, R., Cole, S., Martinez, F.*, et al.* (2016). Sequential Notch activation regulates ventricular chamber development. Nat Cell Biol *18*, 7-20.

Da Vinci, L. (1983). Leonardo on the human body (Dover Publications, Inc).

de Alboran, I.M., O'Hagan, R.C., Gartner, F., Malynn, B., Davidson, L., Rickert, R., Rajewsky, K., DePinho, R.A., and Alt, F.W. (2001). Analysis of C-MYC function in normal cells via conditional gene-targeted mutation. Immunity *14*, 45-55.

Del Monte, G., Grego-Bessa, J., Gonzalez-Rajal, A., Bolos, V., and De La Pompa, J.L. (2007). Monitoring Notch1 activity in development: evidence for a feedback regulatory loop. Dev Dyn *236*, 2594-2614.

del Toro, R., Prahst, C., Mathivet, T., Siegfried, G., Kaminker, J.S., Larrivee, B., Breant, C., Duarte, A., Takakura, N., Fukamizu, A.*, et al.* (2010). Identification and functional analysis of endothelial tip cell-enriched genes. Blood *116*, 4025-4033.

Deng, T., Yan, G., Song, X., Xie, L., Zhou, Y., Li, J., Hu, X., Li, Z., Hu, J., Zhang, Y.*, et al.* (2018). Deubiquitylation and stabilization of p21 by USP11 is critical for cell-cycle progression and DNA damage responses. Proc Natl Acad Sci U S A *115*, 4678-4683.

Diaz-Trelles, R., Scimia, M.C., Bushway, P., Tran, D., Monosov, A., Monosov, E., Peterson, K., Rentschler, S., Cabrales, P., Ruiz-Lozano, P.*, et al.* (2016). Notch-independent RBPJ controls angiogenesis in the adult heart. Nat Commun *7*, 12088.

Dill, M.T., Rothweiler, S., Djonov, V., Hlushchuk, R., Tornillo, L., Terracciano, L., Meili-Butz, S., Radtke, F., Heim, M.H., and Semela, D. (2012). Disruption of Notch1 induces vascular

remodeling, intussusceptive angiogenesis, and angiosarcomas in livers of mice. Gastroenterology *142*, 967-977 e962.

Ding, B.S., Nolan, D.J., Butler, J.M., James, D., Babazadeh, A.O., Rosenwaks, Z., Mittal, V., Kobayashi, H., Shido, K., Lyden, D.*, et al.* (2010). Inductive angiocrine signals from sinusoidal endothelium are required for liver regeneration. Nature *468*, 310-315.

Dobie, R., Wilson-Kanamori, J.R., Henderson, B.E.P., Smith, J.R., Matchett, K.P., Portman, J.R., Wallenborg, K., Picelli, S., Zagorska, A., Pendem, S.V.*, et al.* (2019). Single-Cell Transcriptomics Uncovers Zonation of Function in the Mesenchyme during Liver Fibrosis. Cell Rep *29*, 1832-1847 e1838.

Domigan, C.K., Warren, C.M., Antanesian, V., Happel, K., Ziyad, S., Lee, S., Krall, A., Duan, L., Torres-Collado, A.X., Castellani, L.W.*, et al.* (2015). Autocrine VEGF maintains endothelial survival through regulation of metabolism and autophagy. J Cell Sci *128*, 2236-2248.

Dou, G.R., Wang, Y.C., Hu, X.B., Hou, L.H., Wang, C.M., Xu, J.F., Wang, Y.S., Liang, Y.M., Yao, L.B., Yang, A.G.*, et al.* (2008). RBP-J, the transcription factor downstream of Notch receptors, is essential for the maintenance of vascular homeostasis in adult mice. FASEB J *22*, 1606-1617.

Duan, J.L., Ruan, B., Yan, X.C., Liang, L., Song, P., Yang, Z.Y., Liu, Y., Dou, K.F., Han, H., and Wang, L. (2018). Endothelial Notch activation reshapes the angiocrine of sinusoidal endothelia to aggravate liver fibrosis and blunt regeneration in mice. Hepatology *68*, 677-690.

Duarte, A., Hirashima, M., Benedito, R., Trindade, A., Diniz, P., Bekman, E., Costa, L., Henrique, D., and Rossant, J. (2004). Dosage-sensitive requirement for mouse Dll4 in artery development. Genes Dev *18*, 2474-2478.

Ehling, M., Adams, S., Benedito, R., and Adams, R.H. (2013). Notch controls retinal blood vessel maturation and quiescence. Development *140*, 3051-3061.

Eilken, H.M., and Adams, R.H. (2010). Dynamics of endothelial cell behavior in sprouting angiogenesis. Curr Opin Cell Biol *22*, 617-625.

el-Deiry, W.S., Harper, J W., O'Connor, P. M., Velculescu, V. E., Canman, C. E ., Jackman, J., Pietenpol, .J A., Burrell, M., Hill, D. E ., Wang, Y. (1994). <waf1cip1 is induced in p53 mediated g1 arrest and apoptosis.pdf>. Cancer Research.

Fang, J.S., Coon, B.G., Gillis, N., Chen, Z., Qiu, J., Chittenden, T.W., Burt, J.M., Schwartz, M.A., and Hirschi, K.K. (2017). Shear-induced Notch-Cx37-p27 axis arrests endothelial cell cycle to enable arterial specification. Nature communications *8*, 2149.

Favre, C.J., Mancuso, M., Maas, K., McLean, J.W., Baluk, P., and McDonald, D.M. (2003). Expression of genes involved in vascular development and angiogenesis in endothelial cells of adult lung. Am J Physiol Heart Circ Physiol *285*, H1917-1938.

Fernandez-Chacon, M., Casquero-Garcia, V., Luo, W., Francesca Lunella, F., Ferreira Rocha, S., Del Olmo-Cabrera, S., and Benedito, R. (2019). iSuRe-Cre is a genetic tool to reliably induce and report Cre-dependent genetic modifications. Nat Commun *10*, 2262.

Ferrara, N., Carver-Moore, K., Chen, H., Dowd, M., Lu, L., O'Shea, K.S., Powell-Braxton, L., Hillan, K.J., and Moore, M.W. (1996). Heterozygous embryonic lethality induced by targeted inactivation of the VEGF gene. Nature *380*, 439-442.

Ferrara, N., Gerber, H.P., and LeCouter, J. (2003). The biology of VEGF and its receptors. Nat Med *9*, 669-676.

Fisher, F., Crouch, D.H., Jayaraman, P.S., Clark, W., Gillespie, D.A., and Goding, C.R. (1993). Transcription activation by Myc and Max: flanking sequences target activation to a subset of CACGTG motifs in vivo. EMBO J *12*, 5075-5082.

Franco, C.A., Jones, M.L., Bernabeu, M.O., Geudens, I., Mathivet, T., Rosa, A., Lopes, F.M., Lima, A.P., Ragab, A., Collins, R.T.*, et al.* (2015). Dynamic endothelial cell rearrangements drive developmental vessel regression. PLoS Biol *13*, e1002125.

Gaengel, K., Genove, G., Armulik, A., and Betsholtz, C. (2009). Endothelial-mural cell signaling in vascular development and angiogenesis. Arterioscler Thromb Vasc Biol *29*, 630-638.

Gale, N.W., Dominguez, M.G., Noguera, I., Pan, L., Hughes, V., Valenzuela, D.M., Murphy, A.J., Adams, N.C., Lin, H.C., Holash, J.*, et al.* (2004). Haploinsufficiency of delta-like 4 ligand results in embryonic lethality due to major defects in arterial and vascular development. Proc Natl Acad Sci U S A *101*, 15949-15954.

Garcia-Gonzalez, I., Mühleder, S., Fernández-Chacón, M., and Benedito, R. (2020). Genetic Tools to Study Cardiovascular Biology. Frontiers in Physiology *11*.

Garcia-Marques, F., Trevisan-Herraz, M., Martinez-Martinez, S., Camafeita, E., Jorge, I., Lopez, J.A., Mendez-Barbero, N., Mendez-Ferrer, S., Del Pozo, M.A., Ibanez, B.*, et al.* (2016). A Novel Systems-Biology Algorithm for the Analysis of Coordinated Protein Responses Using Quantitative Proteomics. Mol Cell Proteomics *15*, 1740-1760.

Georgakilas, A.G., Martin, O.A., and Bonner, W.M. (2017). p21: A Two-Faced Genome Guardian. Trends Mol Med *23*, 310-319.

George, S.H., Gertsenstein, M., Vintersten, K., Korets-Smith, E., Murphy, J., Stevens, M.E., Haigh, J.J., and Nagy, A. (2007). Developmental and adult phenotyping directly from mutant embryonic stem cells. Proc Natl Acad Sci U S A *104*, 4455-4460.

Gerhardt, H., and Betsholtz, C. (2003). Endothelial-pericyte interactions in angiogenesis. Cell Tissue Res *314*, 15-23.

Gerhardt, H., Golding, M., Fruttiger, M., Ruhrberg, C., Lundkvist, A., Abramsson, A., Jeltsch, M., Mitchell, C., Alitalo, K., Shima, D.*, et al.* (2003). VEGF guides angiogenic sprouting utilizing endothelial tip cell filopodia. J Cell Biol *161*, 1163-1177.

Gordon, W.R., Zimmerman, B., He, L., Miles, L.J., Huang, J., Tiyanont, K., McArthur, D.G., Aster, J.C., Perrimon, N., Loparo, J.J.*, et al.* (2015). Mechanical Allostery: Evidence for a Force Requirement in the Proteolytic Activation of Notch. Dev Cell *33*, 729-736.

Goveia, J., Rohlenova, K., Taverna, F., Treps, L., Conradi, L.C., Pircher, A., Geldhof, V., de Rooij, L., Kalucka, J., Sokol, L.*, et al.* (2020). An Integrated Gene Expression Landscape Profiling Approach to Identify Lung Tumor Endothelial Cell Heterogeneity and Angiogenic Candidates. Cancer Cell *37*, 21-36 e13.

Gregory, T.R. (2005). The Evolution of the Genome. Elsevier Academic Press, 41-45.

Gridley, T. (2010). Notch Signaling in the Vasculature. In Notch Signaling, pp. 277-309.

Guo, M., Du, Y., Gokey, J.J., Ray, S., Bell, S.M., Adam, M., Sudha, P., Perl, A.K., Deshmukh, H., Potter, S.S.*, et al.* (2019). Single cell RNA analysis identifies cellular heterogeneity and adaptive responses of the lung at birth. Nat Commun *10*, 37.

Haigh, J.J., Morelli, P.I., Gerhardt, H., Haigh, K., Tsien, J., Damert, A., Miquerol, L., Muhlner, U., Klein, R., Ferrara, N.*, et al.* (2003). Cortical and retinal defects caused by dosage-dependent reductions in VEGF-A paracrine signaling. Dev Biol *262*, 225-241.

Halpern, K.B., Shenhav, R., Massalha, H., Toth, B., Egozi, A., Massasa, E.E., Medgalia, C., David, E., Giladi, A., Moor, A.E.*, et al.* (2018). Paired-cell sequencing enables spatial gene expression mapping of liver endothelial cells. Nat Biotechnol *36*, 962-970.

Halpern, K.B., Shenhav, R., Matcovitch-Natan, O., Toth, B., Lemze, D., Golan, M., Massasa, E.E., Baydatch, S., Landen, S., Moor, A.E.*, et al.* (2017). Single-cell spatial reconstruction reveals global division of labour in the mammalian liver. Nature *542*, 352-356.

Han, H., Tanigaki, K., Yamamoto, N., Kuroda, K., Yoshimoto, M., Nakahata, T., Ikuta, K., and Honjo, T. (2002). Inducible gene knockout of transcription factor recombination signal binding protein-J reveals its essential role in T versus B lineage decision. Int Immunol *14*, 637-645.

Hasan, S.S., Tsaryk, R., Lange, M., Wisniewski, L., Moore, J.C., Lawson, N.D., Wojciechowska, K., Schnittler, H., and Siekmann, A.F. (2017). Endothelial Notch signalling limits angiogenesis via control of artery formation. Nat Cell Biol *19*, 928-940.

Heffner, C.S., Herbert Pratt, C., Babiuk, R.P., Sharma, Y., Rockwood, S.F., Donahue, L.R., Eppig, J.T., and Murray, S.A. (2012). Supporting conditional mouse mutagenesis with a comprehensive cre characterization resource. Nature communications *3*, 1218.

Hellstrom, M., Phng, L.K., Hofmann, J.J., Wallgard, E., Coultas, L., Lindblom, P., Alva, J., Nilsson, A.K., Karlsson, L., Gaiano, N.*, et al.* (2007). Dll4 signalling through Notch1 regulates formation of tip cells during angiogenesis. Nature *445*, 776-780.

Herbert, S.P., Huisken, J., Kim, T.N., Feldman, M.E., Houseman, B.T., Wang, R.A., Shokat, K.M., and Stainier, D.Y. (2009). Arterial-venous segregation by selective cell sprouting: an alternative mode of blood vessel formation. Science *326*, 294-298.

Hernandez-Segura, A., Nehme, J., and Demaria, M. (2018). Hallmarks of Cellular Senescence. Trends Cell Biol *28*, 436-453.

Hoare, M., Ito, Y., Kang, T.W., Weekes, M.P., Matheson, N.J., Patten, D.A., Shetty, S., Parry, A.J., Menon, S., Salama, R.*, et al.* (2016). NOTCH1 mediates a switch between two distinct secretomes during senescence. Nat Cell Biol *18*, 979-992.

Hofmann, J.J., and Iruela-Arispe, M.L. (2007). Notch signaling in blood vessels: who is talking to whom about what? Circ Res *100*, 1556-1568.

Hogan, B.M., Herpers, R., Witte, M., Helotera, H., Alitalo, K., Duckers, H.J., and Schulte-Merker, S. (2009). Vegfc/Flt4 signalling is suppressed by Dll4 in developing zebrafish intersegmental arteries. Development *136*, 4001-4009.

Hong, S.K., Yoon, S., Moelling, C., Arthan, D., and Park, J.I. (2009). Noncatalytic function of ERK1/2 can promote Raf/MEK/ERK-mediated growth arrest signaling. J Biol Chem *284*, 33006-33018.

Hori, K., Sen, A., and Artavanis-Tsakonas, S. (2013). Notch signaling at a glance. Journal of Cell Science *126*, 2135-2140.

Horn, H.F., and Vousden, K.H. (2007). Coping with stress: multiple ways to activate p53. Oncogene *26*, 1306-1316.

Hrabe de Angelis, M., McIntyre, J., 2nd, and Gossler, A. (1997). Maintenance of somite borders in mice requires the Delta homologue DII1. Nature *386*, 717-721.

Hsieh, W.J., Hsieh, S.C., Chen, C.C., and Wang, F.F. (2008). Human DDA3 is an oncoprotein down-regulated by p53 and DNA damage. Biochem Biophys Res Commun *369*, 567-572.

Ileana Dumbrava, E.E., Mills, G.B., and Yap, T.A. (2018). Targeting gamma secretase: has progress moved up a Notch? Ann Oncol *29*, 1889-1891.

Jabs, M., Rose, A.J., Lehmann, L.H., Taylor, J., Moll, I., Sijmonsma, T.P., Herberich, S.E., Sauer, S.W., Poschet, G., Federico, G.*, et al.* (2018). Inhibition of Endothelial Notch Signaling Impairs Fatty Acid Transport and Leads to Metabolic and Vascular Remodeling of the Adult Heart. Circulation *137*, 2592-2608.

Jakobsson, L., Franco, C.A., Bentley, K., Collins, R.T., Ponsioen, B., Aspalter, I.M., Rosewell, I., Busse, M., Thurston, G., Medvinsky, A.*, et al.* (2010). Endothelial cells dynamically compete for the tip cell position during angiogenic sprouting. Nat Cell Biol *12*, 943-953.

James, A.C., Szot, J.O., Iyer, K., Major, J.A., Pursglove, S.E., Chapman, G., and Dunwoodie, S.L. (2014). Notch4 reveals a novel mechanism regulating Notch signal transduction. Biochim Biophys Acta *1843*, 1272-1284.

Je, Y., Schutz, F.A.B., and Choueiri, T.K. (2009). Risk of bleeding with vascular endothelial growth factor receptor tyrosine-kinase inhibitors sunitinib and sorafenib: a systematic review and meta-analysis of clinical trials. The Lancet Oncology *10*, 967-974.

Jones, E.A., le Noble, F., and Eichmann, A. (2006). What determines blood vessel structure? Genetic prespecification vs. hemodynamics. Physiology (Bethesda, Md *21*, 388-395.

Joutel, A. (2011). Pathogenesis of CADASIL: transgenic and knock-out mice to probe function and dysfunction of the mutated gene, Notch3, in the cerebrovasculature. Bioessays *33*, 73-80.

Joutel, A., Vahedi, K., Corpechot, C., Troesch, A., Chabriat, H., Vayssière, C., Cruaud, C., Maciazek, J., Weissenbach, J., Bousser, M.-G.*, et al.* (1997). Strong clustering and stereotyped nature of Notch3 mutations in CADASIL patients. The Lancet *350*, 1511-1515.

Kaczmarczyk, S.J., and Green, J.E. (2001). A single vector containing modified cre recombinase and LOX recombination sequences for inducible tissue-specific amplification of gene expression. Nucleic Acids Res *29*, E56-56.

Kageyama, R., Niwa, Y., Shimojo, H., Kobayashi, T., and Ohtsuka, T. (2010). Ultradian Oscillations in Notch Signaling Regulate Dynamic Biological Events. In Notch Signaling, pp. 311-331.

Kalucka, J., de Rooij, L., Goveia, J., Rohlenova, K., Dumas, S.J., Meta, E., Conchinha, N.V., Taverna, F., Teuwen, L.A., Veys, K.*, et al.* (2020). Single-Cell Transcriptome Atlas of Murine Endothelial Cells. Cell *180*, 764-779 e720.

Karaiskos, N., Rahmatollahi, M., Boltengagen, A., Liu, H., Hoehne, M., Rinschen, M., Schermer, B., Benzing, T., Rajewsky, N., Kocks, C.*, et al.* (2018). A Single-Cell Transcriptome Atlas of the Mouse Glomerulus. J Am Soc Nephrol *29*, 2060-2068.

Kasahara, Y., Tuder, R.M., Taraseviciene-Stewart, L., Le Cras, T.D., Abman, S., Hirth, P.K., Waltenberger, J., and Voelkel, N.F. (2000). Inhibition of VEGF receptors causes lung cell apoptosis and emphysema. J Clin Invest *106*, 1311-1319.

Kerr, B.A., West, X.Z., Kim, Y.W., Zhao, Y., Tischenko, M., Cull, R.M., Phares, T.W., Peng, X.D., Bernier-Latmani, J., Petrova, T.V.*, et al.* (2016). Stability and function of adult vasculature is sustained by Akt/Jagged1 signalling axis in endothelium. Nat Commun *7*, 10960.

Khan, S., Taverna, F., Rohlenova, K., Treps, L., Geldhof, V., de Rooij, L., Sokol, L., Pircher, A., Conradi, L.C., Kalucka, J.*, et al.* (2019). EndoDB: a database of endothelial cell transcriptomics data. Nucleic Acids Res *47*, D736-D744.

Kim, K.J., Li, B., Winer, J., Armanini, M., Gillett, N., Phillips, H.S., and Ferrara, N. (1993). Inhibition of vascular endothelial growth factor-induced angiogenesis suppresses tumour growth in vivo. Nature *362*, 841-844.

Knoepfler, P.S., Cheng, P.F., and Eisenman, R.N. (2002). N-myc is essential during neurogenesis for the rapid expansion of progenitor cell populations and the inhibition of neuronal differentiation. Genes Dev *16*, 2699-2712.

Koch, S., and Claesson-Welsh, L. (2012). Signal transduction by vascular endothelial growth factor receptors. Cold Spring Harb Perspect Med *2*, a006502.

Koch, U., Fiorini, E., Benedito, R., Besseyrias, V., Schuster-Gossler, K., Pierres, M., Manley, N.R., Duarte, A., Macdonald, H.R., and Radtke, F. (2008). Delta-like 4 is the essential, nonredundant ligand for Notch1 during thymic T cell lineage commitment. J Exp Med *205*, 2515-2523.

Kopan, R., and Ilagan, M.X. (2009). The canonical Notch signaling pathway: unfolding the activation mechanism. Cell *137*, 216-233.

Krebs, L.T., Shutter, J.R., Tanigaki, K., Honjo, T., Stark, K.L., and Gridley, T. (2004). Haploinsufficient lethality and formation of arteriovenous malformations in Notch pathway mutants. Genes Dev *18*, 2469-2473.

Krebs, L.T., Xue, Y., Norton, C.R., Shutter, J.R., Maguire, M., Sundberg, J.P., Gallahan, D., Closson, V., Kitajewski, J., Callahan, R.*, et al.* (2000). Notch signaling is essential for vascular morphogenesis in mice. Genes Dev *1;14(11):1343-52.*

Kress, T.R., Sabo, A., and Amati, B. (2015). MYC: connecting selective transcriptional control to global RNA production. Nat Rev Cancer *15*, 593-607.

Kwon, Y.H., Jovanovic, A., Serfas, M.S., Kiyokawa, H., and Tyner, A.L. (2002). P21 functions to maintain quiescence of p27-deficient hepatocytes. J Biol Chem *277*, 41417-41422.

Lavina, B., Castro, M., Niaudet, C., Cruys, B., Alvarez-Aznar, A., Carmeliet, P., Bentley, K., Brakebusch, C., Betsholtz, C., and Gaengel, K. (2018). Defective endothelial cell migration in the absence of Cdc42 leads to capillary-venous malformations. Development *145*.

Lawson, N.D., Scheer, N., Pham, V.N., Kim, C.H., Chitnis, A.B., Campos-Ortega, J.A., and Weinstein, B.M. (2001). Notch signaling is required for arterial-venous differentiation during embryonic vascular development. Development *128(19)*, 3675–3683.

Lawson, N.D., Vogel, A.M., and Weinstein, B.M. (2002). sonic hedgehog and vascular endothelial growth factor Act Upstream of the Notch Pathway during Arterial Endothelial Differentiation. Developmental Cell *3*, 127-136.

Lee, S., Chen, T.T., Barber, C.L., Jordan, M.C., Murdock, J., Desai, S., Ferrara, N., Nagy, A., Roos, K.P., and Iruela-Arispe, M.L. (2007). Autocrine VEGF signaling is required for vascular homeostasis. Cell *130*, 691-703.

Leslie, J.D., Ariza-McNaughton, L., Bermange, A.L., McAdow, R., Johnson, S.L., and Lewis, J. (2007). Endothelial signalling by the Notch ligand Delta-like 4 restricts angiogenesis. Development *134*, 839-844.

Leveen, P., Pekny, M., Gebre-Medhin, S., Swolin, B., Larsson, E., and Betsholtz, C. (1994). Mice deficient for PDGF B show renal, cardiovascular, and hematological abnormalities. Genes Dev *8*, 1875-1887.

Levine, A.J. (1997). p53, the Cellular Gatekeeper for Growth and Division. Cell *88*, 323-331.

Li, B., and Dewey, C.N. (2011). RSEM: accurate transcript quantification from RNA-Seq data with or without a reference genome. BMC Bioinformatics *12*, 323.

Li, J.L., Sainson, R.C., Shi, W., Leek, R., Harrington, L.S., Preusser, M., Biswas, S., Turley, H., Heikamp, E., Hainfellner, J.A.*, et al.* (2007). Delta-like 4 Notch ligand regulates tumor angiogenesis, improves tumor vascular function, and promotes tumor growth in vivo. Cancer Res *67*, 11244-11253.

Liberzon, A., Birger, C., Thorvaldsdottir, H., Ghandi, M., Mesirov, J.P., and Tamayo, P. (2015). The Molecular Signatures Database (MSigDB) hallmark gene set collection. Cell Syst *1*, 417-425.

Liberzon, A., Subramanian, A., Pinchback, R., Thorvaldsdottir, H., Tamayo, P., and Mesirov, J.P. (2011). Molecular signatures database (MSigDB) 3.0. Bioinformatics *27*, 1739-1740.

Limbourg, F.P., Takeshita, K., Radtke, F., Bronson, R.T., Chin, M.T., and Liao, J.K. (2005). Essential role of endothelial Notch1 in angiogenesis. Circulation *111*, 1826-1832.

Liu, G., Zhang, Q., Xia, L., Shi, M., Cai, J., Zhang, H., Li, J., Lin, G., Xie, W., Zhang, Y.*, et al.* (2019). RNA-binding protein CELF6 is cell cycle regulated and controls cancer cell proliferation by stabilizing p21. Cell Death Dis *10*, 688.

Liu, J., Willet, S.G., Bankaitis, E.D., Xu, Y., Wright, C.V., and Gu, G. (2013). Non-parallel recombination limits cre-loxP-based reporters as precise indicators of conditional genetic manipulation. Genesis *51*, 436-442.

Lobov, I.B., Cheung, E., Wudali, R., Cao, J., Halasz, G., Wei, Y., Economides, A., Lin, H.C., Papadopoulos, N., Yancopoulos, G.D.*, et al.* (2011). The Dll4/Notch pathway controls postangiogenic blood vessel remodeling and regression by modulating vasoconstriction and blood flow. Blood *117*, 6728-6737.

Lobov, I.B., Renard, R.A., Papadopoulos, N., Gale, N.W., Thurston, G., Yancopoulos, G.D., and Wiegand, S.J. (2007). Delta-like ligand 4 (Dll4) is induced by VEGF as a negative regulator of angiogenic sprouting. Proc Natl Acad Sci U S A *104*, 3219-3224.

Lohela, M., Bry, M., Tammela, T., and Alitalo, K. (2009). VEGFs and receptors involved in angiogenesis versus lymphangiogenesis. Curr Opin Cell Biol *21*, 154-165.

Lukowski, S.W., Patel, J., Andersen, S.B., Sim, S.L., Wong, H.Y., Tay, J., Winkler, I., Powell, J.E., and Khosrotehrani, K. (2019). Single-Cell Transcriptional Profiling of Aortic Endothelium Identifies a Hierarchy from Endovascular Progenitors to Differentiated Cells. Cell Rep *27*, 2748-2758 e2743.

Luo, W., Garcia-Gonzalez, I., Fernández-Chacón, M., Casquero-Garcia, V., Sanchez-Muñoz, MS., Mühleder, S., Garcia-Ortega, L., Andrade, J., Potente, M., Benedito, R. (2020). Arterialization requires the timely suppression of cell growth. Nature.

Mack, J.J., Mosqueiro, T.S., Archer, B.J., Jones, W.M., Sunshine, H., Faas, G.C., Briot, A., Aragon, R.L., Su, T., Romay, M.C.*, et al.* (2017). NOTCH1 is a mechanosensor in adult arteries. Nat Commun *8*, 1620.

MacParland, S.A., Liu, J.C., Ma, X.Z., Innes, B.T., Bartczak, A.M., Gage, B.K., Manuel, J., Khuu, N., Echeverri, J., Linares, I.*, et al.* (2018). Single cell RNA sequencing of human liver reveals distinct intrahepatic macrophage populations. Nat Commun *9*, 4383.

Malinverno, M., Maderna, C., Abu Taha, A., Corada, M., Orsenigo, F., Valentino, M., Pisati, F., Fusco, C., Graziano, P., Giannotta, M.*, et al.* (2019). Endothelial cell clonal expansion in the development of cerebral cavernous malformations. Nat Commun *10*, 2761.

Marshall, C.J. (1995). Specificity of receptor tyrosine kinase signaling: Transient versus sustained extracellular signal-regulated kinase activation. Cell *80*, 179-185.

Martin, D.I., and Whitelaw, E. (1996). The vagaries of variegating transgenes. Bioessays *18*, 919-923.

Martin, M. (2011). Cutadapt removes adapter sequences from high-throughput sequencing reads. EMBnetjournal *17(1):10-12*.

Martinez-Acedo, P., Nunez, E., Gomez, F.J., Moreno, M., Ramos, E., Izquierdo-Alvarez, A., Miro-Casas, E., Mesa, R., Rodriguez, P., Martinez-Ruiz, A.*, et al.* (2012). A novel strategy for global analysis of the dynamic thiol redox proteome. Mol Cell Proteomics *11*, 800-813.

Martinez-Bartolome, S., Navarro, P., Martin-Maroto, F., Lopez-Ferrer, D., Ramos-Fernandez, A., Villar, M., Garcia-Ruiz, J.P., and Vazquez, J. (2008). Properties of average score distributions of SEQUEST: the probability ratio method. Mol Cell Proteomics *7*, 1135-1145.

McDonald, A.I., Shirali, A.S., Aragon, R., Ma, F., Hernandez, G., Vaughn, D.A., Mack, J.J., Lim, T.Y., Sunshine, H., Zhao, P.*, et al.* (2018). Endothelial Regeneration of Large Vessels Is a Biphasic Process Driven by Local Cells with Distinct Proliferative Capacities. Cell Stem Cell *23*, 210-225 e216.

Menon, R., Otto, E.A., Hoover, P., Eddy, S., Mariani, L., Godfrey, B., Berthier, C.C., Eichinger, F., Subramanian, L., Harder, J.*, et al.* (2020). Single cell transcriptomics identifies focal segmental glomerulosclerosis remission endothelial biomarker. JCI Insight *5*.

Meyer, N., and Penn, L.Z. (2008). Reflecting on 25 years with MYC. Nat Rev Cancer *8*, 976-990.

Milano, J., McKay, J., Dagenais, C., Foster-Brown, L., Pognan, F., Gadient, R., Jacobs, R.T., Zacco, A., Greenberg, B., and Ciaccio, P.J. (2004). Modulation of notch processing by gamma-secretase inhibitors causes intestinal goblet cell metaplasia and induction of genes known to specify gut secretory lineage differentiation. Toxicol Sci *82*, 341-358.

Mohtashami, M., Shah, D.K., Nakase, H., Kianizad, K., Petrie, H.T., and Zuniga-Pflucker, J.C. (2010). Direct comparison of Dll1- and Dll4-mediated Notch activation levels shows differential lymphomyeloid lineage commitment outcomes. J Immunol *185*, 867-876.

Mondor, I., Jorquera, A., Sene, C., Adriouch, S., Adams, R.H., Zhou, B., Wienert, S., Klauschen, F., and Bajenoff, M. (2016). Clonal Proliferation and Stochastic Pruning Orchestrate Lymph Node Vasculature Remodeling. Immunity *45*, 877-888.

Mouillesseaux, K.P., Wiley, D.S., Saunders, L.M., Wylie, L.A., Kushner, E.J., Chong, D.C., Citrin, K.M., Barber, A.T., Park, Y., Kim, J.D.*, et al.* (2016). Notch regulates BMP responsiveness and lateral branching in vessel networks via SMAD6. Nat Commun *7*, 13247.

Moya, I.M., Umans, L., Maas, E., Pereira, P.N., Beets, K., Francis, A., Sents, W., Robertson, E.J., Mummery, C.L., Huylebroeck, D.*, et al.* (2012). Stalk cell phenotype depends on integration of notch and smad1/5 signaling cascades. Dev Cell *22*, 501-514.

Munch, J., Grivas, D., Gonzalez-Rajal, A., Torregrosa-Carrion, R., and de la Pompa, J.L. (2017). Notch signalling restricts inflammation and serpine1 expression in the dynamic endocardium of the regenerating zebrafish heart. Development *144*, 1425-1440.

Munoz-Espin, D., and Serrano, M. (2014). Cellular senescence: from physiology to pathology. Nat Rev Mol Cell Biol *15*, 482-496.

Murakami, M., Nguyen, L.T., Zhuang, Z.W., Moodie, K.L., Carmeliet, P., Stan, R.V., and Simons, M. (2008). The FGF system has a key role in regulating vascular integrity. J Clin Invest *118*, 3355-3366.

Murphy, P.A., Kim, T.N., Lu, G., Bollen, A.W., Schaffer, C.B., and Wang, R.A. (2012). Notch4 normalization reduces blood vessel size in arteriovenous malformations. Sci Transl Med *4*, 117ra118.

Muzumdar, M.D., Tasic, B., Miyamichi, K., Li, L., and Luo, L. (2007). A global double-fluorescent Cre reporter mouse. Genesis *45*, 593-605.

Nandagopal, N., Santat, L.A., LeBon, L., Sprinzak, D., Bronner, M.E., and Elowitz, M.B. (2018). Dynamic Ligand Discrimination in the Notch Signaling Pathway. Cell *172*, 869-880 e819.

Navarro, P., Trevisan-Herraz, M., Bonzon-Kulichenko, E., Nunez, E., Martinez-Acedo, P., Perez-Hernandez, D., Jorge, I., Mesa, R., Calvo, E., Carrascal, M.*, et al.* (2014). General statistical framework for quantitative proteomics by stable isotope labeling. J Proteome Res *13*, 1234-1247.

Navarro, P., and Vazquez, J. (2009). A refined method to calculate false discovery rates for peptide identification using decoy databases. J Proteome Res *8*, 1792-1796.

Noguera-Troise, I., Daly, C., Papadopoulos, N.J., Coetzee, S., Boland, P., Gale, N.W., Lin, H.C., Yancopoulos, G.D., and Thurston, G. (2006). Blockade of Dll4 inhibits tumour growth by promoting non-productive angiogenesis. Nature *444*, 1032-1037.

Nolan, D.J., Ginsberg, M., Israely, E., Palikuqi, B., Poulos, M.G., James, D., Ding, B.S., Schachterle, W., Liu, Y., Rosenwaks, Z.*, et al.* (2013). Molecular signatures of tissue-specific microvascular endothelial cell heterogeneity in organ maintenance and regeneration. Dev Cell *26*, 204-219.

Noseda, M., Chang, L., McLean, G., Grim, J.E., Clurman, B.E., Smith, L.L., and Karsan, A. (2004). Notch activation induces endothelial cell cycle arrest and participates in contact inhibition: role of p21Cip1 repression. Mol Cell Biol *24*, 8813-8822.

Nus, M., Martinez-Poveda, B., MacGrogan, D., Chevre, R., D'Amato, G., Sbroggio, M., Rodriguez, C., Martinez-Gonzalez, J., Andres, V., Hidalgo, A.*, et al.* (2016). Endothelial Jag1-RBPJ signalling promotes inflammatory leucocyte recruitment and atherosclerosis. Cardiovasc Res *112*, 568-580.

Otto, T., and Sicinski, P. (2017). Cell cycle proteins as promising targets in cancer therapy. Nat Rev Cancer *17*, 93-115.

Palomero, T., Lim, W.K., Odom, D.T., Sulis, M.L., Real, P.J., Margolin, A., Barnes, K.C., O'Neil, J., Neuberg, D., Weng, A.P.*, et al.* (2006). NOTCH1 directly regulates c-MYC and activates a feed-forward-loop transcriptional network promoting leukemic cell growth. Proc Natl Acad Sci U S A *103*, 18261-18266.

Panier, S., and Boulton, S.J. (2014). Double-strand break repair: 53BP1 comes into focus. Nat Rev Mol Cell Biol *15*, 7-18.

Panin, V.M., Papayannopoulos, V., Wilson, R., and Irvine, K.D. (1997). Fringe modulates Notch-ligand interactions. Nature *387*, 908-912.

Pardali, E., Goumans, M.J., and ten Dijke, P. (2010). Signaling by members of the TGF-beta family in vascular morphogenesis and disease. Trends Cell Biol *20*, 556-567.

Patenaude, A., Fuller, M., Chang, L., Wong, F., Paliouras, G., Shaw, R., Kyle, A.H., Umlandt, P., Baker, J.H., Diaz, E.*, et al.* (2014). Endothelial-specific Notch blockade inhibits vascular function and tumor growth through an eNOS-dependent mechanism. Cancer Res *74*, 2402-2411.

Phng, L.K., and Gerhardt, H. (2009). Angiogenesis: a team effort coordinated by notch. Dev Cell *16*, 196-208.

Pitulescu, M.E., Schmidt, I., Benedito, R., and Adams, R.H. (2010). Inducible gene targeting in the neonatal vasculature and analysis of retinal angiogenesis in mice. Nature protocols *5*, 1518-1534.

Pitulescu, M.E., Schmidt, I., Giaimo, B.D., Antoine, T., Berkenfeld, F., Ferrante, F., Park, H., Ehling, M., Biljes, D., Rocha, S.F., *et al.* (2017). Dll4 and Notch signalling couples sprouting angiogenesis and artery formation. Nat Cell Biol *19*, 915-927.

Poisson, J., Lemoinne, S., Boulanger, C., Durand, F., Moreau, R., Valla, D., and Rautou, P.E. (2017). Liver sinusoidal endothelial cells: Physiology and role in liver diseases. J Hepatol *66*, 212-227.

Pontes-Quero, S., Fernandez-Chacon, M., Luo, W., Lunella, F.F., Casquero-Garcia, V., Garcia-Gonzalez, I., Hermoso, A., Rocha, S.F., Bansal, M., and Benedito, R. (2019). High mitogenic stimulation arrests angiogenesis. Nat Commun *10*, 2016.

Pontes-Quero, S., Heredia, L., Casquero-Garcia, V., Fernandez-Chacon, M., Luo, W., Hermoso, A., Bansal, M., Garcia-Gonzalez, I., Sanchez-Munoz, M.S., Perea, J.R., *et al.* (2017). Dual ifgMosaic: A Versatile Method for Multispectral and Combinatorial Mosaic Gene-Function Analysis. Cell *170*, 800-814 e818.

Potente, M., and Carmeliet, P. (2017). The Link Between Angiogenesis and Endothelial Metabolism. Annu Rev Physiol *79*, 43-66.

Potente, M., Gerhardt, H., and Carmeliet, P. (2011). Basic and therapeutic aspects of angiogenesis. Cell *146*, 873-887.

Pumiglia, K.M., and Decker, S.J. (1997). Cell cycle arrest mediated by the MEK/mitogen-activated protein kinase pathway. Proc Natl Acad Sci U S A *94*, 448-452.

Radtke, F., Wilson, A., Stark, G., Bauer, M., van Meerwijk, J., MacDonald, H.R., and Aguet, M. (1999). Deficient T Cell Fate Specification in Mice with an Induced Inactivation of Notch1. Immunity *10*, 547-558.

Rafii, S., Butler, J.M., and Ding, B.S. (2016). Angiocrine functions of organ-specific endothelial cells. Nature *529*, 316-325.

Ramachandran, P., Dobie, R., Wilson-Kanamori, J.R., Dora, E.F., Henderson, B.E.P., Luu, N.T., Portman, J.R., Matchett, K.P., Brice, M., Marwick, J.A., *et al.* (2019). Resolving the fibrotic niche of human liver cirrhosis at single-cell level. Nature *575*, 512-518.

Rangarajan, A., Talora, C., Okuyama, R., Nicolas, M., Mammucari, C., Oh, H., Aster, J.C., Krishna, S., Metzger, D., Chambon, P., *et al.* (2001). Notch signaling is a direct determinant of keratinocyte growth arrest and entry into differentiation. EMBO J *20*, 3427-3436.

Ridgway, J., Zhang, G., Wu, Y., Stawicki, S., Liang, W.C., Chanthery, Y., Kowalski, J., Watts, R.J., Callahan, C., Kasman, I., *et al.* (2006). Inhibition of Dll4 signalling inhibits tumour growth by deregulating angiogenesis. Nature *444*, 1083-1087.

Risau, W., and Flamme, I. (1995). Vasculogenesis. Annu Rev Cell Dev Biol *11*, 73-91.

Ritchie, M.E., Phipson, B., Wu, D., Hu, Y., Law, C.W., Shi, W., and Smyth, G.K. (2015). limma powers differential expression analyses for RNA-sequencing and microarray studies. Nucleic Acids Res *43*, e47.

Ritschka, B., Storer, M., Mas, A., Heinzmann, F., Ortells, M.C., Morton, J.P., Sansom, O.J., Zender, L., and Keyes, W.M. (2017). The senescence-associated secretory phenotype induces cellular plasticity and tissue regeneration. Genes Dev *31*, 172-183.

Roman, B.L., and Hinck, A.P. (2017). ALK1 signaling in development and disease: new paradigms. Cell Mol Life Sci *74*, 4539-4560.

Rostama, B., Turner, J.E., Seavey, G.T., Norton, C.R., Gridley, T., Vary, C.P., and Liaw, L. (2015). DLL4/Notch1 and BMP9 Interdependent Signaling Induces Human Endothelial Cell

Quiescence via P27KIP1 and Thrombospondin-1. Arterioscler Thromb Vasc Biol *35*, 2626-2637.

Ruzankina, Y., Pinzon-Guzman, C., Asare, A., Ong, T., Pontano, L., Cotsarelis, G., Zediak, V.P., Velez, M., Bhandoola, A., and Brown, E.J. (2007). Deletion of the developmentally essential gene ATR in adult mice leads to age-related phenotypes and stem cell loss. Cell Stem Cell *1*, 113-126.

Sabbagh, M.F., Heng, J.S., Luo, C., Castanon, R.G., Nery, J.R., Rattner, A., Goff, L.A., Ecker, J.R., and Nathans, J. (2018). Transcriptional and epigenomic landscapes of CNS and non-CNS vascular endothelial cells. Elife *7*.

Sanganalmath, S.K., and Bolli, R. (2013). Cell therapy for heart failure: a comprehensive overview of experimental and clinical studies, current challenges, and future directions. Circ Res *113*, 810-834.

Sato, T.N., Tozawa, Y., Deutsch, U., Wolburg-Buchholz, K., Fujiwara, Y., Gendron-Maguire, M., Gridley, T., Wolburg, H., Risau, W., and Qin, Y. (1995). Distinct roles of the receptor tyrosine kinases Tie-1 and Tie-2 in blood vessel formation. Nature *376*, 70-74.

Schlereth, K., Weichenhan, D., Bauer, T., Heumann, T., Giannakouri, E., Lipka, D., Jaeger, S., Schlesner, M., Aloy, P., Eils, R.*, et al.* (2018). The transcriptomic and epigenetic map of vascular quiescence in the continuous lung endothelium. Elife *7*.

Schmidt-Supprian, M., and Rajewsky, K. (2007). Vagaries of conditional gene targeting. Nat Immunol *8*, 665-668.

Schonhuber, N., Seidler, B., Schuck, K., Veltkamp, C., Schachtler, C., Zukowska, M., Eser, S., Feyerabend, T.B., Paul, M.C., Eser, P.*, et al.* (2014). A next-generation dual-recombinase system for time- and host-specific targeting of pancreatic cancer. Nat Med *20*, 1340-1347.

Scoumanne, A., Cho, S.J., Zhang, J., and Chen, X. (2011). The cyclin-dependent kinase inhibitor p21 is regulated by RNA-binding protein PCBP4 via mRNA stability. Nucleic Acids Res *39*, 213-224.

Sennett, R. (1994). Carne y Piedra : el cuerpo y la ciudad en la civilización occidental (Alianza Editorial).

Seo, S., and Kume, T. (2006). Forkhead transcription factors, Foxc1 and Foxc2, are required for the morphogenesis of the cardiac outflow tract. Dev Biol *296*, 421-436.

Serra, H., Chivite, I., Angulo-Urarte, A., Soler, A., Sutherland, J.D., Arruabarrena-Aristorena, A., Ragab, A., Lim, R., Malumbres, M., Fruttiger, M.*, et al.* (2015). PTEN mediates Notch-dependent stalk cell arrest in angiogenesis. Nat Commun *6*, 7935.

Shalaby, F., Rossant, J., Yamaguchi, T.P., Gertsenstein, M., Wu, X.F., Breitman, M.L., and Schuh, A.C. (1995). Failure of blood-island formation and vasculogenesis in Flk-1-deficient mice. Nature *376*, 62-66.

Shetty, S., Lalor, P.F., and Adams, D.H. (2018). Liver sinusoidal endothelial cells - gatekeepers of hepatic immunity. Nat Rev Gastroenterol Hepatol *15*, 555-567.

Shin, M., Beane, T.J., Quillien, A., Male, I., Zhu, L.J., and Lawson, N.D. (2016). Vegfa signals through ERK to promote angiogenesis, but not artery differentiation. Development *143*, 3796-3805.

Shutter, J.R., Scully, S., Fan, W., Richards, W.G., Kitajewski, J., Deblandre, G.A., Kintner, C.R., and Stark, K.L. (2000). Dll4, a novel Notch ligand expressed in arterial endothelium. Genes Dev *14*, 1313-1318.

Siekmann, A.F., and Lawson, N.D. (2007). Notch signalling limits angiogenic cell behaviour in developing zebrafish arteries. Nature *445*, 781-784.

Siemerink, M.J., Klaassen, I., Vogels, I.M., Griffioen, A.W., Van Noorden, C.J., and Schlingemann, R.O. (2012). CD34 marks angiogenic tip cells in human vascular endothelial cell cultures. Angiogenesis *15*, 151-163.

Sivakumar, S., Daum, J.R., Tipton, A.R., Rankin, S., and Gorbsky, G.J. (2014). The spindle and kinetochore-associated (Ska) complex enhances binding of the anaphase-promoting complex/cyclosome (APC/C) to chromosomes and promotes mitotic exit. Mol Biol Cell *25*, 594-605.

Sorensen, I., Adams, R.H., and Gossler, A. (2009). DLL1-mediated Notch activation regulates endothelial identity in mouse fetal arteries. Blood *113*, 5680-5688.

Soriano, P. (1994). Abnormal kidney development and hematological disorders in PDGF beta-receptor mutant mice. Genes Dev *8*, 1888-1896.

Soriano, P. (1999). Generalized lacZ expression with the ROSA26 Cre reporter strain. Nat Genet *21*, 70-71.

Srinivas, S., Watanabe, T., Lin, C.S., William, C.M., Tanabe, Y., Jessell, T.M., and Costantini, F. (2001). Cre reporter strains produced by targeted insertion of EYFP and ECFP into the ROSA26 locus. BMC Dev Biol *1*, 4.

Su, T., Stanley, G., Sinha, R., D'Amato, G., Das, S., Rhee, S., Chang, A.H., Poduri, A., Raftrey, B., Dinh, T.T*., et al.* (2018). Single-cell analysis of early progenitor cells that build coronary arteries. Nature *559*, 356-362.

Subramanian, A., Tamayo, P., Mootha, V.K., Mukherjee, S., Ebert, B.L., Gillette, M.A., Paulovich, A., Pomeroy, S.L., Golub, T.R., Lander, E.S*., et al.* (2005). Gene set enrichment analysis: a knowledge-based approach for interpreting genome-wide expression profiles. Proc Natl Acad Sci U S A *102*, 15545-15550.

Suchting, S., Freitas, C., le Noble, F., Benedito, R., Breant, C., Duarte, A., and Eichmann, A. (2007). The Notch ligand Delta-like 4 negatively regulates endothelial tip cell formation and vessel branching. Proc Natl Acad Sci U S A *104*, 3225-3230.

Sundlisaeter, E., Edelmann, R.J., Hol, J., Sponheim, J., Kuchler, A.M., Weiss, M., Udalova, I.A., Midwood, K.S., Kasprzycka, M., and Haraldsen, G. (2012). The alarmin IL-33 is a notch target in quiescent endothelial cells. Am J Pathol *181*, 1099-1111.

Suri, C., Jones, P.F., Patan, S., Bartunkova, S., Maisonpierre, P.C., Davis, S., Sato, T.N., and Yancopoulos, G.D. (1996). Requisite Role of Angiopoietin-1, a Ligand for the TIE2 Receptor, during Embryonic Angiogenesis. Cell *87*, 1171-1180.

Sweeney, M.D., Zhao, Z., Montagne, A., Nelson, A.R., and Zlokovic, B.V. (2019). Blood-Brain Barrier: From Physiology to Disease and Back. Physiol Rev *99*, 21-78.

Swift, M.R., and Weinstein, B.M. (2009). Arterial-venous specification during development. Circ Res *104*, 576-588.

Taimeh, Z., Loughran, J., Birks, E.J., and Bolli, R. (2013). Vascular endothelial growth factor in heart failure. Nat Rev Cardiol *10*, 519-530.

Tammela, T., Zarkada, G., Nurmi, H., Jakobsson, L., Heinolainen, K., Tvorogov, D., Zheng, W., Franco, C.A., Murtomaki, A., Aranda, E*., et al.* (2011). VEGFR-3 controls tip to stalk conversion at vessel fusion sites by reinforcing Notch signalling. Nat Cell Biol *13*, 1202-1213.

Tateishi, Y., Matsumoto, A., Kanie, T., Hara, E., Nakayama, K., and Nakayama, K.I. (2012). Development of mice without Cip/Kip CDK inhibitors. Biochem Biophys Res Commun *427*, 285-292.

Teuwen, L.A., Geldhof, V., Pasut, A., and Carmeliet, P. (2020). COVID-19: the vasculature unleashed. Nat Rev Immunol *20*, 389-391.

Tikhonova, A.N., Dolgalev, I., Hu, H., Sivaraj, K.K., Hoxha, E., Cuesta-Dominguez, A., Pinho, S., Akhmetzyanova, I., Gao, J., Witkowski, M.*, et al.* (2019). The bone marrow microenvironment at single-cell resolution. Nature *569*, 222-228.

Tillmann, S., Bernhagen, J., and Noels, H. (2013). Arrest Functions of the MIF Ligand/Receptor Axes in Atherogenesis. Front Immunol *4*, 115.

Touyz, R.M., and Herrmann, J. (2018). Cardiotoxicity with vascular endothelial growth factor inhibitor therapy. NPJ Precis Oncol *2*, 13.

Travisano, S.I., Oliveira, V.L., Prados, B., Grego-Bessa, J., Pineiro-Sabaris, R., Bou, V., Gomez, M.J., Sanchez-Cabo, F., MacGrogan, D., and de la Pompa, J.L. (2019). Coronary arterial development is regulated by a Dll4-Jag1-EphrinB2 signaling cascade. Elife *8*.

Trevisan-Herraz, M., Bagwan, N., García-Marqués, F., Rodriguez, J.M., Jorge, I., Ezkurdia, I., Bonzon-Kulichenko, E., Vázquez, J., and Valencia, A. (2019). SanXoT: a modular and versatile package for the quantitative analysis of high-throughput proteomics experiments. Bioinformatics *35*, 1594-1596.

Trichas, G., Begbie, J., and Srinivas, S. (2008). Use of the viral 2A peptide for bicistronic expression in transgenic mice. BMC Biol *6*, 40.

Ubezio, B., Blanco, R.A., Geudens, I., Stanchi, F., Mathivet, T., Jones, M.L., Ragab, A., Bentley, K., and Gerhardt, H. (2016). Synchronization of endothelial Dll4-Notch dynamics switch blood vessels from branching to expansion. Elife *5*.

Uyttendaele, H., Ho, J., Rossant, J., and Kitajewski, J. (2001). Vascular patterning defects associated with expression of activated Notch4 in embryonic endothelium. Proc Natl Acad Sci U S A *98*, 5643-5648.

Vanlandewijck, M., He, L., Mae, M.A., Andrae, J., Ando, K., Del Gaudio, F., Nahar, K., Lebouvier, T., Lavina, B., Gouveia, L.*, et al.* (2018). A molecular atlas of cell types and zonation in the brain vasculature. Nature *554*, 475-480.

Varga, Z., Flammer, A.J., Steiger, P., Haberecker, M., Andermatt, R., Zinkernagel, A.S., Mehra, M.R., Schuepbach, R.A., Ruschitzka, F., and Moch, H. (2020). Endothelial cell infection and endotheliitis in COVID-19. The Lancet *395*, 1417-1418.

Venkatesh, D., Fredette, N., Rostama, B., Tang, Y., Vary, C.P., Liaw, L., and Urs, S. (2011). RhoA-mediated signaling in Notch-induced senescence-like growth arrest and endothelial barrier dysfunction. Arterioscler Thromb Vasc Biol *31*, 876-882.

Villa, N., Walker, L., Lindsell, C.E., Gasson, J., Iruela-Arispe, M.L., and Weinmaster, G. (2001). Vascular expression of Notch pathway receptors and ligands is restricted to arterial vessels. Mechanisms of Development *108*, 161-164.

Wakabayashi, T., Naito, H., Suehiro, J.-i., Lin, Y., Kawaji, H., Iba, T., Kouno, T., Ishikawa-Kato, S., Furuno, M., Takara, K.*, et al.* (2018). CD157 Marks Tissue-Resident Endothelial Stem Cells with Homeostatic and Regenerative Properties. Cell Stem Cell *22*, 384-397.e386.

Wang, H.U., Chen, Z.-F., and Anderson, D.J. (1998). Molecular Distinction and Angiogenic Interaction between Embryonic Arteries and Veins Revealed by ephrin-B2 and Its Receptor Eph-B4. Cell *93*, 741-753.

Wang, Y., Nakayama, M., Pitulescu, M.E., Schmidt, T.S., Bochenek, M.L., Sakakibara, A., Adams, S., Davy, A., Deutsch, U., Luthi, U.*, et al.* (2010). Ephrin-B2 controls VEGF-induced angiogenesis and lymphangiogenesis. Nature *465*, 483-486.

Weng, A.P., Millholland, J.M., Yashiro-Ohtani, Y., Arcangeli, M.L., Lau, A., Wai, C., Del Bianco, C., Rodriguez, C.G., Sai, H., Tobias, J.*, et al.* (2006). c-Myc is an important direct target of Notch1 in T-cell acute lymphoblastic leukemia/lymphoma. Genes Dev *20*, 2096-2109.

Widlansky, M.E., Gokce, N., Keaney, J.F., and Vita, J.A. (2003). The clinical implications of endothelial dysfunction. Journal of the American College of Cardiology *42*, 1149-1160.

Wieland, E., Rodriguez-Vita, J., Liebler, S.S., Mogler, C., Moll, I., Herberich, S.E., Espinet, E., Herpel, E., Menuchin, A., Chang-Claude, J.*, et al.* (2017). Endothelial Notch1 Activity Facilitates Metastasis. Cancer Cell *31*, 355-367.

Wilhelm, K., Happel, K., Eelen, G., Schoors, S., Oellerich, M.F., Lim, R., Zimmermann, B., Aspalter, I.M., Franco, C.A., Boettger, T.*, et al.* (2016). FOXO1 couples metabolic activity and growth state in the vascular endothelium. Nature *529*, 216-220.

Williams, A.B., and Schumacher, B. (2016). p53 in the DNA-Damage-Repair Process. Cold Spring Harb Perspect Med *6*.

Wisniewski, J.R., Zougman, A., Nagaraj, N., and Mann, M. (2009). Universal sample preparation method for proteome analysis. Nat Methods *6*, 359-362.

Wong, G.T., Manfra, D., Poulet, F.M., Zhang, Q., Josien, H., Bara, T., Engstrom, L., Pinzon-Ortiz, M., Fine, J.S., Lee, H.J.*, et al.* (2004). Chronic treatment with the gamma-secretase inhibitor LY-411,575 inhibits beta-amyloid peptide production and alters lymphopoiesis and intestinal cell differentiation. J Biol Chem *279*, 12876-12882.

Woods, D., Parry, D., Cherwinski, H., Bosch, E., Lees, E., and McMahon, M. (1997). Raf-induced proliferation or cell cycle arrest is determined by the level of Raf activity with arrest mediated by p21Cip1. Mol Cell Biol *17*, 5598-5611.

Xu, C., Hasan, S.S., Schmidt, I., Rocha, S.F., Pitulescu, M.E., Bussmann, J., Meyen, D., Raz, E., Adams, R.H., and Siekmann, A.F. (2014). Arteries are formed by vein-derived endothelial tip cells. Nature communications *5*, 5758.

Xue, Y., Gao, X., Lindsell, C.E., Norton, C.R., Chang, B., Hicks, C., Gendron-Maguire, M., Rand, E.B., Weinmaster, G., and Gridley, T. (1999). Embryonic lethality and vascular defects in mice lacking the Notch ligand Jagged1. Hum Mol Genet *8*, 723-730.

Yan, M., Callahan, C.A., Beyer, J.C., Allamneni, K.P., Zhang, G., Ridgway, J.B., Niessen, K., and Plowman, G.D. (2010). Chronic DLL4 blockade induces vascular neoplasms. Nature *463*, E6-7.

Yan, M.S., and Marsden, P.A. (2015). Epigenetics in the Vascular Endothelium: Looking From a Different Perspective in the Epigenomics Era. Arterioscler Thromb Vasc Biol *35*, 2297-2306.

Yang, L.T., Nichols, J.T., Yao, C., Manilay, J.O., Robey, E.A., and Weinmaster, G. (2005). Fringe glycosyltransferases differentially modulate Notch1 proteolysis induced by Delta1 and Jagged1. Mol Biol Cell *16*, 927-942.

Yoshida, Y., Hayashi, Y., Suda, M., Tateno, K., Okada, S., Moriya, J., Yokoyama, M., Nojima, A., Yamashita, M., Kobayashi, Y.*, et al.* (2014). Notch signaling regulates the lifespan of vascular endothelial cells via a p16-dependent pathway. PLoS One *9*, e100359.

You, L.R., Lin, F.J., Lee, C.T., Demayo, F.J., Tsai, M.J., and Tsai, S.Y. (2005). Suppression of Notch signalling by the COUP-TFII transcription factor regulates vein identity. Nature *435*, 98-104.

Zhang, Y., Ulvmar, M.H., Stanczuk, L., Martinez-Corral, I., Frye, M., Alitalo, K., and Makinen, T. (2018). Heterogeneity in VEGFR3 levels drives lymphatic vessel hyperplasia through cell-autonomous and non-cell-autonomous mechanisms. Nature communications *9*, 1296.

Zheng, B., Sage, M., Sheppeard, E.A., Jurecic, V., and Bradley, A. (2000). Engineering mouse chromosomes with Cre-loxP: range, efficiency, and somatic applications. Mol Cell Biol *20*, 648-655.

PUBLICATIONS

The work described in the second chapter of this thesis is included in the following article:

Fernández-Chacón M, Casquero-García V, Luo W, Lunella F, Rocha SF, Del Olmo-Cabrera S, Benedito R*****. *iSuRe-Cre is a genetic tool to reliably induce and report Cre-dependent genetic modifications.* ***Nature Commun.*** (2019). DOI: 10.1038/s41467-019-10239-4.

The collaboration in other research projects during the development of the thesis has resulted in the following publications:

Luo W, Garcia-Gonzalez I, **Fernández-Chacón M,** Casquero-Garcia V, Sanchez-Muñoz MS, Mühleder S, Garcia-Ortega L, Andrade J, Potente M, Benedito R*. *Arterialization requires the timely suppression of cell growth.* ***Nature*** (2020).

Pontes-Quero S, **Fernández-Chacón M**, Luo W, Lunella FF, Casquero-Garcia V, Garcia-Gonzalez I, Hermoso A, Rocha SF, Bansal M, Benedito R*. *High mitogenic stimulation arrests angiogenesis.* ***Nat Commun.*** (2019). DOI: 10.1038/s41467-019-09875-7.

Pontes-Quero S, Heredia L, Casquero-García V, **Fernández-Chacón M**, Luo W, Hermoso A, Bansal M, Garcia-Gonzalez I, Sanchez-Muñoz MS, Perea JR, Galiana-Simal A, Rodriguez-Arabaolaza I, Del Olmo-Cabrera S, Rocha SF, Criado-Rodriguez LM, Giovinazzo G, Benedito R*. *Dual ifgMosaic: A Versatile Method for Multispectral and Combinatorial Mosaic Gene-Function Analysis.* ***Cell*** (2017). DOI: 10.1016/j.cell.2017.07.031.

During the development of the thesis, the following reviews have been published:

Mühleder S, **Fernández-Chacón M,** Garcia-Gonzalez I, Benedito R***.** *Endothelial Sprouting, Proliferation or Senescence: tipping the balance from physiology to pathology.* Accepted at ***Cell. Mol. Life Sci*** Sept (2020). DOI: 10.1007/s00018-020-03664-y

Garcia-Gonzalez I, *Mühleder S,* **Fernández-Chacón M,** Benedito R***.** *Genetic tools to study cardiovascular biology.* ***Front. Physio***. (2020). DOI: 10.3389/fphys.2020.01084